

Alma Mater Studiorum – Università di Bologna

DOTTORATO DI RICERCA IN
INGEGNERIA CIVILE ED AMBIENTALE

Ciclo XXVI

Settore Concorsuale di afferenza: 08/A1

Settore Scientifico disciplinare: ICAR/01

**A WEB GIS DECISION SUPPORT SYSTEM FOR COASTAL RISK
ASSESSMENT AND MITIGATION PLANNING**

Presentata da:

Stefano Bagli

Coordinatore Dottorato

Relatore

Chiar.mo Prof. Alberto Lamberti

Prof.ssa Barbara Zanuttigh

Esame finale anno 2015

Acknowledgements

To my SISTER INVICTUS

*Out of the night that covers me,
Black as the pit from pole to pole,
I thank whatever gods may be
For my unconquerable soul.*

*In the fell clutch of circumstance
I have not winced nor cried aloud.
Under the bludgeonings of chance
My head is bloody, but unbowed.*

*Beyond this place of wrath and tears
Looms but the Horror of the shade,
And yet the menace of the years
Finds and shall find me unafraid.*

*It matters not how strait the gate,
How charged with punishments the scroll,
I am the master of my fate,
I am the captain of my soul.*

William Ernest Henley (1849–1903)

I give special thanks to my friends and colleagues in GECOSistema Valerio Luzzi, Alberto Pistocchi and Paolo Mazzoli, for their qualified co-operations and suggestions in the development of the Web-GIS MARASMA DSS and raster-based coastal flooding models.

I wish to express my gratitude to Prof.ssa Barbara Zanuttigh and to the PhD course coordinator Prof. Alberto Lamberti for their very valuable supervision, support and recommendations throughout the study.

The support of the European Commission through the project “Innovative Technologies for safer European coasts in a changing climate” (THESEUS), Contract 244104, FP7.2009-1, www.theseusproject.eu, is gratefully acknowledged.

Index

1	Abstract.....	9
2	Objectives	10
3	Structure	12
4	Coastal Flooding Risk Assessment	13
4.1	Introduction.....	13
4.2	Flood Definitions and Characteristics	15
4.3	Flood Risk Assessment and EU Legislation	18
4.4	Definition of Risk in Flood Hazard	20
4.5	Vulnerability Definition	23
4.6	Flood Risk Assessment.....	24
4.6.1	Multi Criteria Analysis	28
4.6.2	A Qualitative Approach: Costal Vulnerability Index (CVI)	29
4.7	Coastal Risk Assessment Framework: The SPRC approach	32
4.7.1	SOURCE CHARACHTERIZATION	36
4.7.1.1	Sea Level Rise – Cesenatico case study.....	38
4.7.1.2	Typical and Extreme Climate Scenario.....	39
4.7.2	PATHWAYS- HAZARD ASSESSMENT	43
4.7.3	Receptors and Consequences	45
4.8	Data for coastal risk assessment	47
4.8.1	Land Use Map	48
4.8.2	Ecological Habitats	48
4.8.3	Census Data.....	50
4.8.4	Bathymetry and DTM	51
5	Mapping and Modeling Coastal Flooding - State of the art	53
5.1	Introduction.....	53
5.2	Coastal Flooding Modeling Approach– raster VS Numerical.....	55
5.3	Numerical Hydrodynamic model: Shallow Water Equation	62
5.4	2D Zero Inertial Raster-based flooding model.....	69
5.5	0D DEM-based flood spreading models	74

5.5.1	0D DEM-based flood model: Literature review.....	78
5.6	New GIS-raster-based model for modeling coastal flooding characteristics.....	86
5.6.1	A flat water 0D GIS-based Storm Surge coastal flooding model with infinite volume of water for open coast – FLOODSURGEMAP.....	87
5.6.1.1	Pre-Processing topography : DEM/Lidar.....	87
5.6.1.2	Mathematical Morphology and Watershed Segmentation algorithm	93
5.6.1.3	Model Benchmark.....	96
5.6.1.4	FLOODSURGEMAP Model Application.....	97
5.6.1.5	FLOODSURGEMAP: A watershed segmentation algorithm for mapping flood extent and water depth in estuarine	107
5.6.2	FLOODTOPMAP algorithm Finite Volume Overtopping Model.....	110
5.6.3	FLOODVELMAP raster based for mapping flood velocity.....	119
5.6.4	FLOODDURMAP raster based for mapping floodplain time duration.....	125
6	Flood Vulnerability and Damage Assessment.....	129
6.1	Introduction.....	129
6.2	Economic Damage Model.....	136
6.3	Social Damage Model.....	140
6.4	Environmental Damage Model.....	145
7	Quantitative GIS-Based risk evaluation	148
8	Multicriteria Risk Assessment.....	153
9	MARASMA: A web GIS DSS for mapping coastal risk assessment and mitigation planning	164
9.1	What is a Decision Support System (DSS)?.....	164
9.2	DSS in the context of coastal flood risk assessment: A review.....	166
9.3	The Web-GIS MARASMA DSS Frameworks	169
9.3.1	Conceptual Framework:.....	171
9.3.2	Methodological Framework: The SPRC methodology.....	172
9.3.3	Technological Framework: Architecture and Software.....	177
9.3.3.1	The user requirements	177
9.3.3.2	The methods	177
9.3.3.3	System Architecture and Software	178
9.3.3.3.1	A web mapping server.....	178
9.3.3.3.2	The web GUI	180
9.3.3.3.3	Spatial DB	184

9.3.3.3.4	Raster Based Models	185
9.3.4	Scenario Generation	185
9.3.5	Source of Flooding	185
10	MARASMA DSS: Cesenatico Case Study	187
10.1	Cesenatico Study Area.....	187
10.2	Cesenatico Coastal Flooding Risk Assessment.....	191
11	Conclusions.....	192
12	Appendix	194
12.1	FLOODSURGEMAP	194
12.2	VELOCITY	207
12.3	FLOW DURATION.....	208
13	Bibliography.....	210

Figures

Figure 1 Illustration of the ‘two-faced nature’ of floods bringing with them both hazards and benefits (He et al 2014).....	17
Figure 2 EU Flooding Directive.	18
Figure 3 Risk Triange Paradigm.	22
Figure 4 CVI Workflow Bagdanaviciute et al. 2015	30
Figure 5 SPRC paradigm FLOODsite EU FP7 Project	32
Figure 6 SPRC FLOODsite EU FP7 Project	34
Figure 7 Models involved in SPRC	35
Figure 8 total water level components	36
Figure 9 Average sea level measured in Ravenna. The change in subsidence growth rate due to the law stopping water pumping from the subsoil in the agricultural surrounding land is evident.	39
Figure 10 Maximum, average and minimum sea level rise predictions based on the historical data collected from Trieste measurement station. Kindly provided by Ralf Weisse, HZG.	39
Figure 11 Overtopping	42
Figure 12 Coastal Mortality based upon large-scale events - Jonkman and Vrijling, 2008	46
Figure 13 Cesenatico CORINE Land Cover data.....	48
Figure 14 Cesenatico natural and artificial habitats.....	49
Figure 15 Bellocchio natural and artificial habitats.....	50
Figure 16 Cesenatico ISTA POPULATION DENSITY	50
Figure 17 Costal Area variability and resolution	52
Figure 18 Cesenatico topography	52
Figure 19 0D Equilibrium model – bath-tube approach (A) and seeded region growing (B) ..	75
Figure 20 connectivity and resolution effect on 0D DEM-based flood modeling - Poulter et al. 2008	78
Figure 21 ISIS-FAST - Gouldby et al. (2008)	80
Figure 22 IMPACT ZONE - Gouldby et al. (2008)	81
Figure 23 River Cross-section interpolation - Merwade et al 2008.....	90

Figure 24 River Cross-section interpolation – Case Study Cesenatico	90
Figure 25 Integration of the channel bathymetries with the surrounding datasets	92
Figure 26 Cesenatico topography/bathymetry	93
Figure 27 Bellocchio topography/bathymetry	93
Figure 28 Flooding a DEM and dam building (a), catchment basins (b) Beucher and Meyer 1993	95
Figure 29 Comparison among flooded areas obtained with the simplified modeling tool (yellow areas) and the maximum flood extension derived from simulations with MIKE 21 (red contours). Two areas are show in the pictures above: Lido degli Estensi and Lido di Spina (to the top) and the outlet of Foce Rento (to the bottom). Scenario with Tr=50 years Scenario 2010	97
Figure 30 Cesenatico and Bellocchio case studies	98
Figure 31 Cesenatico storm surge flooding – TR=10 years Scenario 2010.....	99
Figure 32 Cesenatico storm surge flooding – TR=20 years Scenario 2010.....	100
Figure 33 Cesenatico storm surge flooding – TR=50 years Scenario 2010.....	100
Figure 34 Cesenatico storm surge flooding – TR=10 years Scenario 2020.....	101
Figure 35 Cesenatico storm surge flooding – TR=20 years Scenario 2020.....	101
Figure 36 Cesenatico storm surge flooding – TR=20 years Scenario 2020.....	102
Figure 37 Teignmouth Case Study.....	102
Figure 38 Projected sea level rise.....	104
Figure 39 Flood Hazard Maps (water depth) for present, short, mid and longterm scenario with return period 100 years – ARCGIS Model Kwan 2011.....	105
Figure 40 Flood Hazard Maps (water depth) FLOODSURGEMAP for longterm scenario with return period 20 years	106
Figure 41 Flood Hazard Maps (water depth) FLOODSURGEMAP for longterm scenario with return period 100 years	106
Figure 42 Gironde Case Study TELEMAC flood modeling.....	109
Figure 43 Gironde Case Study FLOODSURGEMAP flood modeling	110
Figure 44 Iterative procedure for finite volume overtopping	111
Figure 45 Finte Volume overtopping – 50000 m3.....	112
Figure 46 Finte Volume overtopping – 100000 m3.....	112
Figure 47 Finte Volume overtopping – 200000 m3.....	113
Figure 48 Water Level VS Volume of Water.....	113
Figure 49 Relative increase of LOG(volume) VS Water Level.....	114

Figure 50 Algorithm flow chart	115
Figure 51 Schematic of finite volume reduction algorithm.....	116
Figure 52 Cumulative cost distance is calculated for each cell by summing up the costs of moving from a cell centre to another via least-cost route.....	117
Figure 53 Pseudo code algorithm proposed by Beucher 2011 -	119
Figure 54 Qualitative summary of the influence of impact parameters on flood damage Kreibich et al 2009	120
Figure 55 Map of flow velocity – FEMA formulation	122
Figure 56 Map of flow velocity – FLOODVELMAP formulation	123
Figure 57 MIKE21, FEMA and FLOODVELMAP comparison in transec 1.....	124
Figure 58 MIKE21, FEMA and FLOODVELMAP comparison in transec 3.....	124
Figure 59 Expected damages to grain crops (wheat, rye, barley, corn), oilseed plants (canola), root crops (potatoes and sugar beets) and grass based on flooding occurrence categorized on a monthly basis - Forster et al., 2008.	125
Figure 60 Diagram of infiltration curve and infiltration rate as related to storage in soil.....	126
Figure 61 Ksat map in Cesenatico cm/sec.....	127
Figure 62 Map of flow duration in hours – Storm surge water level 127 cm and depth of water table $z = 3\text{m}$	128
Figure 63 Depth–damage functions and corresponding maximum damage figures for the CORINE land use class “continuous urban fabric” (Jongman et al. 2012).	134
Figure 64 Flow Diagram of the methodology for damage assessment.....	136
Figure 65 Land Use Map – CORINE LAND COVER.....	138
Figure 66 Cesenatico Land Use values UCL euro/mq	138
Figure 67 Cesenatico a_{ij} proportional constant	139
Figure 68 Cesenatico b_{ij} proportional constant	139
Figure 69 Cesenatico Economic Damage Map	140
Figure 70 Observed and fitted mortality function for zone with rapidly rising flood water (Jonkman, 2007).....	141
Figure 71 Population in Cesenatico.....	143
Figure 72 Population density in Cesenatico	143
Figure 73 Cesenatico Residential Building	144
Figure 74 Cesenatico indicator of exposed Population	144
Figure 75 EVI – Flow Duration	147
Figure 76 Risk – Damage Vs Probability Meyer et al. 2007	148
Figure 77 Risk – Trapezoidal Rule Meyer et al. 2007	149

Figure 78 Raster Based Risk Framework - Vanneuille et al. 2003.....	151
Figure 79 MCA Steps wise procedure	155
Figure 80 Risk Reduction Example Meyer et al. 2007	156
Figure 81 Example of criteria used in flood risk MCA Meyer et al. 2007	158
Figure 82 MCA approach fro flood risk maps - Malczewski, 1999	162
Figure 83 Multicriteria Risk Mapping Framework.....	162
Figure 84 Conceptual, methodological and technological frameworks.....	170
Figure 85 Methodological framework of MARASAM DSS.....	172
Figure 86 Methodological framework of MARASAM DSS – detail RASTER BASED MODULE	173
Figure 87 Aerial view of the site.....	188
Figure 88 Hydraulic network with indication of the lamination basins in green colour	188
Figure 89 Mitigation measures: the “Gardens of Cesenatico”: dike behind bathing facilities; sea gate in correspondence of the Canal Harbour.....	190
Figure 90 Total Flooding Risk - Cesenatico	191

Tables

Table 1 CVI Criteria and Weight Bagdanaviciute et al. 2015	31
Table 2 Extreme conditions (surge is the first variable of the joint statistics) in Cesenatico. Storm surge level Z_m , associated significant wave height H_s , sea level rise Z_r . Wave direction $>90^\circ N$	40
Table 3 Selected climate conditions representative of the typical average annual wave climate in Cesenatico. Significant Wave height H_s , mean wave direction Dir , sea level associated to wave height Z_m , frequency of the climate condition in one year f . Calm 0%.....	41
Table 4 Example of GIS applications for natural hazard management Marfai 2003.....	54
Table 5 Advantages and disadvantages of flooding model approach Wicks et al. 2004.....	61
Table 6 Numerical hydrodynamic flood modeling approach - Pender 2006	62
Table 7 Main hydrodynamic flooding models characteristics Nèelz and Pender 2009	66
Table 8 Extreme storm surge (Z_m) and wave height (H_s) scenario	99
Table 9 The predicted extreme water levels at Teignmouth	103
Table 10 Sea-level rise scenarios for flood simulation	103
Table 11 Extreme sea-levels for 16 sea-level rise scenarios at Teignmouth	104
Table 12 Selected sea-level rise scenarios for display in time series	105
Table 13 Different Dimensions of flood damages (Jonkman et al. 2008)	130
Table 14 Damage influencing factor (Merz et al. 2010)	133
Table 15 Land use values UCL (annual € per m^2) in Cesenatico.....	137
Table 16 Parameters for economic consequences in Cesenatico	137
Table 17 Step change categories for EVI	145
Table 18 Review of existing DSS for coastal risk assessment	167

1 Abstract

Coastal flooding poses serious threats to coastal areas around the world, billions of dollars in damage to property and infrastructure, and threatens the lives of millions of people. Therefore, disaster management and risk assessment aims at detecting vulnerability and capacities in order to reduce coastal flood disaster risk. In particular, non-specialized researchers, emergency management personnel, and land use planners require an accurate, inexpensive method to determine and map risk associated with storm surge events and long-term sea level rise associated with climate change.

This study contributes to the spatially evaluation and mapping of social-economic-environmental vulnerability and risk at sub-national scale through the development of appropriate tools and methods successfully embedded in a Web-GIS Decision Support System.

A new set of raster-based models were studied and developed in order to be easily implemented in the Web-GIS framework with the purpose to quickly assess and map flood hazards characteristics, damage and vulnerability in a Multi-criteria approach.

The Web-GIS DSS is developed recurring to open source software and programming language and its main peculiarity is to be available and usable by coastal managers and land use planners without requiring high scientific background in hydraulic engineering.

The effectiveness of the system in the coastal risk assessment is evaluated through its application to a real case study.

2 Objectives

The main goal of this thesis is to develop a Web-GIS Decision Support System able to assist coastal managers in real-time assessing and mapping the risk of floods in the coastal area due to storms and related effects such as storm surge and wave overtopping. The flexibility and the short running time of the evaluation performed by the Web-GIS DSS allow to evaluate costal risk under multiple scenario such as land use change, climate change and subsidence driven.

The peculiarity of the developed system is the possibility to perform quickly simplified but still enough accurate coastal risk assessment evaluation directly from the web without installing locally (desktop) complex software, numerical models etc., and without requiring high scientific knowledge in the field of hydrodynamic modeling and risk assessment. The user, a costal manager or land use planner, can perform risk assessment directly from the browser, available in his PC or mobile device, and quickly sharing results with other colleagues or stakeholders. The GUI of the DSS is user friendly and developed as Wizard tool able to guide step by step the users in the risk analysis.

The SDSS named with acronym **Web-GIS MARASMA: Web Map-based SDSS for costAl Risk AssesSment and Mitigation plAnning**, will be developed with the purpose of assisting a costal manager in assessing and mapping the multicriteria aggregated coastal risk for economy, environment and people under multiple source (climate change and subsidence) and mitigation options scenarios.

The development of Web-GIS MARASMA follows the research activities that were developed within the EU FP7 THESEUS GRANT 244104 (Zanuttigh et al 2014¹) research project for the implementation of a SDSS with similar characteristics.

The system developed and described in this thesis is a conceptual and technological evolution respect the coastal flooding risk assessment DSS available in literature and currently operational .

Conceptually, the design and development of new simple raster-based models for simulating costal flooding effects and assessing the related damages and risks, represents a step forward in terms of the possibility to quickly assess and compare multiple risk scenarios. The new models allows to predict and map floods main characteristics, such as flood extent, water depth, flow velocity and flood duration, without recurring to complex and time

consuming hydrodynamic numerical models. Moreover the implemented Spatial Multicriteria Analysis tools allow to evaluate and map total risk posed by flood on multiple receptors overcoming the limitation of the usually adopted Cost Benefit Analysis (CBA).

From the technological point of view, the MARASMA-DSS consists in a Web based application developed recurring to open source software and programming language. The Web application is considered as an important evolution respect the usually available desktop-based DSS. In fact they can be easily accessible by a wide range of different users without the need to have strong hydraulic or engineering background. Moreover all the implemented function and tools for coastal flooding risk assessment are quickly available without installing any software and models but simply browsing through the dedicated Graphical User Interface (GUI).

To achieve the general objective the following task and milestones are identified and described in the chapters of the thesis:

- 1) Definition and identification of a coastal risk assessment methodology to be implemented in the DSS: The SPRC and THESEUS approach
- 2) Development of new simplified GIS raster-based non hydrodynamic model for assessing and mapping the coastal flooding characteristics:
 - a. Extent of flooding and water depth
 - b. flow velocities in the floodplain
 - c. flood duration time in the floodplain
- 3) Raster based algorithm for mapping vulnerability, consequences and risk related to coastal flooding
- 4) Spatial Multicriteria raster analysis algorithm for aggregating the total risk evaluated for the different criteria: economic activity, social aspects and environmental/ecological habitats.
- 5) Development of a web-GIS DSS recurring exclusively to a open source library and programming language as: python, GDAL, mamba
- 6) Application of Web GIS DSS to Cesenatico Case Study

The Web-GIS MARASMA DSS will be available on-line since June 2015 at the following web address

<http://54.85.129.171/marasma/view/index/>

3 Structure

The thesis is structured in 13 chapters with the following contents:

Chapter 1 Abstract

Chapter 2 Objective

Chapter 3 Structure

Chapter 4 Coastal flooding risk assessment framework

Chapter 5 Modeling coastal flooding: hydrodynamic and simple raster based models

Chapter 6 Raster-based model for mapping Vulnerability, damage

Chapter 7 Raster-based model for mapping risk

Chapter 8 Spatial Multicriteria Assessment

Chapter 9 The Web-GIS DSS MARASMA

Chapter 10 Application to case studies

Chapter 11 Conclusion

Chapter 12 Appendix A – Software Code

Chapter 13 Bibliography

4 Coastal Flooding Risk Assessment

4.1 Introduction

Among the most important and dynamic natural environments worldwide, the approximately 440 000 km long coastal area is one of a small group of systems where several human, animal, vegetal and geomorphologic activities interact (Castillio et al. 2012²) Coastal area with its invaluable landscape and ecological richness make it a very desirable zone to develop social, industrial, economic and recreational infrastructure. As reported in Nicholls 1995³ the coastal area includes a high concentration of the world's biggest cities and produce a considerable proportion of global GDP (Turner et al. 1996⁴)

Costal zones are attacked by different natural phenomena, mostly from hydrometeo sources, such as waves, wind, tides, and rainfall which can reach extraordinary magnitudes during the occurrence of events like hurricanes and tsunamis. The direct consequences of these extreme events are flooding (derived from mea sea level rise or wave overtopping) and beach erosion (as a result of the increase in current velocities and wave energy), a combination of these causes land loss, damage to infrastructure and natural habitats, ecological depletion, economic damage and loss of lives and injuries (Jha et al. 2011⁵, Castillio et al 2012⁶).

Coastal flooding poses serious threats to coastal areas around the world, billions of dollars in damage to property and infrastructure, and threatens the lives of millions of people (Dasgupta et al. 2009⁷; Nicholls 2004⁸; Nicholls et al. 2008⁹, Ward et al 2011¹⁰).

The phenomena mentioned above are commonly grouped under the generic term of "hazards" or "dangers", and the combination of these with the vulnerability of the natural and/or artificial elements found at the coast gives the risk of a specific coastal area. In the last decade, the interest shown in the assessment of risks comes from the evidence of an increase in the magnitude of natural dangers, added to the expansion of human activities in coastal zones which results in a higher level of risk (Vellinga et al 1993¹¹, Balliger et al. 1994¹², Zenger et al. 2002¹³, Duxbury et al. 2007¹⁴). In turn, while not arguing against it nor agreeing on the causes of it, the fact that there is a changing climate represents an increase

in the risks to coastal areas (IPCC 2007¹⁵, El-Raey et al. 1997¹⁶, Nicholls et al 1999¹⁷, Magnan et al 2009¹⁸).

The vulnerability of coastal communities and economic sectors to coastal flooding is expected to increase in the coming decades to century due to both environmental and socioeconomic changes (IPCC 2007¹⁹; Rosenzweig and Solecki 2001²⁰, Ward et al. 2011²¹).

Firstly, global sea-level rise will lead to an increase in flood hazard in coastal regions (IPCC 2007). Secondly, many coastal and deltaic areas suffer from land subsidence due to a combination of glacial-isostatic adjustments (e.g. Peltier 1998²²), natural subsidence in deltaic areas (e.g. Meckel et al. 2007²³), and human activities (e.g. Ericson et al. 2006²⁴; Nicholls et al. 2007, 2008²⁵).

A third environmental factor is the possible increase in peak wind intensities as a result of climate change (IPCC 2007²⁶), which may lead to increased storm surge heights in some regions (Nicholls et al. 2008²⁷).

A storm-surge is an increase in the ocean water level above what is expected from the normal tidal level that can be predicted from astronomical observations and is most often caused by the winds and low pressure of atmospheric storms. Global sea-level rise, as predicted by climate change models, will increase the risk due to storm surges making more coastal areas vulnerable to flooding (Church et al 2001²⁸).

Finally, the vulnerability of coastal cities will also increase due to socioeconomic trends such as the continued demographic and economic expansion in these areas (Bouwer et al. 2007²⁹). The work of Nicholls et al. 2008 made an important contribution to this process, providing a first estimate of the exposure of 136 port cities (with populations above one million) to coastal flooding and examining how this exposure may change under future scenarios of climate change, subsidence, and socioeconomic development. Dasgupta et al. 2009³⁰ assessed the consequences of global sea-level rise for 84 coastal developing countries using a spatially disaggregated global database.

River and Coastal Flood damages and loss of lives are mitigated through flood risk management (Leskens et al. 2014³¹). This includes the design of structural protection measures such as dikes and dams; the planning of a flood resilient environment; and flood disaster management.

4.2 Flood Definitions and Characteristics

Hazardous flooding can be defined as having too much water in the wrong place and/or at the wrong time and as such is a problem generated by humans.

Flood is defined as extremely high flows or levels of rivers, lakes, ponds, reservoirs and any other water bodies, whereby water inundates outside of the water bodies area. Flooding also occurs when the sea level rises extremely or above coastal lands due to tidal sea and sea surges. In many regions and countries floods are the most damaging phenomena that effect to the social and economic of the population (Smith et, al., 1998³²).

Such water sources are conveyed along a variety of pathways (as overland flow, through the subsurface, in rivers or over fluvial and coastal floodplains) to risk receptors where the adverse effects of flooding occur. This source-pathway-receptor model therefore defines the types of floods that hydrologists typically refer to: flash floods, dam break floods, fluvial or river floods, groundwater floods, and coastal floods. Flooding is therefore driven by a variety of physical processes, and it only becomes a problem when either economic damage or threats to human life, well-being, and security occur.

Many factors cause floods. In general, the reasons for increasing flooding in many parts of the world are:

- Climatological events; such as excessively prolonged rainfall cause river floods. Estuarine and coastal floods are usually caused by combination of high tides and the elevated sea level and large waves associated with storm surges, which result from severe cyclonic weather systems.
- Changes in Landuse and increasing population; changeover from rural area to built up area potentially causes floods. Many of the sites that are subject to flooding, such as coastal plains, estuarine areas, lakes shores, and floodplains are also subject to preferential location by industries, commerce and private housing. Urbanization, building density and population density have on effect to drainage capacity and soil infiltration capacity, and well finally increase overland flow on the volume of runoff. Although urban areas occupy less than 3% of the earth's land surface, the effect of urbanization on flood hazards is disproportionately large.
- Land subsidence; land subsidence is the process by which the level of the ground is lowered from its previous elevation. When a tidal wave comes from the sea or water overflow from the river, the lower parts of the ground due to the land subsided will

be inundated. Land subsidence in coastal and alluvial floodplain areas causes extensive flood inundation.

- Climate Change; “a change of climate which is attributed directly or indirectly to human activity that alters the composition of the global atmosphere and which is in addition to natural climate variability observed over comparable time periods” (United Nations General Assembly, 1992³³). The current knowledge on climate modelling suggests that climate change will be a determining factor in intensifying the hydrological cycle (Christensen and Christensen, 2007³⁴; van der Linden and Mitchell, 2009³⁵). This will most likely lead to an increase in the magnitude and frequency of intense precipitation events in many parts of Europe (see, e.g., Frei et al., 2006; Christensen and Christensen, 2007; Fowler and Ekström, 2009³⁶; van der Linden and Mitchell, 2009³⁷; Nikulin et al., 2011³⁸), which may lead to an increase in future flood hazard in those regions (e.g., Dankers and Feyen, 2009³⁹; Whitfield, 2012⁴⁰). Moreover global sea-level rise induced by climate change will lead to an increase in flood hazard in coastal regions (IPCC 2007⁴¹). As reported in Gallien et al. 2011⁴², absolute sea levels are projected to rise 1–1.4m along the California coast in the next century. A statewide impact assessment indicates a wide range of critical infrastructure including 5600 km of roadways, 450 km of railways, 29 wastewater treatment facilities and countless buildings and contents valued at over \$100 billion dollars are at risk (Heberger et al., 2009⁴³), and there have been calls for statewide adaptation planning and action at the local level.

The dangers of floodwaters are associated with a number of different characteristics of the flood. A summary of the characteristics and related hazards (Kingma, 2002⁴⁴) is given below:

- Depth of water; building stability against flotation and foundation failures, flood proofing, and vegetation survival, have different degrees of tolerance to inundation.
- Duration; time of inundation applies to structural safety, the effect of interruption in communication, industrial activity and public services, and the life of plants.
- Velocity; high velocities of flow create high erosive forces and hydrodynamic pressures. This features often result in complete or partial failure of structures by creating instability or destroying foundation support.
- Sediment load; high rates of sedimentation can especially in agricultural areas cause high damage depending on the growing season.
- Rate of rise; the importance of rate of rise of river level and discharge is in its relation to the time available for evacuation and flood fighting arrangements.

- Frequency of occurrence; cumulative frequency of occurrence of the various hazards is therefore a major factor in the development of Landuse.

The nature of floods is, however, two-faced (Few 2003⁴⁵). Despite being perceived as a ‘hazard,’ humans have coevolved and coexisted with floods and floodplains. Floodplains have always been favored sites for human settlement because of their multiple functions in providing drinking water, hydropower, sites for waste disposal, fertile soils for agriculture, navigation waterways, flat terrain for building, ‘waterfront’ view, and leisure activities, and so on (Alexander and Marriott 1999⁴⁶; Bridge 2003⁴⁷). Floods can also bring extensive economic and environmental benefits, although often less acknowledged by people (Blaikie et al. 2003⁴⁸; Smith, 1996; Handmer et al. 1999⁴⁹; Alexander and Marriott 1999; Bridge 2003). These include habitat creation to sustain biodiversity, alluvium fertilization for agriculture, sediment mobilization and redeposition for materials exchange, and surface or subsurface water recharge and nutrient circulation. It is therefore reasonable that many residents of developing countries perceive floods with an ambivalent attitude and prefer ‘living with floods’ to engineering measures that prevent them (Few 2003). In fact, this is increasingly true for all people as the desire for sustainable or green living takes root in the world. Figure 1 summarizes both the hazardous and beneficial features of floods.



Figure 1 Illustration of the ‘two-faced nature’ of floods bringing with them both hazards and benefits (He et al 201450).

4.3 Flood Risk Assessment and EU Legislation

At European level the Water Framework Directive, Floods Directive and other water policies has been emanated and implemented by Member State in order to reduce natural hazard impacts on European territory.

In the EU Floods Directive (see textboxes), the term ‘flood’ means *“the temporary covering by water of land not normally covered by water. This shall include floods from rivers, mountain torrents, Mediterranean ephemeral water courses, and floods from the sea in coastal areas, and may exclude floods from sewerage systems”*.

The EU Floods Directive: some details

Preliminary flood risk assessment (Articles 4 & 5)

It is essential that flood mitigation actions are only taken in areas where potential significant flood risks exist or are reasonably foreseeable in the future. If in a particular river basin, sub-basin or stretch of coastline no potential significant flood risk exists or is reasonably foreseeable in the future, Member States can identify them in the preliminary flood risk assessment. For these river basins and/or sub-basins no further action need be taken.

Flood hazard and flood risk maps (Article 6)

Flood hazards and risks are to be mapped for the river basins and sub-basins with significant potential risk of flooding for three scenarios:

- Floods with a low probability or extreme event scenarios
- Floods with a medium probability (likely return period > 100 years)
- Floods with high probability, where appropriate

The maps may show information on flood extent, depths and velocity of water, and the potential adverse consequences.

Flood risk management plans (Article 7)

Flood risk management plans are to be developed and implemented at river basin or sub-basin level to reduce and manage the flood risk where identified as necessary in the preliminary flood risk assessment. These plans are to focus on the reduction of potential adverse consequences of flooding for human health, the environment, cultural heritage and economic activity, and, if considered appropriate, with non-structural initiatives and/or on the reduction of the likelihood of flooding. They are to address all phases of the flood risk management cycle but focus particularly on:

- Prevention (i.e. preventing damage caused by floods by avoiding construction of houses and industries in present and future flood-prone areas or by adapting future developments to the risk of flooding),
- Protection (i.e. taking measures to reduce the likelihood of floods and/or the impact of floods in a specific location such as restoring flood plains and wetlands) and
- Preparedness (e.g. providing instructions to the public on what to do in the event of flooding).

Boundaries and international basins (Article 8)

Article 8 covers the boundaries of plans and in particular the need for collaboration between Member States for international river basins which extend across several Member States or beyond the boundaries of the Community.

Figure 2 EU Flooding Directive.

In the last few years, the EU developed a set of guidelines to support these regulations, by implementing the risk assessment and mapping processes (EC, 2010⁵¹) and by developing a community framework on disaster prevention and risk evaluation (EC, 2009⁵²).

Furthermore, the Council of European Union developed these guidelines aiming to reduce the national gaps on the risk assessment methodologies and to further develop a national risk management procedure before the end of 2011. Besides, it has to be underlined that all Member States have to make available to Commission, before the end of 2012, any relevant information on natural hazards risk, in order to develop an overview of the major risks that Europe will face in the next future (EC, 2010⁵³). In particular, these guidelines are focused on the reduction of three different types of natural hazards impacts, which are:

- Human impacts, as the number of affected people (the number of deaths, the number of injured or ill people and the number of permanently displaced people);
- Economic and environmental impacts, as the sum of the costs of cure or healthcare, immediate or longer-term emergency measures, restoration of buildings, property damage, cultural heritage, environmental restoration and other associated costs between environment and economy; and
- Political/social impacts, as public outrage or social psychological impact, on public order and safety, or political implications.

The objective of the Council is to minimize these impacts, trying to reduce their potential negative consequences and improving the local preparedness (EC, 2009⁵⁴). Therefore, the EU guideline for national risk assessment and mapping have as main objectives the gradually development in each Member State of a coherent and consistent risk assessment methodology and terminology; to provide the risk management instruments for authorities, policy-makers, and public or private stakeholders involved; to develop a knowledge-based disaster prevention policy and to contribute the raising of public awareness on disaster prevention measures .

Here, the basic steps of the risk assessment process are defined, which have to be followed by all Member States:

1. Risk identification, which is the process of finding, recognizing and describing risks. It is a screening exercise and serves as a preliminary step for the subsequent risk analysis stage.
2. Risk analysis, which is the process to comprehend the nature of risk and to determine quantitatively the level of risk. Risk is defined as a function of probability, exposure and vulnerability: the risk analysis is focused on these subjects. First it should be estimated the probability that an event or hazard happen, then must be quantified the impact. The level of risk is determined differently for each type of impact: by number of affected people (human impact), by money estimation

(economic - environmental impact in euro) or using risk matrix (political - social impact).

3. Risk evaluation, which is the process of comparing the results of risk analysis with risk criteria to determine whether the risk and/or its magnitude are acceptable or tolerable.

The developed Web-MARSAMA DSS represents an useful tool for coastal managers in order to pursue the EU legislation targets with particular emphasis in mapping coastal flooding risk.

4.4 Definition of Risk in Flood Hazard

In the specialized literature the term “risk” has been analyzed from very diverse points of view; sometimes its definition is stated by the needs of particular decision-makers, which has led to several meanings of risk attending different safety, economic, environmental, and social issues. Some examples of these are:

- Risk involves an “exposure to a chance injury or loss” (Morgan et al. 2003⁵⁵).
- Expected losses (of lives, persons injured, property damaged, and economic activity disrupted), due to a particular hazard, for a given area and reference period. Based on mathematical calculations, risk is the product of hazard and vulnerability (UN 1992⁵⁶).
- Risk is a compound measure combining the probability and magnitude of an adverse effect (Adams 2003⁵⁷).
- risk = impact of hazard X elements at risk X vulnerability of elements at risk (Kelman 2003⁵⁸).
- risk = hazard X vulnerability X value of the threatened area/preparedness (Cruz-Reyna 2003⁵⁹).
- Risk is the actual exposure of something of human value to a hazard, and is often regarded as the combination of probability and loss (Smith 2003⁶⁰).
- risk = probability X consequence (Gouldby et al. 2005⁶¹, Helm 2003⁶², Safecoast 2008⁶³, Bellomo 2008⁶⁴)
- Risk is a combination of the chance of a particular event, with the impact that the event would cause if it occurred. Risk therefore has two components: the chance (or probability) of an event occurring and the impact (or consequence) associated with that event (Wallingford 2005⁶⁵).

As reported in Balica et al 2013⁶⁶, The term “risk” in relation to flood hazards was introduced by Knight (1921⁶⁷), and is used in diverse different contexts and topics showing how adaptive any definition can be (Sayers et al., 2011⁶⁸). In the area of natural hazard studies,

many definitions can be found. It is clear that the many definitions related to risk (Slovic, 1987⁶⁹; Alexander, 1993⁷⁰; IPCC, 2001⁷¹; Plate Erich, 2002⁷²; Barredo et al., 2007⁷³) are inter-related and interchangeable and each of them has certain advantages in different applications (e.g. Sayers et al., 2011⁷⁴; Merz et al., 2007⁷⁵).

This study will consider flood risk as the product of two components, the probability of a flood event and of the potential adverse consequences to human health, the environment and economic activity associated with a flood event (FLOODSITE 2009⁷⁶):

Risk = Probability X Consequence

This concept of flood risk is strictly related to the probability that a high flow event of a given magnitude occurs, which results in consequences which span environmental, economic and social losses caused by that event.

Practically, risk is made up of four major building blocks: the probability of flooding, the exposure of the elements-at-risk to a flood with certain characteristics, the value of these elements-at-risk, and the vulnerability of these elements-at-risk (ADAPT 2008⁷⁷)

The EU Flood European Floods Directive 2007/60/EC (EC, 2007) and UNEP (2004) uses this definition of risk where “flood risk” means the combination of the probability of a flood event and of the potential adverse consequences for human health, the environment, cultural heritage and economic activity associated with a flood event.

“The probability of the occurrence of potentially damaging flood events is called flood hazard” (Schanze, 2006⁷⁸). Potentially damaging means that there are elements exposed to floods which may be harmed. Flood hazards include events with diverse characteristics, e.g. a structure located in the floodplain can be endangered by a 20-year flood and a water level of 0.5 m and by 50-year flood and a water level of 1.2 m. Heavy rainfall, coastal or fluvial waves, or storm surges represent the source of flood hazard. Generally these elements are characterised by the probability of flood event with a certain magnitude and other characteristics.

Another formalization of risk related to natural hazard and flooding is called as “Risk Triangle” (Crichton, 1999, 2007⁷⁹) or the interaction of hazard, exposure, and vulnerability:

$$R = f(H, V, E)$$

Climate hazard, or ‘source’, in the risk triangle framework relates to extreme weather events, such as intense rainfall causing surface water flooding. Vulnerability refers to the intrinsic characteristics of the hazards’ receptors (which can be people, infrastructure, economic activities, or other), and defines the extent to which these receptors are

susceptible to harm from, or unable to cope with, hazards. The term ‘exposure’ can be defined as the nature and degree to which a receptor (the urban communities in this study) is exposed to climate or weather hazards (Parry, et al. 2007⁸⁰). Thus, exposure, closely related to the concept of a flooding ‘pathway’ (DEFRA & EA, 2006⁸¹), refers to the geographical location of a receptor, as well as the characteristics of the specific location that can exacerbate or reduce the magnitude of a hazard’s impact. According to this framework, for risks to be realised, the receptors and hazard need to coincide spatially. Further, the magnitude of risk depends on the level of vulnerability of the receptors, the nature of the hazard, and the physical characteristics of the environment defining the exposure (Lindley et al., 2006⁸²).

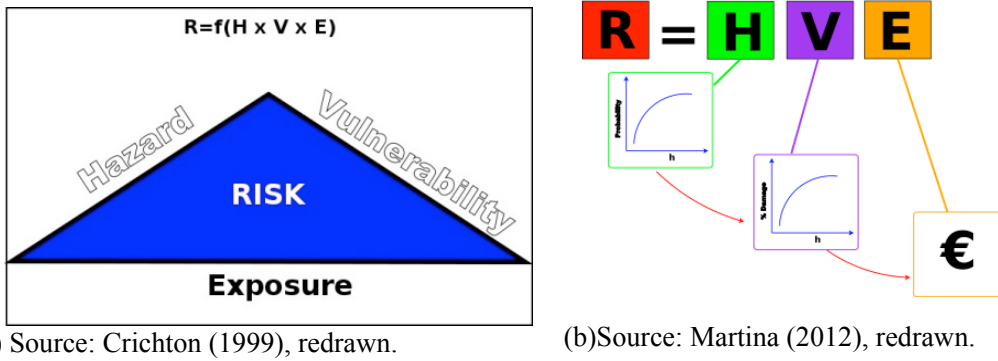


Figure 3 Risk Triange Paradigm.

Considering a specific return period, T, the risk can be expressed as (Castillio et al. 2012):

$$R = CV_T P_T \quad \text{Eq. 1}$$

where VT is the vulnerability related to the return period, PT the probability of occurrence of a certain event in the return period, and C is the value of the exposed goods. If several events are to be considered, the risk is:

$$R_j = \sum_{i=1}^n C_j P(i) \cdot V_j(Y_i) \quad \text{Eq. 2}$$

where the subindex i stands for each return period considered and j refers to each system of interest; P(i) and $V_i(Y_i)$ are the hazard and vulnerability functions, respectively.

4.5 Vulnerability Definition

Vulnerability is the degree of fragility of a (natural or socio-economic) community or a (natural socio- economic) system towards natural hazards. It is a set of conditions and processes resulting from physical, social, economical and environmental factors, which increase the susceptibility of the impact and the consequences of natural hazards. Vulnerability is determined by the potential of a natural hazard, the resulting risk and the potential to react to and/or to withstand it, i.e. its adaptability, adaptive capacity and/or coping capacity.

The most authoritative and widely quoted definition of vulnerability in the context of climate change is from the Fourth Assessment Report (2007): *“Vulnerability is the degree to which a system is susceptible to, and unable to cope with, adverse effects of climate change, including climate variability and extremes. Vulnerability is a function of the character, magnitude, and rate of climate change and variation to which a system is exposed, its sensitivity, and its adaptive capacity”* (IPCC 2007⁸³). The most challenging aspect of the vulnerability definition provided by the IPCC is the concept of adaptive capacity. This is because to make adjustments or changes to current action (adaptation) many social, political, economic, technological and other factors need to be considered. In general terms, without adaptation, a rise in sea-level would inundate and displace wetlands and lowlands, erode shorelines, exacerbate coastal storm flooding, increase the salinity of estuaries, threaten freshwater aquifers, and otherwise impact water quality. The impacts would vary from place to place and would depend on coastal type and relative topography.

While the notion of vulnerability is frequently used within catastrophe research, researchers’ notion of vulnerability has changed several times lately and consequently there have been several attempts to define and capture the meaning of the term. It is now commonly understood that “vulnerability is the root cause of disasters” (Lewis, 1999) and “vulnerability is the risk context” (Gabor and Griffith, 1980⁸⁴). Many authors discuss, define and add detail to this general definition. Some of them give a definition of vulnerability to certain hazards like climate change (IPCC, 2001⁸⁵), environmental hazards Klein et al., 1999⁸⁶; ISDR, 2004⁸⁷), or the definition of vulnerability to floods.

The vulnerability concept is central to the definition of a flooding-related disaster, and acts as the conceptual bridge between changes in the external environment and the responses of

the affected system. The nature of vulnerability only matters to the extent to which it produces insights that will help us to adapt to, or mitigate, external changes. Vulnerability concerns the susceptibility to substantial damage, disruption and casualties as a result of a hazardous event. The recent approach in terms of “coastal vulnerability” studies (since the 90s) is the main tool used nowadays to help managers to evaluate impacts of natural hazards on coastal zones.

This study will use the following definition of vulnerability specifically related to flooding:

The extent to which a system is susceptible to floods due to exposure, a perturbation, in conjunction with its ability (or inability) to cope, recover, or basically adapt.

We represent vulnerability with the following equation:

$$V = f(S, E, R)$$

Eq. 3

where V = vulnerability S = susceptibility E = exposure R = resilience V depends on many factors including landuse, building design and construction concepts, planning paradigm, forecast skill, effective communication of an impending hazard, and willingness and ability to take responsive actions. Naturally, these factors increase flood risk and also affect vulnerability. Increased unmitigated risk will thus result in high or very high vulnerability, especially under existing paradigms that emphasize increased ‘active’ HI (higher dikes, better early warning, etc.). Indirect intervention including smart and sustainable urban design or a paradigm shift from ‘fighting floods’ to ‘living with floods’ can induce passive resistance to flooding and thus reduce vulnerability. Creating multipurpose infrastructure or waterscapes (Amphibious city landscapes) through amphibious urban design appears to be one of the more promising ways forward, given the current state of affairs.

4.6 Flood Risk Assessment

The available literature dealing with analysis and evaluation of risks in coastal zones is quite wide; it includes laws and regulations, guidelines and manuals, research projects and studies published at coastal conferences and workshops. Nevertheless, very few studies really present feasible and effective methodologies for coastal risk assessment. Some of these

studies can be found in Jha et al.⁸⁸, Papathoma and Dominey-Howes⁸⁹, DEFRA/EA⁹⁰, Werritty et al.⁹¹, Kazmierczak and Handley⁹², Narayan et al.⁹³, FLOODsite⁹⁴, THESEUS⁹⁵.

Although risk analysis and risk assessment terms are often confused, some sources separate them. FLOODsite⁹⁶ defines risk analysis as a methodology to determine risk by combining probabilities and consequences; while risk assessment comprises understanding, evaluating, and interpreting the perceptions of risk and societal tolerances of it to inform decisions and actions in the risk management process. The objective of risk assessment methodologies is to come up with an estimate of the probable future risk and to provide an insight into the distribution of risk and its related causes.

Roughly speaking the purpose of flood risk assessment pursued in this thesis is to identify and mapping areas where risk is unacceptably high and where mitigation actions would be necessary.

Flood Hazard/Risk Mapping consists in displaying the spatial distribution of the flood threat, the intensity of flood situation and their associated exceedance probability for either a single or several flood scenarios.

Risk mitigation means to propose, evaluate and select measures to alleviate risks in these areas. Currently, the evaluation of alternative measures is mostly done by means of cost-benefit analysis (CBA) or Multi Criteria Analysis(MCA). In the first approach the costs of a certain measure are compared with their benefits in terms of risk reduction. In theory, this procedure leads to an efficient allocation of funds and finally to an optimized protection against flooding. The MCA is usually considered as a decision making tool more than a risk assessment approach; however, it has been included as a methodology to assess risk by using the same information as risk analysis. The MCA methodology is based on economic, social, and environmental criteria, which are joined together into a single risk estimation.

Different methods to assess or determine hazard, risk and vulnerability to flooding have evolved through ongoing research and practice in recent decades (Xia et al., 2011⁹⁷; Hartanto et al., 2011⁹⁸; Gichamo et al., 2012⁹⁹). Two distinct method types can be distinguished:

- Deterministic modelling or quantitative approaches which use physically based modelling approaches to estimate flood hazard/probability of particular event, coupled with damage assessment models which estimate economic consequence to

provide an assessment of flood risk in an area and to evaluate multiple mitigation options in a CBA or MCA framework.

- Parametric or qualitative approaches which aim to use readily available data of information to build a picture of the vulnerability of an area. Parametric-based approaches are applied to a vast diversity of systems: Environmental Vulnerability Index (EVI), Pratt et al., 2004¹⁰⁰; The Composite Vulnerability Index for Small Island States (CVISIS), Briguglio, 2003¹⁰¹; Global Risk and Vulnerability Index (GRVI), Peduzzi et al., 2001¹⁰²; Climate Vulnerability Index (CVI), Sullivan and Meigh, 2003¹⁰³, etc.

The risk-based scheme evaluated in this thesis and implemented in the Web-GIS DSS refers to the deterministic approach.

As reported in the FLOODsite EU FP7 Project¹⁰⁴ practice of flood risk assessment and management is subjected to the following deficits:

- Defining flood risk by the formula $RISK = Probability \times Consequence$ (Gouldby et al 2005) comprehends all kinds of consequences of flooding. Nevertheless, current practice of risk assessment and cost-benefit analysis still focuses on damages that can be easily measured in monetary terms. More precisely, risk analysis mainly deals with damage to assets, while social and environmental consequences are often neglected. In consequence, flood risk management often manages only certain parts of flood risk. On that basis, an optimised allocation and design of flood mitigation measures cannot be ensured and is the more unlikely, the more social and environmental risks are spatially separated from economic risks.
- The spatial distribution of risks as well as of the benefits of flood mitigation measures is rarely considered. E.g. the evaluation and selection of appropriate mitigation measures is mostly based on their overall net benefit. Therefore, it is often not considered which areas benefit most from a measure and which areas do not. This may lead to spatial disparities of flood risk which are not desirable or acceptable.

The methodological framework discussed, proposed and implemented in the Web-GIS DSS developed in this thesis tries to define solutions for these two deficits.

The first point is addressed recurring to multicriteria analysis (MCA), it represents an appropriate method of incorporating all relevant types of consequences without measuring

them on one monetary scale. It provides an alternative to the complex monetary evaluation and internalisation of intangible consequences in a cost-benefit analysis.

The second point can be considered by mapping risks and risk reducing effects, respectively. GIS with their ability to handle spatial data are an appropriate tool for processing spatial data on flood risk. In our framework we will therefore describe and test approaches which combine MCA with GIS.

In conclusion the purpose is to develop a Web-GIS SDSS able to quantify and spatially represent risk related to coastal flooding for multiple receptors type (economic activities, people and social aspect, environment) with the following characteristics:

- Flood risk mapping is an essential element of flood risk management and risk communication. In many countries risk mapping is regulated by law. The Flood Directive of the European Union, enacted in November 2007, requires member states to create both flood hazard and flood risk maps (European Commission, 2007). Although flood mapping is frequently limited to mapping the flood hazard, there is a lively discussion on flood risk mapping, including the potentially adverse effects on asset values, people and the environment.
- Optimal decisions on flood mitigation measures: safety against floods requires resources, among others large amounts of tax money. It should therefore be secured that these resources are well used economically. This implies that the current flood risk has to be estimated, the potential risk reduction options have to be determined, and benefits and costs of different options have to be quantified and compared. For these steps towards cost-effective risk management, damage assessments are an essential ingredient.

To define the risk related to flooding, some assumptions have to be made. The inundations taken into account in this research are coastal inundations due to overflow (storm surge) and dike breaching or overtopping, which is conceptually taken into account. For example, flooding from sewer systems or channel and river network is not taken into account in this thesis. The proposed methodological approach for coastal risk assessment implemented in a Web-GIS DSS service considers two scale of flooding hazard: the first related to long-term events the second to extreme or episodic events. Cost Benefit Analysis

This approach has been utilized for more than 50 years to quantify in monetary terms as many of the costs and benefits of a feasible proposal, including items for which the market does not provide a satisfactory measure of economic value. CBA examines whether the total benefits of a risk reducing activity, evaluated in terms of money, exceed the costs involved in

utilizing resources. It has undergone continuous refinement and expansion due to the increasing importance of social and environmental concerns in development projects in recent years, by applying monetary values to social and environmental issues.

This approach is unable to take into account the factors and issues that cannot be expressed in monetary terms, such as moral issues, distributional equity, etc. As a result, this kind of risk management often manages only certain parts of risk. Moreover, the spatial distribution of risks as well as the benefits of risk mitigation measures is rarely considered, and the evaluation and selection of appropriate mitigation measures is mostly based on their overall net benefit.

4.6.1 Multi Criteria Analysis

The MCA is usually considered as a decision making tool more than a risk assessment approach; however, it has been included as a methodology to assess risk by using the same information as risk analysis.

The MCA methodology is based on economic, social, and environmental criteria, which are joined together into a single risk estimation. Each criterion is weighted to allow the representation of the relative importance of each risk type. The possibility of this approach for evaluating monetary and non-monetary risk in an integrated way, as well as showing their spatial distribution provides a better supported technique for the comparison of project alternatives. There are various approaches that suggest multi-criteria procedures to map, manage and assess the economic, social and ecological dimension of risk in an integrated manner such as: Tkach and Simonovic 1997¹⁰⁵, Bana et al. 2004¹⁰⁶, Brouwer and van Ek 2004¹⁰⁷, RPA 2004¹⁰⁸, and FLOODsite¹⁰⁹.

Some decision frameworks combining cost-benefit and multi-criteria have been developed; monetary issues are often given more importance but an MCA-based framework is used to involve non-monetary items. This combined methodology has been used for guiding decisions about adaptation measures to climate change induced flooding, as part of the ADAPT Project work.

The multi-criteria approach is often supported on geographical information systems (GISs) technology to evaluate and map damage and risks (Bana et al. 2004¹¹⁰).

4.6.2 A Qualitative Approach: Coastal Vulnerability Index (CVI)

A different, more qualitative, approach for the assessment of shoreline vulnerability due to effects of climate change consists in developing a version of the Coastal Vulnerability Index (CVI). The aim is to make use of the physical characteristic of the coastal system to at least qualitatively classify the potential impacts of climate change on different coastal sections Gornitz and White, 1992¹¹¹ and Gornitz et al., 1994¹¹²; Pendleton et al., 2004¹¹³ developed a Coastal Vulnerability Index (CVI) integrating multi-criteria evaluation to identify areas that are at risk of erosion and/or permanent or temporary extreme climatic events (storms, floods, etc). Grid cells and/or line segments with low reliefs, erodible substrates, histories of subsidence and shoreline retreat, and high wave and tide energies, will have high index values indicating high vulnerability.

The CVI is based on a complex set of coastal factors which identify the risk from a specific coastal hazard. The definition of the vulnerability indices can be determined as a function of coastal erosion (Hedge et al. 2007¹¹⁴), a variation of sea level (Gornitz et al. 1997¹¹⁵), or an ecological and cultural context (Dal Cin 1994¹¹⁶).

The workflow scheme used for the multi-criteria coastal vulnerability assessment (Figure 4) consists of the following major steps (Bagdanaviciute et al. 2015¹¹⁷) :

- (1) Identification of criteria representing geological features and physical processes of the coastal environment which influence coastal vulnerability.
- (2) Quantification of criteria according to the vulnerability scale .
- (3) Reclassification of initial data in order to compile a vulnerability map of each criterion.
- (4) Application of two scenarios (I and II).
- (5) Application of an analytic hierarchy process (AHP) for the assessment of the relative importance (weights) of the criteria.
- (6) Calculation of the coastal vulnerability index (CVI).
- (7) Compilation of vulnerability maps.

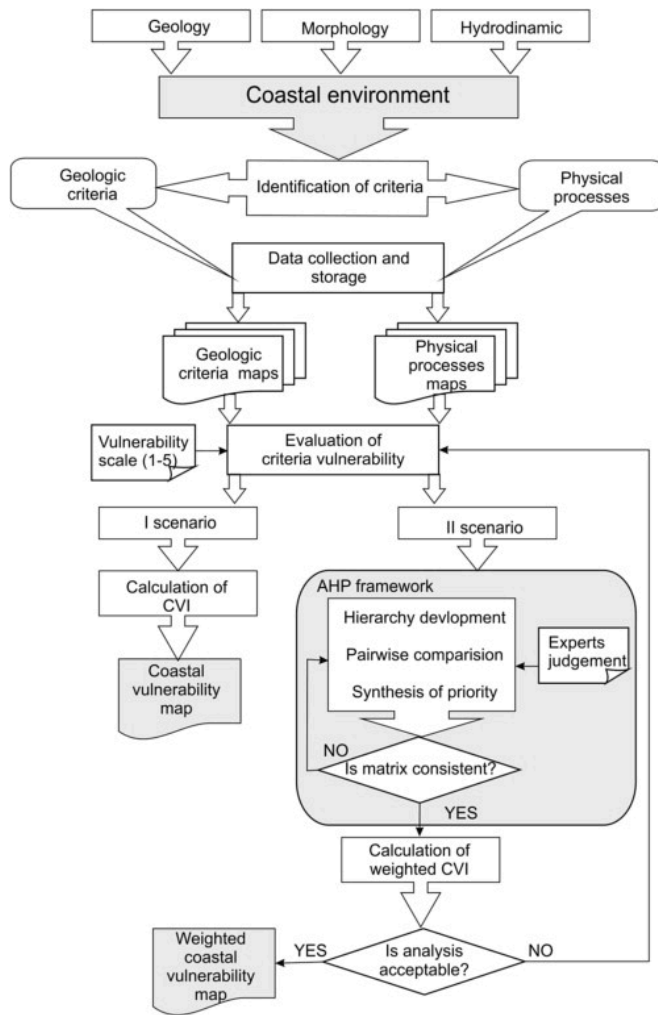


Figure 4 CVI Workflow Bagdanaviciute et al. 2015¹¹⁸

Table 2
Vulnerability ranking of the criteria.

Criteria	Vulnerability ranking				
	Very low 1	Low 2	Moderate 3	High 4	Very high 5
Geologic (a) Historical shoreline change rate (m/yr)	>1	0.3–1	–0.3–0.3	–0.3 –1	<–1.0
(b) Beach width (m)	>60	40–60	30–40	20 –30	<20
(c) Beach height (m)	>4	3–4	2–3	1–2	<1
(d) Beach sediments	Sand/ pebble/ till/ boulders	Sand/ gravel/ pebble	Sand/gravelly sand/sand with gravel	Sand	Sand/ peat/ sapropel
(e) Underwater slope (tan α)	>0.0005	0.0005 –0.001	0.001–0.008 0.001–0.005	0.008 –0.01 0.005 –0.01	>0.01
(f) Sand bars (underwater slope)	>4	3	2	1	0
Physical process	(g) Mean		significant wave height (m)	<0.5	0.5–0.6
	0.6–0.7	0.7–0.8	>0.8		

Table 3
Weighting of the criteria.

Criteria	Expert 1		Expert 2		Combined	
	Weight	Rank	Weight	Rank	Weight	Rank
Historical shoreline change rate	0.242	2	0.310	1	0.277	2
Underwater slope	0.380	6	0.068	5	0.052	5
Beach width	0.130	4	0.098	4	0.112	4
Beach height	0.059	5	0.038	7	0.046	6
Sand bars	0.334	1	0.254	2	0.297	1
Beach sediments	0.028	7	0.048	6	0.036	7
Mean significant wave height	0.170	3	0.185	3	0.179	3
Consistency ratio	0.09		0.04		0.04	

Table 1 CVI Criteria and Weight Bagdanaviciute et al. 2015¹¹⁹

4.7 Coastal Risk Assessment Framework: The SPRC approach

Extreme events in the past decade, such as Hurricane Sandy (Schultz, 2013¹²⁰) and Hurricane Katrina (Seed et al., 2008) in the US and Storm Xynthia in France (Kolen et al., 2010¹²¹), have demonstrated that it is impossible to completely control or prevent damage due to a flood event. Coastal floodplains world-wide are focal points for human settlement (McGranahan et al., 2007¹²²; Small and Nicholls, 2003¹²³) and often span large areas crossing administrative and geo-political boundaries (de Moel et al., 2009¹²⁴; EXCIMAP, 2007). Several large-scale flood risk studies recognise that for effective strategic flood risk management, coastal floodplains should be analysed as regions of interacting physical, socio-economic and ecological systems (Hanson and Nicholls, 2012¹²⁵; Mokrech et al., 2011¹²⁶; Safecoast, 2008¹²⁷). Flood risk studies also recognise the need for expanding the spatial and temporal scales across which floodplains are studied (Dawson et al., 2009¹²⁸). Strategic flood risk management therefore requires risk appraisal models that are rapid as well as comprehensive.

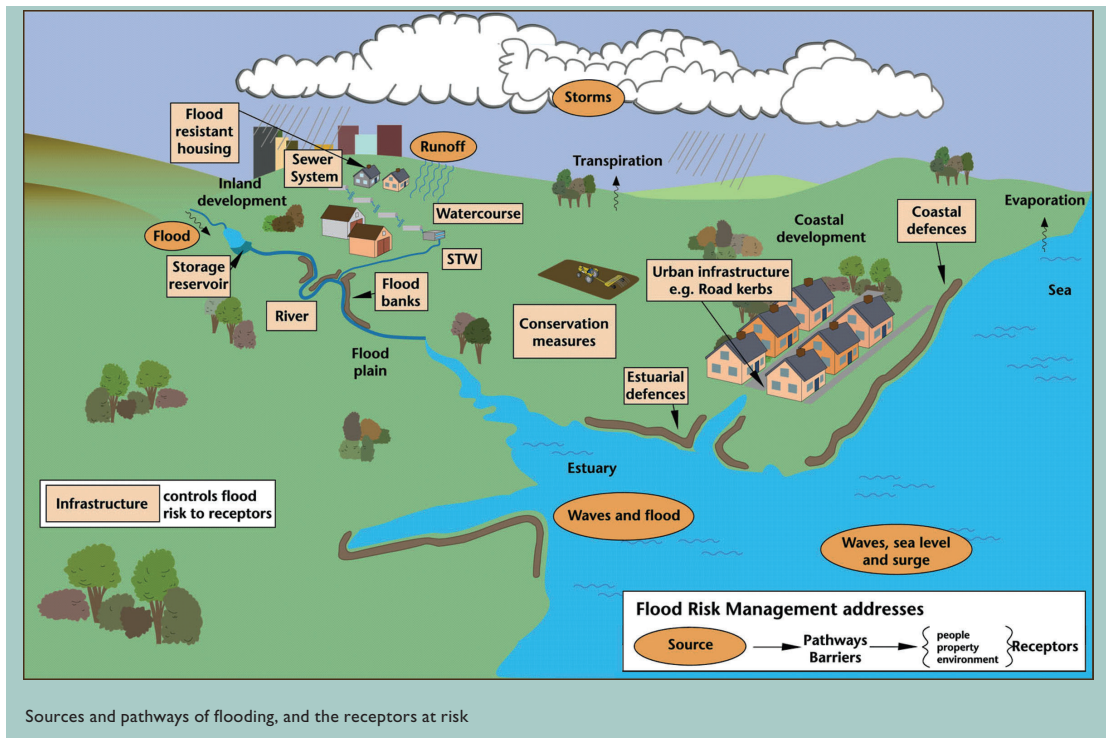


Figure 5 SPRC paradigm FLOODsite EU FP7 Project¹²⁹

The conceptual model for coastal flooding risk assessment proposed for the Web-GIS DSS developed in this thesis is based on Source-Pathway-Receptor-Consequence (SPRC) model

that is widely used in the fields of pollution and natural hazard risk assessment. The SPRC was initially applied in environmental pollution (Holdgate, 1979¹³⁰) to describe the flow of contaminants from a source (an ocean or river) through a pathway (a coastal protection structure or a beach) to a receptor (flood plain/ urban areas / ecosystems, etc.)

The SPRC model is a simple conceptual model for representing flood systems and processes that lead to particular flooding consequences. Effectively, the SPRC represents how the Sources (in this case, waves, tide, storm surge, mean sea level, river discharge, run-off) through the Pathways (including, coastal defence units) affect the Receptors (buildings, infrastructure, habitats, etc.) generating economic, social and environmental Consequences. Scenarios of change will modify the consequences of flooding and, given adverse trends such as sea-level rise and increasing coastal development, will increase them. Mitigation options from a wide menu of engineering, ecological and social options can offset this increase in Consequences, and keep risk at a socially-acceptable level.

In literature risk is recognised as a main concept in coastal flood protection (Evans et al., 2006¹³¹; Sayers et al., 2002¹³²). Coastal flood risk studies conceptualise the coastal floodplain in terms of two components: 1) flood defences that prevent or reduce the ingress of flood water; and 2) the floodplain behind the defences comprising all features considered to be at risk from flooding (Bakewell and Luff, 2008¹³³; FLOODSite Consortium, 2008¹³⁴; Naulin et al., 2012¹³⁵).

Large-scale integrated flood risk assessments use conceptual frameworks to describe the relationship of the coastal floodplain system to external drivers and pressures (e.g., DEFRA 2004¹³⁶, Evans et al., 2004¹³⁷; Sayers et al. 2005¹³⁸, FLOODSite Consortium, 2009¹³⁹; Safecoast, 2008¹⁴⁰; North Carolina Division of Emergency Management, 2009¹⁴¹; Narayan et al 2011¹⁴², Naulin et al., 2012).

In all of these studies, the state of the coastal floodplain is described using a well-established concept — the Source–Pathway–Receptor–Consequence (SPRC) conceptual model (Gouldby and Samuels, 2005¹⁴³). The SPRC model describes the floodplain in terms of the process of flood risk propagation — the initiation of a hazard at the shoreline, and its propagation through a flood pathway to a receptor with particular (negative) consequences (Figure 6)

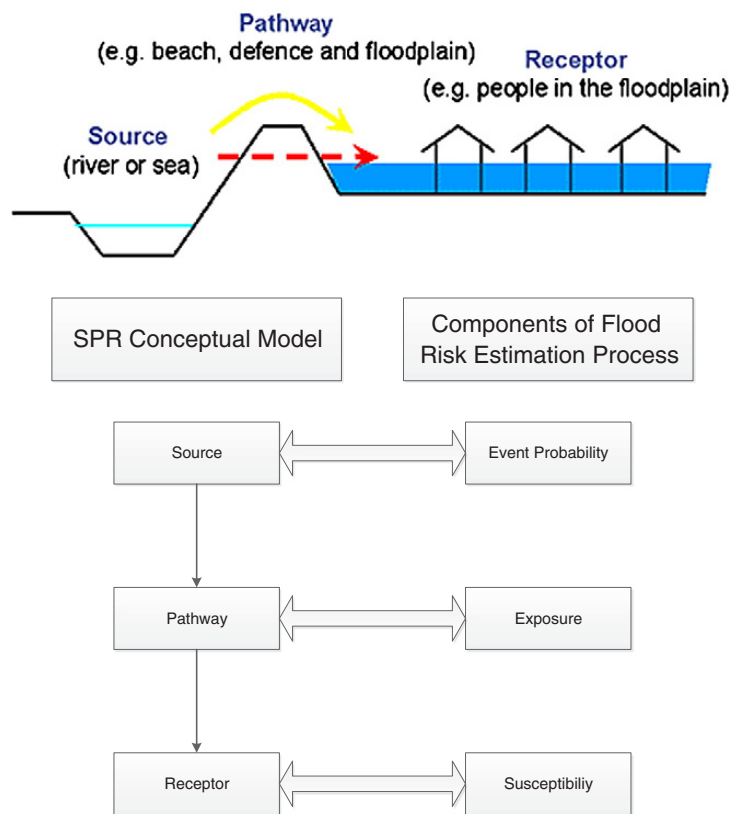


Figure 6 SPRC FLOODsite EU FP7 Project¹⁴⁴

The factor grouping of the SPRC model is defined as follows:

Sources refer to marine forcings inducing the flood event. In this work we have selected two flood risk sources, differentiated primarily by the scales of time and space that affect the coastal zone. The first one is associated to long-term processes which are given by RSLR and, the second one is associated to episodic/extreme events which are given by storm impacts.

Pathway (P): describes the main variables and processes controlling the coastal risk in its way from the source to the receptor. It includes natural and artificial elements such as morphologic processes of flooding, and those related to the behavior and failure mechanisms of defense (overtopping, overflow, breaching, or flood plain inundation).

Receptor (R): are all physical entities exposed to the threat, such as people, buildings, possessions, property, infrastructure, or environment. The characterization of the Receptor refers to the estimation of the flooding effects in the territory, the flood extent and valuation of vulnerability and damage.

Consequence (C): represents all the physical, social, institutional, economic, and environmental adverse effects derived from the occurrence of any hazard. To evaluate the full consequences, direct and indirect losses, social and ecologic resilience as well as acceptance and perception of risk should be considered.

Sources, pathways, receptors, and consequences are spatially and temporally overlaid, thus the division between sources, pathways, and receptors is not strict and depends upon the scale and context of the research (Hall et al. 2003¹⁴⁵).

One reason for the popularity of the SPRC as a conceptual model for floodplain state descriptions is that it readily translates to the components of risk estimation as reported in the next Figure.

The SPRC uses different models at each stage of the process

- (i) Source: storm surge, overtopping, rainfall-runoff, wave climate models.
- (ii) Pathway: coastal hydrodynamic hydrological and hydraulic models, failure models, morphological models.
- (iii) Receptor: exposure data models.
- (iv) Consequence: damage and other vulnerability models.

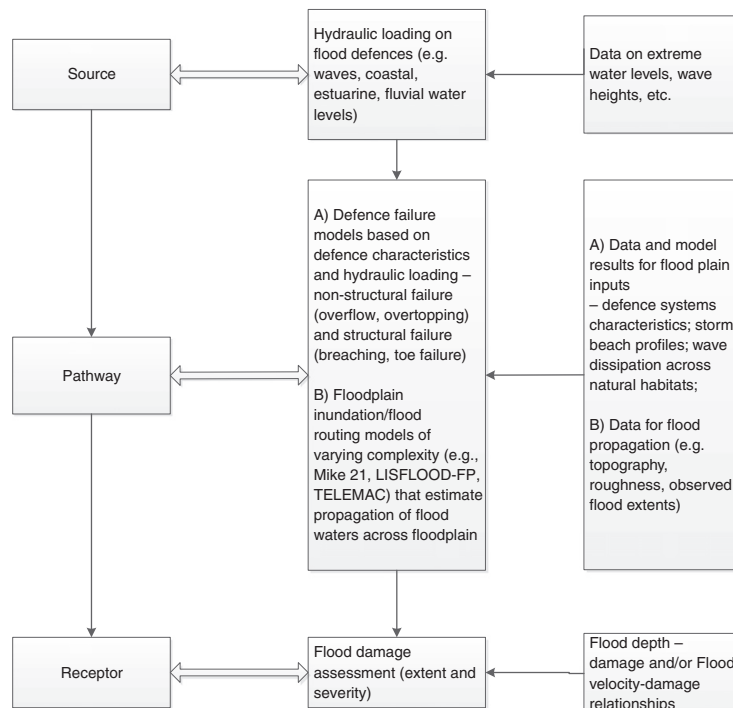


Figure 7 Models involved in SPRC

With the aim of implementing a Web-GIS DSS for coastal flooding risk assessment, the

general methodology of Source-Pathway-Receptor (SPR) developed within the FLOODsite and THESEUS project was used as starting point and adapted to the specific characteristics of this work.

4.7.1 SOURCE CHARACTERIZATION

The main input for calculating costal flood hazard and risk maps under the SPRC framework is a water level associated to a give probability. Following the Directive 2007/60/EC of the European Parliament and of the Council of 23 October 2007 on the Assessment and Management of Flood Risks, flood hazard maps shall cover the geographical areas which could be flooded according to the following scenarios:

- (a) floods with a low probability, or extreme event scenarios;
- (b) floods with a medium probability (likely return period ≥ 100 years);
- (c) floods with a high probability, where appropriate.

With independence of the probability chosen to define the water level to be used as the source for the flooding analysis, the water level is composed by different components associated to different agents varying at different time scales. Figure 8 schematizes the three main components contributing to the total water level: (i) astronomical tide; (ii) storm surge and (iii) run-up.

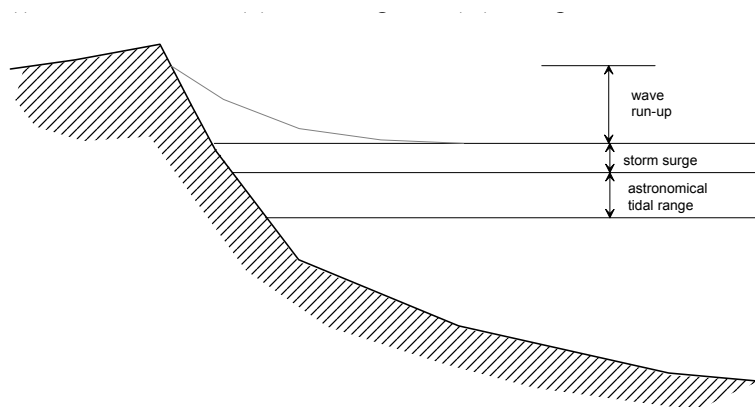


Figure 8 total water level components

The main problem associated to the right estimation of the water level associated to a given probability is to assess the contribution of each component. There are two main options to estimate such level:

- to directly estimate it from existing time series of water levels;

- to estimate it by analysing the integrated contribution of each component.

Extreme distributions to be used in fitting water levels can be seen in Sobey (2005¹⁴⁶) and Pirazzoli and Tomasin (2007)¹⁴⁷ among others (see also Sánchez-Arcilla 2007¹⁴⁸). The main problem of this methodology is that water level records usually do not include wave-induced contributions. Thus, its use should only quantify the water level associated to astronomical and meteorological tides.

In the second case, the contribution of each component has to be estimated and the joint probability has to be calculated. Here two main approaches do exist: (i) response and (ii) event approaches (see e.g. Fema, 2005¹⁴⁹).

The event approach is deterministic, it uses one or more combinations of water level and wave conditions (events) associated to a given probability and it computes the resulting flood level (response). The main problem is that, in many cases, a combination of events with a given probability will not generally result in a response of a different probability. Moreover, the flood associated to the given probability could be produced by many combinations of conditions. On the other hand, the response approach is that in which the water level of interest (associated to a given probability or return period) is directly calculated from a probability distribution of total water levels.

In the DB embedded in the Web-GIS DSS, yearly maximum wave and storm surge conditions were computed and uploaded for an historical period, characterized by significant wave height, peak off-shore wave steepness, wave direction and water elevation (sum of storm surge and tide), were processed to derive the climate statistics describing the yearly probability of occurrence of each storm at present.

In particular for the Cesenatico case study, the Surge levels and wave height projections for the next 100 years are based on different computer simulations of the atmosphere and ocean for a range of emission scenarios. The projections of climates and sea-level rises changes are made using computer models of the Earth's climate. These Global Climate Models also known as 'Global Circulation Models' or 'Atmosphere–Ocean Global Circulation Models' (AOGCMs), simulate the effect on the atmosphere and oceans of different possible future scenarios of greenhouse gas emissions.

The meteorological data are computed as a regional downscaling with the SGA-CLM (COSMO- CLM). SGA-CLM set of simulations, provided by the DWD, are initialized and forced

6 hourly by global coupled model ECHAM5-MPIOM (Max Planck Institute Ocean Model) and provide results with a spatial resolution of 18 km (Keuler et al., 2009¹⁵⁰).

The model used for the hydrodynamic simulation is SHYFEM (Shallow water Hydrodynamic Finite Element Model). SHYFEM is a multidisciplinary numerical modeling tool, structured in a hydrodynamic module coupled with a surface wave module, a sediment transport module and a bed load module. The 3D SHYFEM Model solves the primitive equations and applies the Boussinesq and hydrostatic approximations. It is based on the finite element approach; More info about the SHYFEM Model can be found in Umgiesser et al. (2004)¹⁵¹ and Bellafiore et al. (2008)¹⁵².

The hydrodynamic model is coupled with a wave model, WWMII (Wind Wave Model). WWMII is a finite element 3rd generation spectral wave model. WWMII solves the Wave Action Equation, describing growth, decay, advection and refraction of wind waves due to depths and currents (computed by the hydrodynamic model). WWMII is a new version of the WWM model (Hsu et al., 2005) based on updated numeric schemes, solution procedures and description of the physics of wave growth and decay.

Following the indication of the IPCC, meteorological data produced by the DWD (Deutscher Wetterdienst) and distributed by the Helmholtz-Zentrum Geesthacht, both for the control period (1960-1990) and for three periods of the IPCC A1B scenario (2010-2039, 2040-2069, 2070-2100), were treated to produce forcings for a set of simulations performed with SHYFEM and WWM for the Adriatic Sea basin, particularly for the Northwestern coastal zone, from the Venice Lagoon to the Emilia Romagna Littoral.

4.7.1.1 Sea Level Rise – Cesenatico case study.

Due to the high local subsidence affecting the measurements of sea level in Ravenna (Fig. 15), sea level rise scenarios for Cesenatico were computed by HZG based on the data collected in Trieste, Northern Adriatic Sea. The data together with the predicted scenarios (blue circles and interval) and the IPCC boundaries (red curve and grey coloured field) are reported in Figure 16.

Sea level rise is therefore in the short, mid and long term:

- 2020. From -3 to +16 cm, average + 7 cm
- 2050. From +2 to +23 cm, average +13 cm
- 2080. Based on the IPCC red line, average + 22 cm

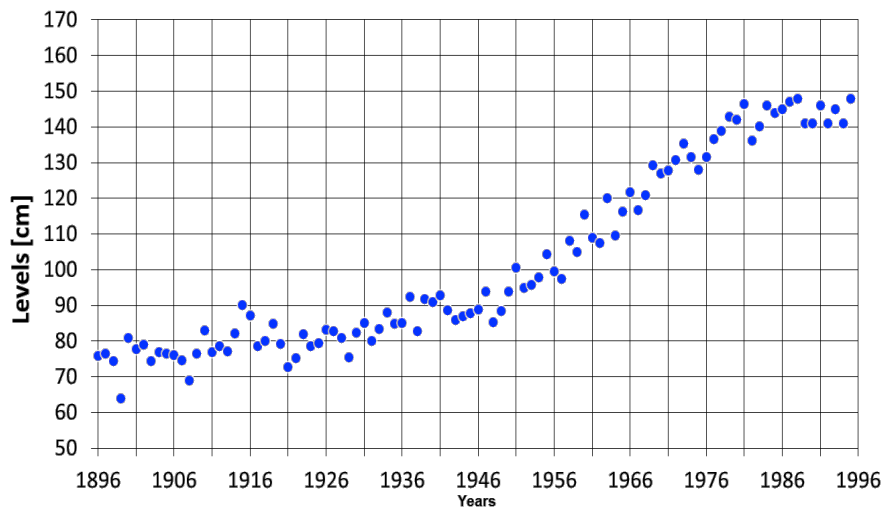


Figure 9 Average sea level measured in Ravenna. The change in subsidence growth rate due to the law stopping water pumping from the subsoil in the agricultural surrounding land is evident.

Sea Level (Trieste)

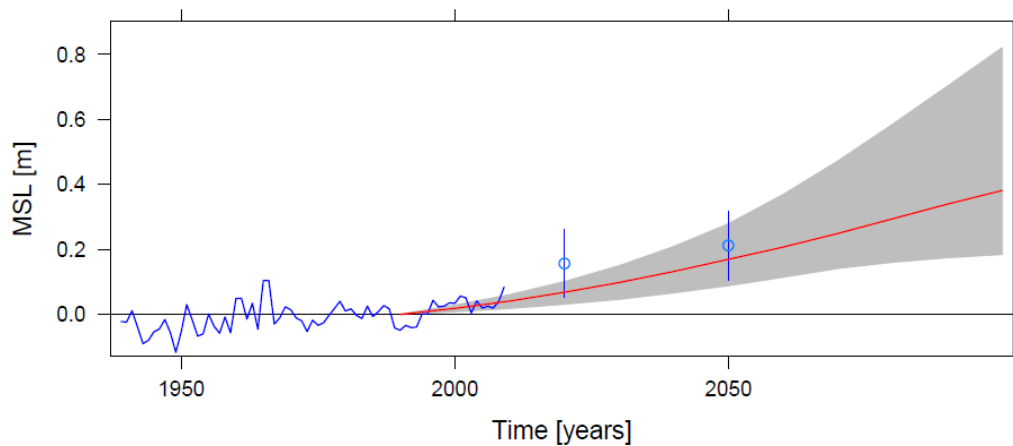


Figure 10 Maximum, average and minimum sea level rise predictions based on the historical data collected from Trieste measurement station. Kindly provided by Ralf Weisse, HZG.

4.7.1.2 Typical and Extreme Climate Scenario

In the case of episodic or extreme events, the process is somewhat more complex, as it is necessary, to determine first what we consider extreme events and their return period.

The first step consists in the estimation of a total water level at the shoreline. The total water level at the shoreline corresponds to the sum of the sea-level, astronomical tides, storm surge and wave runup. This is done by using the response-method approach, which is based on measured or simulated water levels and waves as they occur in nature. The water

level of interest (associated to a given probability or return period) is directly calculated from a probability distribution of total water levels.

In order to calculate the water levels and since our methodology is proposed for a coast without any protection but natural beaches, the runup model proposed by Stockdon et al (2006) has been selected. The runup (R2%) is calculated for each beach profile scenario (according to each beach profile definition method, see below), and wave climate of TR (10, 50, 100 years and extreme).

Wave run-up is computed by means of Stockdon et al. (2006)¹⁵³:

$$R_{u2\%} = 1.1 \cdot \left\{ 0.35 \cdot \tan \beta (H_s L_0)^{1/2} + 0.5 \cdot \left[H_0 L_0 (0.563 \cdot \tan \beta^2 + 0.004) \right]^{1/2} \right\} \quad \text{Eq. 4}$$

The differences in runup magnitude are controlled by the use of a different beach slope since wave conditions are the same in all the cases. Obtained runup values are then added to simultaneous water level data (ζ_m) to build up the total water level time series ($\zeta(t)$).

Total water level data are then fitted to an extreme distribution to estimate the water level associated to given probabilities or return periods.

First, a series with the yearly maximum surge is selected for period of interest (1960-1990, 2010-2039, 2040-2069 and 2070-2100), with the correspondent significant wave height, peak off-shore wave steepness and wave direction

Scenario	Zr, m		Return period, years							
			2	5	10	20	25	30	50	100
2010 Present	0	Sop, %	1.305	1.977	2.329	2.619	2.703	2.770	2.946	3.163
		Zm, m	1.143	1.238	1.287	1.328	1.340	1.349	1.374	1.404
		Hs, m	2.204	3.072	3.537	3.923	4.036	4.124	4.358	4.647
2020 Short term	0.07	Sop, %	1.208	1.713	1.976	2.194	2.258	2.308	2.439	2.603
		Zm, m	1.110	1.201	1.248	1.287	1.298	1.307	1.331	1.360
		Hs, m	2.132	2.754	3.070	3.326	3.399	3.457	3.607	3.790
2050 Mid term	0.13	Sop, %	1.596	2.746	3.348	3.845	3.989	4.103	4.404	4.776
		Zm, m	1.150	1.261	1.319	1.367	1.381	1.392	1.421	1.457
		Hs, m	2.397	3.779	4.585	5.286	5.495	5.661	6.106	6.668
2080 Long term	0.22	Sop, %	1.524	2.223	2.589	2.890	2.978	3.047	3.230	3.456
		Zm, m	1.175	1.305	1.372	1.428	1.444	1.457	1.491	1.533
		Hs, m	2.362	3.120	3.512	3.831	3.923	3.995	4.184	4.416

Table 2 Extreme conditions (surge is the first variable of the joint statistics) in Cesenatico. Storm surge level Zm, associated significant wave height Hs, sea level rise Zr. Wave direction >90°N

The value of surge for each scenario associated to the 7 waves are obtained by averaging the surface elevation observed in the large set of conditions represented by each wave. It was found that surge did not influence the surge significantly (1 cm difference), and therefore the average surge across scenarios was taken.

Typical annual climate is reconstructed in Tables 5 and 6 respectively for Bellocchio and Cesenatico. It can be seen that the wave climate does not show relevant modifications, with the exception of a slight tendency to an increase of storms coming from Scirocco.

				2010	2020	2050	2080
Hs, m	Dir, °N	Sop	Zm	f, %	f, %	f, %	f, %
0.3	50	0.025	0.21	26.00%	26.50%	25.70%	24.10%
1.5	50	0.035	0.25	5.66%	5.70%	5.15%	4.78%
2.5	50	0.035	0.37	1.71%	1.63%	1.48%	1.21%
0.85	80	0.035	0.25	23.60%	24.20%	25.30%	26.30%
3	80	0.035	0.62	0.77%	0.69%	0.45%	0.63%
0.3	120	0.025	0.29	39.70%	38.70%	39.70%	40.70%
1.5	120	0.035	0.56	2.63%	2.67%	2.18%	2.30%

Table 3 Selected climate conditions representative of the typical average annual wave climate in Cesenatico. Significant Wave height Hs, mean wave direction Dir, sea level associated to wave height Zm, frequency of the climate condition in one year f. Calm 0%.

Wave Overtopping

Once the target total water level has been estimated, the next step is to calculate overtopping rates (Q) for those cases where the runup exceeds the beach/barrier crest. This will determine the volume of floodwater penetrating to the hinterland and, in consequence, determining the extension of the flood hazard area. The overtopping volume has been calculated following the method used by FEMA (2003) to estimate the inundation in low-lying coasts. The following describes in detail the formulas used in this part of the methodology.

Wave overtopping occurs when the barrier crest height is lower than the potential runup level Figure 11. Waves will flow or splash over the barrier crest, typically to an elevation less than the potential runup elevation (R). The exact overtopping water surface and overtopping rate will depend on the incident water level and wave conditions and on the barrier geometry and roughness characteristics. Moreover, overtopping rates can vary over several orders of magnitude, with only subtle changes in hydraulic and barrier characteristics, and are difficult to predict accurately.

Under random wave attack, overtopping discharges can change in several orders of magnitude from one wave to another, meaning that wave overtopping is a non-linear function of wave height and wave period. This time variation is difficult to measure and quantify in the laboratory and therefore overtopping discharges are most often given in terms of average discharge.

Due to the complexity of overtopping processes and the wide variety of structures over which overtopping can occur, wave overtopping is highly empirical and generally based on laboratory experimental results and on relatively few field investigations.

The wave overtopping on beaches and dunes is important because it helps in the calculation and prediction of sediment overwash, but has not been well studied. Most of these formulations have been developed for laboratory conditions where uniform slopes were used. On natural beaches, the profile is more complex and thus an appropriate equivalent slope for use in those predictive formulae is not straightforward. Different slope definitions can lead to substantial differences in overtopping estimates.

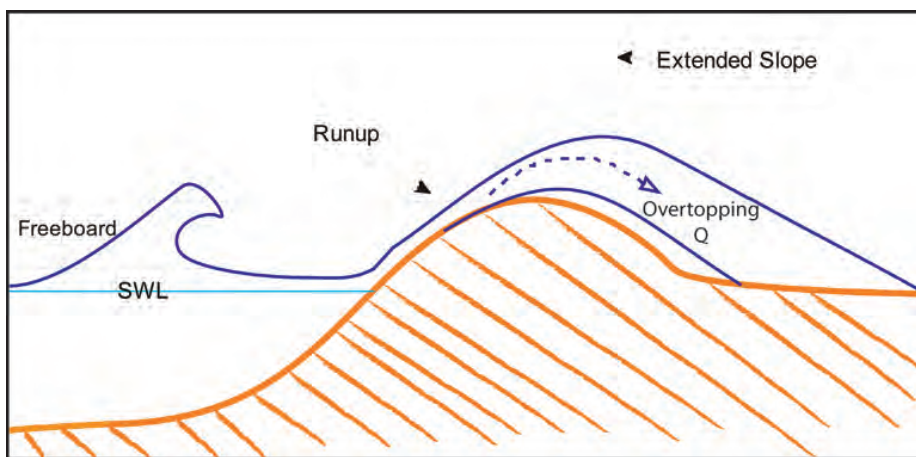


Figure 11 Overtopping

Overtopping guidance of FEMA (2003) is based largely on the work of Owen (1980)¹⁵⁴ and Goda (1985)¹⁵⁵. This formulation does not call for overtopping calculations in all instances. Instead it first calls for a comparison of the freeboard, F (the vertical distance between the base flood stillwater elevation and the crest elevation), and the mean runup height, R . If $F > 2 R$, then the guidance assumes that overtopping can be neglected. If $F < 2 R$, then the mean overtopping rate Q for a nonvertical slope is calculated according to:

$$Q = Q^* \sqrt{gH_s^3}$$

$$Q^* = 8 * 10^{-5} \exp \left[3.1 \left(rR^* - \frac{F}{H_s} \right) \right]$$

$$R^* = \frac{1.5m}{\sqrt{(H_s/L_{op})}} \text{Eq. 5}$$

where:

Q^* = dimensionless overtopping, R^* = estimated extreme runup normalized by r = the roughness coefficient, F = freeboard, H_s = incident significant wave height at toe of overtopped barrier, g = gravitational constant, m = the cotangent of the slope angle of the overtopped barrier, and L_{op} = deepwater wavelength.

4.7.2 PATHWAYS- HAZARD ASSESSMENT

Pathways are the route and processes which are active during a flood event and there must be at least one pathway between the source and receptor otherwise no consequences can occur. Pathways are a relative concept and they include the components of the flood system and management through or over which flood waters flow, such as habitats relevant for coastal protection, hard and soft coastal defences, and infrastructure. It is worth remembering that an individual pathway may lead to multiple receptors and individual receptors may have multiple pathways (Narayan et al., 2014). The DSS model needs to be able to describe multiple sets of flood routings.

Once the storm impacts on the coast the floodplain will be inundated if the total water level exceed the crest of the coastal structure and overtopping occurs.

Failure or gaps in coastal flood defences can allow seawater or tidally-locked freshwater, to propagate landward of the shoreline and come into contact with receptors.

Flooding can arise from 'functional' failures when wave and water level conditions exceed those for which the defence is designed, or structural failure where some element or components of the defence do not perform as intended under the design conditions (Reeve et al., 2009¹⁵⁶).

Once water enters land due to a combination of extreme sea levels and exceedance of defence systems, inundation characteristics are primarily dependent upon the type of defence failure(s) and the floodplain topography (e.g. gradient, barriers, and obstacles). Water levels and flow patterns are also influenced by features that accelerate, obstruct or retain water (e.g. buildings, vegetation, walls, fences and drainage features). Urban floodplains are highly complex to model due to many interacting variables (Dawson et al.,

2008¹⁵⁷), containing hard structures, surfaces, people and debris. Urban floodplain processes are also characterised by turbulence, inertia, and flow transitions due to the spatially dense presence of obstacles, obstructions and features that cause rapid flow constrictions and variations in floodplain friction.

In rural floodplains, natural topography is likely to be the predominant influence upon flow characteristics; although frictional resistance may also be critical and be dominated by drag due to vegetation. These complexities are represented to varying degrees by numerical models, which are described in the following subsection.

As explained further in chapter 6, variants of flood map are an important component of flood risk analysis and management. These may be generated by inundation analysis, which can be used to spatially express flood risk, or emphasize different types of consequence. Flood maps can be used for operational flood warning management or planning.

Advances in geographical information systems (GIS) and high resolution topographic floodplain data have benefited the analysis and visualisation of inundation. A form of floodplain elevation data considered effective for flood modelling is airborne topographic Light Detection and Ranging (LiDAR). This is an implementation of laser ranging incorporating the representation of the ground surface at high resolutions, which increases the ability to predict flood inundation extent and depths more precisely (Marks and Bates, 2000¹⁵⁸). Such systems are capable of providing elevations of the earth's surface to decimetre-level precision or better. In coastal environments, the root mean square error (RMSE) is dependent on slope and has been noted to yield points that are ± 0.3 m of reality (Xharde et al., 2006¹⁵⁹; Webster et al., 2006¹⁶⁰). Such data can be used to construct a digital elevation model (DEM) and subsequently generate flood maps if combined with other layers such as boundary water levels and features such as roads, building etc.

One of the simplest forms of inundation map is to lay a return period planar still water level³ across a DEM and generate a flood outline, to determine what is within or beneath this theoretical flood extent. Although capable of providing a quick overview of land that could be affected by flooding, this method can significantly over-predict the spatial extent of inundation; and it is often preferable to use methods which account for hydraulic connectivity and mass conservancy (Bates et al., 2005¹⁶¹; Gallien et al., 2011¹⁶²), particularly for complex or low gradient floodplains, and where defences play a significant role (Nicholls et al., 2005¹⁶³; Dawson et al., 2005¹⁶⁴).

Relatively recent advances in flood propagation algorithms and collection and processing of topographic elevation data have supported the widespread application of hydraulic models

to aid flood prediction (Brown et al., 2007¹⁶⁵); by defining a computational domain, boundary conditions and using a two-dimensional solver to simulate the free surface elevation of floodplain flow (depending on the complexity of the 2D model an initial condition, and depth-averaged velocity vector may also be incorporated). The application of more complex models which solve the three-dimensional Reynolds- averaged Navier Stokes equations (Cugier and Le Hir, 2002¹⁶⁶) is rare due to computational cost and lack of necessity, whereas one dimensional modelling is more suited to problems where there are well- defined channels or subsurface flow networks; and nowadays rarely used for coastal flooding predictions due to the supremacy of 2D codes. Hence 2D models are now widely used; by coupling coastal boundary conditions and such models to allow numerical simulation of floodplain flow processes and propagation of the flood wave. 2D hydraulic numerical modelling of inundation can also allow analysis of a wide range of scenarios (Bates et al., 2005).

4.7.3 Receptors and Consequences

Receptors are the final target of the flooding event, this phase of SPRC methodology consist in the definition and localization of different type of receptors located in the flooded floodplain. The receptor characterization consist in defining the Vulnerability (see chap 4.5) that concerns the susceptibility to substantial damage, disruption and casualties as a result of a hazardous event.

The exposure assessment requires the localization of the people potentially affected by the hazard, which can be defined using census data of population density within the residential areas. Fatalities are widely viewed as the worst type of impact of a flood event; and analysis of a global database has suggested that large scale coastal flood events are associated with greater mortality than for inland floods (Jonkman and Vrijling, 2008¹⁶⁷).

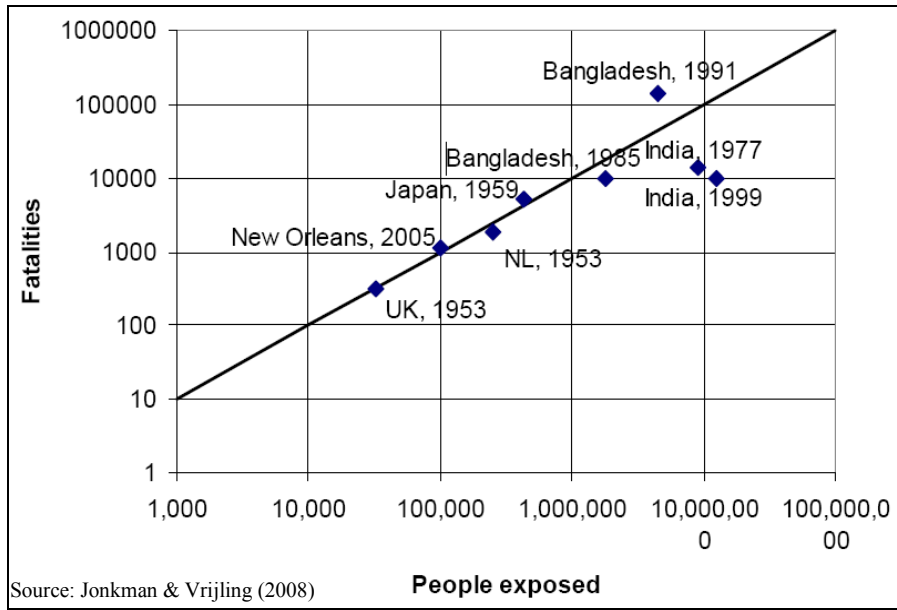


Figure 12 Coastal Mortality based upon large-scale events - Jonkman and Vrijling, 2008

4.8 Data for coastal risk assessment

To properly build flood hazard and risk maps in the coastal zone, different type of data to characterize the coastal domain are required. These are necessary to build the following main layers:

- The digital terrain model DTM of the floodplain to be flooded
- The morphology of the coastal fringe where waves and storm surge will impact during the flood event
- The bathymetry where waves and surge will propagate during their approach towards the coast
- Layers for characterizing the receptors (economic, environmental, social) vulnerability
 - Land Use Maps
 - Census Data- ISTAT
 - GDP
 - Ecological Habitat

All these data are GIS raster and vector data that uploaded by the user in the Web-GIS DSS in a specific format: Tiff for Raster and ESRI Shapefile for Vector.

The next paragraphs describes the data that are used in the Cesenatico and Bellocchio Case Study.

4.8.1 Land Use Map

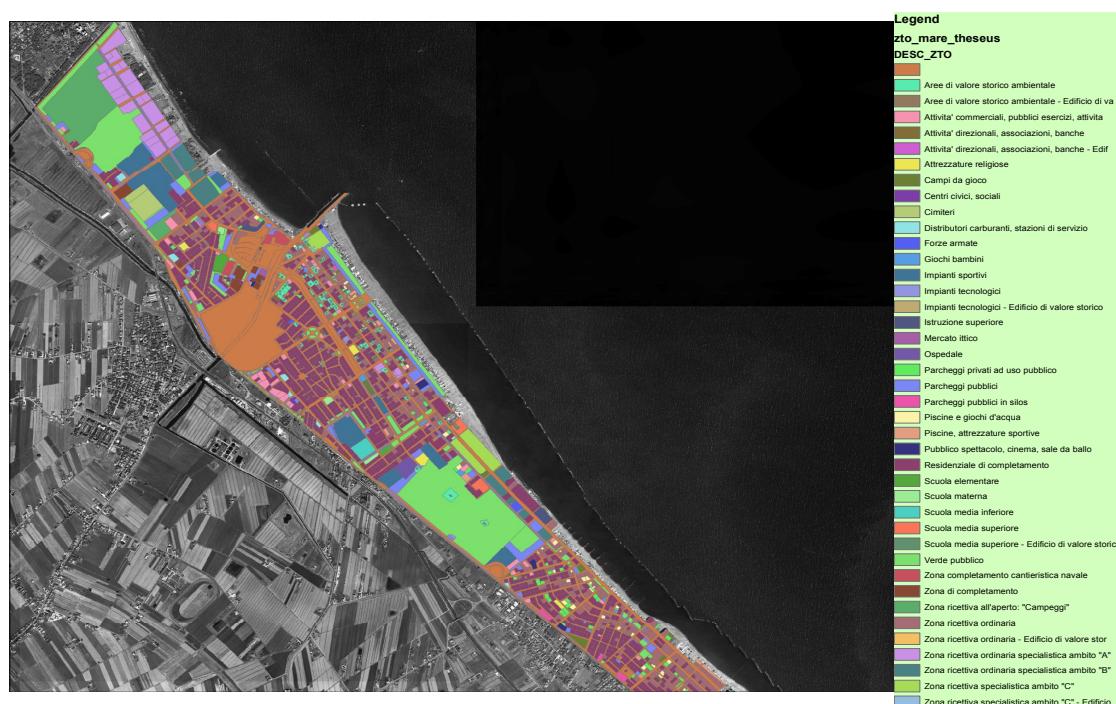


Figure 13 Cesenatico CORINE Land Cover data

4.8.2 Ecological Habitats

Cesenatico offers an example of the depleted ecological conditions of the Region (Figure 81). Nowadays no saltmarshes, seagrasses, mussel beds, oyster beds nor other relevant biogenic habitats are present in Cesenatico. The only natural habitats remaining are some scattered vegetated patches of limited naturalistic value (Figure 82).

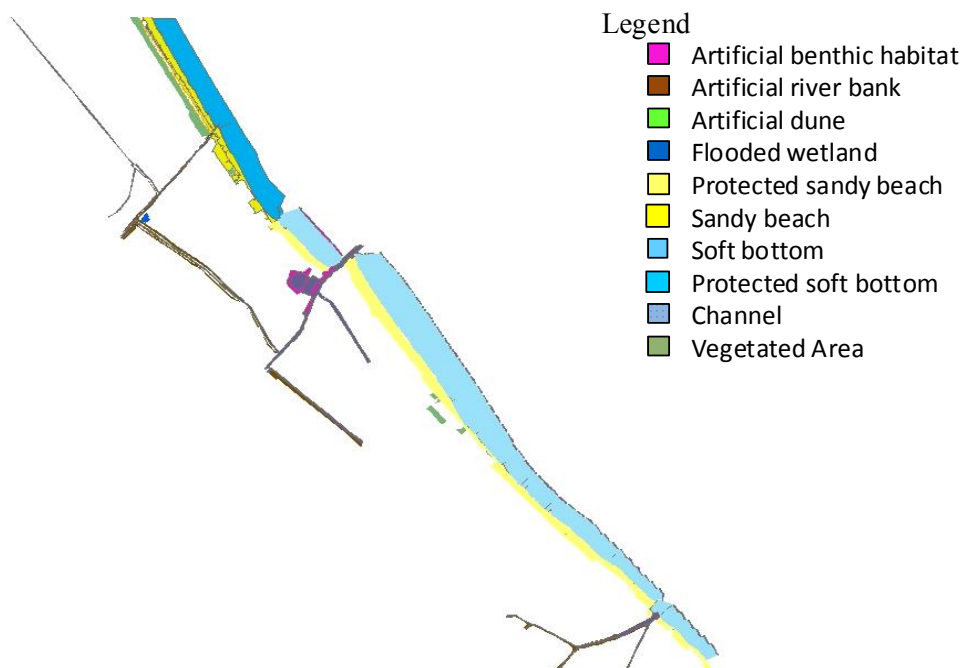


Figure 14 Cesenatico natural and artificial habitats

The seabed is gently sloping (about 6 m/Km), and a wide surf zone is exposed to waves raised by prevailing south-easterly and north-easterly winds in summer and winter, respectively. Shallow subtidal bottom sediments consist of fine to medium sands, and are colonised by assemblages generally dominated by bivalves. The coastline is protected by an uninterrupted sequence of hard defence structures, except for a small unprotected gap in the northern area. These breakwaters are colonized by assemblages typical of artificial structures in the region such as: *Mytilus galloprovincialis*, *Crassostrea gigas*, *Ulva* spp., *Sabellaria alveolata*, *Patella caerulea*.

Bellocchio comprises an extremely valuable naturalistic area of the territory of the Emilia-Romagna Region, between the provinces of Ferrara and Ravenna. The site is classified and protected as a nature reserve and has been proposed as “Sites of community importance” for the EU network Natura 2000. It is a brackish lagoon formed by a clay plateau with a large landfill on the left bank of the river Reno. The area is subject to cyclical flooding of the river Reno with their contribution of sediment and marine ingressions dependent on tides and storms. As for the flora, the habitats of Community importance within the meaning of Annex I to Directive 92/43/EEC are reported in Figure 83.

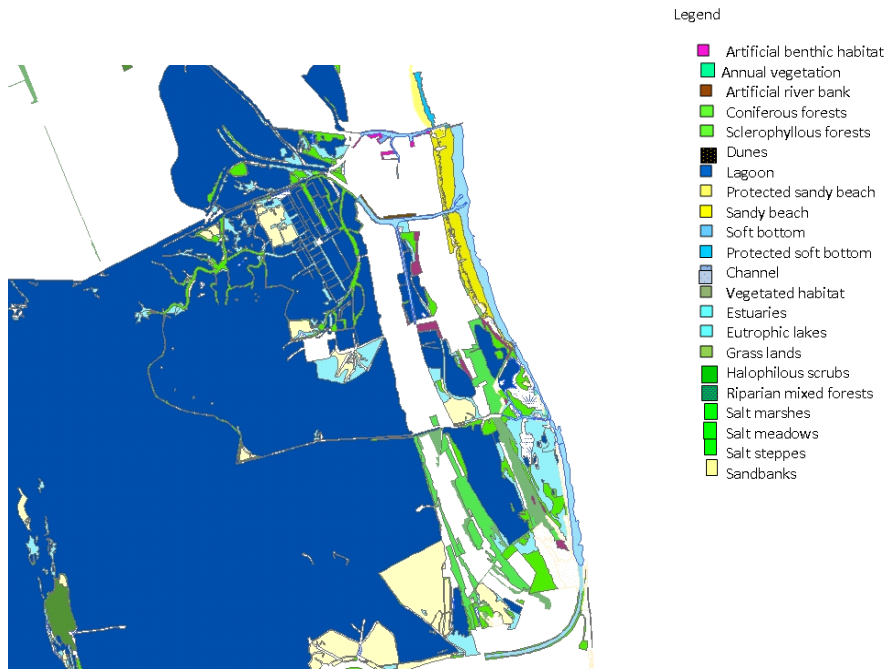


Figure 15 Bellocchio natural and artificial habitats

4.8.3 Census Data

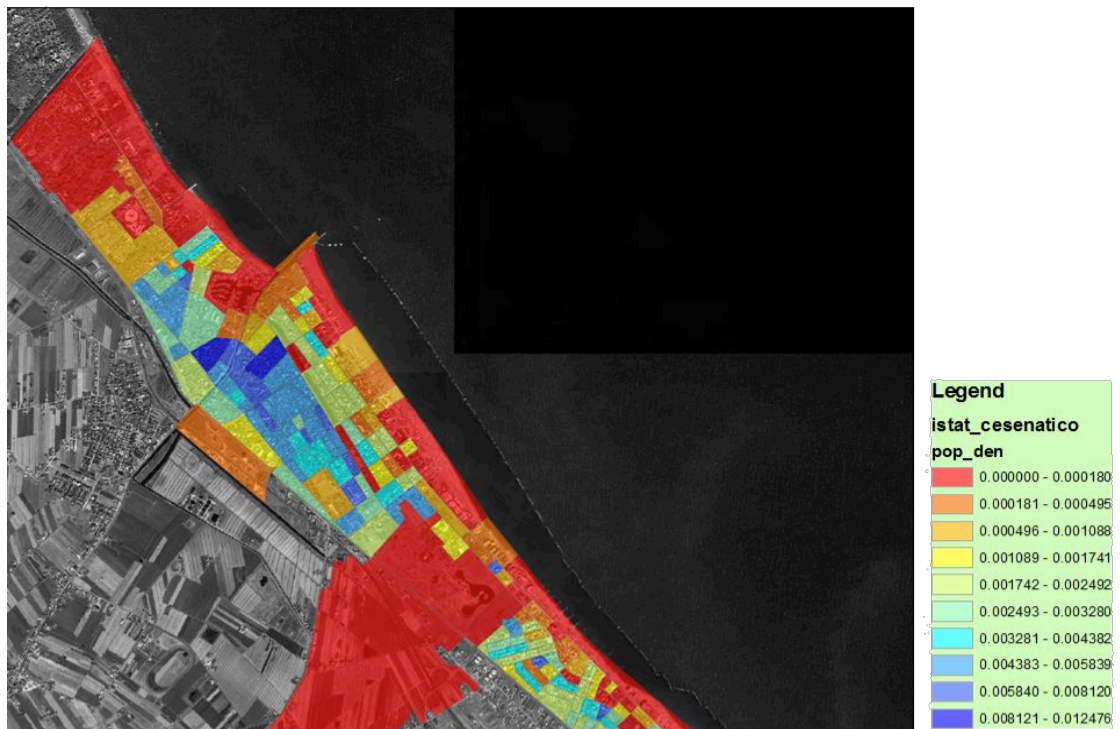


Figure 16 Cesenatico ISTA POPULATION DENSITY

4.8.4 Bathymetry and DTM

Both numerical hydrodynamic models and simple raster-based equilibrium models require accurate DTM in order to produce reliable outputs concerning the flood extent and velocity in the floodplain.

The importance of the data quality on the quality of the final product (map) is underlined by the procedure implemented by the Federal Emergency Management Agency (FEMA) who has produced a series of guidelines and specifications on aerial mapping and surveying within the programme on Flood Map Modernization (FEMA, 2003¹⁶⁸). They provide guidelines on different practical aspects of surveying (e.g. ground surveys of control points, hydraulic structures, topographic mapping using photogrammetry, Lidar, etc.) and, also, they serve to specify the quality of the spatial data products to be produced which are later used as base maps to produce different Flood Maps

There exist different technologies to measure the elevation in the territory, ranging from remote sensing techniques (e.g. photogrammetry, Lidar, SAR, etc.) to ground-truth methods such as DGPS, each one with different limitations on accuracy, cost-effectiveness, time-consumption, feasibility, and applicability. One of the first main points to be considered is that the most frequent situation is that in which the area to be analysed for flooding purposes is large or very large (100s of km²). This makes that ground-truth methods are not practical since they are very costly in terms of time requirements and costs. As a consequence of this, data actually being used in most of the flood hazard mapping exercises are obtained by remote sensing based techniques

Finally, it has to be stressed that if the quality of the data used to produce the DTM affects the accuracy of the flood map, the resolution of the generated DTM also affects the accuracy of the map (e.g. see Haile and Rientjes, 2005¹⁶⁹).

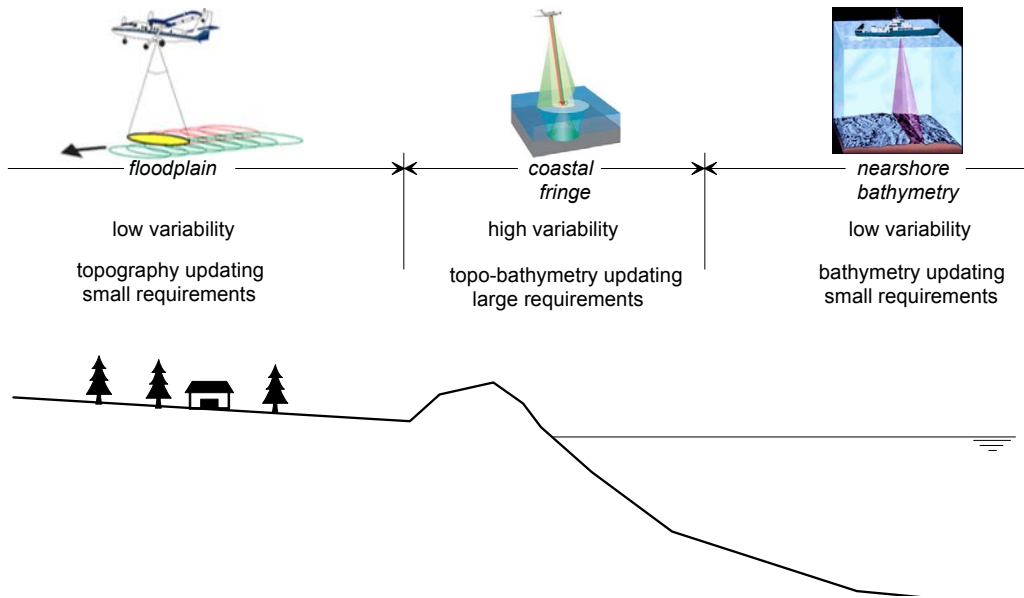


Figure 17 Costal Area variability and resolution

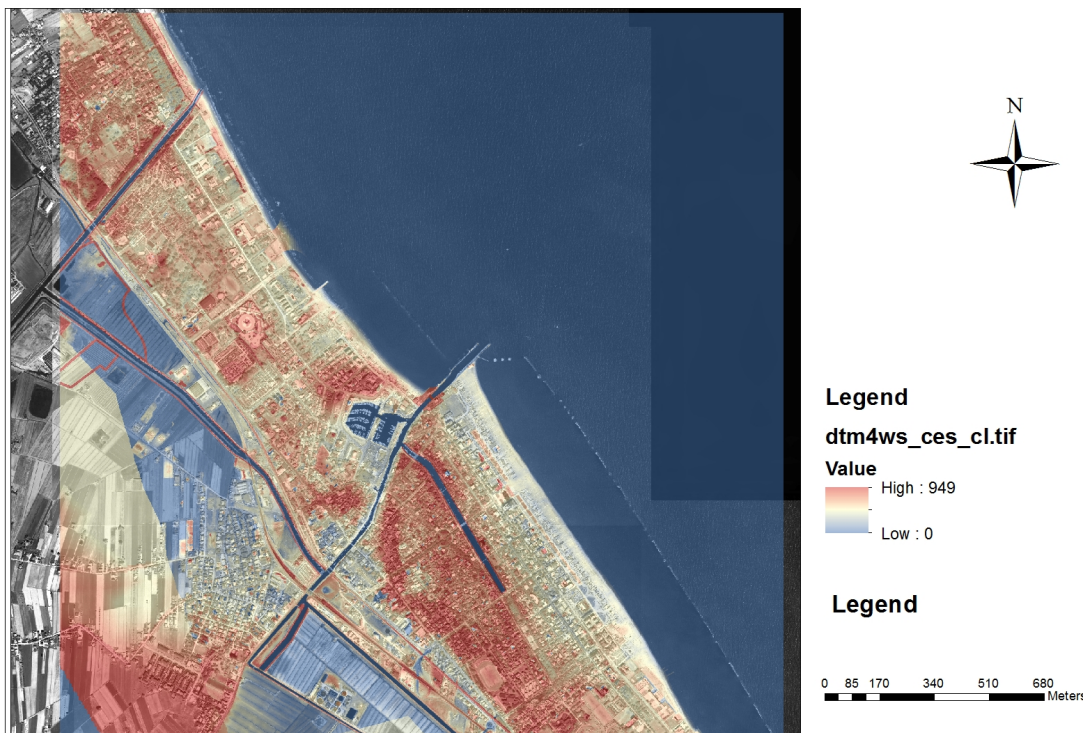


Figure 18 Cesenatico topography

5 Mapping and Modeling Coastal Flooding - State of the art

5.1 Introduction

In this chapter we analyze the use of flood simulation models for mapping floods characteristics such as water depth, velocity and duration, and for supporting the coastal managers in flood risk assessment and in mitigation measures planning through the use of a dedicated Web-GIS DSS.

As reported in the description of the SPRC framework, modeling of flood effects and characteristics is a key aspect for damage and risk assessment.

The demand for predictions of flooding damage and risk posed by natural events of different return period, or in multiple scenarios associated with different potential futures, has increased significantly (Middelkoop et al., 2004¹⁷⁰; Ashley et al., 2005¹⁷¹; Hall et al., 2005¹⁷²; Dawson et al., 2005¹⁷³).

Flood simulation play a very important role and make a real contribution to the work against flood hazards (Hunter et al 2007¹⁷⁴). Coastal Flood simulation models can support coastal managers in estimating the consequences of floods, in terms of water depths, flow velocities or damages. They can also be used to test the effectiveness under multiple scenario defined combining coastal hazards (climate change, subsidence, storm) and mitigation measure adoption.

A flood hazard map shows the spatial distribution of the flood threat, the intensity, in term for example of velocity and duration of flood situation, and their associated exceedance probability for either a single or several flood scenarios.

In the past Flood Hazard Mapping (FHM) was traditionally carried out by gathering, collecting, and analyzing coastal/wave or hydrological data, which involved a large number of field observations and calculations. This traditional approach uses historical data of flood events to delineate the extent and return times of floods. With the development of remote sensing and computer analysis techniques, the traditional sources can be supplemented, thus yielding to improvements in FHM, and this leading in turn to better planning.

Nowadays, in FHM several types of approaches are used, after an extensive review, we can consider two major types of approaches. The first is completely based on theoretical and numerical hydrodynamic flooding, flood simulation models are computer programs based

on physical equations, features of an area, such as elevation and roughness resistance, and external forces, such as storm events and dam breaches (Al-Sabhan et al., 2003¹⁷⁵; Bates and De Roo, 2000¹⁷⁶; De Moel and Aerts, 2011¹⁷⁷; Stelling, 2012¹⁷⁸). This approach requires a rather large degree of hydraulic expertise and is computational demanding. The other one, also called as equilibrium or planar model, uses as input the water level of the storm surge and distribute this over a DEM by means of some kind of flow-connectivity algorithm. For this approach Digital Elevation Model and Geographic Information Systems (GIS) are the basic working tool for delineating flooded area. As discussed later we will consider the more simplified GIS-based planar approach to be appropriate for the kind of rapid assessment and decision support tool to be developed here.

Over the previous decade, the field of flood simulation modeling has rapidly grown, resulting in the development of many new and sophisticated models. The growth in model development has occurred for two main reasons:

(1) advances in computer technology, spatial data analysis (GIS) and modeling methods have opened new possibilities for modeling and simulating complex systems;

(2) unprecedented socio-economic and technical conditions have put new demands on decision-makers for complex and ready to use flood information (McCarthy et al., 2007¹⁷⁹).

The key to graphical visualizations on the flooding modelling is the inclusion of the series data within a spatial interface, such as a Geographical Information System (GIS). Nowadays, the state of the art technology in the field of Geographic Information System (GIS) allows spatial analysis as well as to generate the modelling for a flood hazard phenomenon.

In term of natural hazard studies, GIS give contribution for data display, storage and retrieval, site selection, impact assessment, and modelling. Table 4 is shown an example of GIS application for natural hazard management, (DRDE-US, 1991¹⁸⁰).

Function	Potential Applications
Data display	Aid in the analysis of spatial distribution of socio-economic infrastructure and natural hazard phenomena
	Use of thematic maps to enhance reports and/or presentations
	Link with other databases for more specific information
Land Information Storage and Retrieval	Filing, maintaining, and updating land-related data (land ownership, previous records of natural events, permissible uses, etc.)
Zone and District Management	Maintain and update district maps, such as zoning maps or floodplain maps
	Determine and enforce adequate land-use regulation and building codes
Site Selection	Identification of potential sites for particular uses
Hazard Impact Assessment	Identification of geographically determined hazard impacts
Development/Land Suitability Modelling	Analysis of the suitability of particular parcels for development

Table 4 Example of GIS applications for natural hazard management Marfai 2003¹⁸¹

Further, advances in geospatial technologies have revived interest in storage cell based simplified flood models introduced by Cunge et al. (1980¹⁸²). In particular Storage cell based flood models easily harmonize with GIS data formats and with increasing availability of high resolution Digital Elevation Model (DEM), such flood models are being applied even for urban areas (Bates and DeRoo, 2000; Bates et al., 2010). Normally, sophisticated flood models are data intensive and use geospatial datasets, a requirement which can only be addressed by research level organizations. Adoption of such models by stakeholders or local communities may be difficult due to model complexity, poor understanding of underlying assumptions, tedious model calibration, lack of skill in handling geospatial datasets, besides high maintenance costs of the system. Thus, the usefulness of advances in geospatial technologies and high resolution data cannot be fully utilized by stakeholders unless it is offered in a suitable form (Miller et al., 2004¹⁸³).

In this chapter we examine and discuss different modeling approach for coastal flooding suitable to be implemented in a Web-GIS DSS with the purpose to quickly simulate multiple flooding scenarios in order to assist coastal managers in mapping risk and selecting the best mitigation options.

5.2 Coastal Flooding Modeling Approach– raster VS Numerical

In this section the models that are available for assessing coastal vulnerability to coastal flooding due to storm or sea-level rise are discussed. The models presented here raise problems of scale; some are good for local purposes and not very good for large study areas and others vice versa. In the case of large coastal areas, the lack of good quality and homogeneous data among regions-countries is a key bottleneck, for instance meteorological data or consistent and high accurate height information (DTM) for Europe (Vaze *et al.*, 2010¹⁸⁴, Horritt *et al.*, 2001¹⁸⁵).

The physics of floodplain inundation remains a challenge to scientists (Bates et al. 2012¹⁸⁶). Recently, laboratory experimentation (e.g., Knight and Shiono 1996¹⁸⁷; Sellin and Willets 1996), field experimentation (e.g., Babaeyan-Koopaei et al. 2002¹⁸⁸; Nicholas and Mitchell 2003¹⁸⁹), and remote sensing observations (e.g., Alsdorf et al. 2000, 2007; Bates et al. 2006¹⁹⁰; Pavelsky and Smith 2008¹⁹¹; Schumann et al. 2007¹⁹², 2008¹⁹³) have all resulted in significant advances in understanding of floodplain processes. We now understand much

more about turbulent flow around structures during overbank flood flows and the dynamics of shallow plain flooding over complex topography.

The best representation of the physics that is currently conceivable would be to numerically model both river channel and floodplain flows as being fully three dimensional (3D), including turbulence, with solution of the full Navier–Stokes equations.

The main stimulus for numerical modeling proliferation has been the increasing availability of high resolution topography and the continued development of new and more efficient numerical tools and scheme for predicting flood characteristics mainly mapping the flood extent and flow velocity.

In particular the advances in remote sensing and computing power have made distributed numerical models (e.g. Hromadka and Yen, 1986¹⁹⁴; Syme, 1991¹⁹⁵; Bates and De Roo, 2000; Horritt, 2004) an increasingly attractive solution where spatial predictions of the potential damage of future flooding episodes are required.

There are numerous hydrodynamic numerical models able to simulate the propagation of flood water across floodplain areas generated by coastal or river flooding.

These models generally solve a form of the two-dimensional shallow water equations (Katapodes and Strelkoff, 1979¹⁹⁶; Kawahara and Yokoyama, 1980¹⁹⁷; Iwasa and Inoue, 1982¹⁹⁸; Zhang and Cundy, 1989¹⁹⁹), or simplified approximations in which the inertia terms or ‘acceleration slopes’ are omitted from the controlling equations (Xanthopoulos and Koutitas, 1976²⁰⁰; Cunge et al., 1980²⁰¹; Hromadka and Yen, 1986²⁰²; Julien et al., 1995²⁰³) to give what is sometimes known as a “zero-inertia model” and range in complexity from raster-based approaches (Lhomme et al. 2004²⁰⁴, Bates et al. 2000²⁰⁵) that assume the flow between cells to be uniform and are based on the Manning equation, to more complex finite volume approaches that solve numerically the full two-dimensional equations.

Solving the full Saint-Venant (RANS Reynolds Averaged Navier-Stokes) equations over complex topography using finite difference (Smith, 1978²⁰⁶), finite element (Zienkiewicz and Cheung, 1965²⁰⁷) or finite volume (Hirsch, 1988²⁰⁸) algorithms for undertaking high-resolution hydrodynamic modelling of coastal and river–floodplain systems and producing assessments of flood risk at very fine spatial and temporal scales is not a panacea.

In fact, these models are computationally expensive to run, can suffer from instability and convergence problems (Liggett and Woolhiser, 1967²⁰⁹) and are time consuming to set up.

Moreover as reported in Leskens et al. 2014²¹⁰ complex numerical flooding models despite the advantages in providing very detailed results in terms of mapping flood extent and characteristics (flow velocity, duration, et), experience in the field of risk assessment have

proven that the information from these models is of limited use in flood risk assessment and management. Morss et al. (2005²¹¹) show that practitioners of flood disaster management, operating under regulatory, institutional, political, resource, and other constraints, prioritize other concerns over more sophisticated model information about flood risk, particularly when they cannot readily see the feasibility or value of incorporating new or more detailed information from models. Decision-makers, acting under these circumstances, tend to discard information that seems to increase the complexity they already have to deal with (Gray, 1989²¹²; Janis and Mann, 1977²¹³; Kahneman and Tversky, 1979²¹⁴; MacCrimmon and Taylor, 1976²¹⁵). This indicates that the modelers community develops models that provide information that is often not useful for practitioners of flood risk management.

Numerical and complex models were considered to be too static as a consequence of fixed options in the model that did not allow recalculation of the scenarios that were under consideration. Multiple coastal flooding risk scenarios should be evaluated quickly in order to communicate scenario results to decision makers.

Their application within the context of risk-based flood system models that require consideration of multiple breach and loading scenarios can be impractical (B. Gouldby et al. 2008²¹⁶). In particular, non-specialized researchers, emergency management personnel, and land use planners require an accurate, inexpensive method to determine and map risk associated with storm surge events and long-term sea level rise associated with climate change (Webster et al. 2008)²¹⁷.

For the reasons discussed above full numerical shallow water models are not suitable for the development of a Web-GIS DSS where users need rapid response for assessing multiple coastal risk flooding scenario.

A simplification is represented by reduced complexity or Zero Inertial inundation models. They are based on the application of the Manning's formula or weir overflow equations on irregular grids. These approaches have a long history, with the first applications dating back to the 1970s (Cunge, 1975²¹⁸), and have experienced a renaissance in the recent years (Moussa and Bocquillon, 2009²¹⁹; Castellarin et al., 2011²²⁰). The floodplain is represented by interconnected storage cells of irregular shapes. Water volume fluxes between cells are typically computed by the Manning's equation or weir-type formulas, whereas water levels within the cells are derived from water stage-volume functions.

The strengths of this reduced-complexity model structure derive from its explicit dependence on a regular gridded digital elevation model (DEM) to parameterize flows through riparian areas. This approach offers order of magnitude gains in computational

efficiency over more complex finite element and volume codes, and so enables a more critical examination of parameter and structural model sensitivities and predictive uncertainty using Monte Carlo methods (Aronica et al., 2002²²¹).

Among the 2D reduced complexity inundation models, one can further distinguish between models based on continuity and simplified momentum equations and those based solely on the continuity or floodplain connectivity. Particularly, models based on discretization of the diffusive wave equation over the 2D Cartesian grids were extensively used in recent years (Bates and de Roo, 2000; Bradbrook et al., 2005²²²; Hunter et al., 2005²²³; Vorogushyn et al., 2010²²⁴). Particularly, the widely used LISFLOOD-FP model (Bates and de Roo, 2000) was successfully applied to a number of catchments, among others to the large-scale basins such as Amazon (Wilson et al., 2007²²⁵; Trigg et al., 2009²²⁶) and Ob (Biancamaria et al., 2009²²⁷).

The ability to combine a simplified descriptions of surface flow with very detailed descriptions of topography to produce model outputs that can be easily calibrated/validated using remotely-sensed data of a commensurate resolution. Changing the model discretization from user-defined polygons to a regular grid or TIN-based format that can interface with remotely-sensed data held within Geographical Information Systems is a relatively simple undertaking, yet one that facilitates model construction, whilst at the same time improving utility and ease of coding.

It is therefore not surprising that such simple modifications have led to the recent widespread proliferation of reduced complexity modelling studies in hydraulics

However although Zero Inertial model represents a step forward in simplification and reduction of computational time, they are still difficult to be implemented in DSS for coastal risk assessment due to complex pre-processing phase and long running time.

Moreover in the context of coastal risk assessment, the complexity of hydraulic models, both in a full expression or simplified version (Raster Based Zero Inertial), is not required for either steady state simulations or applications where only maximum flood extent is required.

As underlined by Sayers et al. 2005²²⁸, we might even question whether we actually need a hydrodynamic inundation model at all, or just a GIS-based flood spreading algorithm is sufficient for risk assessment evaluations.

Recent research in hydraulics and risk-based flooding has begun to (re-)examine reduced complexity approaches from raster based mono and two-dimensional hydraulic modelling to simple DEM-based flood spreading method as a solution to some of these problems.

This flooding models are represented by so called 0D (Pender et al. 2006²²⁹), planar model, static flood modeling, bath-tube or Rapid Flood Spreading methods (Gouldby et al. 2008²³⁰) which are the subject of some research in the context of national scale flood risk assessment (for which simulation run times many orders of magnitudes shorter than conventional 2D models are needed). These methods are based on much simpler representations of the physical processes than 2D-models and the removal of the time discretisation in the computation. These methods do not involve any modelling of the physical processes of inundation. One may consider emulation techniques making use of a limited number of training runs of a hydraulic model (see, for example, Beven et al. 2008²³¹) to belong to this category. Simple geometric methods which project river or sea water levels horizontally over a floodplain can also be termed 0D as far as the modelling of floodplain inundation is concerned (this is also referred to as the “bath tub” approach). These can be applied to both river and coastal inundation cases.

This approach does not use hydraulic physically based models but aims to map the extent of the flood through the spreading of water level using a GIS-raster based approach.

This approach is highly recommended in case the user need to run in a faster and easy mode multiple flooding scenario. The use of numerical model must be avoided in order to achieve a good time response of the DSS.

The computational engine functions are based on a set of rules governing the transfer of water between neighbouring pixels on the floodplain. The model is forced by introducing the total volume of water associated with the flood at a single point on the domain.

As reported in Poulter et al. 2008²³² **two** different 0D GIS-based approach can be used in order to map the flood extension using raster data without implementing hydrodynamic equation : The first is a simple **'bathtub' or 'contour'** (Brown, 2006²³³) based approach (referred to as a 'zero-side rule') in which a grid cell became flooded if its elevation was less than the projected sea level. The **second** approach specified that the grid cell was flooded only if its elevation was below sea level and if it was connected to an adjacent grid cell that was flooded or open water.

Reduced complexity codes, such as raster-based and 0D GIS models, are designed to perform very specific (often pragmatic) tasks by deliberately ignoring processes deemed incidental to these objectives, yet their very success in such applications may lead to over-confidence in their wider ability. There is also a danger that model-specific conclusions may be applied generally without a detailed appreciation of the subtle differences between codes.

In moving to reduced complexities codes, it's important to ask if it's acceptable to use a code that we know to be wrong in elements of detail just because at some aggregate level it produces realistic predictions.

The unprecedented scope for undertaking high-resolution numerical hydrodynamic modelling of coastal/river–floodplain systems and producing assessments of flood risk at very fine spatial and temporal scales seems to be not a panacea.

The aim of developing and using models that are ‘as realistic as possible’ for the purpose of risk-based flood system models must be balanced against a number of other important considerations. These include:

- the computational burden of the hydrodynamic calculations
- investment in bespoke data collection and model set-up
- requirements of the end user: capable to generate hydraulic information (water depth and velocity)
- possibility to embed floodplain inundation models inside GIS and Spatial DSS for risk assessment
- performing modeling scenario from spatial resolution grids of urban areas to large domain size represented by catchment scenarios
- develop multiple flood risk analysis

In other words methods for modelling flood inundation should be reliable, practicable in terms of computational expense and input data, easily coupled with GIS and DSS, and capable of generating the required hydraulic information (e.g. water depth, flood duration, water velocity) in an appropriate format and level of detail.

The debate between the use of complex hydrodynamic models respect the use of simplified codes in the area of flooding simulation can find a solution in asking the following question: “how simple can a model be and still be physically realistic?”.

To put this question more generally: to what extent is it acceptable to use a code that we know to be wrong in elements of detail just because at some aggregate level it produces realistic predictions? Such questions are an inevitable consequence of moving to reduced complexity codes, but can actually be asked of all models because of they way in which they (to different extents) simplify reality.

For these reasons, reduced complexity codes have had a significant recent impact in hydraulic modelling and have led to a re-examination of a number of long standing research questions. In particular, they have allowed us to address the relative importance of process representation and topographic complexity in determining floodplain inundation and shown

clearly that the latter is the more dominant effect. They have also led us to question what are the dominant flow process at particular spatial scales during a flood event. They have allowed us to more accurately assess the effect of friction on model results and demonstrated the equifinal nature of much hydraulic modelling. They have opened up significant new application areas and forced a search for more appropriate calibration-validation data that needs to continue and accelerate if we are to further develop such approaches. Whilst not a panacea, they have so far proved very useful as an experimental framework for science studies and for advancing our ability to make practical predictions. In the next paragraphs is reported a review of different modeling approach, reported in the literature, focused in coastal flooding.

2D Modelling Approach	Advantages	Disadvantages
Quasi 2D flood cells (with 1D model)	<ul style="list-style-type: none"> • Short run times • Existing links to available 1D hydrodynamic models 	<ul style="list-style-type: none"> • Flow routes within flood cells not defined • Difficult to define flood cells (subjective) • Poor or lack definition of velocities and flood hazard
2D raster routing	<ul style="list-style-type: none"> • Quick to apply • Makes good use of LiDAR/SAR data 	<ul style="list-style-type: none"> • Potentially long run times • Time step and grid size dependency (difficult to get both depth/extent and travel time correct) • Lack of velocity data
Full 2D regular grid (finite difference schemes)	<ul style="list-style-type: none"> • Finite difference schemes more stable than finite element schemes. • Straight forward to apply a regular grid given a DEM 	<ul style="list-style-type: none"> • May not provide adequate topographic definition where grid resolution is too coarse. • Potentially long run times
Full 2D irregular grid (finite element schemes)	<ul style="list-style-type: none"> • Allows the use of a coarse mesh over expansive areas of unchanging terrain. • Potentially the most accurate for the 2D domain 	<ul style="list-style-type: none"> • Long run times • Long set up times
Combined 1D and full 2D	<ul style="list-style-type: none"> • 1D elements used for complex structures (eg sluice gates and culverts) • Easy to apply regular grid for 2D domain • Faster run times as 1D elements where 2D not necessary 	<ul style="list-style-type: none"> • Work involved in defining the link between 1D and 2D elements
Rapid Flood Inundation Models	<ul style="list-style-type: none"> • Extremely short run times • Rapid prediction of flood depths • Flow Path results to help understand flooding mechanisms • Can be combined with 1D model elements • Makes good use of LiDAR/SAR data 	<ul style="list-style-type: none"> • Lack of velocity or flow output • More detailed model required for design purposes

Table 5 Advantages and disadvantages of flooding model approach Wicks et al. 2004²³⁴

5.3 Numerical Hydrodynamic model: Shallow Water Equation

Numerical Flood modeling methods currently in use can be divided into a number of approaches as reported in Table 6 (Pender 2006²³⁵), characterized by their dimensionality or the way they combine approaches of different dimensionalities.

Method	Description	Application	Typical computation times	Outputs	Example Models
1D	Solution of the one-dimensional St-Venant equations.	Design scale modelling which can be of the order of 10s to 100s of km depending on catchment size.	Minutes	Water depth, cross-section averaged velocity, and discharge at each cross-section. Inundation extent if floodplains are part of 1D model, or through horizontal projection of water level.	Mike 11 HEC-RAS ISIS InfoWorks RS
1D+	1D plus a storage cell approach to the simulation of floodplain flow.	Design scale modelling which can be of the order of 10s to 100s of km depending on catchment size, also has the potential for broad scale application if used with sparse cross-section data.	Minutes	As for 1D models, plus water levels and inundation extent in floodplain storage cells	Mike 11 HEC-RAS ISIS InfoWorks RS
2D-	2D minus the law of conservation of momentum for the floodplain flow.	Broad scale modelling and applications where inertial effects are not important.	Hours	Inundation extent Water depths	LISFLOOD-FP JFLOW
2D	Solution of the two-dimensional shallow water equations.	Design scale modelling of the order of 10s of km. May have the potential for use in broad scale modelling if applied with very coarse grids.	Hours or days	Inundation extent Water depths Depth-averaged velocities	TUFLOW Mike 21 TELEMAC SOBEK InfoWorks-2D
2D+	2D plus a solution for vertical velocities using continuity only.	Predominantly coastal modelling applications where 3D velocity profiles are important. Has also been applied to reach scale river modelling problems in research projects.	Days	Inundation extent Water depths 3D velocities	TELEMAC 3D
3D	Solution of the three-dimensional Reynolds averaged Navier Stokes equations.	Local predictions of three-dimensional velocity fields in main channels and floodplains.	Days	Inundation extent Water depths 3D velocities	CFX

Table 6 Numerical hydrodynamic flood modeling approach - Pender 2006²³⁶

Hydrodynamic models based on the two-dimensional shallow water equations are classed here as 2D approaches. The 2D shallow water equations (also referred to as 2D St-Venant equations) can be derived by integrating the Reynolds-averaged Navier-Stokes equations over the flow depth. In this integration process, a hydrostatic pressure distribution is assumed. A solution to these equations can be obtained from a variety of numerical methods (such as finite difference, finite element or finite volume) and use different numerical grids (such as Cartesian or boundary fitted, structured or unstructured) all of which have advantages and disadvantages in the context of floodplain modelling

The governing equations of fluid flow, including shallow water flow, are based on the conservation of mass, momentum, and energy and the second law of thermodynamics. The principle of conservation requires that the three aforementioned fundamental quantities are neither created nor destroyed. The consideration of the conservation of mass is simple but the conservation of energy and momentum is more difficult, owing to the interrelationship between these quantities and the numerous phenomena that influence these quantities. For simplicity the following discussion, as with many classical texts (Laney 1998²³⁷, Chorinand 1979²³⁸], begins by eliminating all influences on momentum and energy, save for redistribution and pressure, by initially only considering inviscid flows of perfect fluids free of forces except for pressure. Various forces can then be added to describe more complex flows.

There are several approaches that can be used to develop the depth-averaged shallow water wave equations. The following most closely follows the text of Liggett²³⁹ which begins with the aforementioned hydrodynamic equations to stress the necessary assumptions and approximations of shallow water theory

Shallow water theory makes three important assumptions regarding the nature of the fluid being studied. The fluid is assumed to be incompressible, irrotational and inviscid. The latter two assumptions were made when deriving Euler's equations. The construction of the depth-averaged shallow water equations also requires three main assumptions about the spatial domain. Shallow water flows only exist in bodies of fluid with a vertical extent D of Ω that is 'much smaller' than the horizontal extent L . By 'much smaller' we mean the ratio of horizontal and vertical extent is much smaller than one. That is $\varrho = D/L \ll 1$. In addition pressure is assumed to increase linearly with depth and there is assumed to be negligible vertical acceleration within the fluid.

The two-dimensional shallow water equations expressed in vector form are:

$$\frac{\partial U}{\partial t} + \frac{\partial F}{\partial x} + \frac{\partial G}{\partial y} = H \quad \text{Eq. 6}$$

where x and y are the two spatial dimensions. The four vectors U , F , G , H are defined as follows:

$$U = \begin{pmatrix} h \\ hu \\ hv \end{pmatrix}, \quad F = \begin{pmatrix} hu \\ g \frac{h^2}{2} + hu^2 \\ huv \end{pmatrix}, \quad G = \begin{pmatrix} hv \\ huv \\ g \frac{h^2}{2} + hv^2 \end{pmatrix}, \quad H = \begin{pmatrix} 0 \\ gh(S_{0x} - S_{fx}) \\ gh(S_{0y} - S_{fy}) \end{pmatrix} \quad \text{Eq. 7}$$

where u and v are the depth-averaged velocities in the x and y directions, respectively. S_{0x} and S_{0y} are the bed slopes in the x and y directions. The friction slopes in the x and y directions can be expressed in a manner analogous to the 1D formulation, as follows (assuming the use of Manning's n):

$$S_{fx} = -\frac{n^2 u \sqrt{u^2 + v^2}}{h^{4/3}} \quad \text{and} \quad S_{fy} = -\frac{n^2 v \sqrt{u^2 + v^2}}{h^{4/3}} \quad \text{Eq. 8}$$

The non-linear hyperbolic nature of the shallow water wave equations makes finding analytic solutions to these equations difficult. The equations admit both continuous and discontinuous solutions even when initial conditions are smooth. Consequently numerical schemes are needed to solve most practical problems. The approaches can be divided into three categories – finite difference methods, finite volume methods and finite element methods.

Finite difference methods

Finite difference (FD) methods rely on Taylor series expansions to express the value taken by a variable (h , u , v and so on) at a given point, as a function of the values at neighbouring points and of local derivatives of increasing orders. These Taylor series are then combined to yield approximate expressions for the derivatives involved in the shallow water equations, as a function of a finite number of neighbouring point values. The accuracy of the approximations can be controlled by the order to which the Taylor series expansions are developed (the order of the so-called *truncation*), which is also linked to the number of neighbouring points involved.

The implementation of finite difference methods is significantly more straightforward on a structured grid, which is a computational grid that can effectively be represented on a square matrix (in 2D applications). This explains to some extent why their popularity is currently in decay in the academic community (Alcrudo 2004²⁴⁰), as unstructured grids lend themselves better to the modelling of environmental flows. Software packages based on FD methods, however, are popular with a number of UK consultants, due mainly to their compatibility with high resolution digital terrain models and digital bathymetric models created from LiDAR and sonar surveys.

Finite element methods

In finite element methods, the solution space is divided into a number of elements in 2D. In each element, the unknown variables are approximated by a linear combination of

piecewise linear functions called trial functions. There are as many such functions as there are vertices defining the element, and each takes the value of one at one vertex and the value of zero at all other vertices. A global function based on this approximation is substituted into the governing partial differential equations. This equation is then integrated with weighting functions and the resulting error is minimised to give coefficients for the trial functions that represent an approximate solution (Wright 2005²⁴¹). A number of methods to do this exist, including the *Galerkin* method (see for example Ottosen and Petersson 1992²⁴²).

Finite element methods benefit from a rigorous mathematical foundation (Alcrudo 2004²⁴³) that allows a better understanding of their accuracy (Hervouet 2007²⁴⁴); however, the technique has not been used as much as other approaches in commercial software, perhaps because it is less accessible conceptually and produces models that result in large run-times. Also, generating meshes can be time-consuming when a suitable mesh generation tool is not available (Sauvaget *et al.* 2000²⁴⁵).

Finite volume methods

In the finite volume method, space is divided into so-called finite volume which are 2D (in this context) regions of any geometric shapes. The shallow water equations (in conservative form) are integrated over each control volume to yield equations in terms of fluxes through the control volume boundaries. Flux values across a given boundary (calculated using interpolated variables) are used for both control volumes separated by the boundary, resulting in the theoretically perfect mass and momentum conservativeness of the approach (a flux into a finite volume through a boundary is always equal to a flux out of a neighbouring one through the same boundary). In 1D, finite volume methods are equivalent to finite difference methods. Finite volume methods are increasingly popular and have become the most widely used method in the area of Shallow Water flow modelling (see for example Caleffi *et al.* 2003²⁴⁶, DHI 2007²⁴⁷, Villanueva and Wright 2005²⁴⁸, Alcrudo and Mulet YEAR²⁴⁹, Kramer and Stelling 2008²⁵⁰, Begnudelli & Sanders, 2006²⁵¹). This can be explained by their advantages in terms of conservativeness, geometric flexibility and conceptual simplicity (Alcrudo 2004)

(1) Name	(2) Physics	(3) Further information on numerical scheme	(4) Shock capturing	(5) Developer	(6) Status	(7) Linkages
FINITE DIFFERENCE SCHEMES						
TUFLOW	SWE	Alternating Direct. Implicit	No	BMT-WBM	Commercial	Own 1D river and pipes solver
DIVAST	SWE	Alternating Direct. Implicit	No	Cardiff Univ.	Research	As part of ISIS 2D
DIVAST-TVD	SWE	Explicit TVD- MacCormack	Yes	Cardiff Univ.	Research	
ISIS 2D	SWE	Alternating Direct. Implicit	No	Halcrow	Commercial	Own 1D river solver
MIKE 21	SWE	Alternating Direct. Implicit	No	DHI	Commercial	As part of MIKE FLOOD
MIKE FLOOD	SWE	MIKE 21	No	DHI	Commercial	Own 1D river (MIKE 11) and urban drainage (MIKE URBAN) solvers
SIPSON/UIM	SWE	Alternating Direct. Implicit	No	U. of Exeter	Research	Own multiple linking element
SOBEK	SWE	Implicit - Staggered grid	Yes	DELTA RES	Commercial	Own 1D river solver, vertical link
JFLOW	Diffusive wave	Explicit	No	JBA	Internal	
FINITE ELEMENT SCHEMES						
TELEMAC 2D	SWE		No	EDF	Commercial	
FINITE VOLUME SCHEMES						
TELEMAC 2D	SWE	Tbc	Yes	EDF	Commercial	
MIKE 21 FM	SWE	Godunov based	Yes	DHI	Commercial	As part of MIKE FLOOD
MIKE FLOOD	SWE	MIKE 21 FM	Yes	DHI	Commercial	Own 1D river (MIKE 11) and urban drainage (MIKE URBAN) solvers + MOUSE (?)
InfoWorks-RS	SWE	Roe's Riemann solver	Yes	Wal'ford Softw	Commercial	Own 1D river solver
InfoWorks-CS	SWE	Roe's Riemann solver	Yes	Wal'ford Softw	Commercial	Own 1D urban drainage solver
HEMAT	SWE	Roe's Riemann solver	Yes	Iran Wat. Res. Cent. & Cardiff	Research	
BreZo	SWE	Explicit- R Riemann solver	Yes	U. of California	Research	
TRENT	SWE	Explicit- R Riemann solver	Yes	Nottingham U.	Research	

Table 7 Main hydrodynamic flooding models characteristics Nèlz and Pender 2009²⁵²

Four numerical hydrodynamic codes were evaluated in this thesis for the purpose of coastal flooding risk assessment. The numerical codes were used as benchmark models for testing the results obtained through the new 0D raster-based spreading models developed discussed in this thesis and embedded in the Web-GIS MARASMA DSS.

Hereafter a brief description of the 4 numerical models

TELEMAC - www.opentelemac.org

The Computational Fluid Dynamics (CFD) software suite, TELEMAC^{253 254}, is a powerful integrated modelling tool for simulating offshore, coastal and river systems, and shallow lagoons and estuaries. The software is able to model free-surface flows, including flooding and drying effects, and discharges of pollutants or fresh-water. The suite has been continuously developed by EDF R&D for over 20 years. The main codes within the TELEMAC suite include TELEMAC-2D, which uses the depth-integrated shallow water (hydrostatic) equations to describe the conditions when the horizontal length scale of the flow is greater than the vertical scale, and TELEMAC-3D, where the full Navier–Stokes (or non-hydrostatic) equations are solved.

BREZO - <http://sanders.eng.uci.edu/brezo.html>

BreZo (Begnudelli and Sanders, 2008²⁵⁵), is a two-dimensional Godunov-type finite volume models based on shallow-water wave theory. This type of numerical approach is relatively new to flood inundation modeling but have been shown to support an accurate and stable prediction of inundation dynamics (flooding and drainage) in complex urban landscapes (e.g. Gallegos et al., 2009²⁵⁶). These models have overcome long standing stability and

conservation problems posed by a moving wet/dry interface which constitutes a singularity in the governing equations (e.g. Begnudelli & Sanders, 2006²⁵⁷), and allow for a wide range of flow regimes to be resolved including supercritical breach flows without case-specific parameter tuning. Godunov-type shallow-water models therefore constitute an attractive basis for integrated embayment flood event modeling as described above, i.e., seamlessly resolving embayment long wave dynamics, overtopping, breach flows, and overland flow into low lying terrain.

MIKE21 - <http://www.mikepoweredbydhi.com>

The modelling system is based on the numerical solution of the two/three-dimensional incompressible Reynolds averaged Navier-Stokes equations subject to the assumptions of Boussinesq and of hydrostatic pressure. Thus, the model consists of continuity, momentum, temperature, salinity and density equations and it is closed by a turbulent closure scheme. The density does not depend on the pressure, but only on the temperature and the salinity. The modelling system has been developed for complex applications within oceanographic, coastal and estuarine environments. However, being a general modelling system for 2D and 3D free- surface flows it may also be applied for studies of inland surface waters, e.g. overland flooding and lakes or reservoirs.

ANUGA - <https://anuga.anu.edu.au>

The Australian Government through Geoscience Australia (GA) has collaborated with the Australian National University (ANU) to develop and validate an inundation modelling software tool called ANUGA. ANUGA is Free and Open Source Software (FOSS).

AnuGA uses a finite-volume method for solving the shallow water wave equations (Zoppou and Roberts, 1999²⁵⁸). The study area is represented by a mesh of triangular cells in which water depth h , and horizontal momentum (uh , vh), are determined. The size of the triangles may be varied within the mesh to allow greater resolution in regions of particular interest.

Fluxes across cell boundaries are calculated using the central-upwind scheme of Kurganov, Noelle and Petrova (2001)²⁵⁹. One advantage of this approach is that the traditional characteristic decompositions and Riemann solvers are replaced by one simple scheme that efficiently addresses super- and sub critical flows, wetting and drying as well as faithful reproduction of planar surfaces. ANUGA uses a second order spatial reconstruction to produce a piece-wise linear representation of the conserved quantities. This surface is allowed to be discontinuous across the edges of the cells, but the slopes are limited to avoid artificially introduced oscillations. As a consequence wave fronts can be arbitrarily steep

allowing for stable resolution of bores and hydraulic shocks. The algorithms underlying solution of the shallow water wave equations are discussed further in the user manual and paper by Toro (1992)²⁶⁰.

The mathematical model behind ANUGA is suitable for modelling complex flows in shallow water involving hydraulic jumps (shock waves), rapidly changing flow regimes and flows into dry beds. The study area in an ANUGA model is represented by an unstructured triangular mesh. Further general information on ANUGA may be obtained from the ANUGA user manual freely available from <http://datamining.anu.edu.au/anuga> and the ANUGA software may be downloaded from <http://sourceforge.net/projects/anuga>.

Most AnuGA components are written in the object-oriented programming language Python. Software written in Python can be produced quickly and can be readily adapted to changing requirements throughout its lifetime. Computationally intensive components are written for efficiency in C routines working directly with the Numerical Python structures.

The inundation model will be released under an OSS license in 2006. This strategy will enable free access to the software and allow the risk research community to use, validate and contribute to the development of AnuGA.

5.4 2D Zero Inertial Raster-based flooding model

As discussed in the previous paragraph modeling coastal flooding with 2D hydrodynamic numerical codes solving the SWE may be impractical in case the user needs to evaluate multiple risk assessment scenario evaluation as requested in the development of DSS.

In fact numerical fully 2D SWE models requires an heavy input pre/post-processing phase, excessive computational costs and finally they are subjected to numerical instabilities related to small water depths and the wetting and drying process as well as.

The use of raster-based models overcomes these difficulties and provides a way to work with a large number of floodplain grid elements. Additionally, this approach has the advantages of taking into account the spatial variability of floodplain physical characteristics (elevation and roughness) and of being easily integrated into a geographic information system (GIS) with simplification of pre-processing input data.

The ability to combine a simplified description of surface flow with a very detailed descriptions of topography to produce model outputs that can be easily calibrated/validated using remotely-sensed data of a commensurate resolution. Changing the model discretization from user-defined polygons to a regular grid or TIN-based format that can interface with remotely-sensed data held within Geographical Information Systems is a relatively simple undertaking, yet one that facilitates model construction, whilst at the same time improving utility and ease of coding. It is therefore not surprising that such simple modifications have led to the recent widespread proliferation of reduced complexity modelling studies in hydraulics.

These models were developed simplifying the full Saint-Venant equations and meanwhile endeavor to maintain a reasonable physical representation of flood waves. One of the strategies is to simplify the governing equations using zero-inertia approaches whenever justified by the physical conditions (Ponce et al., 1978²⁶¹; Vieira, 1983²⁶²).

The Zero-Inertia Models (ZIMs) or Diffusion-Wave Models (DWMs) fall in this category. Based on the assumption of slow-varying flood waves, the zero-inertia governing equation can be derived from the fully 2D shallow water equations by neglecting the momentum dynamic terms where the three shallow water equations are simplified and finally combined into a single zero-inertia equation.

Considering the one-dimensional Saint-Venant or Shallow Water momentum equations expressed in (Hunter et al. 2007²⁶³):

$$\frac{\partial u}{\partial t} + u \frac{\partial u}{\partial x} + g \left(\frac{\partial h}{\partial x} + S_f - S_0 \right) = 0. \quad \text{Eq. 9}$$

(i) (ii) (iii) (iv) (v)

where (i) represents the local inertia (or acceleration) term, (ii) represents the advective inertia term, (iii) represents the pressure differential term and (iv) and (v) account for the friction and bed slope respectively.

A simplified version of flood flow model can be generated, depending on which of these terms is assumed to be negligible respect the others terms

From many floodplains flow advection (ii) is relative unimportant as demonstrated by Hunter et al. 2007, and is possible to neglect this term. In particular is intuitive that flows over long reaches can be adequately modeled by kinematic or diffusive approximations, whereas small scale features require full dynamic approach. The length scale defining long and short reaches in this case is give by setting the Froude number equal to 1:

$$R = \frac{Lgn^2}{h_0^{4/3}} \quad \text{Eq. 10}$$

where L is a typical length scale of perturbation S_0 is the bed slope, g is acceleration due to gravity, n is Manning's roughness coefficient.

For typical flow depths (about 1 m) and Manning's n values (about $0.03 \text{ m}^{-1/3} \text{ s}$), this gives a length scale of the order of 100 m, and again this will have implications for model selection at particular resolutions. Models with grid cells bigger than this length scale will not be able to represent processes at a length scale small enough to generate significant advective processes, and there is therefore little point in including advection terms.

A diffusion-wave (DWM) approach was first proposed by Cunge et al. (1976), and similar methods have been used by Estrela and Quintas (1994)²⁶⁴ and Bechteler et al. (1994)²⁶⁵. It uses an explicit 2D treatment of mass conservation, but a highly simplified representation of momentum conservation, commonly based upon determining the magnitude of flow between any two adjacent cells according to the water surface elevation difference and the Manning equation.

More recently, raster-based models have gained credence in the modelling of floodplain flow inundation extent (Bates and De Roo, 2000²⁶⁶; Horritt and Bates 2001²⁶⁷,^b²⁶⁸; Bradbrook et al., 2004²⁶⁹).

Bates and De Roo (2000) developed a raster-based model (LISFLOOD-FP) based on this concept and compared it with a relatively coarse resolution (50–250 m) 2D finite-element scheme. Unlike other models, this model was specifically designed to predict flood

inundation and ignored or minimized the representation of processes that were not considered central to the aim. Tentatively, these results indicated that topography and a basic process representation were more important than a complete process representation for effective prediction of inundation extent.

The LISFLOOD equation development will be described here briefly, a more detailed derivation is provided by Bates et al. (2010). The inertia model solves the continuity and momentum equations of the Saint-Venant equations with the latter one neglecting the advective inertial term only:

$$\frac{\partial h^{i,j}}{\partial t} = \frac{q_x^{i-1,j} - q_x^{i,j} + q_y^{i-1,j} - q_y^{i,j}}{\Delta x}$$

Eq. 11 continuity

$$\frac{\partial v}{\partial t} + v \frac{\partial v}{\partial x} = -g \frac{\partial h}{\partial x} + gS_f - gS_0$$

local and advective acceleration term pressure term friction term bed slope

Eq. 12 momentum

where, $h_{i,j}$ is the water free surface height, $q_{i,j}$ is the specific flow per unit width at the node (i, j), Δx is the cell dimension, v is velocity, g is gravity, S_f is the friction slope and S_0 is the bed slope.

Expressing the momentum in terms of specific flow per unit width and approximating the hydraulic radius with the flow depth between cells (h_{flow}), the explicit equation for q at time $t+\Delta t$ reads:

$$q_{t+\Delta t} = \frac{q_t - gh_{flow} \Delta t S_f}{(1 + gh_{flow} \Delta t + n^2 |q_t| / h_{flow}^{10/3})}$$

Eq. 13

where n is the Manning's roughness coefficient and Δt is the time step. The fluxes across cell boundaries in x and y directions are computed independently of each other and are used to update the water level using the continuity equation.

As such, explicit solutions are often favored as they are simple to program and allow straightforward integration of models within a dynamic GIS environment (VanDeursen and Wesseling, 1996²⁷⁰; Burrough, 1998²⁷¹)

However, the numerical scheme is not unconditionally stable. The time step for a stable numerical solution is constrained by the Courant-Friedrichs-Levy criterion:

$$\Delta t_{max} = \alpha \frac{\Delta x}{\sqrt{gh_{flow}}}$$

Eq. 14

where α was introduced by Bates et al. (2010), as a factor reducing Δt_{max} to enhance model stability. Bates et al. (2010) indicated a value ranging between 0.2 and 0.7 as sufficient for most floodplain flow situations.

The inclusion of the inertia term implies that the water mass can gradually accelerate and decelerate that precludes the flow overshooting and resulting instabilities known for this type of codes (Bates et al., 2010²⁷²). However, previous studies (Bates et al., 2010; Dottori and Todini, 2011²⁷³; Neal et al., 2011b²⁷⁴) indicated a small difference between the diffusive storage cell code and the inertia formulation regarding model accuracy. Nevertheless the inertia model requires by far less computational time because of the stabilizing effect of inertia on the numerical solution that allows using larger time steps compared to the diffusive wave approximation.

Reasonable results have been obtained by several authors with this modelling approach in terms of reproducing floodplain spatial inundation patterns (Horritt and Bates, 2001a²⁷⁵; Bates et al., 2006; Wilson et al., 2007).

Horritt and Bates (2001b²⁷⁶) compared LISFLOOD-FP with a 2D finite-element model (TELEMAC-2D). Though the raster-based and the 2D finite-element models showed similar performance, insufficiently accurate validation data and the lack of friction parameterization data made it difficult to distinguish between the two kinds of model formulations. More recently, the ability of the LISFLOOD-FP model to predict flood extent has been compared with a 1D model (HEC-RAS) and a 2D model (TELEMAC-2D) using independent calibration data from hydrometric and satellite sources (Horritt and Bates, 2002²⁷⁷). Results revealed that the LISFLOOD-FP model required independent inundation area data for calibration in order to achieve good predictions of inundation extent

A simplified 2D numerical modeling of coastal flooding was developed in 2005 by Bates et al.²⁷⁸, LISFLOOD-FP is a physically-based flood inundation model that uses the simplest possible process representation capable of simulating the water depth in each grid cell at each time step. The model consists of a one-dimensional kinematic wave approximation for channel flow solved using an explicit finite-difference scheme and a two-dimensional diffusion wave approximation for floodplain flow. The basic component of the model is a raster DEM and those elements of the floodplain topography considered necessary to flood inundation prediction.

Yu and Lane in 2005²⁷⁹ developed a 2D raster-based diffusion-wave model to determine patterns of fluvial flood inundation in urban areas using high resolution topographic data

and explores the effects of spatial resolution upon estimated inundation extent and flow routing process. Model response shows that even relatively small changes in model resolution have considerable effects on the predicted inundation extent and the timing of flood inundation

In 2011 Dottori and Todini²⁸⁰ presented a reduced complexity model based on the cellular automata (CA) approach and the diffusive wave equations, specifically designed to simulate flood inundation events involving wide areas.

The rule based model are defined as Cellular Automata (CA), they represents a simple, attractive and alternative modelling technique respect to traditional numerical models that solve differential equations to describe complex phenomena (Toffoli, 1984). Cellular Automata are dynamical systems which are discrete in space and time, operate on a uniform, regular lattice and are characterised by local interactions.

Reduced complexity models are generally faster when applied on coarse grids (25–100 m) and wide areas (see, for example, Horritt and Bates, 2002), but run times can become prohibitive as the computation grid is refined, due to time step restrictions (Hunter et al., 2008). Recently Pender and Néelz (2010) have compared several 2D hydraulic models in different cases, and they did not observe a consistent saving in computational effort by applying simplified equations models as compared to full shallow water equations models.

5.5 0D DEM-based flood spreading models

Modeling the propagation of flood water across floodplain areas with 2D numerical models, solving fully and simplified SWE, is in many situation impractical, examples include real time flood inundation forecasting, probabilistic and risk analysis and national scale flood mapping.

In fact despite their potential accuracy, such models are complex and involve issues such as definition of the computational mesh, description of initial boundary conditions, and the interpretation of hydraulic roughness from land cover data. Moreover they require simulation run times lasting many hours (especially where computational cells sizes are less than 10m)

Even if simpler finite-difference (raster) models have been shown to be quicker than finite-element models (Bates and de Roo, 2000²⁸¹; Horritt and Bates, 2001a), but even with these a grid mesh of 10^6 cells can require considerable calibration effort and possibly model run-time (depending on the number of iterations).

As a consequence of the effort required to calibrate, run and validate hydrodynamic models, especially over larger areas, more general methods of strategic flood-risk assessment have been developed, typically taking advantage of Geographical Information Systems (GIS) which can provide an effective framework to integrate and analyse disparate environmental data sources (Argent, 2004²⁸²).

A new class of 2D model has evolved over recent years to meet this need and make best use of the increased availability of digital terrain data (e.g. LiDAR and SAR).

The approach of mapping flood extension and related water depth through non hydrodynamic models but adopting simple raster DEM based on spreading models is widely described in literature as previously reported.

So called 'rapid flood spreading (or inundation) models', 0D, planar or equilibrium models focus on replacing the time consuming components of the computation with simplified representations that run much faster but retain sufficient accuracy for specific uses.

This approach is highly recommended in case the user need to run in a faster and easy mode multiple flooding scenario. The use of numerical model must be avoided in order to achieve a good time response of the DSS.

The flat-water model assumes that water level is a horizontal plane. In this method, flooding of cities or coastal areas due to storms or rise of water level can be modeled relatively easily (Demirkesen et al., 2007²⁸³; Wang et al., 2002²⁸⁴).

As reported in Poulter et al. 2008²⁸⁵ and Shen et al. 2015²⁸⁶, **two** different GIS-based approach can be used in order to map the flood extension using raster data without implementing hydrodynamic equation :

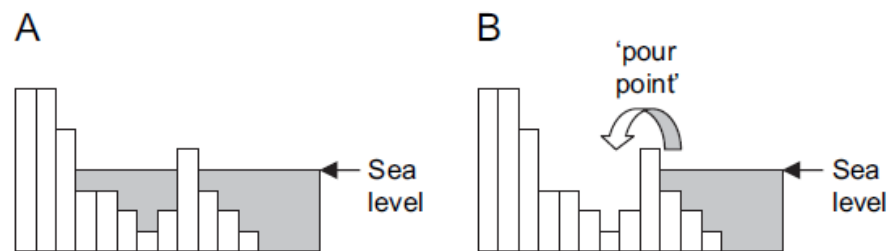


Figure 19 0D Equilibrium model – bath-tube approach (A) and seeded region growing (B)

The **first** is a simple **'bathtub' or 'zero-side rule' or 'contour'** (Moorhead and Brinson, 1995²⁸⁷; Titus and Richman, 2001²⁸⁸; Brown, 2006²⁸⁹) based approach (referred to as a 'zero-side rule') in which a grid cell became flooded if its elevation was less than the projected sea level. The 'zero-side rule' does not consider surface connectivity at all between grid cells and is the approach used in previous studies of sea-level rise (Moorhead and Brinson 1995²⁹⁰, Titus and Richman 2001²⁹¹).

All the DEM grid cells whose elevation values are below floodwater level are regarded as flooded areas, and the inundation extent consisted of DEM grid coverage, as expressed by

$$\text{Flood Extent} = \{\text{cell}:Z_{\text{cell}} < Z_{\text{water level}}, \text{cell} \in Q\}$$

where Z_{cell} is the elevation value of DEM grid cell, $Z_{\text{water level}}$ fixes the level of floodwater, and Q is the assemblage of DEM grid cells

The Bathtub or Inundation model can be better described as a set of tools (i.e. GIS software) which allows the mapping of sea-level rise in all studied locations (NOAA, 2010) rather than a model to simulate flooding along the coast or rivers. The intersection of this surface with a Digital Elevation Model provides a predicted planar surface. All areas below this surface are classified as flooded (Priestnall, 2000²⁹²).

The simple method may be suitable for a very rapid and simple risk assessment over large areas but it does not take into account the presence of intervening topographic ridges or other features (e.g. man-made defences) that can separate a lowlying area from the source of flooding. This criticism is particularly applicable to coastal floodplains, especially on

barrier coasts such as in the case study, where series of dune ridges and embankments prevent the lower hinterland from flooding in most sea conditions.

The **second** approach, referred as seeded region growing, considers DEM grid cell connectivity specifying that the grid cell was flooded only if its elevation was below sea level and if it was connected to an adjacent grid cell that was flooded or open water. Two connectivity definitions were used; a ‘four-side rule’, where the grid cell was connected if any of its cardinal directions were adjacent to a flooded cell, and an ‘eight-side rule’, where the grid cell was connected if its cardinal and diagonal directions were connected to a flooded grid cell specifying whether water flows from one cell to another along only the flat sides of a grid cell (four flow directions, D4), the diagonals or corners of the grid cell, or both (eight flow directions, D8)

This approach usually chooses some inundated DEM grid cells as seeds and then simulates the flood diffusion by four-side or eight-side rule. The flood extent consists of the coverage of DEM grid, as expressed

$$\text{Flood Extent} = \{ \text{cell} : Z_{\text{cell}} < Z_{\text{water level}} \wedge \text{cell connect with point, cell} \in Q, \text{point} \in P, P \subseteq Q \}$$

where Z_{cell} is the elevation value of DEM grid cell, $Z_{\text{water level}}$ fixes the level of floodwater, point is a real inundated seeded grid cell, Q is the assemblage of DEM grid cells, and P is the assemblage of inundated seeded grid cells among the whole DEM grid.

The connectivity rule selected and spatial resolution of the DEM cells act together to influence the accuracy of our depiction of connectivity for different topographic surface features at different spatial scales. The following equation describes how the model was used to predict flooding (F):

$$F_{x,y} = \begin{cases} E_{x,y} \leq S, 1 \\ E_{x,y} > S, 0 \end{cases} \cdot C_i \quad \text{Eq. 15}$$

where F is binomial, either flooded (1) or not flooded (0), E is DEM/lidar elevation at location x, y , S is projected sea level, C represents connectivity (connected (1) or not connected (0)), and i is an integer specifying the ‘bathtub’, cardinal, or cardinal and diagonal connectivity rules (‘zero-side rule’, ‘four-side rule’, or ‘eight-side rule’, respectively).

Usually this is obtained flooding all the raster pixel of the floodplain which respect the following topological and physical rules:

1. is connected to the source of flooding (river or coast)
2. the pixel elevation is above the flood water height
3. the volume of flooding is enough to flood the pixel (water budget)

The DEM/LIDAR flat water inundation model can be easily developed using raster data-set in a GIS using the principles of map algebra (Tomlin, 1990²⁹³), cellular automata or using the mathematical morphology operators such as watershed segmentation algorithm (Meyer and Beucher (1990) and in Soille and Ansoult (1990)).

This class of raster model are defined also as Priority-Flood Algorithm and they may be applied to either integer or floating-point DEMs and is optimal for both; the general algorithm is also indifferent as to the underlying connectedness of the DEM and works equally well on 4-, 6-, or 8-connected grids, as well as meshes.

The computational engine functions are based on a set of rules governing the transfer of water between neighbouring catchments on the floodplain. The model is forced by introducing the total volume of water associated with the flood at a single point on the domain.

As reported in Poulter et al. 2008²⁹⁴ horizontal DEM resolution play an important role in flood extent mapping with the simple raster inundation models, the difference between DEM resolution was greatest at low sea-level-rise projections (.0.3m) and decreased at high projections (.0.8m).

Specifying connectivity (four- or eight-side rule) resulted in lower inundation estimates than the zero-side rule (no connectivity). As expected, the four-side rule reduced the number of connections between flooded cells and decreased the area of the landscape that was flooded. The eight-side rule increased the number of connections (relative to the four-side rule) and consequently, and the area that was flooded increased accordingly. Enforcing hydrological connectivity increased the importance of fine-scale landscape features such as ditches and dikes. In the presence of topographic barriers, connectivity forced water to pass around rather than flood low-elevation cells in front of and behind the obstructions. For example, in one location, a dike associated with a road prevented inland inundation only when the four-side rule for connectivity was specified (Figure 20). However, at this same location, flooding extended inland with the zero or eight-side rule because the dike was not recognized with the less constrained connectivity assumptions.

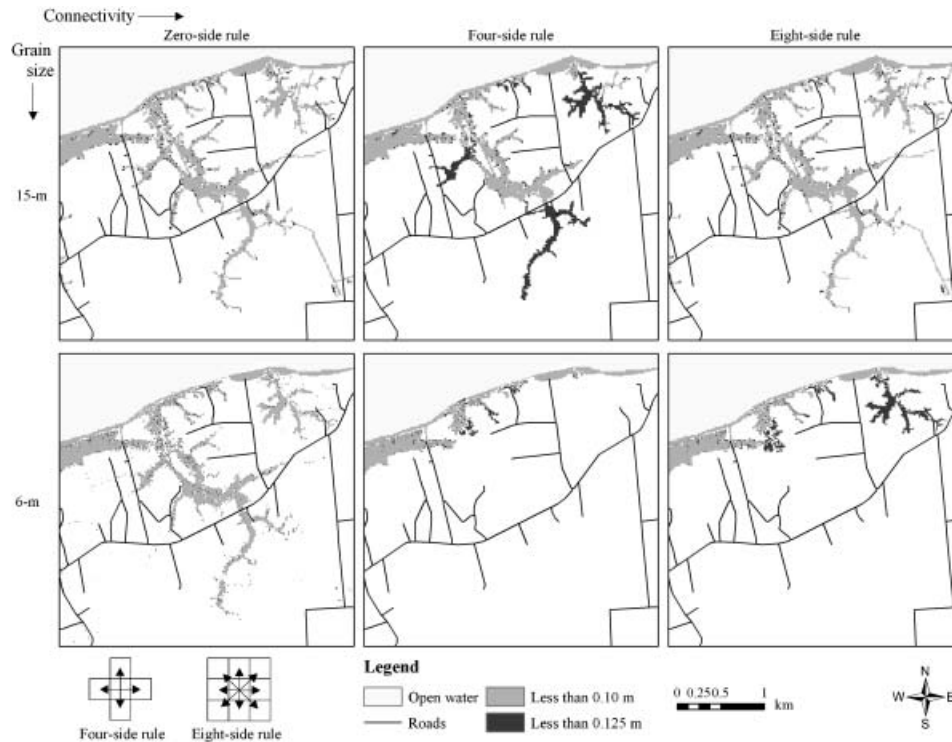


Figure 20 connectivity and resolution effect on 0D DEM-based flood modeling - Poulter et al. 2008²⁹⁵

There are three main advantages of using flat water GIS inundation models. The tools do not require high expertise, so the analysis is cheaper in terms of man hours. Furthermore, this ease of use is complemented with fast production of vulnerability maps of the coastal areas. The final advantage is that policy makers can easily understand and interpret the model results.

The disadvantages of this sort of model are also clear. There is a lack of inclusion of urban infrastructures (i.e. dikes), sediment data, storm tide, waves, wind, and precipitation information and also, feedback systems on hydrological and ecological issues. All this makes the model not very accurate, especially for local purposes. Thus, the inundation model commonly overestimates the flooding areas due to sea-level rise.

5.5.1 0D DEM-based flood model: Literature review

Examples of these rapid models include Gouldby et al. (2008)²⁹⁶, Lhomme et al (2008)²⁹⁷, Liu et al (2009)²⁹⁸ and ISIS FAST(Wicks et al, 2011²⁹⁹).

ISIS-FAST - www.halcrow.com/isisfast

ISIS-FAST is a flood volume spreading algorithm that follows a set of rules governing the routing of water through a series of depressions or 'catchments' on the floodplain, similar in essence to the rapid flood spreading model (RFSM) described in Gouldby et al. (2008)³⁰⁰, Lhomme et al (2008)³⁰¹.

The basic sequence of calculations can be broken down to the following steps:

- Pre-processing of the input raster grid. The pre-processor identifies every point in the DTM that has all its neighbouring points at a higher elevation than itself. Correspondingly, it also finds the set of all points such that water falling on these points will flow towards an identified low point. This set of points is termed a 'depression'. Hence, the entire DTM can be broken into a collection of depressions. Further, the pre-processor sets up stage-area-volume relationships for each depression, defines its neighbours and finds the minimum connection level with each neighbour.
- Main computation phase. The computational engine now introduces water into the depressions linked to the boundary conditions specified. It then checks the water level in each depression. If the water level in any depression is higher than the connection level with its neighbouring depression (and the water level in the neighbour is lower than the water level in depression being considered), then water is distributed between the depression and its neighbour such that volume is conserved and water levels equalized.
- Post-processing phase. Finally, the post-processor projects final water levels for each depression on to the DTM to generate the flood maps.

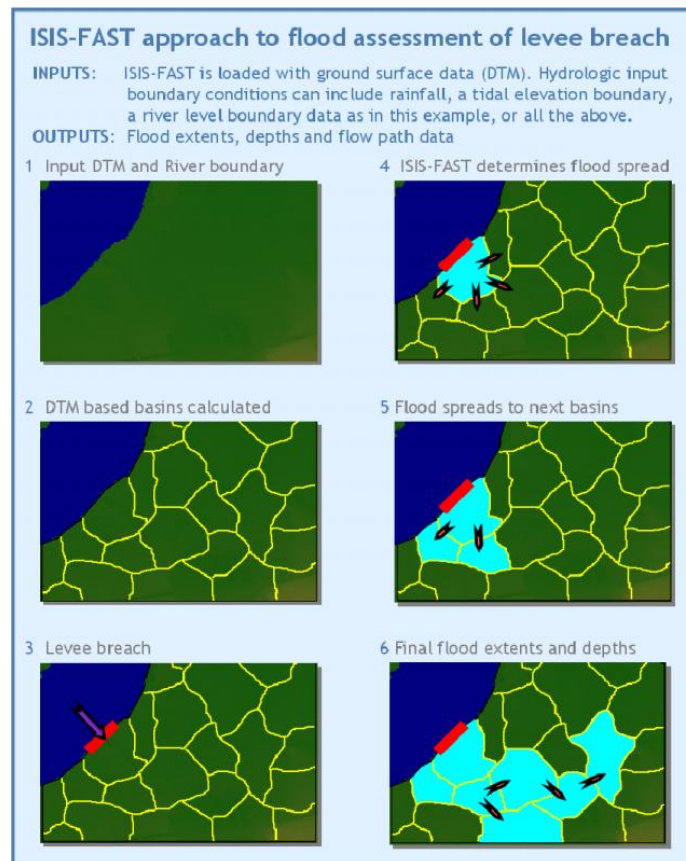


Figure 21 ISIS-FAST - Gouldby et al. (2008)³⁰²

RFSM

Rapid Flood Spreading Model is an irregular storage cell model developed by HR Wallingford (HR Wallingford, 2006³⁰³, Gouldby et al. 2008, Lhomme et al. 2008, Lhomme et al 2009³⁰⁴). RFSM is a simplified hydraulic model that takes as input flood volumes discharged into floodplain areas from breached or overtopped defences, RFSM determines the final inundation extent by distributing a given water volume over the storage cells.

It then spreads the water over the floodplain accounting for the floodplain topography. The output from the model is a flood depth grid of the floodplain area resulting from the input volumes at each defence. The model was specifically developed to provide a fast solution to the flood spreading problem for use in probabilistic flood risk models that consider defence failures (i.e. where many model runs, involving different defence failure combinations, are required).

The pre-process divides the floodplain in elementary areas called Impact Zones (IZs). The IZs represent topographic depressions in the floodplain where the water accumulates in case of flooding (Figure 22).

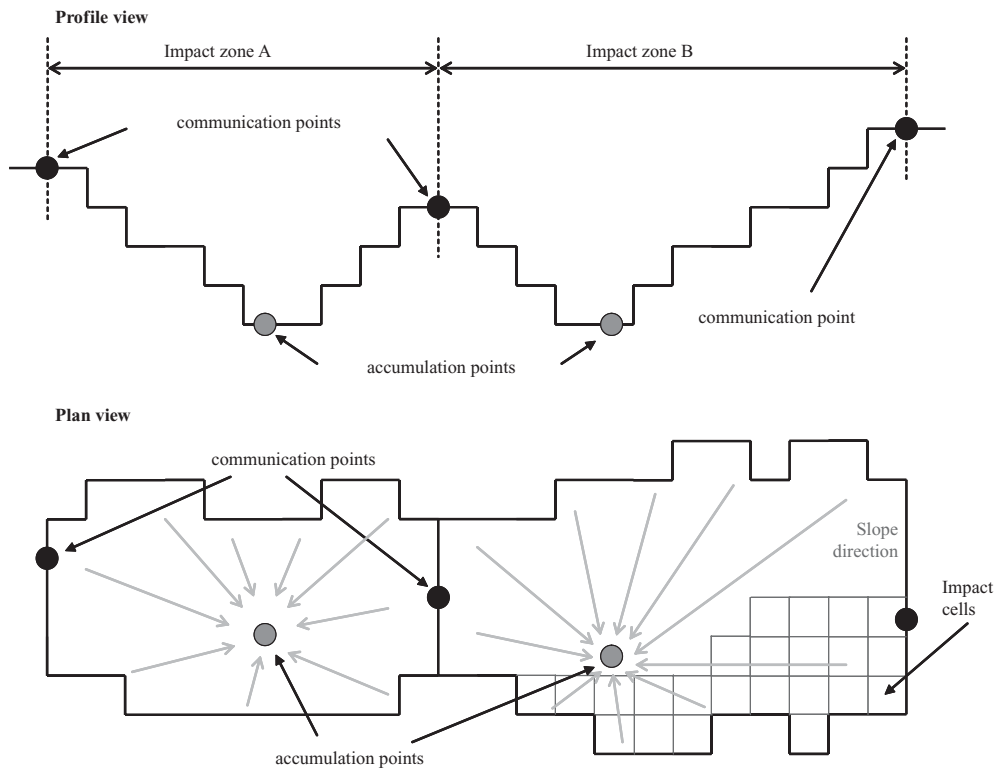


Figure 22 IMPACT ZONE - Gouldby et al. (2008)³⁰⁵

HR Wallingford, 2006³⁰⁶,

The RFSM spreads the flood volumes by filling the IZs adjacent to the input points and spilling the excess to the neighbour IZs. This filling/spilling process is repeated as long as some IZs have volume in excess. When two or more neighbour IZs have the same water level, they are merged into a unique IZ. When all the input volumes have been spread in the IZs and no IZ has excess volume, it is considered that the flood has reached its final state.

This process can be summarized in 5 steps as shown in Figure 3:

- Step 1, the overtopped volume is passed to the IZ adjacent to the defense (IZ B).
- Step 2, the water level is set to the first CL, this allows to calculate the volume stored in the IZ and the excess volume. The excess volume is spilled towards one or more neighbour IZs (IZ C).
- Step 3, the water level in IZ C being set to the first CL, IZ C has the same water level as IZ B.
- Step 4, IZs B and C are merged. The CLs of this merged IZ (IZ BC) are calculated and the water level is set to the first CL. The excess volume is calculated and spilled towards one or more neighbour IZs (IZ A).
- Step 5, the water volume is lower than the capacity of the IZ and the process stops.

Sampson et al 2012³⁰⁷ benchmarked LISFLOOD-FP (Bates 2010³⁰⁸, Bates 2000³⁰⁹, Hunter 2005³¹⁰), a regular grid finite difference model solving a simplified form of the 2D St. Venant Equation (Zero Inertial approach) and the ISIS-FAST (Gouldby³¹¹, Shaad³¹²) a volume spreading method whereby the inflow water volume is transferred between neighbouring grid cells until a steady state water depth has been achieved. The first is an hydrodynamic model that conserve the mass and solve a simplified version of momentum equation, the second is not an hydrodynamic model and conserve only the mass without solving momentum equation. Model have been used to simulate flood events over DEMs derived from terrestrial laser scanning data and airborne LIDAR data at 10 cm and 1 m scales. The variation due to a change from terrestrial to airborne data at 1 m was typically greater than that seen between 10 cm and 1 m simulations run on the terrestrial data alone, and the flood spreading algorithm employed by ISIS-FAST was more sensitive to changes in the DEM than the reduced complexity shallow water formulation employed by LISFLOOD-FP.

ISIS-FAST would be able to tackle considerably larger domains at decimetre scale or, alternatively, undertake Monte-Carlo type studies to address other sources of uncertainty.

(Zerger, 2002)³¹³ and (Zerger, Smith, Hunter, & Jones, 2002)³¹⁴ developed a flat-water (bathtub approach) inundation model to estimate the coastal storm-surge risk in Cairns, Australia. This simple inundation model is implemented using the Arc/Info GIS (ESRI, 1997) and the Arc Macro Language (AML).

(Chen, Hill, & Urbano, 2009)³¹⁵ developed and evaluated a GIS-based urban flood inundation model (GUFIM) in two urban areas in the USA. GUFIM is GIS-based non hydraulic model suitable for places where high-resolution topographic data and/or a hydraulic over-land inundation model are not available.

The flooding model is based in a routing algorithm that iteratively increases water depth of wet cells from topographic depressions (routing-start points) and simultaneously expands wet cells to surrounding low 'dry' cells.

It is very useful for urban planning and emergency preparation because of its time-efficient performance and low to input and hardware requirements

(Wang, Wan, & Palmer, 2010)³¹⁶ presented a water level calculation process for the assessment of optimal flood protection levels in urban flood risk management. The flood spreading model process is treated as a search for optimization problem, where is devised to

move the flood front edges, (initially that are the river boundaries), outwards utilising the standard gradient descent (or steepest descent) method integrated with the digital terrain model to minimize the flood contour energy function(Kass et al. 1987³¹⁷) on the digital terrain's geometrical elevation map. This can determine the flood flow direction and inundation area created with the total flood volume known. The energy function guides the motion of the flood contour towards the final inundation boundaries

Fewtrell et al 2011³¹⁸ describes benchmark testing of a diffusive and an inertial formulation of the de St. Venant equations implemented within the LISFLOOD-FP hydraulic model using high resolution terrestrial LiDAR data. The sensitivity of water elevation and velocity simulations to model formulation and grid resolution are analyzed. The differences in depth and velocity estimates between the diffusive and inertial approximations are within 10% of the simulated value but inertial effects persist at the wetting front in steep catchments

Webster and Stiff 2008³¹⁹ developed a set of spatial analysis tools within a GIS were applied for the construction of flood risk map and to support communities that are vulnerable to coastal flooding from storm surge during high tide which results in flooding and coastline erosion. The accuracy of flood extent mapping with simple raster based models is becoming appropriate with the availability of high resolution topography provided by Airborne Lidar data. Using the ArcMap® environment and Visual Basic Scripting, a toolbox containing a storm surge script was developed which will flood a region of a given Digital Elevation Model (DEM) based on connectivity at user specified increments.

M. G. F. Werner 2001³²⁰ estimates the extent of the river flooding by subtracting the terrain elevation from the water level in the river cross section and computing with a simple cost distance algorithm (ESRI 1996) the accumulated cost to travel from the source of flooding, in this case represented by the river, to each cell of the study area where cost of travelling through each individual pixel along the route is determined by the friction map generated previously by the subtraction.

Marfai 2004³²¹ 2008³²² developed a raster based tidal flood model using ILIWI GIS environment in order to calculate the flooded area using an iterative neighborhood approach. The neighborhood function for tidal flood spreading calculation is an iterative procedure, the calculation stops when difference of the output compared to the input is negligible as show

in the next figure. With the Marfai procedure the extent of flooding is obtained taking into account the pixel elevation and the connectivity with the source of flooding. The inundated area has a logical extent whereby all flooded cells are connected to each other along a (flow) path, rather than simply assuming that all cells lower than the extreme sea-level height will be inundated.

The RASP model developed by Hall et al. (2003³²³) relates the frequency of flooding in a grid cell to the combined probability of defence types within that compartment failing at critical thresholds, thereby generating an expected depth of water, and this model has been used at an aggregated level for a national assessment of flood risk on a 10-km grid within England and Wales

At a more regional level, Nicholls and Wilson (2002) used a GIS-based analysis on a 5-km grid in eastern England to explore links between flooding, biodiversity and agriculture under different future scenarios of climate and socio-economic change.

In Falter et al 2012, two simplified hydraulic models, an inertia-based raster model and the Dynamic RFSM, were compared to a benchmark scenario. The objective was to investigate their ability to simulate a hypothetical inundation scenario, in comparison to the fully dynamic InfoWorks model. The accomplished tests included a sensitivity analysis of the raster model to grid size and of the Dynamic RFSM to time step, with respect to model accuracy and run time. As was expected, the raster-based model delivered the best results at the finest tested grid resolution of 25m corresponding to the original DEM resolution used for the benchmark model. However, the total computational time at this resolution becomes intractable in view of the national scale application. It was shown that the model accuracy deteriorates with increasing grid size, as one would have expected, when the topographic constraints become smoothed by interpolation. Indeed, the inertia model tends to overestimate the inundation extent at coarser grids compared to the benchmark result. Even with its simplified structure that uses a diffusive- wave approximation on an irregular grid, the Dynamic RFSM was able to simulate the maximum inundation extent and depths in a reasonable manner, although problems occurred with very large impact zones delineated in the flat regions of the case study area. Isolated ponds of inundation were simulated in the study area. This effect is caused by the filling of the impact zones that starts from the lowest point. Whenever an impact zone is not completely filled, the crest between the considered impact zone and its neighbours is not inundated. This effect increases with larger inundation

zones and leads to a marked underestimation of inundation extent in the affected areas. These problems are likely to be less dominant in areas with a complex topography where generally smaller inundation zones are delineated

The literature review reported above shows that in order to easily represent and map the patterns of coastal and river flooding GIS raster based models are widely used with particular emphasis in risk assessment applications.

The equilibrium models can be used to map the flood extension related to finite volume discharges (eg. overtopping wave on dune or dikes) through a simple and faster iterative approach that identify the corresponding water level map characterized with a volume of water closest to the computed volume discharge.

Since the raster flooding approach does not require the resolution of PDE equations but rather consists in a simplified method that actually proceeds in the classification or segmentation of topography where the pixels are divided into two classes, flooded or not flooded, as a function solely of the terrain height and the topographic connection with the source of flooding, it follows that it is not necessary, once you accept the simplifying assumptions of the approach, a strong phase of verification and testing of the model similar to what you might require for numerical hydraulic models solving differential equations of S. Venant.

5.6 New GIS-raster-based model for modeling coastal flooding characteristics

This chapter describes the development of new simplified 0D GIS raster-based non hydrodynamic models and routines able to quickly mapping costal flooding characteristics in order to evaluate the risk posed on multiple receptors: population, environment and economy. The coastal flooding characteristics to be modeled for supporting the damage and risk assessment methodology implemented in the Web-GIS DSS are:

- Flooding Extent and Water Depth due to Storm Surge and Wave Overtopping
- Magnitude of flows velocity
- Temporal duration of flooding in the floodplain

Five different models were developed and implemented in the DSS:

1. A flat water 0D GIS-based Storm Surge coastal flooding model with infinite volume of water for open coast – FLOODSURGEMAP
2. A flat water 0D GIS-based Storm Surge coastal flooding model with infinite volume of water for estuarine – FLOODESTSURGEMAP
3. A flat water and mass balance 0D GIS-based finite volume Dike/Dune overtopping flooding model– FLOODTOPMAP
4. A raster based manning coastal flooding flow velocity model – FLOODVELMAP
5. A raster based coastal flooding floodplain duration model – FLOODDURMAP

The above listed models were developed recurring to raster map algebra (Tomlin, 1990³²⁴), watershed segmentation algorithm based on mathematical morphology operator (Meyer and Beucher, 1990³²⁵; Soille and Ansoult, 1990³²⁶) and cost-distance function (ESRI 1996).

The new algorithms were recurring exclusively Open-source software and written with Python programming language exploiting the following libraries:

- Numpy, Scipy
- GDAL
- Mamba
- PIL

The GIS-based models were implemented in the DSS in order to produce flood maps characteristic's as main input for the THESEUS DSS (Zanuttigh et al. 2014) (FP7 Research

Program Innovative technologies for safer European coasts in a changing climate) and for the Web-GIS MARASMA DSS developed in this Thesis.

The algorithms results were evaluated in specific real case studies of the THESEUS EU Project : Bellocchio and Cesenatico in Italy, Santander in Spain, Gironde in France and Teighnmouth in England.

The accuracy of the results is evaluated troughs the comparison with the flooding maps obtained through 2D numerical hydrodynamic models such as MIKE21, TELEMAC.

In the following paragraphs a detailed description of the code is discussed.

In Appendix is reported the code of the models.

5.6.1 A flat water 0D GIS-based Storm Surge coastal flooding model with infinite volume of water for open coast – FLOODSURGEMAP

Here is presented a new 0D GIS-based flat water model for simulating sea level rise induced by storm surge characterized by an infinite volume of water able to fill and flood all the interest floodplain pixels.

The developed model is a seeded region growing type, is based on spreading water between cells in the floodplain taking into account the following main flooding criteria:

- The model floods pixels at low altitude respect the sea water level and connected to the source of flooding (sea)

This model doesn't solve hydrodynamic equation in terms of mass and momentum but simply assess the flood extent and water depth propagating water level across the pixels of a DEM floodplain.

The FLOODSURGEMAP requires as input simply an high resolution topography/bathymetry, usually obtained from topographic DEM or remotely sensed LIDAR, and the specification of water levels for the storm surge scenario.

An important pre-processing phase consists in acquiring the topography and check its consistency in representation of main hydraulic structures such as : river banks, sea walls, dunes, roads, etc.

5.6.1.1 Pre-Processing topography : DEM/Lidar

Both numerical 2D/3D hydrodynamic and 0D flat-water models require an integrated continuous surface combining elevation from the sea/river bed (bathymetry) with the topography from adjacent areas covering the floodplain. This may eventually be complemented by the inclusion of more detailed data representing features that influence

the spread of flooding, such as dykes, dunes, river banks or roads (Poulter and Halpin, 2008³²⁷).

Results of inundation modelling processes are known to be dependent on the properties of the elevation model (Ali et al., 2009³²⁸, Weaver and Slinn, 2010³²⁹ and Cea and French, 2012³³⁰). The channel bathymetry, namely the horizontal resolution, is known to affect the results of models, such as the rate, extent and timing in inundation mapping (Hardy et al., 1999, Omer et al., 2003, Horritt et al., 2006, Buttner, 2007, Raber et al., 2007, Poulter and Halpin, 2008 and Merwade et al., 2008b). Despite these known effects, changes of scale, which result in distinct horizontal resolutions for the input elevation data, may be necessary to obtain files that do not overload the hydrodynamic model.

To create the digital elevation model (DEM) for the simulation stages, data from several sources, formats and acquisition and processing techniques, have to be combined: discrete bathymetry points, surveyed cross-sections, satellite and aerial elevation models and/or imagery, DEMs obtained from paper or digitalized topographic maps (contours and height spots), topographic features such as thalwegs and artificial constructions such as dykes, piers or culverts. These spatial data may be acquired through a range of techniques, such as aerophotogrammetry (Yamano, 2007³³¹ and DiGruttolo and Mohamed, 2011³³²), LiDAR (Coveney and Stewart Fotheringham, 2011³³³ and Pe'eri and Long, 2011³³⁴) or videogrammetry (Long, 2005³³⁵), but the application of those techniques, which provide high-resolution data, is only justified in large areas.

Merwade et al., 2008³³⁶ present a varied set of GIS techniques for merging the datasets of bathymetry and topography from surrounding areas, and acquired by different techniques, in order to create a continuous river and floodplain elevation model. For this, a series of procedures for interpolating and merging those varied datasets is described, but only focused on DEM production

The first step of the methodology consists in processing and integrating the LiDAR data of the study area in order to obtain an a terrain model suitable for the storm surge flood inundation analysis and mapping.

River banks and coastal dune/dikes delineation.

An other key aspect consists in generating a detailed river terrain model with a good representation of centerline, thalweg and river banks and integrating it into LIDAR DEM. The LIDAR in fact can't detect river cross section elevation due to water obstacle.

Bank delineation represent a crucial step in order to represents accurately the storm surge flood for the river connected to coastline.

Delineation of river boundary is one of the key inputs in hydraulic modeling, floodplain mapping, channel migration studies, habitat classification, hydraulic geometry relationships, etc. In most cases, the river banks are manually delineated using aerial photographs.

As reported in Merwade et al 2008³³⁷ multiple approaches are used to create river terrain models for 2D/3D hydrodynamic modeling and flood inundation mapping. These include interpolation of surveyed cross-sections, interpolation of discrete bathymetry points collected using echosounding techniques, and integration of surrounding topography with surveyed cross-sections and/or bathymetry points including breaklines (e.g., thalweg).

Because geometric descriptions of channel bathymetry and its surrounding topography affect hydrodynamic modeling of river channels including storm surge inundation mapping (Hardy et al., 1999³³⁸; Horritt et al., 2006³³⁹; Buttner, 2007³⁴⁰; Raber et al., 2007³⁴¹), it is important to understand and address the issues associated with creating river terrain models using conventional approaches.

In this case, the GIS simple linear interpolation technique for cross-sections developed by Merwade et al. 2008 is applied to the river cross sections present in the study area. Thanks to the LIDAR high accuracy a semi-automatic GIS procedure was applied in order to correct the LIDAR "errors", such as the detection of "holes" along the river banks. Each river bank area was identified by a buffer zone of 10 m from the river boundary. The GIS interpolation techniques produce an interpolated mesh of cross-sections and profile-lines as shown in the Figure 23

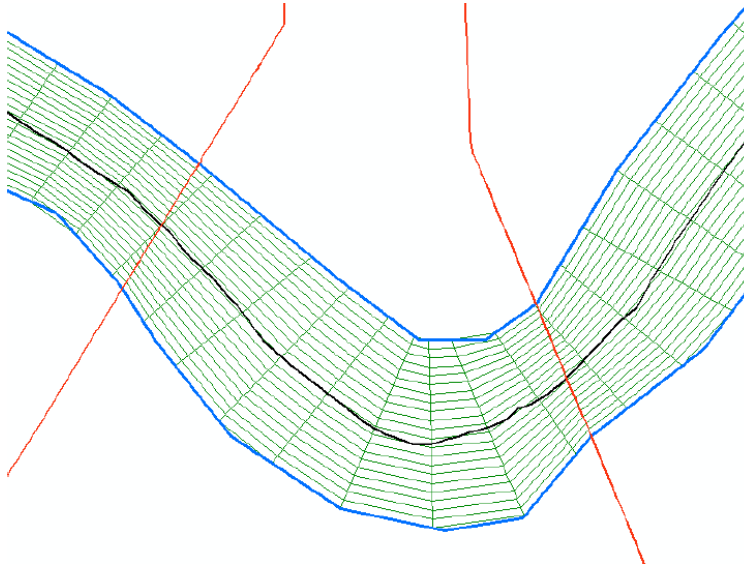


Figure 23 River Cross-section interpolation - Merwade et al 2008³⁴²

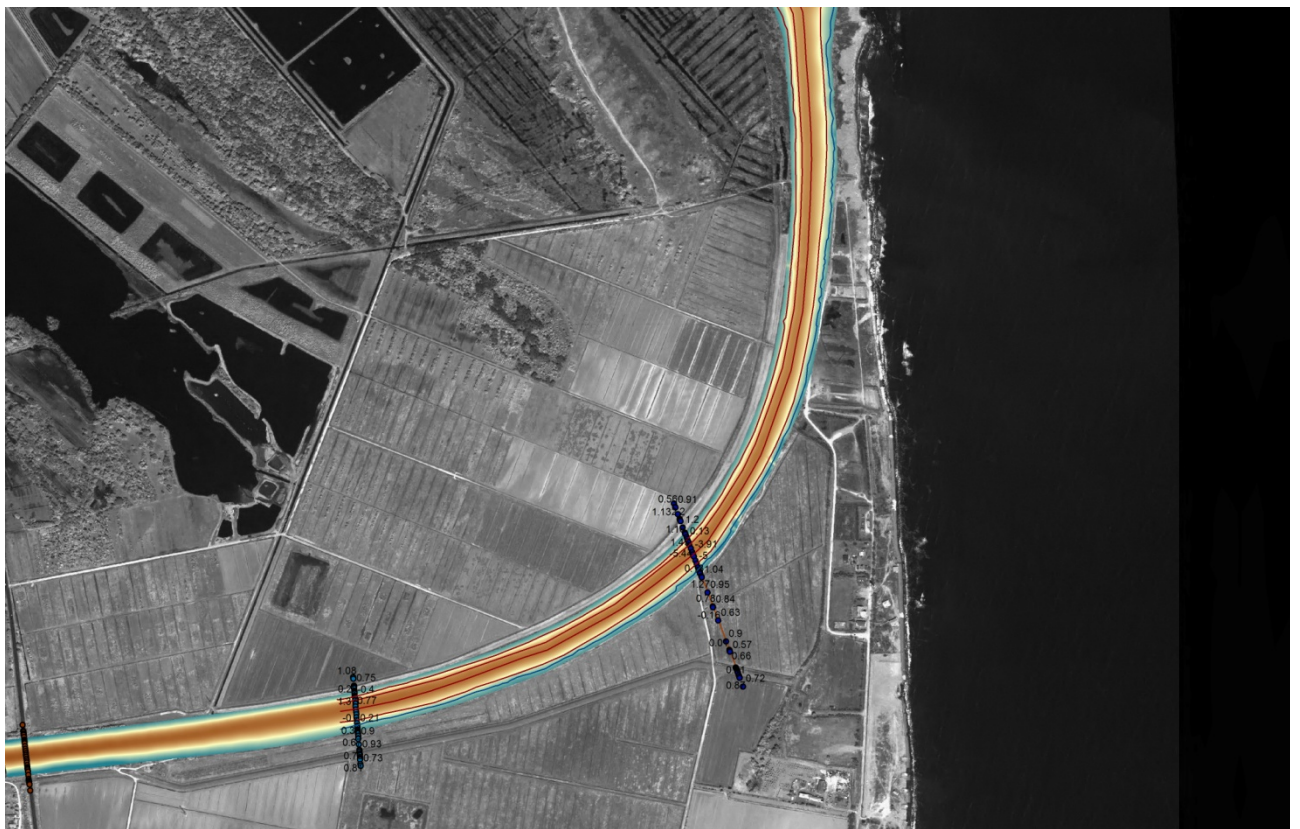


Figure 24 River Cross-section interpolation – Case Study Cesenatico

River Banks Delineation

Automatic GIS and image-processing methodology were developed (Venkatesh Merwade and David Maidment) for delineating river bank from aerial photographs and LIDAR data. Due to high accuracy of the LIDAR a semi-automatic procedure was applied in order to correct the LIDAR error (hole) detection in the river bank zone. In particular for each river

bank area identified by a buffer zone of 10 m from the river boundary was developed a semi automatic GIS procedure in order to fill the holes that may be present.

The GIS bank delineation algorithm assign for each pixel in the buffer bank area an altitude value that is:

$\max(Z_{\text{lidar}} \text{ and } Z_{\text{bank}})$

where

- Z_{lidar} is the altitude detected by the LIDAR
- Z_{bank} is an user defined value of the bank height retrieved by direct measure (GPS) or design information

A future development of the algorithm will be to introduce an automatic river bank delineation procedure based on GIS and Image segmentation function to the LIDAR data.

<http://www.shim.bc.ca/methods/top%20of%20bank%20report.pdf>

<http://proceedings.esri.com/library/userconf/proc05/papers/pap2041.pdf>

Terrain Data Integration

The last step of the pre-processing phase consist in integrating main channel bathymetry with surrounding topography .

This simplified approach neglects the following complex issues:

- the boundaries of the main channels do not always match exactly with the channel representation in the surrounding topography datasets;
- LIDAR data for floodplains are usually processed through a filtering algorithm to remove vegetation effects. The density of vegetation and assumptions made in applying filtering algorithms may affect the capability of LIDAR to accurately represent channel bank elevations.

Considering these issues, a simple smoothing algorithm –following Merwade et al. (2008) was introduced with the sole objective of creating a smooth transition between integrated datasets .

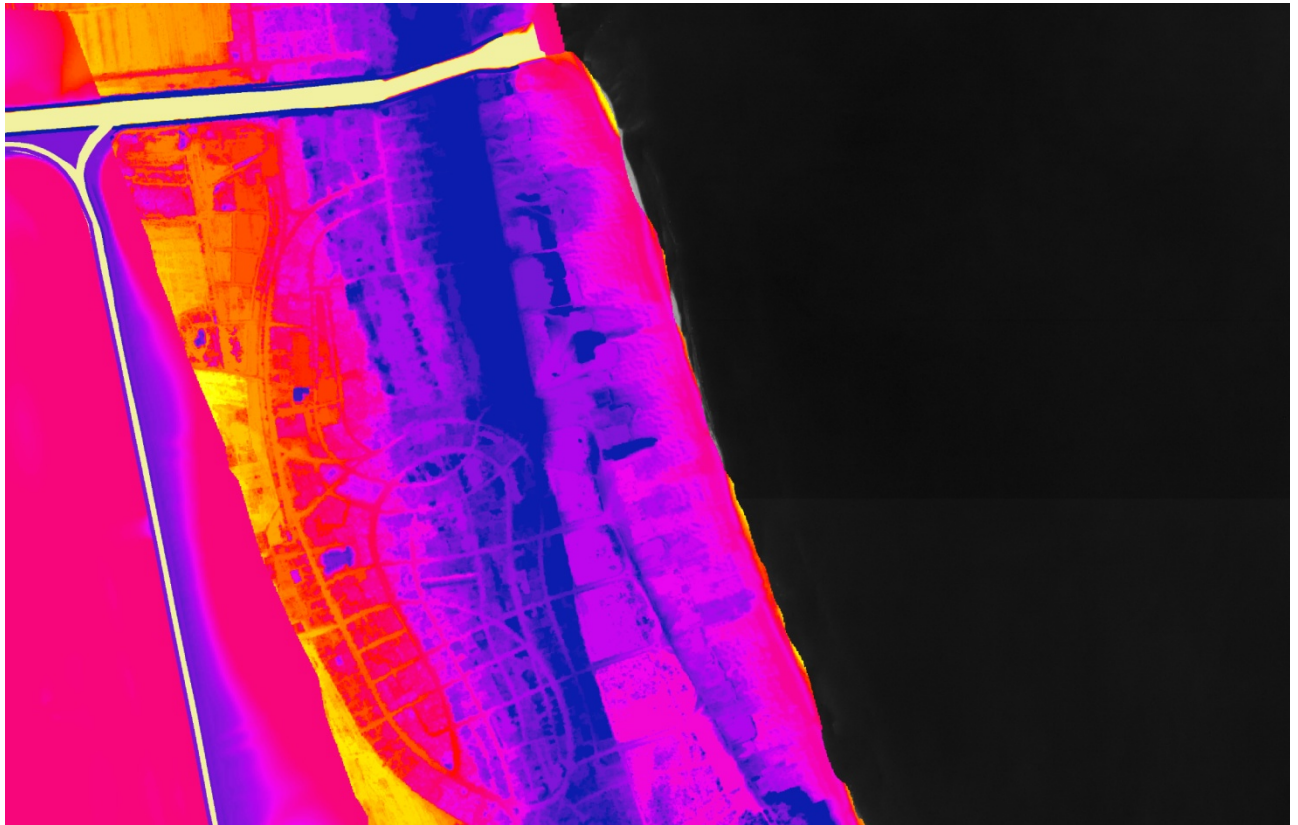


Figure 25 Integration of the channel bathymetries with the surrounding datasets

In the next figure is reported the processed topography for the Cesenatico study site, obtained integrating and processing LIDAR, topographic contour levels and river cross section provided by Regione Emilia Romagna.

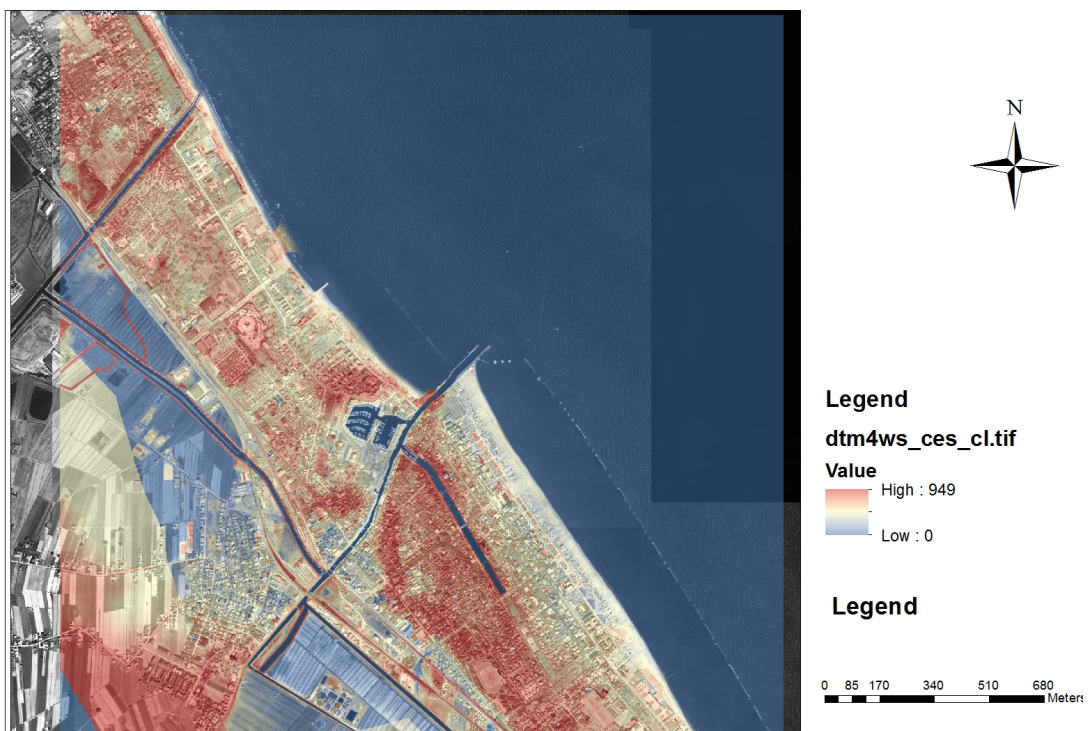


Figure 26 Cesenatico topography/bathymetry

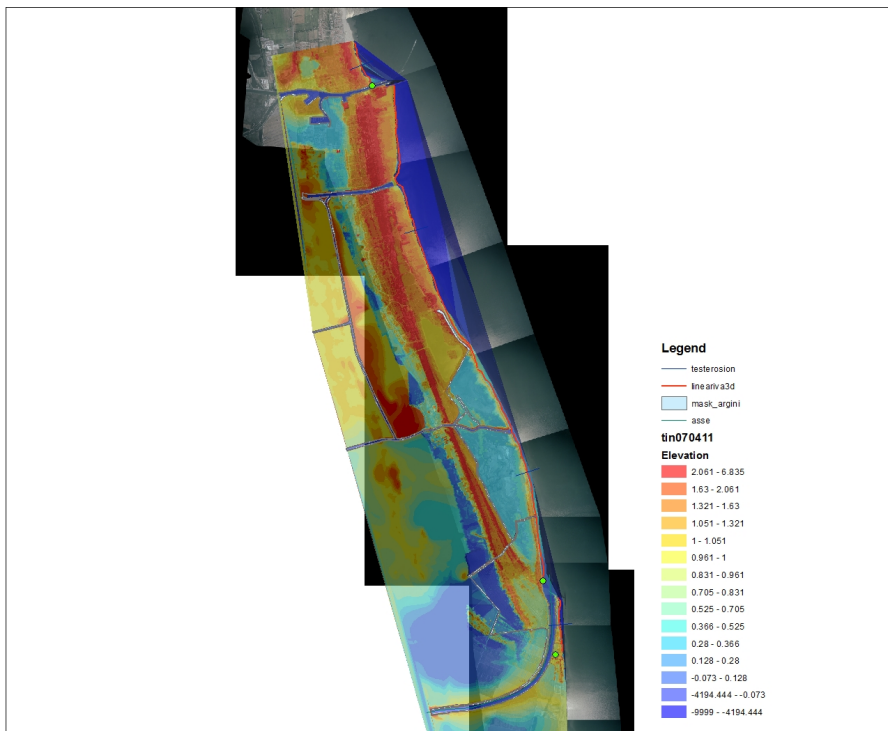


Figure 27 Bellocchio topography/bathymetry

5.6.1.2 Mathematical Morphology and Watershed Segmentation algorithm

Mapping of flooded area due to a specific storm surge height or water inundation head can be developed in a raster based scheme using the marker controlled watershed segmentation algorithm as described in by Meyer and Beucher (1990) and in Soille and Ansout (1990³⁴³), Soille 2003³⁴⁴.

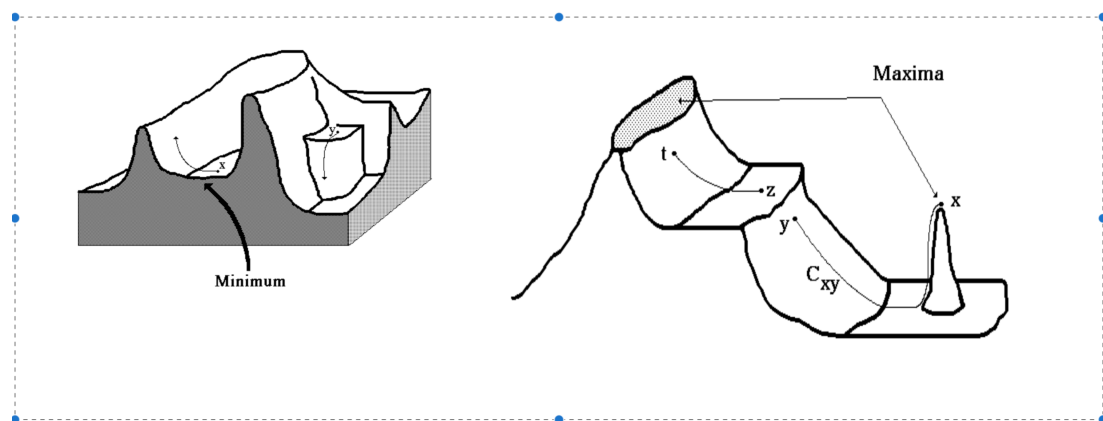
In grey scale mathematical morphology the watershed transform, originally proposed by Digabel and Lantuejoul^{345 346} and later improved by Beucher and Lantuejoul³⁴⁷, is the method of choice for image segmentation (Beucher 1990³⁴⁸, Vincent and Soille 1991³⁴⁹ Serra 1982³⁵⁰). Generally spoken, image segmentation is the process of isolating objects in the image from the background, i.e., partitioning the image into disjoint regions, such that each region is homogeneous with respect to some property, such as grey value or texture (Haralick and Shapiro 1985³⁵¹).

The concept of watersheds comes from the field of topography, referring to the division of a landscape in several basins or water catchment areas. A good example is the *continental divide* that separates the USA into two main regions: one associated with the Atlantic Ocean,

and another associated with the Pacific Ocean. So, on rainy days, all the drops of rain that fall on one side of the divide flow into one ocean, while rain falling on the other side of the division will flow into the other ocean. It is clear that the water will reach the ocean provided that it is not trapped in a local minimum along the way. Both regions are usually named catchment basins, and each one has an associated minimum (the oceans).

The border line that separates both basins is called the watershed line, corresponding to the continental divide in the example. From this point of view, we can consider the image as a topographic surface where each pixel is a point situated at some altitude as a function of its grey level.

The watershed transform can be classified as a region-based segmentation approach. The intuitive idea underlying this method comes from geography: it is that of a landscape or topographic relief which is flooded by water, watersheds being the divide lines of the domains of attraction of rain falling over the region. An alternative approach is to imagine the landscape being immersed in a lake, with holes pierced in local minima. Basins (also called 'catchment basins') will fill up with water starting at these local minima, and, at points where water coming from different basins would meet, dams are built. When the water level has reached the highest peak in the landscape, the process is stopped. As a result, the landscape is partitioned into regions or basins separated by dams, called watershed lines or simply watersheds.



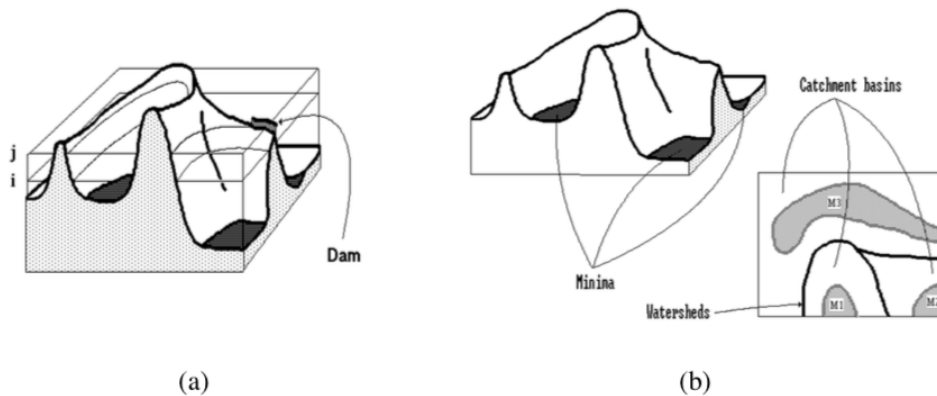


Figure 28 Flooding a DEM and dam building (a), catchment basins (b) Beucher and Meyer 1993³⁵²

The traditional implementation of the watershed segmentation algorithm simulates the flooding process over the image surface. First, regional minima are detected and uniquely labelled with integer values. Then, the algorithm simulates the flooding process using a hierarchical queue (Beucher and Meyer 1993³⁵³, Meyer 1994³⁵⁴, Beucher and Beucher 2011³⁵⁵).

In this case the watershed segmentation flooding concept is applied to a real DEM in order to extract all the pixel flooded by a specific water level and connected to the source of flooding. In particular the source of flooding represented by a single pixel located in the sea or where overtopping can occur is considered as local minima or the source/hole from which inundation initiate to filling the DEM until a specific water level is reached. The result is a binary image (flooding extent), representing a partition of DEM in non-flooded and flooded pixel for a specific water level propagate from the source.

The map of water depth can be easily computed using the following map algebra equation:

$$\text{Water_Level} * \text{Flood_Extent} - \text{DEM} \quad \text{Eq. 16}$$

The flooding simulation of a DEM with a known source of flooding, in case of coastal flooding related problem is located in the sea, can be modeled using the above described watershed transformation.

This approach can extract flooded pixel that are connected to the source of flooding with a height on sea level less than storm surge or water inundation head.

The algorithm is based on the assumption that the terrain model represented by a floating image can be flooded from a specific seed or source (usually the minima) defining a specific water level. The result is the watershed area flooded by each source.

Through this algorithm is possible to produce inundation flood map for different storm surge water levels and with multiple sources of flood. The algorithm floods each pixel that is

located on a lower level with respect to the fixed storm surge water level and that appears to be connected to the flooding sources.

The flooding using watershed transform is controlled simply by height or water level imposed at the source of flooding. This means that, when the flooding has reached an altitude where it can flood an adjacent catchment basin, this catchment basin and also other catchment basins are immediately totally flooded up to the imposed level of water at the source. The topography of these catchment basins has no importance since the flooding is immediate and not hydrodynamically controlled by these catchment basins.

Usually in case of storm surge events due to sea level rise, the volume of water available can be considered as infinite, and the extent of flooded area is controlled only by the sea water level .

The algorithm FLOODSURGEMAP implement the watershed transform as defined in Beucher and Meyer 1993³⁵⁶ through the use of MAMBA library (<http://www.mamba-image.org>).

In Appendix is reported the python code of the FLOODSURGEMAP.

5.6.1.3 Model Benchmark

In this section the FLOODSURGEMAP model, a new 0D DEM-based coastal flooding model is tested through a benchmarking with results obtained with hydrodynamic 2D numerical models such as MIKE 21 and Telemac.

Several tests were conducted simulating coastal floodplain flooding due to sea level rise induced by storm surge scenarios. The tests were applied in 5 Theseus study sites such as Cesenatico and Bellochio in Italy, Santander in Spain, Plymouth in UK and Gironde in France. In the following figures are reported the results in terms of coastal flooding extent and water depth due to different storm surge scenarios applied in the case studies.

Coastal flooding maps are derived with two methodologies:

- A detailed modeling by means of an ad hoc procedure coupled with a 2DH shallow water model (Mike 21 and Telemac)
- A simplified modeling based on the comparison of bottom elevation and flood level.

The basic idea is to compare the results obtained with the two methods to guarantee that the simplified model – to be used in the Decision Support System tool – provides reasonable results.

Both modeling approaches were applied on the same storm surge scenario and Digital Terrain Model reconstructed from Lidar or topographic data available in the area.

Bellocchio Benchmarking

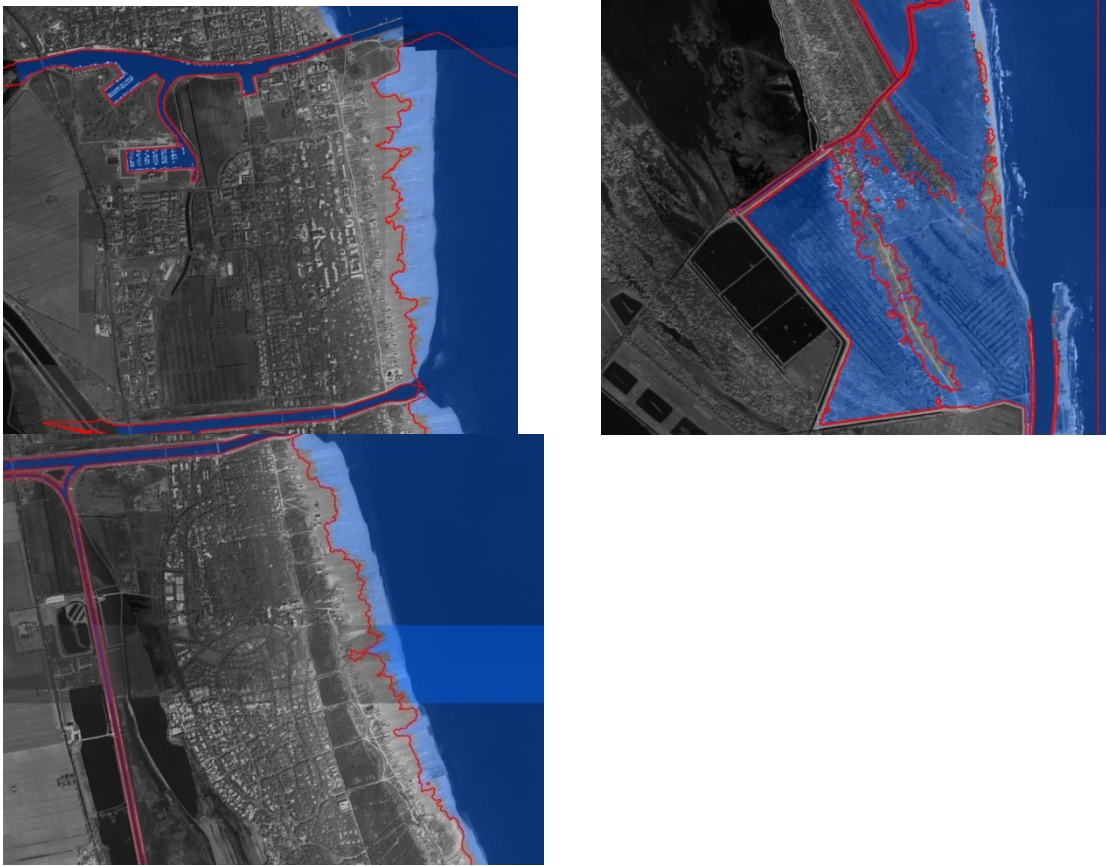


Figure 29 Comparison among flooded areas obtained with the simplified modeling tool (yellow areas) and the maximum flood extension derived from simulations with MIKE 21 (red contours). Two areas are show in the pictures above: Lido degli Estensi and Lido di Spina (to the top) and the outlet of Foce Rento (to the bottom). Scenario with $T_r=50$ years Scenario 2010

The FLOODSURGEMAP output in terms of extent of flooding and water depth is matching the results obtained with MIKE21 and Telemac as reported in previous maps.

The tests conducted comparing the results obtained with hydrodynamic 2D numerical models and the 0D DEM-based equilibrium models, shows how mapping costal flood extent can be conducted with high accuracy with the second approach in case are available high resolution DEM or Lidar.

5.6.1.4 FLOODSURGEMAP Model Application

The developed model is embedded in the THESEUS DSS and in the WEB-GIS MARASMA DSS. Under the Theseus project the model was applied in order to map coastal flooding extent and water depth in Cesenatico/Bellocchio and Teinghamouth.

Cesenatico and Bellocchio Case Study

The two sites on which THESEUS activities are specifically focused are: Cesenatico, an urbanised area with high touristic value, and Bellocchio, an area that is particularly exposed to flooding, characterized by high ecological value (natural park, protected species, Ramsar site), urban areas and fishing activities. Both sites suffer from the interaction of drainage/irrigation systems with the sea during storms. Most intense storm events come from Bora (NE) and Scirocco (SE) with similar intensity; waves may reach 3.5 m every year and rise to 6 m every 100 years. Wind is stronger from the shorter fetch sector of Bora where it frequently reaches an intensity of about 35 knots, whereas from the longer fetch sector of Scirocco it seldom exceeds 30 knots. The tidal range is low, on average spring tide are in the range ± 0.4 m and extreme values around ± 0.85 m.

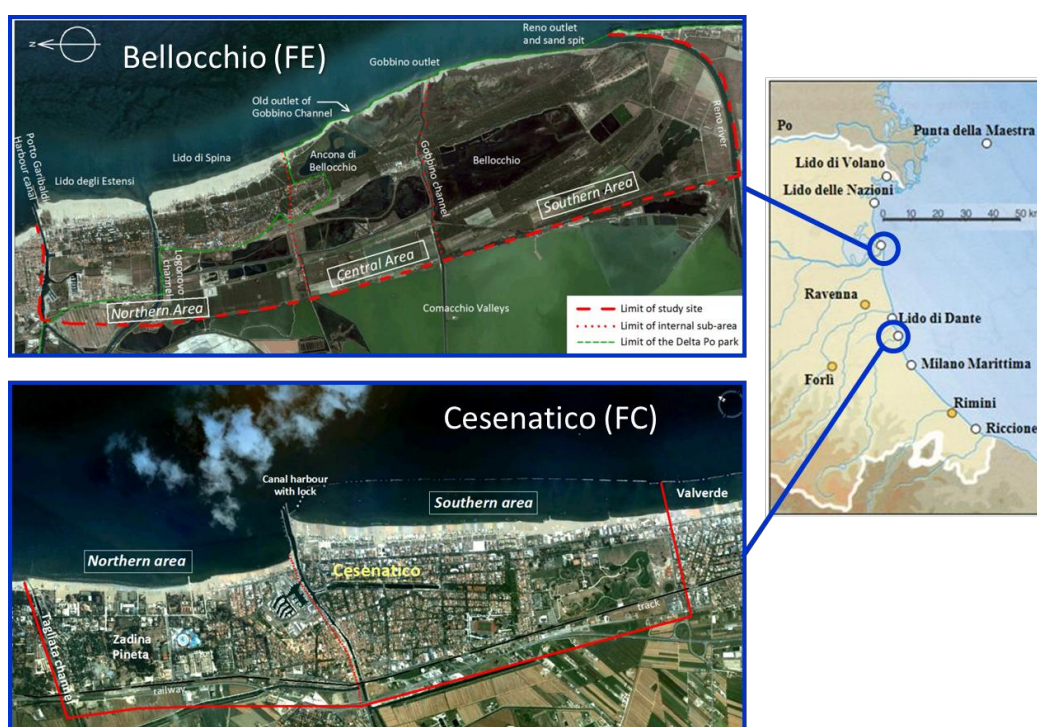


Figure 30 Cesenatico and Bellocchio case studies

The next maps display the coastal flooding extent and water depth related to the storm surge scenario reported in next table.

Scenario	Zr, m		Return period, years							
			2	5	10	20	25	30	50	100
2010 Present	0	Sop, %	1.305	1.977	2.329	2.619	2.703	2.770	2.946	3.163
		Zm, m	1.143	1.238	1.287	1.328	1.340	1.349	1.374	1.404
		Hs, m	2.204	3.072	3.537	3.923	4.036	4.124	4.358	4.647
2020 Short term	0.07	Sop, %	1.208	1.713	1.976	2.194	2.258	2.308	2.439	2.603
		Zm, m	1.110	1.201	1.248	1.287	1.298	1.307	1.331	1.360
		Hs, m	2.132	2.754	3.070	3.326	3.399	3.457	3.607	3.790
2050 Mid term	0.13	Sop, %	1.596	2.746	3.348	3.845	3.989	4.103	4.404	4.776
		Zm, m	1.150	1.261	1.319	1.367	1.381	1.392	1.421	1.457
		Hs, m	2.397	3.779	4.585	5.286	5.495	5.661	6.106	6.668
2080 Long term	0.22	Sop, %	1.524	2.223	2.589	2.890	2.978	3.047	3.230	3.456
		Zm, m	1.175	1.305	1.372	1.428	1.444	1.457	1.491	1.533
		Hs, m	2.362	3.120	3.512	3.831	3.923	3.995	4.184	4.416

Table 8 Extreme storm surge (Zm) and wave height (Hs) scenario

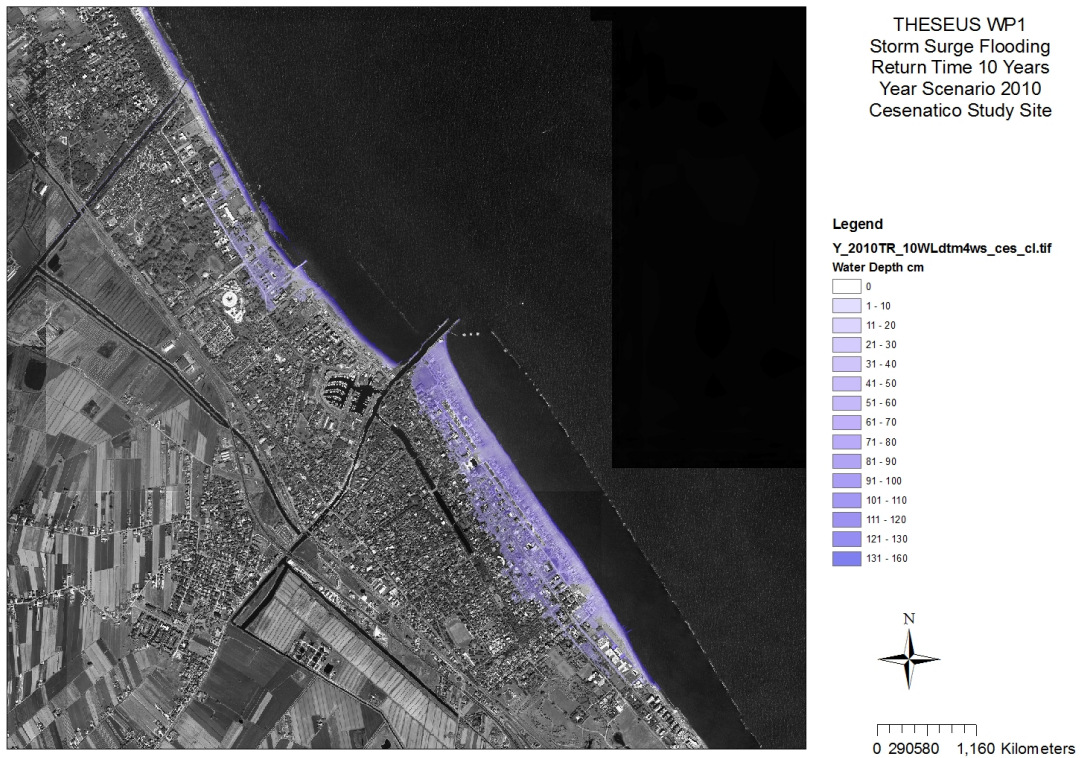


Figure 31 Cesenatico storm surge flooding – TR=10 years Scenario 2010

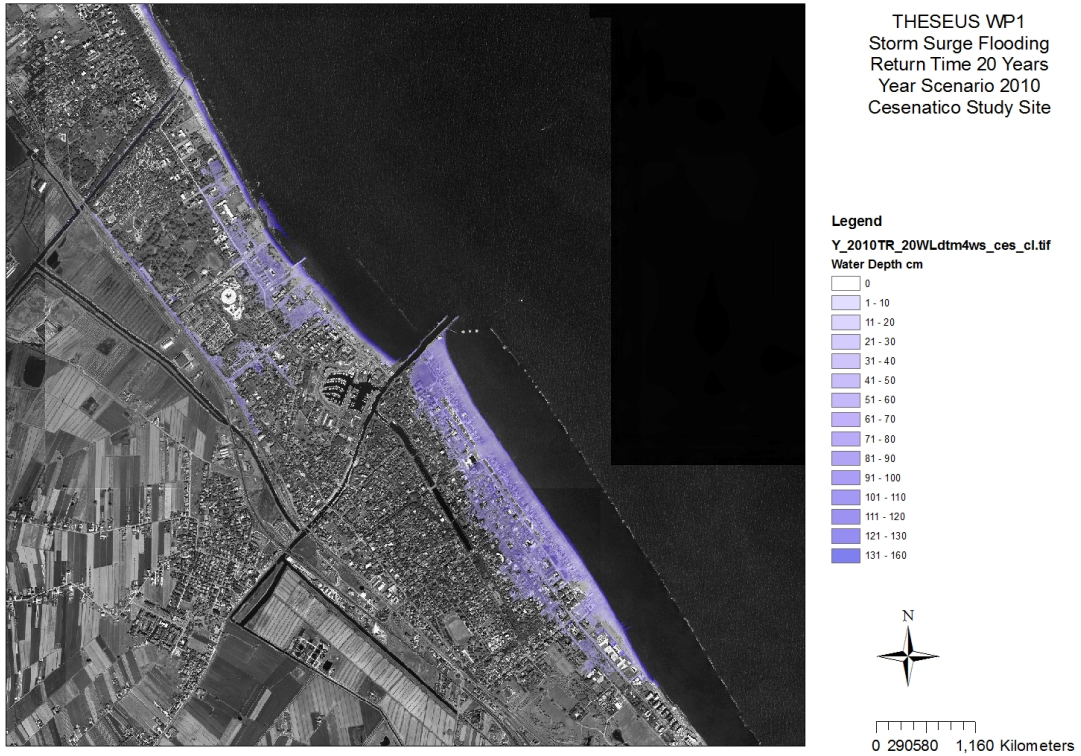


Figure 32 Cesenatico storm surge flooding – TR=20 years Scenario 2010

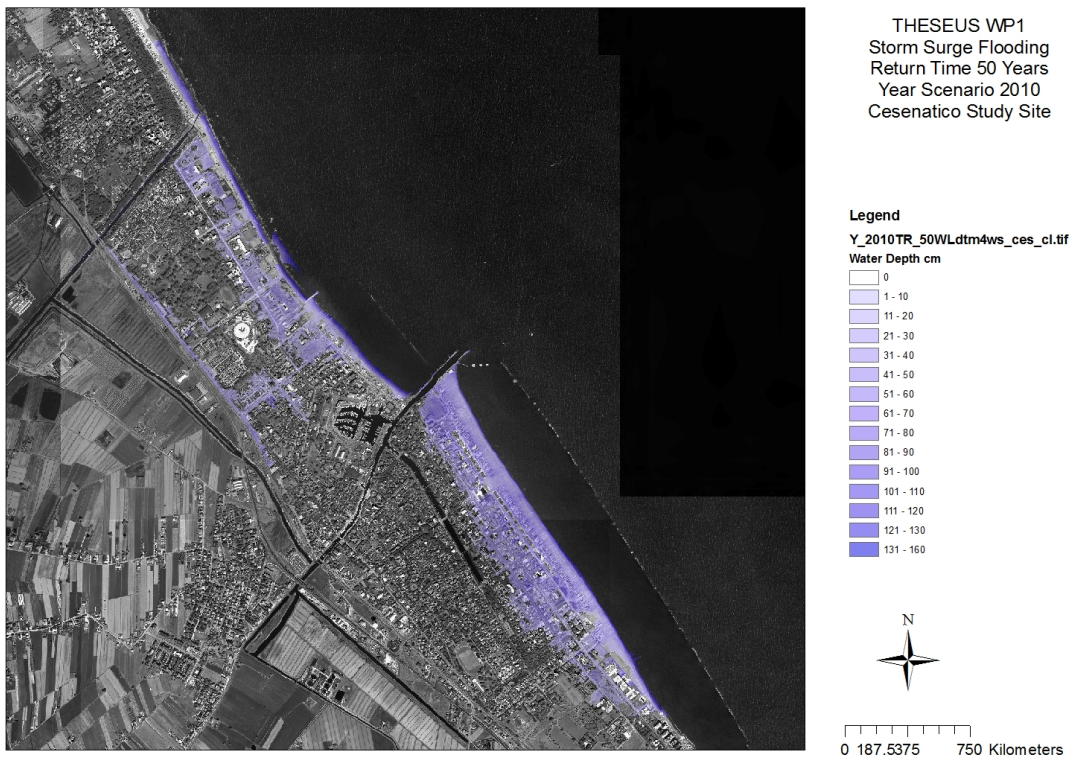


Figure 33 Cesenatico storm surge flooding – TR=50 years Scenario 2010

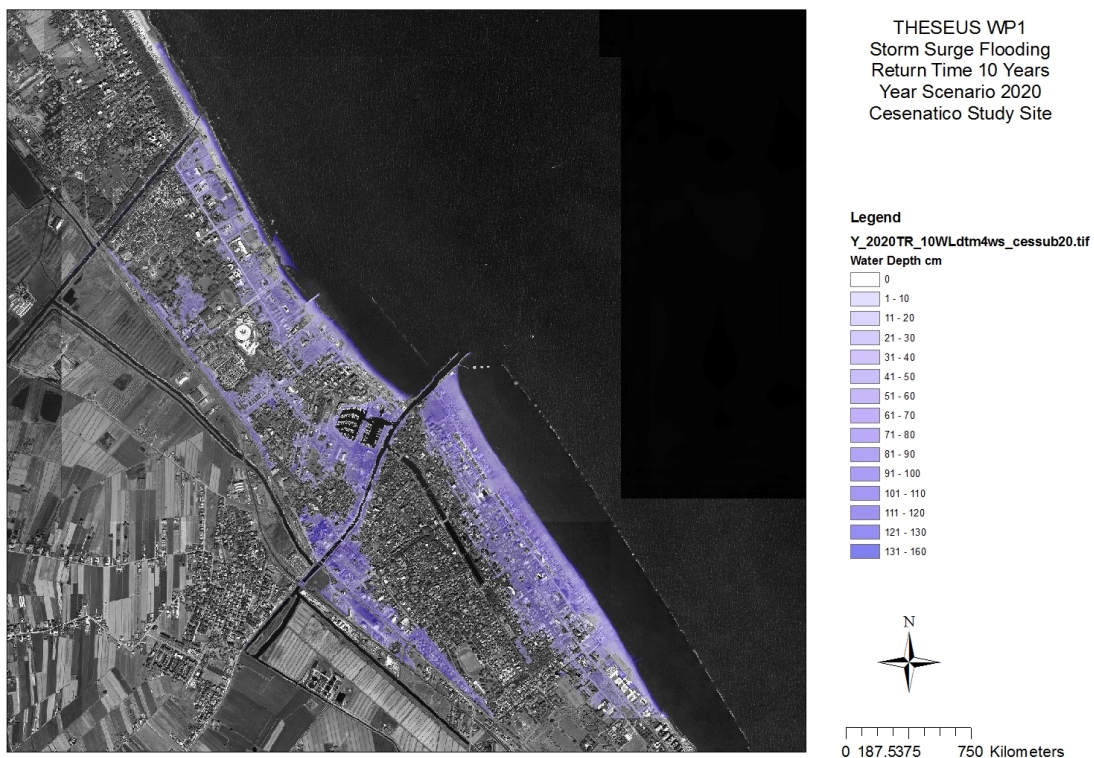


Figure 34 Cesenatico storm surge flooding – TR=10 years Scenario 2020

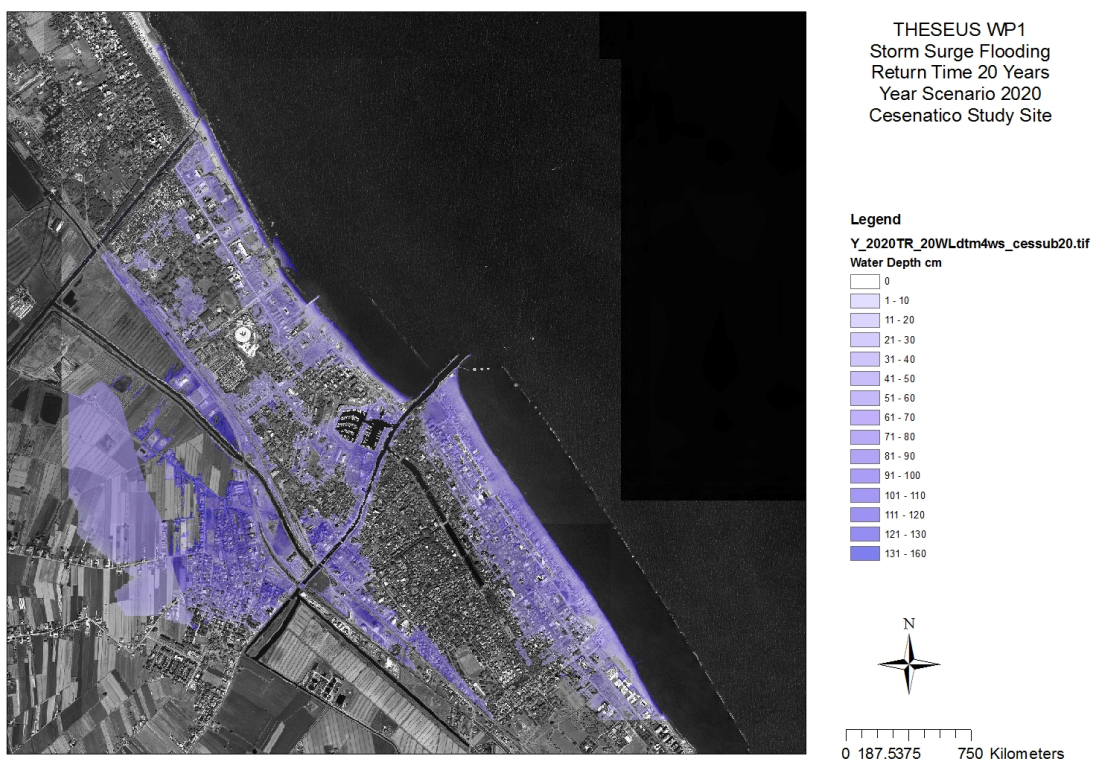


Figure 35 Cesenatico storm surge flooding – TR=20 years Scenario 2020

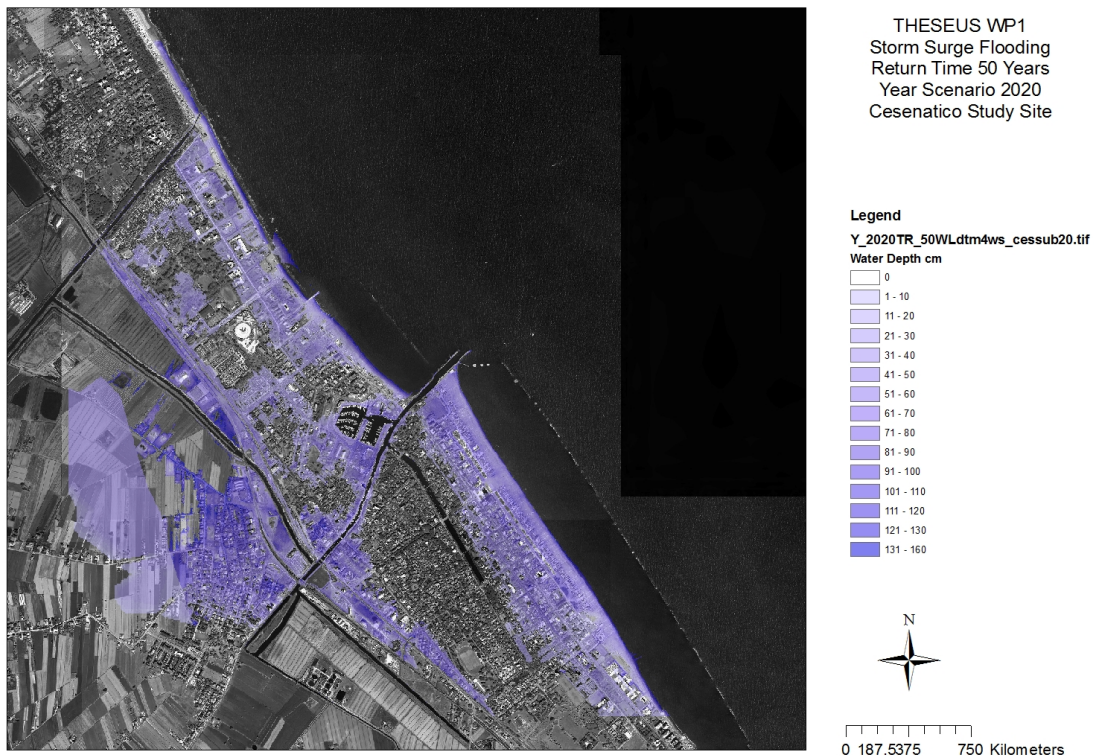


Figure 36 Cesenatico storm surge flooding – TR=20 years Scenario 2020

Teignmouth Case Study

The Teignmouth Sound to Exe Estuary site is located in southwest England, see Figure 53a, encompassing a 100 km stretch of coastline bordered by the English Channel. The site is one of the most diverse coastal settings in Europe and incorporates a range of habitats from exposed rocky and shingle coast to sheltered mud of flooded valleys or 'rias' together with densely populated urbanised and industrial zones of Plymouth Sound, Torbay and Exeter.



Figure 37 Teignmouth Case Study

Four climate scenarios which cover the coming 100 years are (1) Present; (2) Short-term; (3) Mid-term and (4) Long-term scenarios. The year of the Present Scenario is set to be 2010. Details of the other 3 scenarios are given in Table 10. Each of the scenario is subdivided into 4 categories to correspond to the return periods of combined high tide and surge of 1 in 20, 100, 200 and 1,000 years. Altogether there are 16 climate scenarios for analysis.

Return period (year)	Extreme water levels (tide + surge) (mOD)
20	2.955
100	3.157
200	3.244
1,000	3.444

Table 9 The predicted extreme water levels at Teignmouth

Return Period (Year)	Present Scenario (2010)	Short-term Scenario (2010 - 2040)	Mid-term Scenario (2040 - 2070)	Long-term Scenario (2070 - 2100)
	Year of Representation			
	2010	2025	2055	2085
20	<i>Scenario P20</i>	<i>Scenario S20</i>	<i>Scenario M20</i>	<i>Scenario L20</i>
100	<i>Scenario P100</i>	<i>Scenario S100</i>	<i>Scenario M100</i>	<i>Scenario L100</i>
200	<i>Scenario P200</i>	<i>Scenario S200</i>	<i>Scenario M200</i>	<i>Scenario L200</i>
1000	<i>Scenario P1000</i>	<i>Scenario S1000</i>	<i>Scenario M1000</i>	<i>Scenario L1000</i>

Table 10 Sea-level rise scenarios for flood simulation

The projected sea-level rise from year 2010 to 2110 based on PPS25 is plotted in Figure 38. By combining the extreme sea-levels in Table 9 with the projected sea-level rises, the predicted sea-level under each climate scenario is worked out and summarized in Table 11.

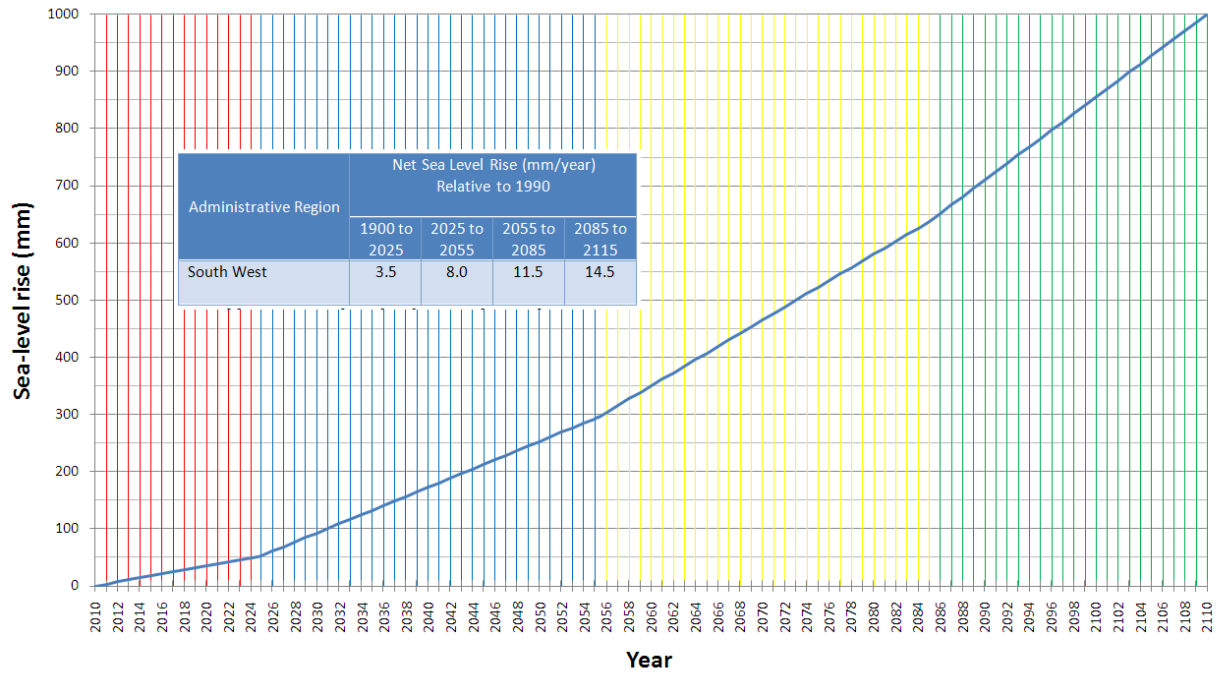


Figure 38 Projected sea level rise

Return Period (year)	Present Scenario (2010)	Short-term Scenario (2010 - 2040)	Mid-term Scenario (2040 - 2070)	Long-term Scenario (2070 - 2100)
	(tide+surge+sea-level rise) (mOD)	(tide+surge+sea-level rise) (mOD)	(tide+surge+sea-level rise) (mOD)	(tide+surge+sea-level rise) (mOD)
20	2.955 + 0 = 2.955	2.955 + 0.053 = 3.008	2.955 + 0.2925 = 3.248	2.955 + 0.6375 = 3.593
100	3.157 + 0 = 3.157	3.157 + 0.053 = 3.210	3.157 + 0.2925 = 3.450	3.157 + 0.6375 = 3.795
200	3.244 + 0 = 3.244	3.244 + 0.053 = 3.297	3.244 + 0.2925 = 3.537	3.244 + 0.6375 = 3.882
1,000	3.444 + 0 = 3.444	3.444 + 0.053 = 3.497	3.444 + 0.2925 = 3.737	3.444 + 0.6375 = 4.082

Table 11 Extreme sea-levels for 16 sea-level rise scenarios at Teignmouth

Return Period (year)	Present Scenario (2010)	Short-term Scenario (2010 - 2040)	Mid-term Scenario (2040 - 2070)	Long-term Scenario (2070 - 2100)
	(tide+surge+sea-level rise) (mOD)	(tide+surge+sea-level rise) (mOD)	(tide+surge+sea-level rise) (mOD)	(tide+surge+sea-level rise) (mOD)
20	P20 = 2.955	S20 = 3.008	M20 = 3.248	L20 = 3.593
100	P100 = 3.157	S100 = 3.210	M100 = 3.450	L100 = 3.795

200	P200 = 3.244	S200 = 3.297	M200 = 3.537	L200 = 3.882
1,000	P1000 = 3.444	S1000 = 3.497	M1000 = 3.737	L1000 = 4.082

Table 12 Selected sea-level rise scenarios for display in time series

In the next figure are displayed the flooding maps obtained using the storm surge levels with return time 100 years and generated using a ARCGIS procedure developed by Kwan 2011 and combining the information from LiDAR and topographical data obtained from the Plymouth Coastal Observatory (<http://www.channelcoast.org>) and from the DIGIMAP (EDINA, 2011³⁵⁷)

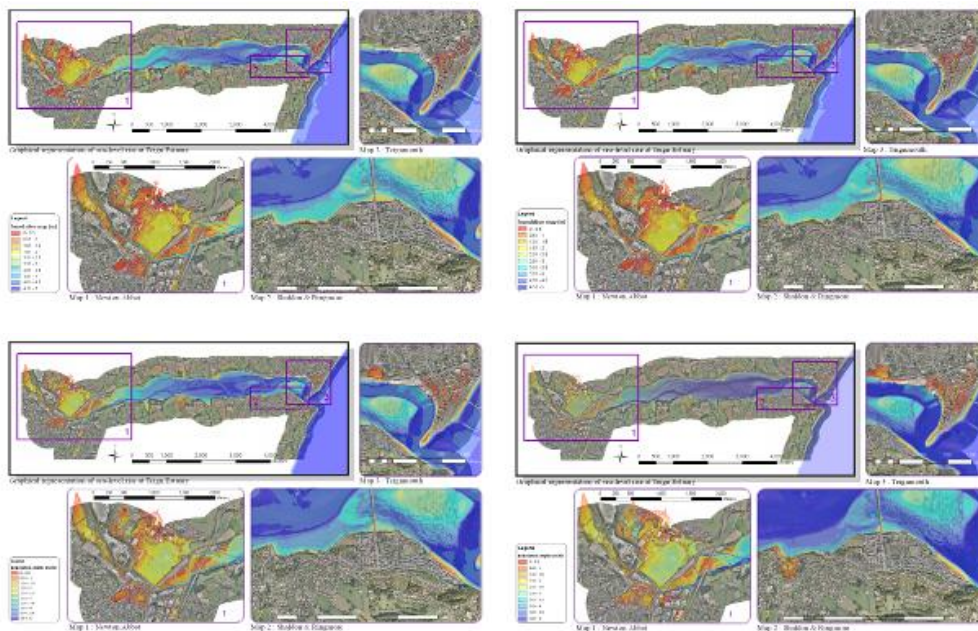


Figure 39 Flood Hazard Maps (water depth) for present, short, mid and longterm scenario with return period 100 years – ARCGIS Model Kwan 2011

In the next maps are displayed the results for the same storm surge scenarios (Return Period 100 years) obtained with the new 0D DEM-based model developed in this thesis.

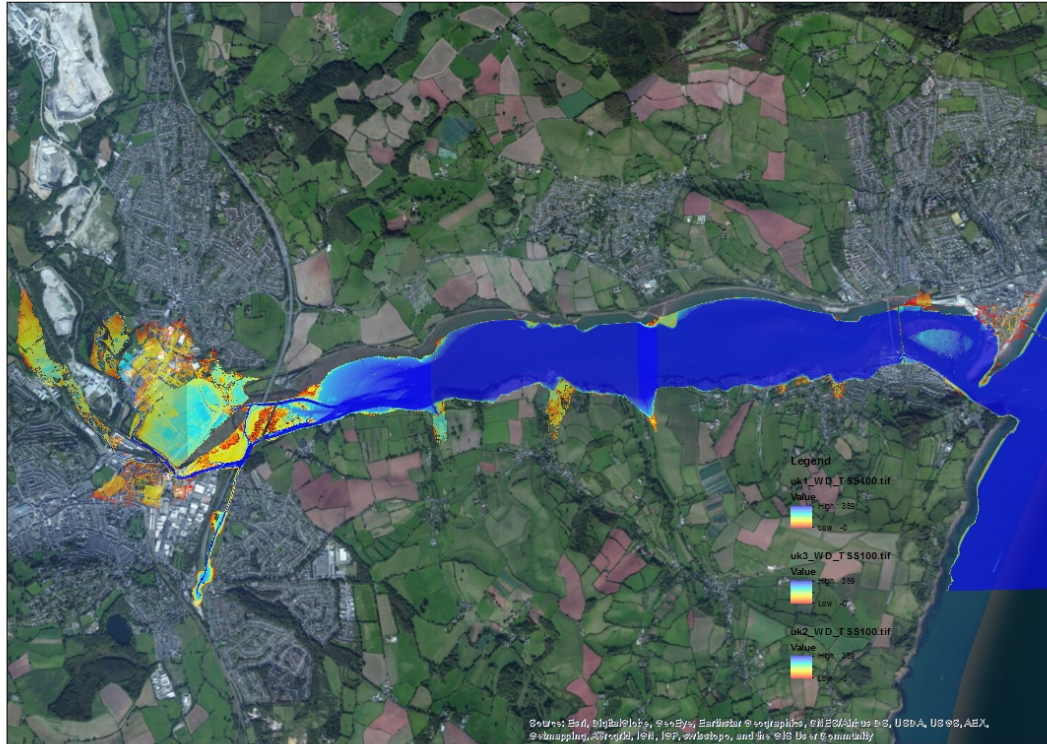


Figure 40 Flood Hazard Maps (water depth) FLOODSURGEMAP for longterm scenario with return period 20 years



Figure 41 Flood Hazard Maps (water depth) FLOODSURGEMAP for longterm scenario with return period 100 years

5.6.1.5 FLOODSURGEMAP: A watershed segmentation algorithm for mapping flood extent and water depth in estuarine

The model FLOODSURGEMAP is able to map coastal flooding due to uniform condition in terms of sea water level over the DEM floodplain. In fact this model is suitable for open coastline where tide or storm surge water levels are uniform along the entire coastline.

In case of large depth estuarine the tide or storm surge level can be different zone by zone, usually the effect of sea level rise decreases towards the inner part of the estuarine.

For this reason a specific version of FLOODSURGEMAP was developed and applied in the Gironde case study.

The user can define multiple storm surge or sea levels along the estuarine and propagate the different water levels inside the floodplain DEM with the same concept implemented in the FLOODSURGEMAP mode.

Gironde Case Study

The estuary of Gironde is the largest estuary in Europe, with a surface of 635 km². It is created from the confluence of the two rivers Garonne and Dordogne which merge near Ambès. From there to the mouth of the estuary, the distance is about 75 km. In average, it is oriented from south-east to north-west in a valley which width changes from 1 kilometers at Bordeaux to 15 km at the mouth near the presqu'île of Grave.

Garonne mainly flows over modern alluvial fields limited by outcrops of early Miocene. Tidal waves can be perceived up to 70 km upstream from Bordeaux, near La Réole.

Near the mouth of the estuary, the tidal wave is almost a semi-diurnal sinusoid with a mean amplitude of 3.20m. Due to the geometry of the estuary, the funnel effect involved by the decrease of width and the bend towards the West, this tidal wave grows when it enters in the estuary (see table 1). Thus in Bordeaux, the mean amplitude is 4.20m. However, the tidal wave is strongly dissymmetric upstream where the water rise is relatively quick (1/3 of the period) whereas ebb tide lasts for 2/3 of the period.

The tidal wave propagates from downstream to Bordeaux in about 2.5 hours for high tide and 5 hours for low tide, during spring tide. For low tide, the difference is lower and the low tide propagates in about 4 hours.

In the next figures are reported some outputs of the model.

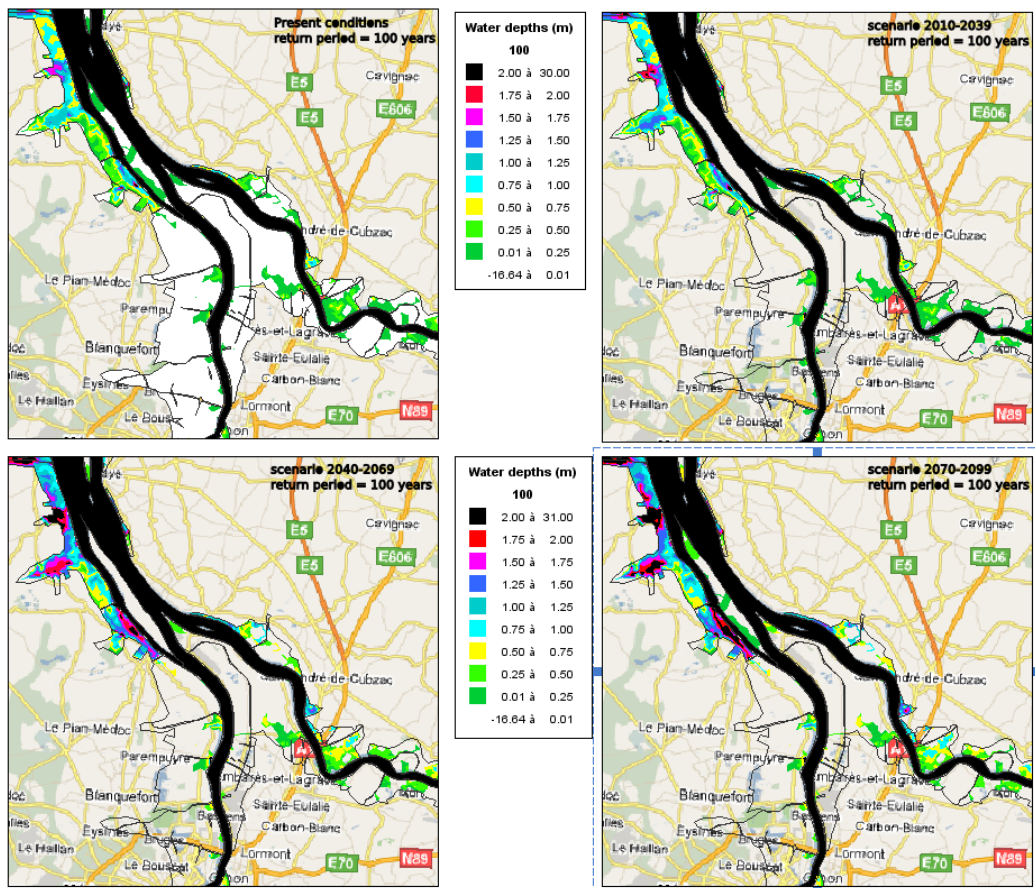


Figure 41: Quantiles of water levels for 100 years return period in the area of Ambes (confluence between Dordogne and Garonne) for present conditions and mid and long terms periods

Flood maps on the Gironde estuary

December 1999 flood

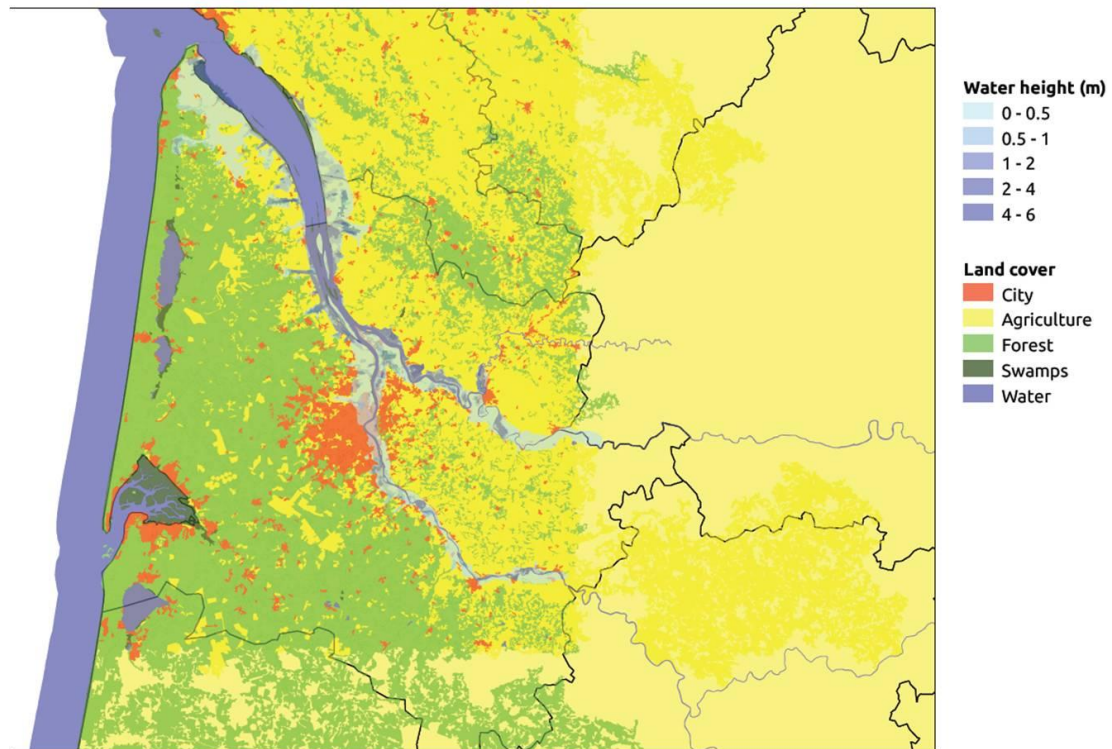


Figure 42 Gironde Case Study TELEMAC flood modeling

The next figure displays the flood map extent related to the same storm surge scenario as modeled by TELEMAC. In the left map are displayed the estuarine sub-regions characterized by different values in term of storm surges.

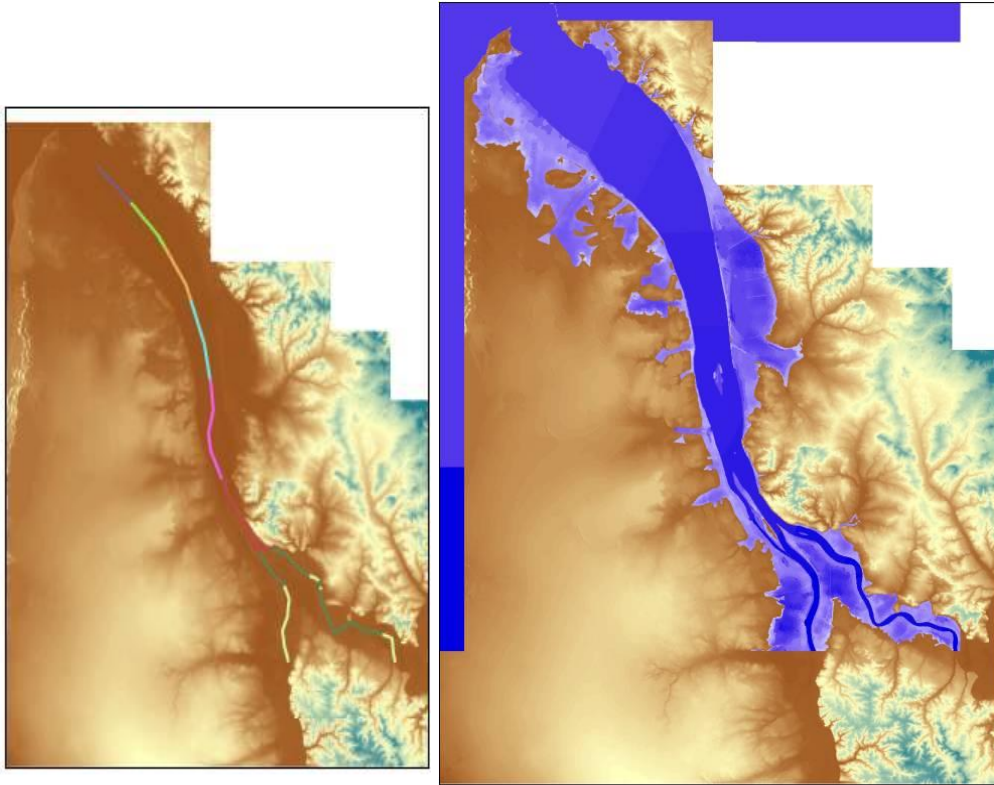


Figure 43 Gironde Case Study FLOODSURGEMAP flood modeling

5.6.2 FLOODTOPMAP algorithm Finite Volume Overtopping Model

In order to map flood extent and water depth due to coastal structure wave overtopping characterized by a finite volume, is possible to use the new approach described above through an iterative procedure.

The new developed raster-based procedure proceed in flooding a DEM floodplain with initial water level (L_0) released from the point source $P(i,j)$ located near by the overtopping point.

The relative maps of flood extent and water depth corresponding to the initial water level (L_0) were processed in order to compute the associated volume of water $V(L_0)$. In case the volume of water is less than the overtopping volume (V_0) computed with overtopping formula described in paragraph 4.7.1 the iteration continue increasing the water level. The procedure is iterate until the water level reach an associate volume of water greater than the overtopping volume (V_0).

The Figure 44 displays the iterative procedure.

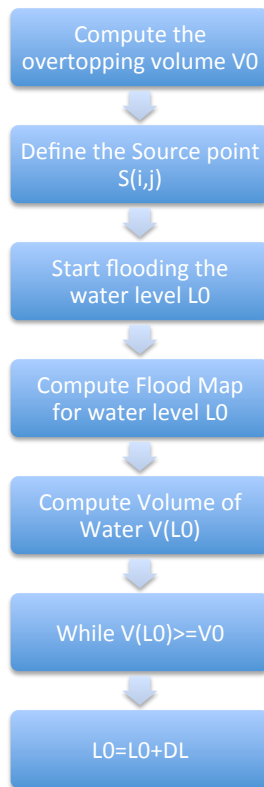


Figure 44 Iterative procedure for finite volume overtopping

The procedure is producing good results if the floodplain is not characterized by the presence of wide flat area. In fact in this case it becomes inaccurate and tends to over-predict the flooded area.

This aspect becomes a strong limit for accuracy in mapping the flood extension when the volume of water in the coastal flooding (storm surge and wave overtopping) becomes comparable with the total flooded volume at the specific water level imposed with the watershed transform.

This limitation is more evident in the case of small flooding volume spreading in a large floodplain area, in this case it is not possible to control small volume by imposing a water level, in fact even a small water level can flood a large portion of the floodplain with a large value of water volume.

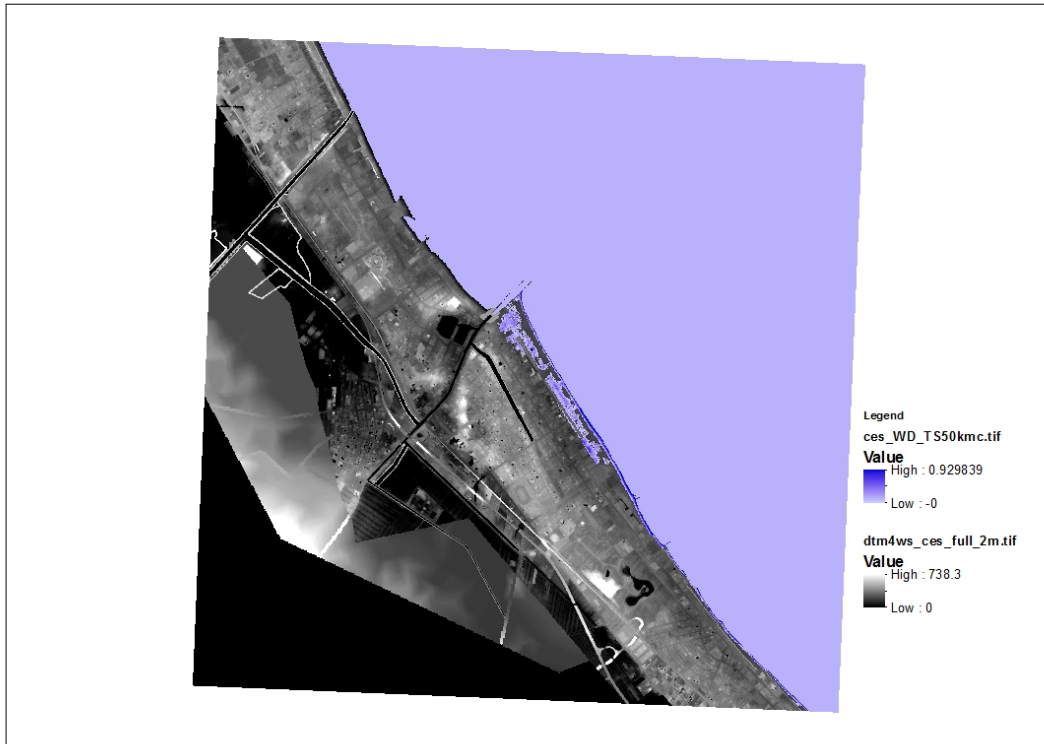


Figure 45 Finte Volume overtopping – 50000 m3

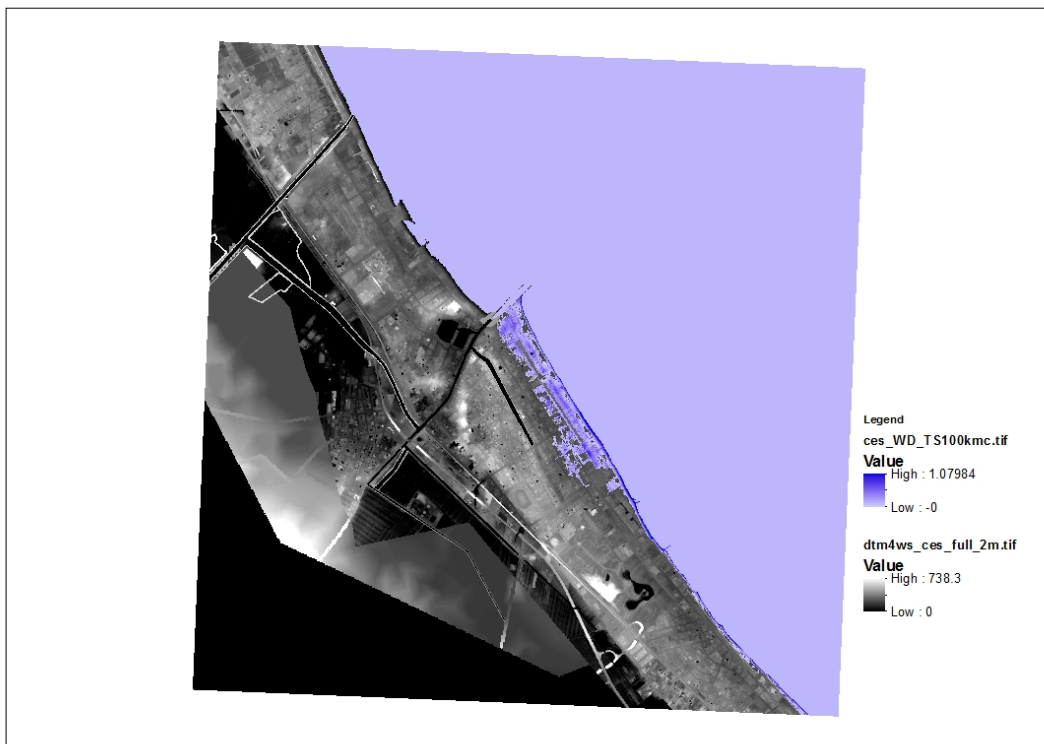


Figure 46 Finte Volume overtopping – 100000 m3

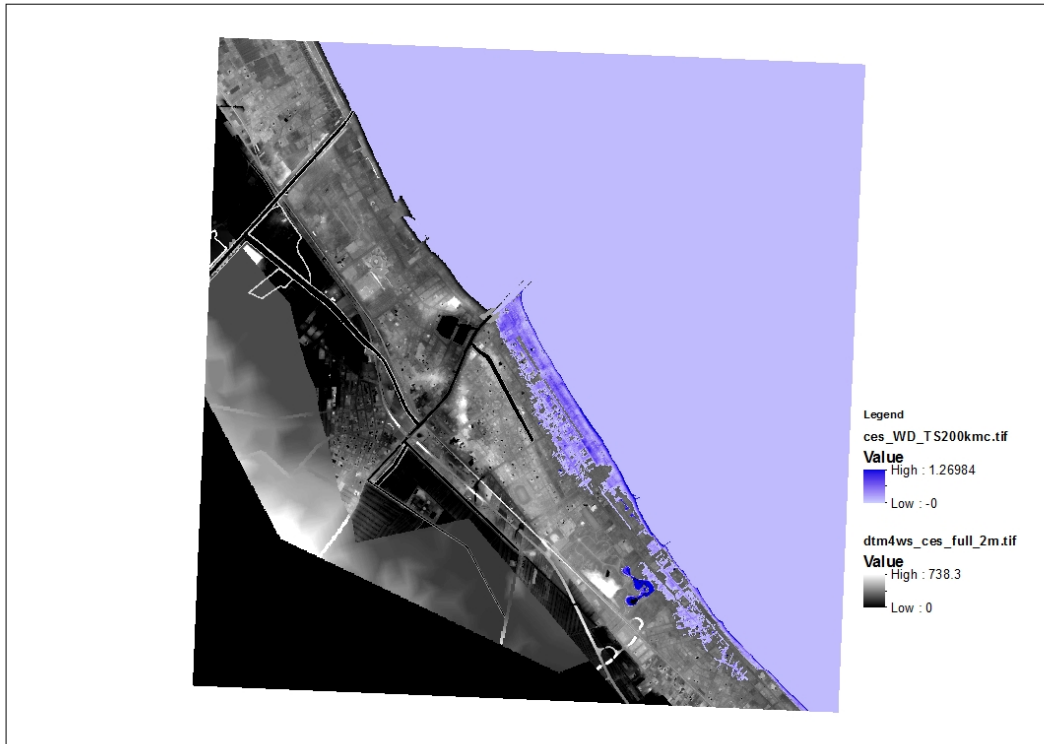


Figure 47 Finte Volume overtopping – 200000 m3

The charts displayed in the Figure 48 reports the increasing of volume (m³) of flooding water in Cesenatico with the water level in cm. It's evident the presence of two relevant discontinuity, the first one is between 125 and 126 cm with associated volume of water that increasing from 199000 m3 to 250000 mc and from 148 cm to 149 cm with an increase of volume exploding from 488000 m3 to 1280000 m3.

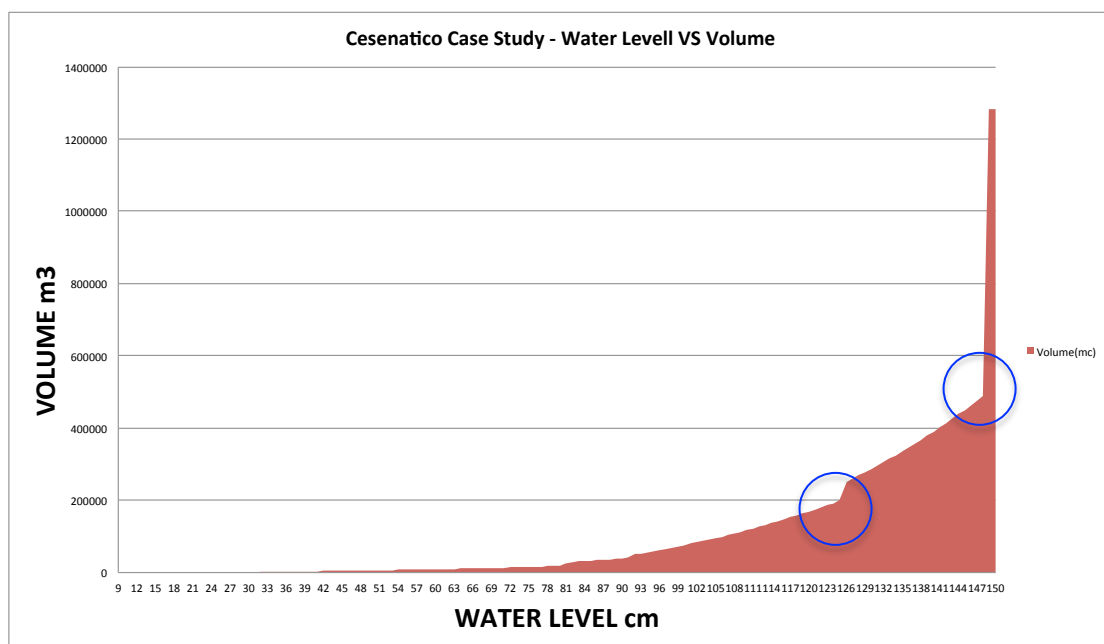


Figure 48 Water Level VS Volume of Water

The next Figure 49 displays the relative increase in flooding water volume, expressed in logarithmic scale, corresponding to an increase of 1 cm of water level. The log of relative volume is increasing rapidly with water level. For this reason the exact representation of a finite water volume become more and more inaccurate with the increase of water level.

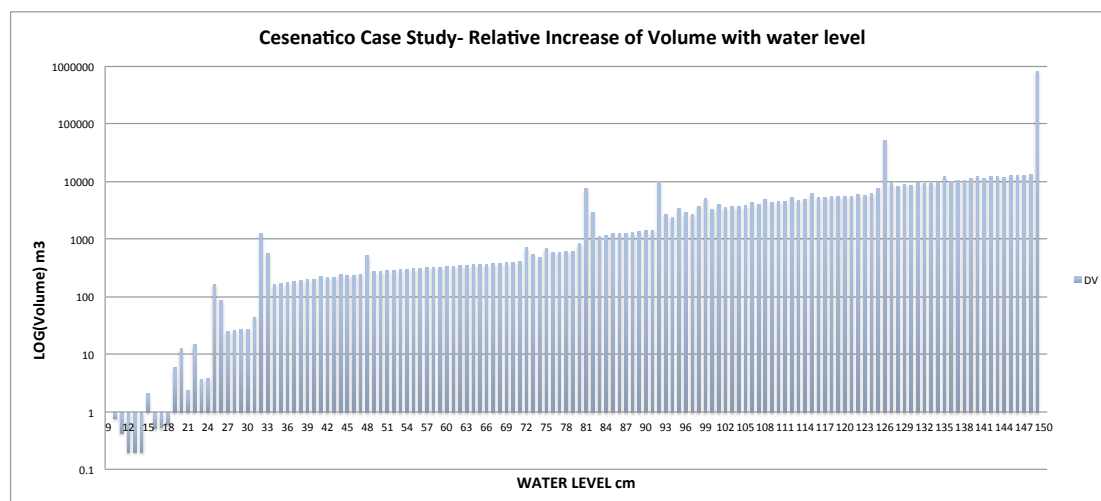


Figure 49 Relative increase of LOG(volume) VS Water Level

Analyzing the graphs reported above, are evident the limits associated with the model in case of finite overtopping volume, for example, if you need to simulate a release equal to 700,000 cubic meters would get a big underestimation by imposing a level equal to 148 cm while a wide overestimation is associated with the next level equal to 149 cm.

In order to overcome the modeling and flood mapping of a finite volume with watershed segmentation algorithm, is developed a revised version of the watershed segmentation algorithm with the capability to map the exact volume of water.

The implemented algorithm is based in the following steps

Input Data

- The DEM of the study area pre-processed as described in paragraph
- The initial source of finite volume flooding $S(i,j)$ localized immediately downstream respect the overtopping structure (dune, dike, etc)
- The maximum volume of overtopping water available V_0

Process

- 1) Identify the elevation Z_0 of the point $S(i,j)$

- 2) Run the watershed algorithm with source of flooding in S and $WL=Z_0+DZ$ where DZ is the increment of water level defined by the user
- 3) Compute the Volume of Water VW associated at the specific WL
- 4) Iterate 2 and 3 incrementing WL while VW is greater than Vmax
- 5) Generate a binary mask of flooded pixels Fmap (0 non flooded, 1 flooded)
- 6) Compute the first Water Depth Map (WDmap) : $Famp*WL-DEM$
- 7) Computing the weighted cost-distance map (CDmask) from the point of volume release with weight the inverse map of Water Depth
- 8) Iteratively Tresholding CDmask (TCDmask) from maximum value until lower level, removing non source connected pixel and generating a mask (mask_i) in order to reduce the volume of WDmap lower than WO
 - a. $WDmap_i=mask_i* WDmap$

The flowchart reported in the next figure describe the above process.

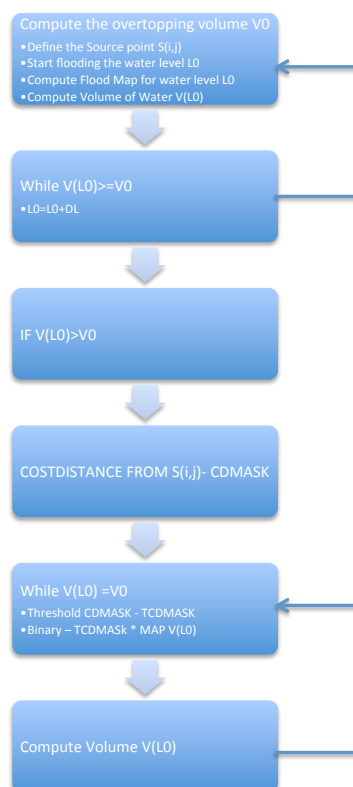


Figure 50 Algorithm flow chart

In the next figures the steps of algorithm are explained.

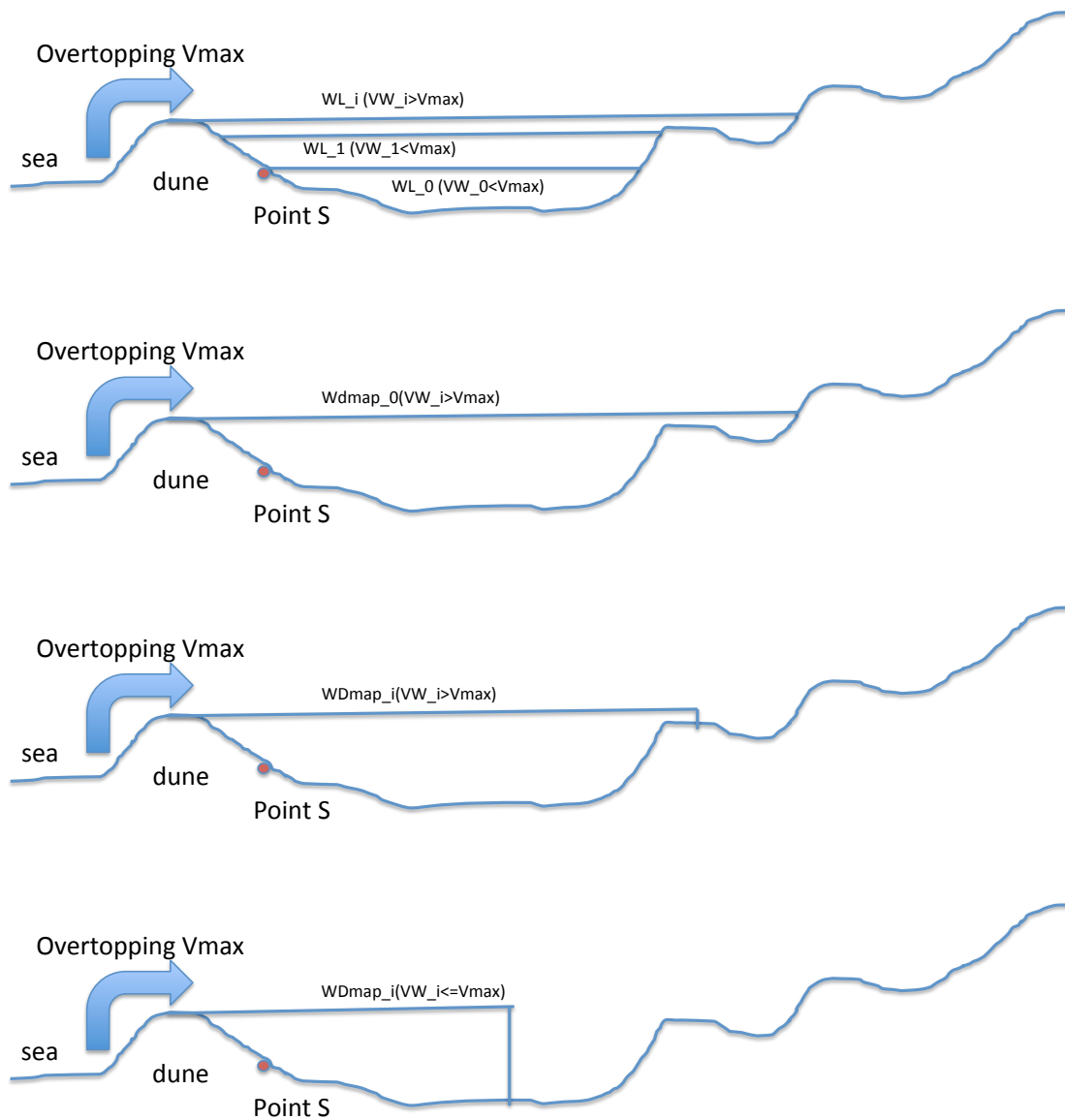


Figure 51 Schematic of finite volume reduction algorithm

The finite volume of water flooding the floodplain is controlled by imposing three main rules

- Imposing a water level
- Connectivity of flooded pixel with the source S of water release
- Weighted cost distance (ESRI 1996³⁵⁸, SAGA-GIS) from the source S(i,j)

Cost distance analysis is a GIS-based modelling technique to calculate a measure of the least accumulative cost to specified source locations over a cost surface. In models, the overall cost of the movement between a source and a target is modelled as a movement over the cost surface. All non-source cells need to be assigned No Data on the source raster. A cost raster assigns a cost involved in moving through any particular cell, which depends on several factors. In this case the source is represented by the overtopping point S(i,j) while

the cost surface is represented by the water depth map. The Figure 52 shows an example of a cost distance calculation when the cell crossing time cost for 10 m cell is set to 0.65 s.

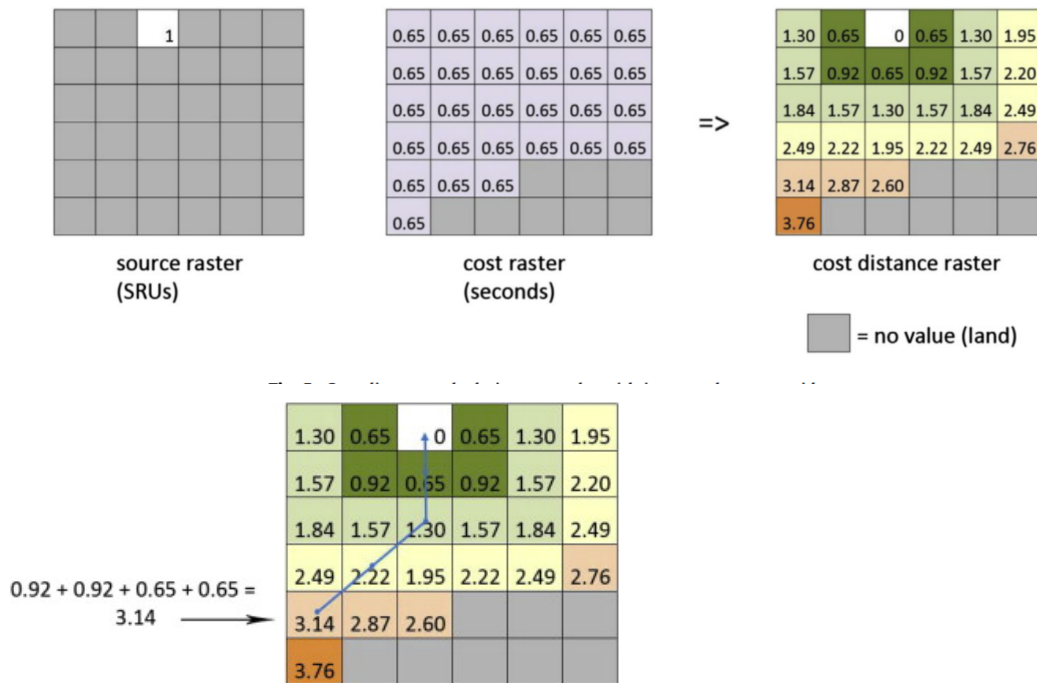


Figure 52 Cumulative cost distance is calculated for each cell by summing up the costs of moving from a cell centre to another via least-cost route.

The described algorithm is a raster-based procedure able to spread a finite volume in a floodplain DEM imposing topological connectivity and water mass balance rules. This approach is not dealing with momentum and energy balance equation, it means that is not an hydrodynamic model.

A more robust approach is for routing a finite overtopping volume using GIS and mathematical morphology operators is proposed by Beucher (November 2011 http://cmm.ensmp.fr/~beucher/publi/DEM_flooding.pdf). The proposed algorithm search the FOZ (First Overflow Zone) using geodesic reconstruction operators and provides a kind of flooding graph which simply indicates which catchment basins (or unions of catchment basins) will be flooded next when a given catchment basin has been flooded. This corresponds to a hierarchy of catchment basins. However, the flooding/overflow procedure is synchronised. This means that the basins belonging to a same level of hierarchy will be flooded simultaneously only when all the catchment basins belonging to the previous level have been flooded (up to their respective FOZ).

It is unlikely that a real flooding would follow this rule. We have, for instance, no control of the rate of flow in this procedure. This rate of flow will surely depend, in the real flooding process, of lots of factors: size of FOZ, dynamics of the flow (speed), etc. Moreover, when a small catchment basin is filled, neighbouring catchment basins will be flooded without waiting for the end of flooding of the other catchment basins belonging to the same hierarchy. Therefore, the calculation of the volume of water involved at each step of the above procedure may be biased and may not correspond to the real situation. Secondly, this procedure does not simulate the flooding itself but it simply gives an idea of the result of this flooding, that is, the regions which could be affected by this flooding. Indeed, this information can be useful to establish risk maps. Thirdly, the described procedure allows to know if the general flooding process is mainly achieved through a classical “watershed-like” flooding or through an overflow, by a very simple way illustrated at Fig 4-c (step 4): when at least two previously flooded regions merge, this means that the process is again a flooding process (a minimal catchment basin has been reached). On the contrary, if a new non connected flooded region appears, this region has been added through an overflow. At the end, the situation where the calculated volume of water corresponds to the real one involved is when the flooded surface is made of a single connected component as illustrated at Fig 1 (if only one flooding source is used). It could be possible, then, to use the catchment basins hierarchy graph obtained by the above procedure to design another more realistic flooding schemes based on graph valuation and propagation. Although there exists morphological operators able to handle this kind of data structure (generalised geodesic operators), it is likely that these flooding schemes would also require the use of other mathematical and simulation tools.

Algorithm description

Here are the different steps of this algorithm.

Initial data:

- The DEM image f_0
- The initial source of flooding, S (it is a set).
- The maximum volume of water available, V_{max} .

Initialisation

1. Compute w , the valued watershed of f_0 .
2. Generate the catchment basins image CB of w (set obtained by thresholding w at 0).
3. Compute $M = \text{build}(CB, S)$; M is the set of all the (even partly) flooded catchment basins at the end of each step.
4. Generate m (valued mask of M , obtained by a convert function).
5. Let the current flooded topography f_i be equal to f_0 .

Process

1. $f_{i-1} = f_i$ (f_{i-1} is the flooded topography at the beginning of each step).
2. $M' = M$ (M' indicates the partly flooded catchment basins at the beginning of each step).
3. Compute m' (convert function applied to M')
4. Calculate $w_i = w \wedge [\delta(m') - m']$
5. Calculate $h_i = R_{w_i}^+(w_i \vee m')$ (dualbuild of $(w_i \vee m')$ over w_i).
6. Calculate $f_i = f_{i-1} \vee h_i$
7. Calculate $V = \text{vol}(f_i - f_0)$, total volume of water consumed since start.
8. Calculate $V_i = \text{vol}(f_i - f_{i-1})$, volume used at step i (optional).
9. Call $\text{getFOZ}(m', w_i, h_i)$, result is the FOZ Z (see description of this function below).
10. Compute $WRK_1 = M' \cup CB \cup Z$
11. $WRK_1 = \text{SKIZ}(WRK_1)$
12. $M = \text{build}(WRK_1, M')$, geodesic reconstruction.
13. If $(V \leq V_{max})$, then go to step 1
14. Else, end of flooding.

Procedure $Z = \text{getFOZ}(m, w, h)$

1. Determine points such that $w = \delta(h \wedge m)$ and store them in Z .
2. Calculate z (numerical convert of Z).
3. $v_0 = \text{vol}(Z)$.
4. $v_i = v_0$
5. Compute $\delta(w \wedge z)$
6. Put points such that $\delta(w \wedge z) = w$ in Z
7. Calculate z

Figure 53 Pseudo code algorithm proposed by Beucher 2011 -

5.6.3 FLOODVELMAP raster based for mapping flood velocity

Another important characteristic of coastal flooding in order to assess the risk posed on economic, environmental and social aspect is the magnitude of velocity. Directive 2007/60/EC of the European Parliament and of the Council on the assessment and management of flood risks" effective from 23 October 2007 (<http://europa.eu/scadplus/leg/en/lvb/l28174.htm>) requires EU member states to develop maps identifying all areas exposed to a risk of flooding and indicating the probability of flooding for each of these areas and the potential damage for local populations, to structures and buildings and the environment.

Flow velocity is presumed to have high influence in flood damage assessment, however as underlined by Kreibich et al 2009³⁵⁹, the flooding damages related to high flow velocity is hardly quantified and virtually no damage models take it into account. A significant influence

of flow velocity on structural damage, particularly on roads, could be shown in contrast to a minor influence on monetary losses and business interruption

impact parameters	damage types				
	structural damage of residential buildings	structural damage of road infrastructure	monetary loss to residential buildings	monetary loss to road infrastructure and companies	business interruption and disruption duration
flow velocity	NO	STRONG	WEAK	NO	NO
water depth	STRONG*	MEDIUM	MEDIUM	NO	MEDIUM
energy head	STRONG*	MEDIUM	MEDIUM	NO	WEAK
indicator for flow force	WEAK*	STRONG	WEAK	NO	NO
intensity	WEAK*	STRONG	WEAK	NO	WEAK

Figure 54 Qualitative summary of the influence of impact parameters on flood damage Kreibich et al 2009³⁶⁰

Numerical hydrodynamic model solving the full or simplified version of SWE can provide flow velocity simulation, but as previously discussed they are not suitable for a Web-GIS DSS integration with risk assessment purposes.

For this reason, this research, has developed a simple raster based approach in order to evaluate the magnitude of flow velocity related to a floodplain coastal flood event.

Several simple approaches are available in literature for evaluating in a preliminary way the flow velocity of a coastal flooding event. The most used are indirect approaches based on deriving flow velocity from water depth.

For example, FEMA P-55, Coastal Construction Manual, gives guidelines on estimating water velocity grids from the stillwater depth grid. In this case map of flow velocity can be easily obtained through a simple map algebra equation:

$$V\left(\frac{feet}{sec}\right) = \sqrt{32.3 * (water_depth)}$$

Another approach consist in solving Bernulli and Momentum equation under the hypothesis of small amplitude waves, in this case the wave velocity is equal to wave celerity and can be expressed by:

$$V = \sqrt{g * (water_depth)}$$

Another approach proposed in TR55 valid for slope less than or equal to 0.005 is:

$V = 16.1345\sqrt{(slope)}$ – unpaved (n=0.05 Manning's coeff. and R=0.4 hydraulic radius)

$V = 20.3282\sqrt{(slope)}$ – paved (n=0.025 Manning's coeff. and R=0.2 hydraulic radius)

Manning's equation is a common and simple way to solve for the average velocity or shear across an open channel cross-section. The general expression of Manning equation is

$$V = \frac{R^{2/3}S^{1/2}}{n}$$

R is the hydraulic radius (m), S is the slope ($m\ m^{-1}$) and n is the Manning roughness coefficient ($m^{-1/3}\ sec$). In case of flooding in the floodplain the hydraulic radius can be assumed equal to water dept.

The Manning equation can easily implemented in a raster based approach in order to compute cell-by-cell velocity (Mondloch 2014³⁶¹), in fact once available water depth, slope and Manning roughness coefficient maps is possible with a simple map algebra computation to obtain the velocity map.

In the particular case of storm surge flooding with water spreading from the coastline towards the inland will be necessary to take into account the spatial variation of Manning parameters. The spatial distribution of average value of Manning parameters moving from the source of coastal flooding (coastline) can be easily obtained computing the cost accumulation distance weighted over the selected parameter (n or R) and dividing by the accumulation of flooded pixels obtained computing cost accumulation over a binary mask indicating the flooded pixels (0 non flooded, 1 flooded).

The Cost Distance or Accumulation surface functions implemented in the new algorithm are provided by SAGA-GIS and are based on Dijkstra algorithm able to accumulate all cells with a distance equal from the origin to the target.

The idea behind the FLOODVELMAP algorithm is to implement the Manning's equation in a raster based approach that takes into account the average value of Manning's coefficient and the water depth moving from the coastline.

The implemented algorithm is here described:

AVERAGE_WD = average water depth in m for each pixel evaluated computing all source of flooding Euclidean connected pixels

- $Costdistance(WD(x,y)/Costdistance(mask_flood(x,y))$
- $WD(x,y)$ Water Depth for each pixel
- $mask_flood(x,y)$ = boolean map (0,1) representing flooded pixels

Slope= $H0-zdem(x,y)/distance(x,y)$

- H_0 = Storm Surge height at source of flooding
- $z_{dem}(x,y)$ = elevation in m
- $Distance(x,y)$ = distance in m from source of flooding

AVERAGE_n = average Manning's roughness coeff for each pixel evaluated computing all source of flooding Euclidean connected pixels.

- $Costdistance(n(x,y)/Costdistance(mask_flood(x,y)))$
- $n(x,y)$ manning coeff.

An application of FLOODVELMAP algorithm to Cesenatico site is here displayed. In particular is reported a comparison between the new approach respect the FEMA formulation and the flow velocity computed by the hydrodynamic 2D model MIKE21.

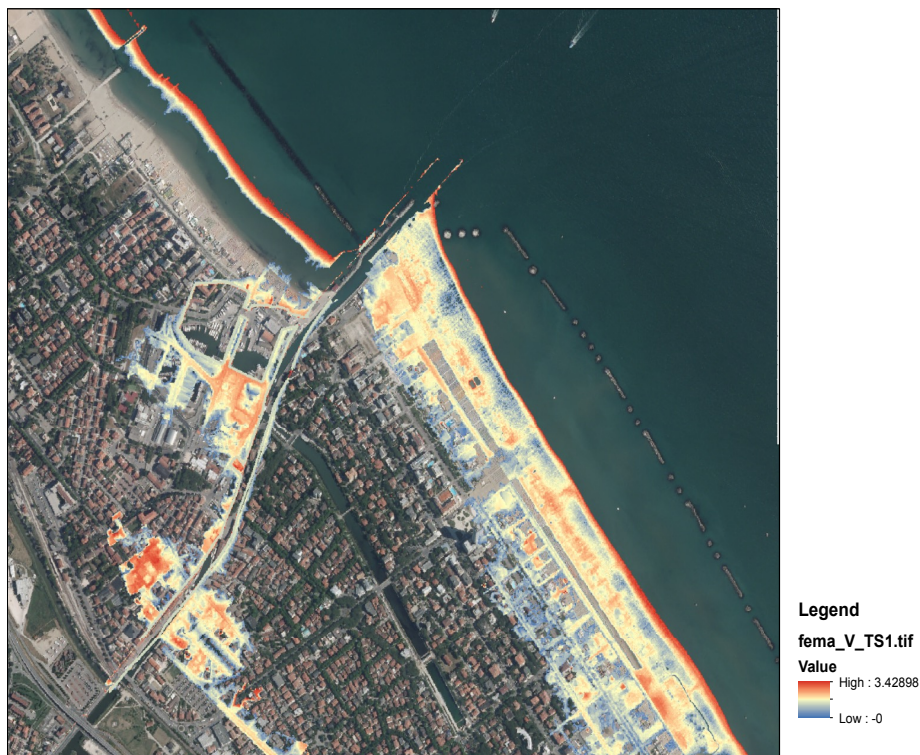


Figure 55 Map of flow velocity – FEMA formulation

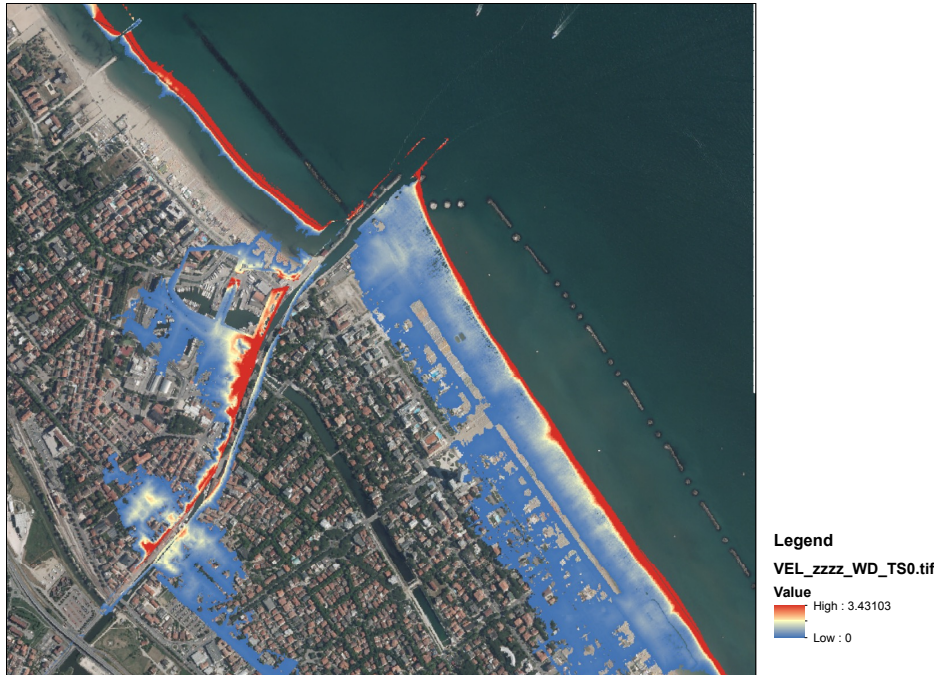
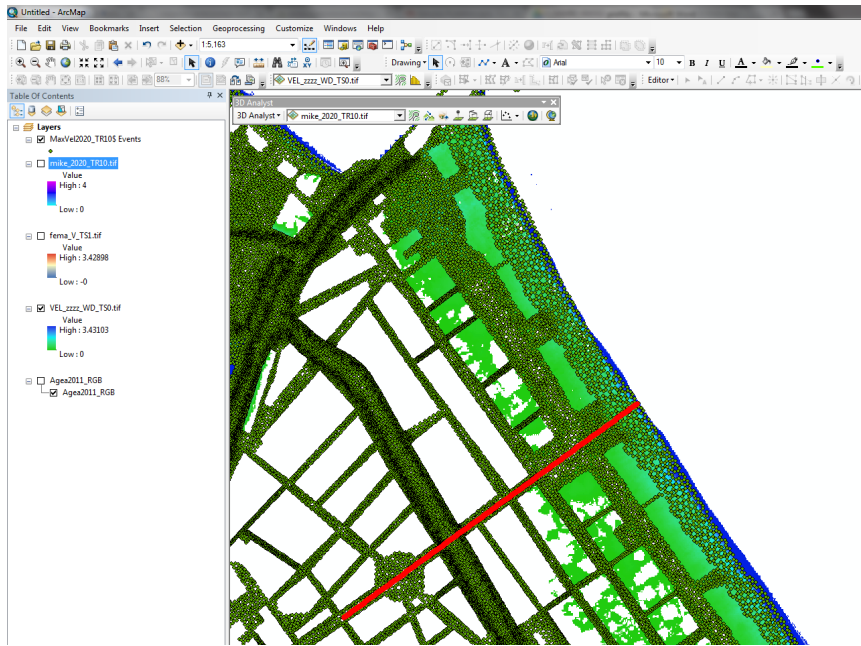


Figure 56 Map of flow velocity – FLOODVELMAP formulation



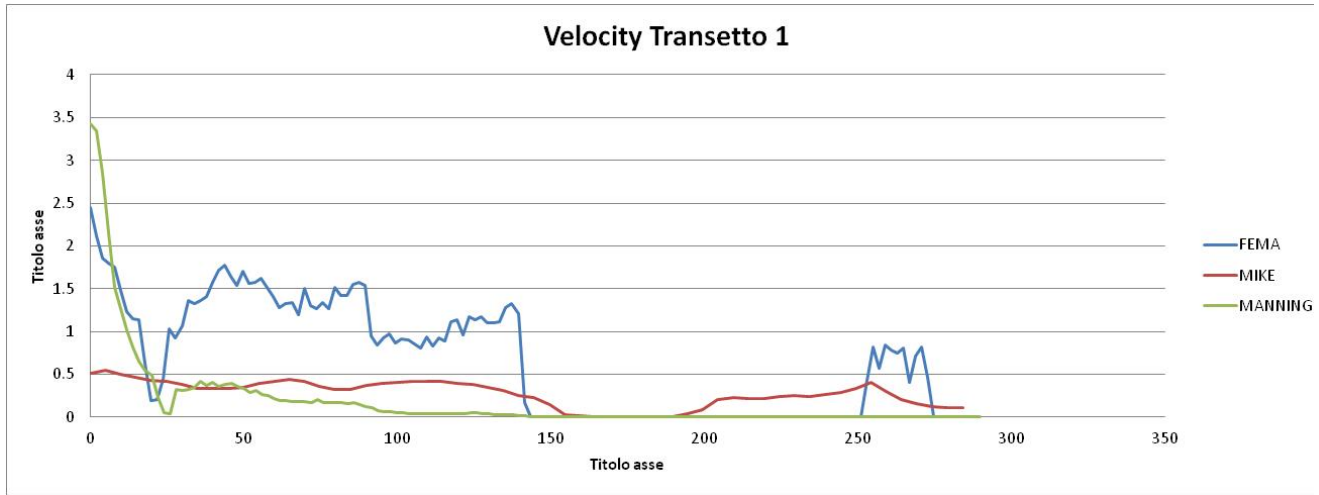


Figure 57 MIKE21, FEMA and FLOODVELMAP comparison in transec 1

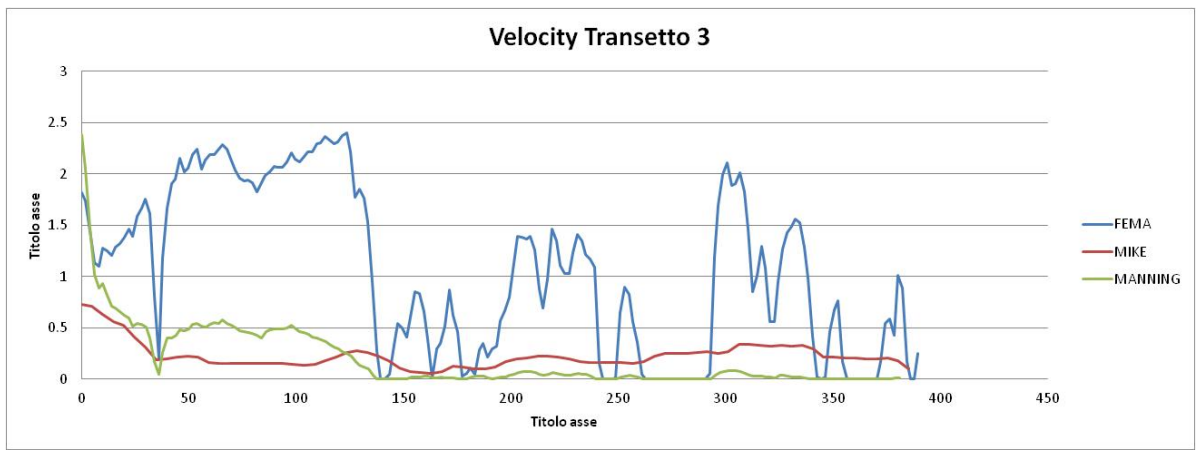
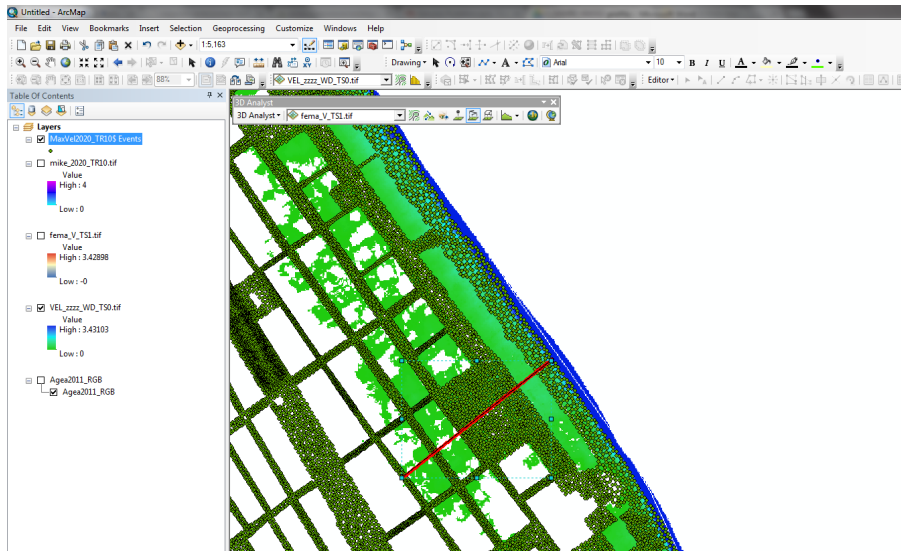


Figure 58 MIKE21, FEMA and FLOODVELMAP comparison in transec 3

5.6.4 FLOODDURMAP raster based for mapping floodplain time duration

Besides the water depth and flow velocity, also other factors determine the resulting flood damages. These factors are often not taken into account in flood damage models. One of these influences is the flood duration. The longer a flooding lasts, the larger the material damage, and especially damage due to interruption will be. Flood duration causes interruptions and extra material damages. Taking into account flood duration can, therefore, theoretically make flood damage models more accurate. In particular for damage to agricultural crops and ecological habitat the time of flooding and the duration of the flood are decisive (Forster et al., 2008³⁶²).

The longer the duration of inundation, the greater the saturation of building structure and contents, the higher the effort for drying, the more severe the anoxia of crops, increasing the probability of damage.

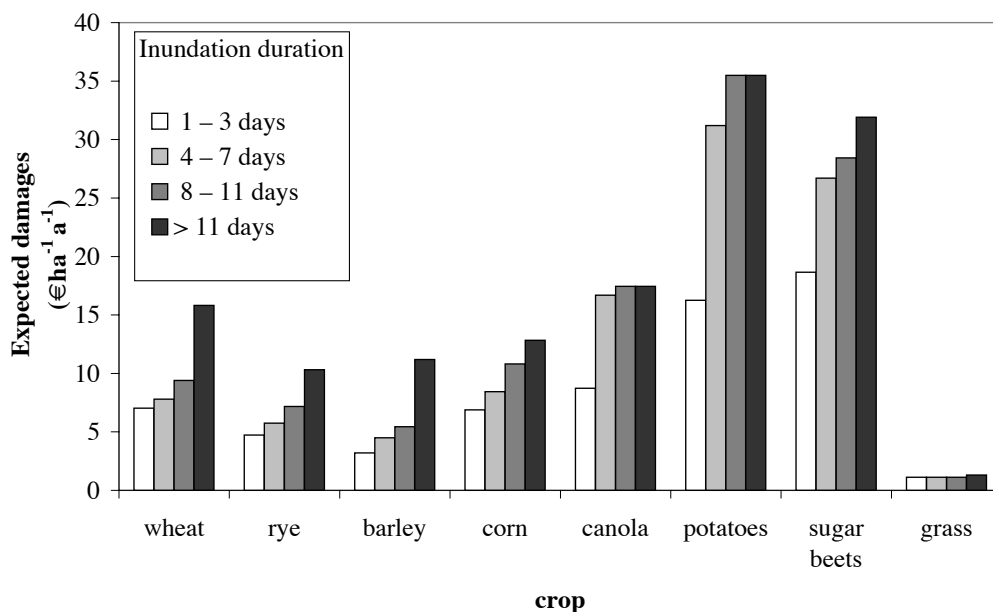


Figure 59 Expected damages to grain crops (wheat, rye, barley, corn), oilseed plants (canola), root crops (potatoes and sugar beets) and grass based on flooding occurrence categorized on a monthly basis - Forster et al., 2008³⁶³.

Flood time duration is dependent on flood volume or water depth, soil infiltration/drainage and storage capacity. The general equation can be expressed as:

$$\text{Flood_Duration} = (\text{Volume of Water} - \text{Soil Water Storage Capacity}) / \text{infiltration capacity}$$

The amount of water that can be stored in the soil mantle is dependent first upon the total pore space available in the soil between the soil particles. This is commonly expressed as porosity in percent of soil volume. The total pore space available within the soil mantle represents the maximum volume of water that can be stored in this soil mantle. When this entire pore space is filled with water, the soil is said to be *saturated*.

Infiltration is a time dependent process (Figure 60). The rate at which water enters the soil, especially dry soil, starts very fast and then declines and eventually approaches a constant rate of entry. This constant rate of infiltration is also referred to as the saturated hydraulic conductivity, K_{sat} , and sometimes called the soil's permeability. In almost all cases, when laypeople refer to an infiltration rate they mean the long-term constant rate, permeability, or K_{sat} .

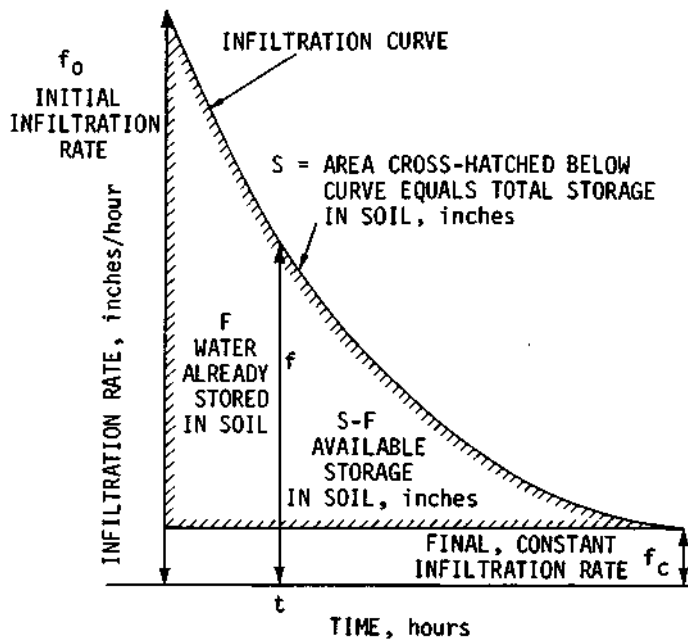


Figure 60 Diagram of infiltration curve and infiltration rate as related to storage in soil.

The FLOODURMAP is a simple raster-based model developed recurring to GIS map algebra techniques under the following hypothesis and equation:

n is the porosity of unsaturated layer and z is the depth of the water table, the map of soil water storage is obtained through the following equation:

$$SWS = z * n$$

Consequently the map of Surface Runoff is equal to

$$SRO = WD - SWS$$

Infiltration rate at any time t by methodology described by Holtan (1950³⁶⁴):

f_c = final constant infiltration rate, in inches per hour (generally equivalent to the saturated conductivity, in inches per hour, of the tightest horizon present in the soil profile)

In order to evaluate the duration of flood water permanence in the floodplain we can assume that the soil is completely saturated and that the infiltration rate is equivalent to the saturated conductivity of the soil.

$$\text{flood_duration} = \text{SRO} / f_c$$

$$f_c = K_{\text{sat}} \text{ in cm/h}$$

INPUT

z = groundwater depth in cm

k_{sat} = hydraulic saturated conductivity in cm/sec

n = soil porosity

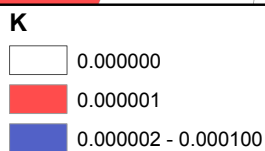


Figure 61 Ksat map in Cesenatico cm/sec

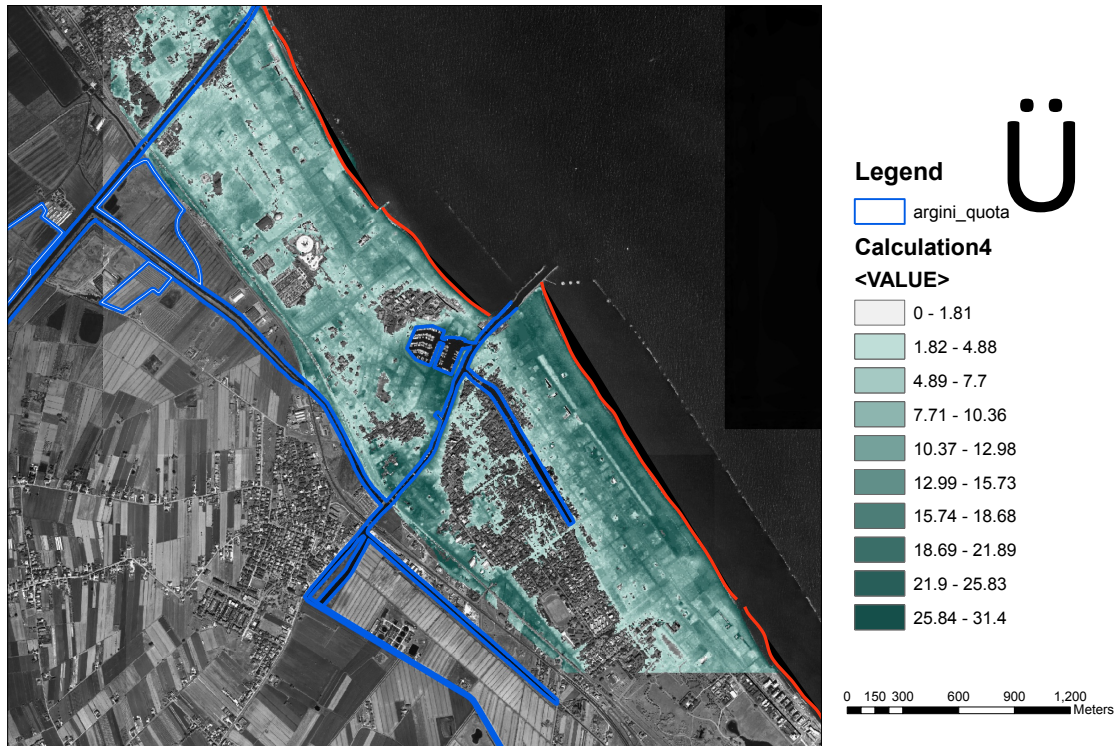


Figure 62 Map of flow duration in hours – Storm surge water level 127 cm and depth of water table $z = 3\text{m}$

6 Flood Vulnerability and Damage Assessment

6.1 Introduction

As reported in the literature, flood damages can be classified into direct and indirect damages. Direct damages are those which occur due to the physical contact of flood water with humans, property or any other objects. Indirect damages are induced by the direct impacts and occur – in space or time – outside the flood event. Both types of damages are further classified into tangible and in- tangible damages, depending on whether or not they can be assessed in monetary values (e.g. Parker et al., 1987³⁶⁵; Smith and Ward, 1998³⁶⁶). Tangible damages are damage to man- made capital or resource flows which can be easily specified in monetary terms, whereas intangible damage is dam- age to assets which are not traded in a market and are difficult to transfer to monetary values. Although the differentiation in direct and indirect, and tangible and intangible dam- age is commonplace, interpretations and delineations differ (Jonkman et al., 2007³⁶⁷). Some examples for the different types of damage are:

- Direct, tangible: damage to private buildings and con- tents; destruction of infrastructure such as roads, rail- roads; erosion of agricultural soil; destruction of harvest; damage to livestock; evacuation and rescue measures; business interruption inside the flooded area; clean up costs.
- Direct, intangible: loss of life; injuries; loss of memorabilia; psychological distress, damage to cultural heritage; negative effects on ecosystems.
- Indirect, tangible: disruption of public services outside the flooded area; induced production losses to companies outside the flooded area (e.g. suppliers of flooded companies); cost of traffic disruption; loss of tax revenue due to migration of companies in the aftermath of floods.
- Indirect, intangible: trauma; loss of trust in authorities.

	Tangible and priced	Intangible and unpriced
Direct	<ul style="list-style-type: none"> • Residences • Capital assets and inventory • Business interruption (inside the flooded area) • Vehicles • Agricultural land and cattle • Roads, utility and communication infrastructure • Evacuation and rescue operations • Reconstruction of flood defences • Clean up costs 	<ul style="list-style-type: none"> • Fatalities • Injuries • Inconvenience and moral damages • Utilities and communication • Historical and cultural losses • Environmental losses
Indirect	<ul style="list-style-type: none"> • Damage for companies outside the flooded area • Adjustments in production and consumption patterns outside the flooded area • Temporary housing of evacuees 	<ul style="list-style-type: none"> • Societal disruption • Psychological traumas • Undermined trust in public authorities

Table 13 Different Dimensions of flood damages (Jonkman et al. 2008)³⁶⁸

The methodology implemented in the Web-GIS DSS developed in this thesis is mainly focused in the estimation of direct tangible and intangible damages. The estimation of direct flood damage is a complex process involving a large number of hydrologic and socioeconomic factors. The structure, inputs and outputs of a specific damage model are defined not only by the available data, but also by the purpose of the model. For example, while insurance companies model the estimated insured damages, government agencies and academics are generally interested in the accurate assessment of total economic losses (Jongman et al. 2012³⁶⁹).

In developing flood damage models two main approaches can be distinguished: **empirical** approaches which use damage data collected after flood events and **synthetic** approaches which use damage data collected via what-if-questions also known as damage function approach.

An example for the first approach is the German flood damage data base HOWAS (Merz et al., 2004³⁷⁰), from which the damage functions of MURL (MURL, 2000³⁷¹) and Hydrotec (Emschergerossenschaft and Hydrotec, 2004³⁷²) were derived. What-if analyses estimate the damage which is expected in case of a certain flood situation, e.g.: “Which damage would you expect if the water depth was 2 m above the building floor?” Examples for this approach are the damage functions for United Kingdom (Penning-Rowse et al., 2005³⁷³).

Synthetic functions are hypothetical curves developed independently from historical flood data for a specific area; therefore, they do not rely on the time-consuming and often difficult collection of damage data. Unlike empirical curves, they can also be used in different areas, enabling unqualified comparisons between these areas (Middelmann-Fernandes 2010³⁷⁴).

. Synthetic functions may be developed using data from surveys, insurance companies, loss adjusters or quantity surveyors, enabling extrapolation to other areas (Greenaway and Smith, 1983³⁷⁵)

Examples of synthetic functions for residential buildings include ANU- FLOOD for Australia (Greenaway and Smith, 1993³⁷⁶), the Blue Manual for the United Kingdom (Penning-RowSELL and Chatterton, 1977; Penning- Rowsell et al., 2003³⁷⁷) and HOWAD (Flood Damage Simulation Model, German: Hochwasser-Schadens-Simulations-Model) for Germany (Neubert et al., 2009³⁷⁸).

Besides the choice of empirical or synthetic damage functions, a choice has to be made between relative or absolute functions

Impact parameter		
Parameter	Description	Selected references
Inundation depth	The higher the inundation depth, the greater the building and contents parts which are damaged and the stronger the buoyancy force.	CH2M Hill (1974); Black (1975), Sangrey et al. (1975), Smith and Tobin (1979), Handmer (1986), Smith (1991), Torterotot et al. (1992), Smith and Greenaway (1994), Hubert et al. (1996), USACE (1996), Islam (1997), Blong (1998), Zerger (2000), Nicholas et al. (2001), Beck et al. (2002), Kato and Torii (2002), Citeau (2003), Dutta et al. (2003), Hoes and Schuurmans (2005), Penning-Rowse et al. (2005), Büchele et al. (2006), Kreibich and Thieken (2008), Thieken et al. (2008a)
Flow velocity	The greater the velocity of floodwaters, the greater the probability of structural building damage due to lateral pressure, scouring, etc. High flow velocities can cause direct damage to crops and may lead to soil degradation from erosion.	CH2M Hill (1974), Black (1975), Sangrey et al. (1975), Smith and Tobin (1979), Handmer (1986), McBean et al. (1988), Smith (1991), Smith and Greenaway (1994), USACE (1996), Islam (1997), Blong (1998), Zerger (2000), Nicholas et al. (2001), Beck et al. (2002), Kato and Torii (2002), Citeau (2003), Schwarz and Maiwald (2007, 2008), Kreibich et al. (2009), Pistrika and Jonkman (2009)
Duration of inundation	The longer the duration of inundation, the greater the saturation of building structure and contents, the higher the effort for drying, the more severe the anoxia of crops, increasing the probability of damage.	Smith and Tobin (1979), Handmer (1986), McBean et al. (1988), Torterotot et al. (1992), Consuegra et al. (1995), Hubert et al. (1996), USACE (1996), Islam (1997), Nicholas et al. (2001), Kato and Torii (2002), Citeau (2003), Dutta et al. (2003), Penning-Rowse et al. (2005), Förster et al. (2008)
Contamination	The greater the amount of contaminants, the greater the damage and the cleanup costs. Inclusion or adsorption of contaminants may even lead to total damage. Examples are the inclusion of small particles in porous material impossible to remove, or the dispersal of microorganisms in moist building material requiring extensive clean up and disinfection.	Smith and Tobin (1979), Handmer (1986), USACE (1996), Nicholas et al. (2001), Kreibich and Thieken (2008), Thieken et al. (2008a)
Debris/sediments	The presence of debris in floodwater, depending on its amount, size and weight, increases the dynamical forces which affect buildings and thus the potential for structural damage. Sediment can damage flooring and mechanical equipment and it may lead to an increased effort for clean up.	Handmer (1986), Penning-Rowse et al. (1994), Kato and Torii (2002)
Rate of rise	As the rate of rise increases, it becomes increasingly difficult to reduce flood damage.	Smith and Tobin (1979), Handmer (1986), Penning-Rowse et al. (1994)
Frequency of inundation	Repeated flooding may have cumulative effects, increasing the probability of damage. On the other hand, preparedness significantly increases, leading to reduced damage.	USACE (1996), Elmer et al. (2010)
Timing	Floods occurring at night may be associated with greater damage owing to ineffective warning dissemination. Floods occurring during holidays may see property owners absent and unable to take damage-reduction measures. The time of year (season) of flood occurrence with respect to crop growth stages and critical field operations plays a crucial role for the magnitude of agricultural damage.	Smith and Tobin (1979), Smith and Greenaway (1984), Smith (1992), Smith (1992), Consuegra et al. (1995), Yeo (1998), Citeau (2003), Dutta et al. (2003),

Resistance parameter		
Parameter	Description	Selected references
Business sector/ use of building	Sectors differ significantly in respect to exposed assets as well as susceptibility. For instance, the manufacturing sector has a relatively high damage potential (high assets and business volumes) but a relatively good preparedness status. In contrast, preparedness is comparatively weak in the financial and service sectors.	MURL (2000), ICPR (2001a), FEMA (2003), Emschergerossenschaft and Hydrotec (2004), Penning-Rowse et al. (2005), Scawthorn et al. (2006)
Building type	Building type may significantly influence the degree of damage. For instance, multistorey buildings are affected by a lower fraction in contrast to single-storey buildings. Additionally, their relation of weight to buoyancy force is advantageous.	Penning-Rowse et al. (2005), Büchele et al. (2006), Kreibich and Thieken (2008), Thieken et al. (2008a)
Building material	Building material reacts differently to exposure to (contaminated) water, e.g. absorbents rates are different. Additionally, drying of material as well as decontamination is more or less difficult. Building material affects also the weight of the building and thus the danger of buoyancy.	Nicholas et al. (2001), Schwarz and Maiwald (2007, 2008)
Precaution	There are various precautionary measures, which are able to reduce flood damage significantly. Examples are structural measures such as elevated building configuration, use of suitable building material or flood adapted interior fitting. Measures like flood secure configuration of oil tanks or secure storage of chemical can prevent contamination.	Kreibich et al. (2005), Büchele et al. (2006), Kreibich and Thieken (2008), Thieken et al. (2008a)
External response/ emergency measures	Emergency measures can be undertaken particularly effective with sufficient warning time and low water levels. Such measures are for instance the dismantling of fixed equipment/machinery, the relocation of inventory, the sealing of openings to prevent water from entering the building. Or quick drying or disinfection which reduce mold building on walls.	
Early warning	Only if the warning time is sufficiently long and if the content is comprehensible, emergency measures can be undertaken efficiently.	McBean et al. (1988), NRE (2000), Penning-Rowse et al. (2005)

Table 14 Damage influencing factor (Merz et al. 2010)³⁷⁹

In almost all models in use today, flood depth is treated as the determining factor for expected damage, sometimes complemented by other parameters like velocity, duration, water contamination, precaution and warning time (Messner et al., 2007³⁸⁰; Merz et al., 2010³⁸¹; Green et al., 2011³⁸²). Some recently developed multi-parameter models are conceptual (Nicholas et al., 2001³⁸³) or developed (and validated) for specific areas, e.g. for Japan (Zhai et al., 2005³⁸⁴) or FLEMO for Germany (Kreibich et al., 2010³⁸⁵).

However, the internationally accepted and most common method for the estimation of direct flood damage is still the application of depth–damage functions (Smith, 1994³⁸⁶; Kelman and Spence, 2004³⁸⁷; Meyer and Messner, 2005³⁸⁸; Merz et al., 2010; Green et al., 2011³⁸⁹).

Depth–damage functions represent relationships between flood depth and the resulting damage indicator such as economic value, loss of people, loss of habitats, etc.

For a given flood depth the function gives expected losses to a specific property, environmental or land use type, either as a percentage of a pre-defined asset value (relative function) or directly in financial terms (absolute function).

A comparison of different damage functions is reported in Figure 63

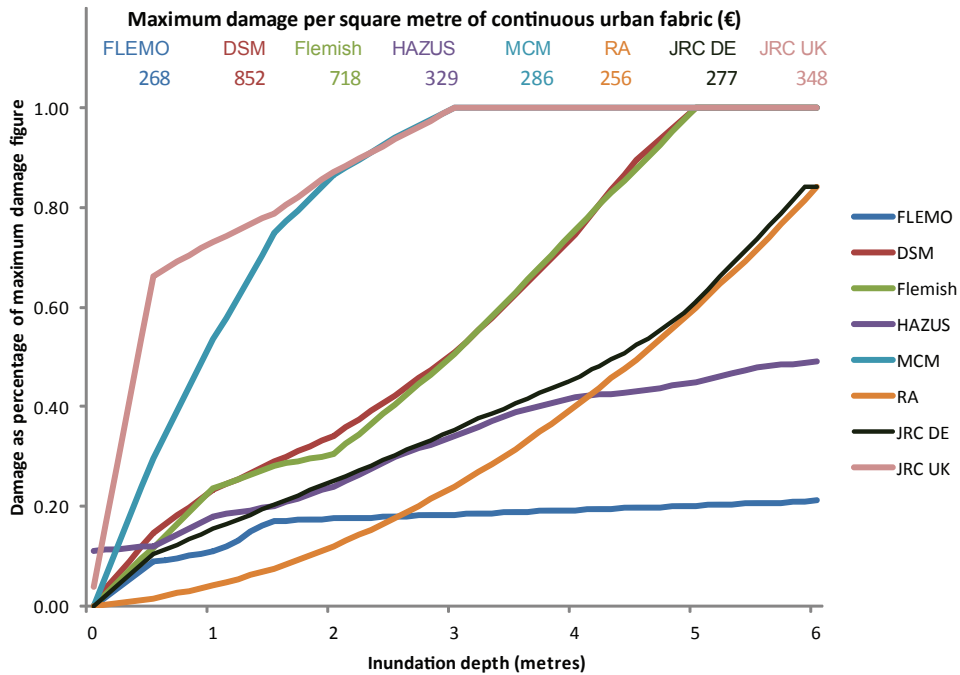


Figure 63 Depth–damage functions and corresponding maximum damage figures for the CORINE land use class “continuous urban fabric” (Jongman et al. 2012³⁹⁰).

There is a large degree of uncertainty in the construction of the damage curves, the asset values connected to these curves and the larger methodological framework (Merz et al., 2004³⁹¹; Hall et al., 2005³⁹²; Meyer and Messner, 2005; Messner et al., 2007; Apel et al., 2008; Freni et al., 2010; Merz et al., 2010; De Moel and Aerts, 2011; Green et al., 2011; Ward et al., 2011)

De Moel and Aerts 2011³⁹³ show that uncertainty in depth–damage curves and corresponding asset values constitutes the most important factor in damage estimation, and has a much stronger effect on the outcome than uncertainties in hydrological and land use (“assets at stake”) inputs.

Jongman et al. 2012 present a qualitative and quantitative assessment of seven flood damage models, using two case studies of past flood events in Germany and the United Kingdom. The qualitative analysis shows that modelling approaches vary strongly, and that current methodologies for estimating infrastructural damage are not as well developed as methodologies for the estimation of damage to buildings. The quantitative results show that

the model outcomes are very sensitive to uncertainty in both vulnerability (i.e. depth–damage functions) and exposure (i.e. asset values), whereby the first has a larger effect than the latter.

We conclude that care needs to be taken when using aggregated land use data for flood risk assessment, and that it is essential to adjust asset values to the regional economic situation and property characteristics.

The purpose of the Web-GIS DSS developed in this thesis is focused on multicriteria risk assessment in order to spatially map the coastal flooding risk and assist managers in mitigation measure selections.

For this reason the damage assessment routines implemented in the DSS were developed in order to assess the environmental (loss of habitats), economical and social damages.

In the context of SMCA (Spatial Multi-Criteria Analysis) risk assessment, the damage models are expressing relation between flood characteristics (water depth, velocity or duration) and indicator relative (percentage of loss) or absolute (number of death, money lost, number of natural habitats, ect).

The basic model implemented in the DSS to calculate flood damages is based on depth/velocity/duration–damage functions which relates the inundation depth/velocity/duration in a grid cell to a fraction of the total value at risk of the corresponding land use. This fraction (usually named ‘ α ’ or ‘damage factor’) is then multiplied with the total value that can get damaged (also based on the land use) to derive a flood damage estimate

The Damage module of the DSS consists in a raster-based algorithm developed using map algebra routines crossing the following elements:

- costal flooding characteristics: water depth, flow velocity and time duration of inundation in the floodplain.
- Receptors characteristics: raster map of asset value (landuse, population, building)
- Vulnerability expressed in terms of damage function

Each damage function represents a relationship between a given flood characteristics (water depth, flow velocity, time duration) (X-axis) and the dependent damage factor (Y-axis) that can be expected for that land use category.

In a flood zone the real damage caused by inundation at a certain water height can be calculated by summing all unique surface entities (i.e., discrete land use categories) and combining the water depth (translated to the corresponding damage function DF_L factor) with the maximum damage of that land use category.

For a generic pixel (i,j) the Damage is evaluate with the following general map algebra equation:

$$Damage(i, j) = UC_L * A_L(i, j) * DF_L(WD(i, j), V(i, j), D(i, j)) \text{ Eq. 17}$$

Where i and j describe the row and column of generic pixel ij, UC_L is the unit value of asset type l (maximal damage) expressed in land value per square meter, A_L is the unita area defined by pixel size, DF_L is the $(WD(i, j), V(i, j), D(i, j))$ -damage function.

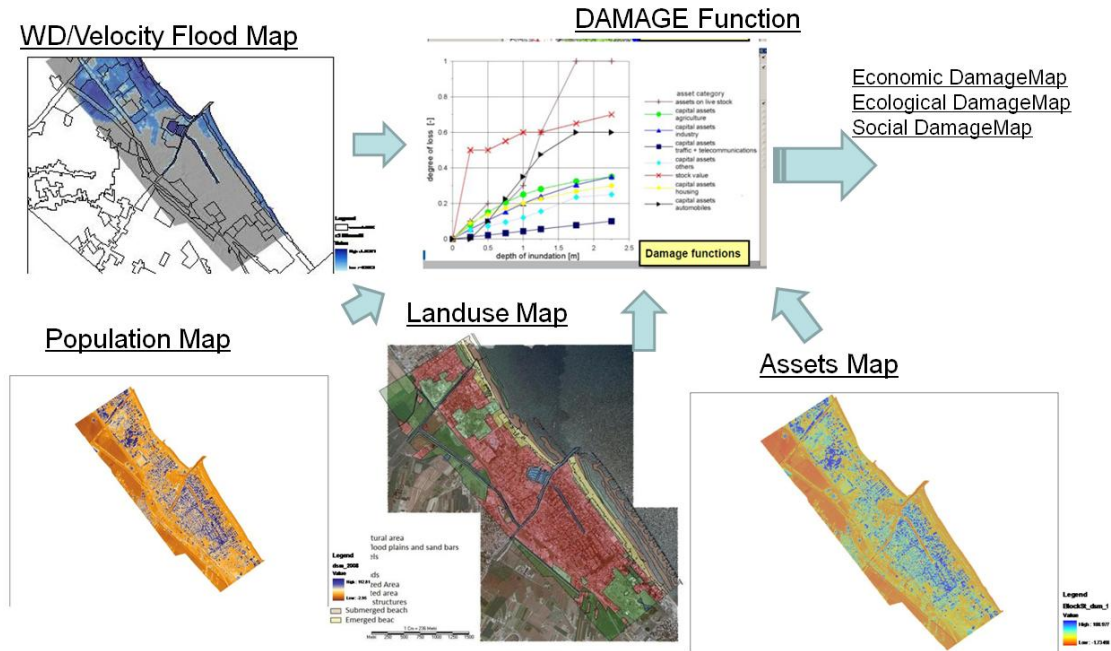


Figure 64 Flow Diagram of the methodology for damage assessment

Hereafter are described the damage models implemented in the Web-GIS DSS.

6.2 Economic Damage Model

The overall Economic Consequences (EC) of flood in terms of flood depth and flood duration are estimated by applying the following formula (Zanuttigh et al. 2014³⁹⁴):

$$Economic_Damage(i, j) = (UC_L * A_L(i, j) * b_{ij} * D(i, j) + UC_L * A_L(i, j) * a_{ij} * \sqrt{WD(i, j)}) \text{ Eq.}$$

18

where UC_L are the values of land uses in euro/m²/year from census statistic data; $D(i, j)$ is flood duration and $WD(i, j)$ is flood depth; a_{ij} are proportionality constants as functions of $WD(i, j)$ that are normalised for each land use j at the maximum value of F_y in 2050 for a storm return period $Tr = 100$ years, assuming different reference percentage of damage

depending on the use (for instance, 50% damage for buildings/homes/hotels, 25% damage for harbours); b_{ij} are proportionality constants as functions of $D(i,j)$ that express the expected period to restore economic activities as a factor of duration, depend on the land use (for instance, a value of 30 is set for hotels and of 20 for private services) and are normalised to annual incomes with the days/year. Note that flood velocity is assumed to be irrelevant.

In the next table are reported the economical data for the study site of Cesenatico (Italy).

ECONOMIC VALUES	Northern West	Southern West	East
Residential homes	130	165	140
Holiday homes	191	217	199
Historical buildings	180	180	180
Hotels	152	152	152
Camp sites	61	0	0
Tourism harbour and infrastructures	97	97	97
Fishing harbour and infrastructures	179	179	179
Private services	3554	3554	3554

Table 15 Land use values UC_L (annual € per m²) in Cesenatico

ECONOMIC VALUES	% damage at max flood depth 0.787 m	a_j	b_j
Residential homes	50	0.564	0
Holiday homes	50	0.564	0
Historical buildings	50	0.564	0
Hotels	50	0.564	30/365
Camp sites	100	1.127	40/365
Tourism harbour and infrastructures	25	0.282	20/365
Fishing harbour and infrastructures	25	0.282	20/365
Private services	75	0.845	20/365

Table 16 Parameters for economic consequences in Cesenatico

Land Use values UC_L per square meters are obtained through reclassification of land use map (Corine Land Cover) and mapped in Figure 65.

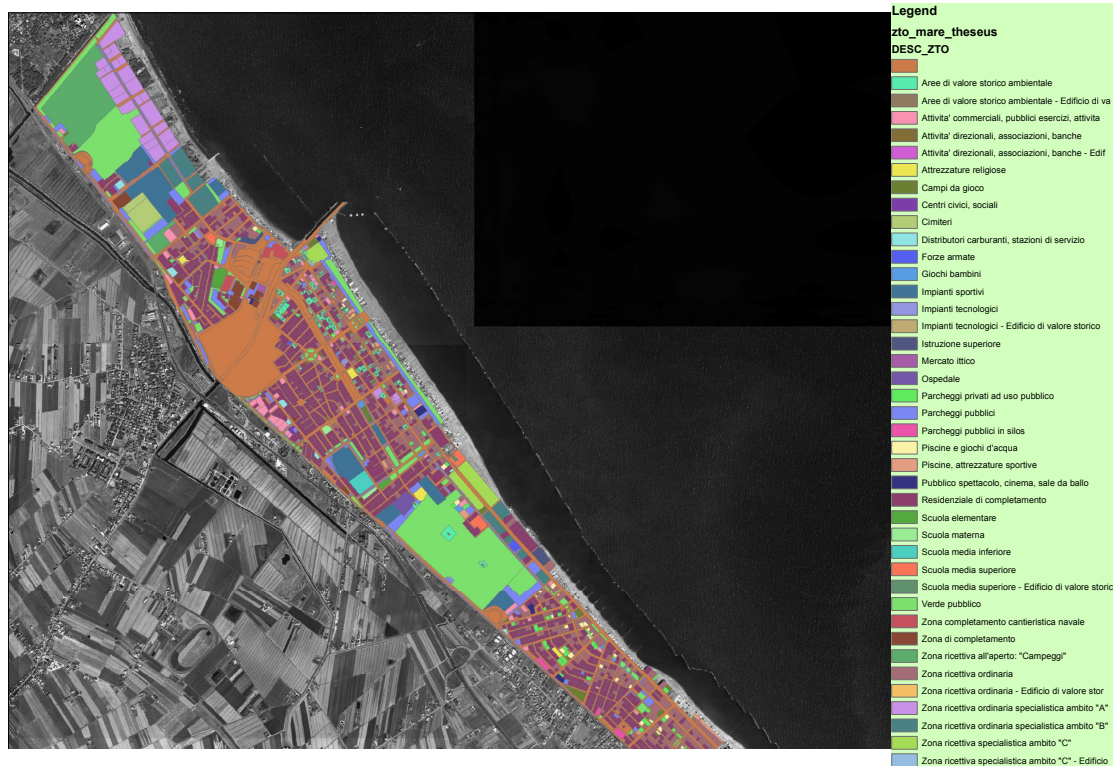


Figure 65 Land Use Map – CORINE LAND COVER

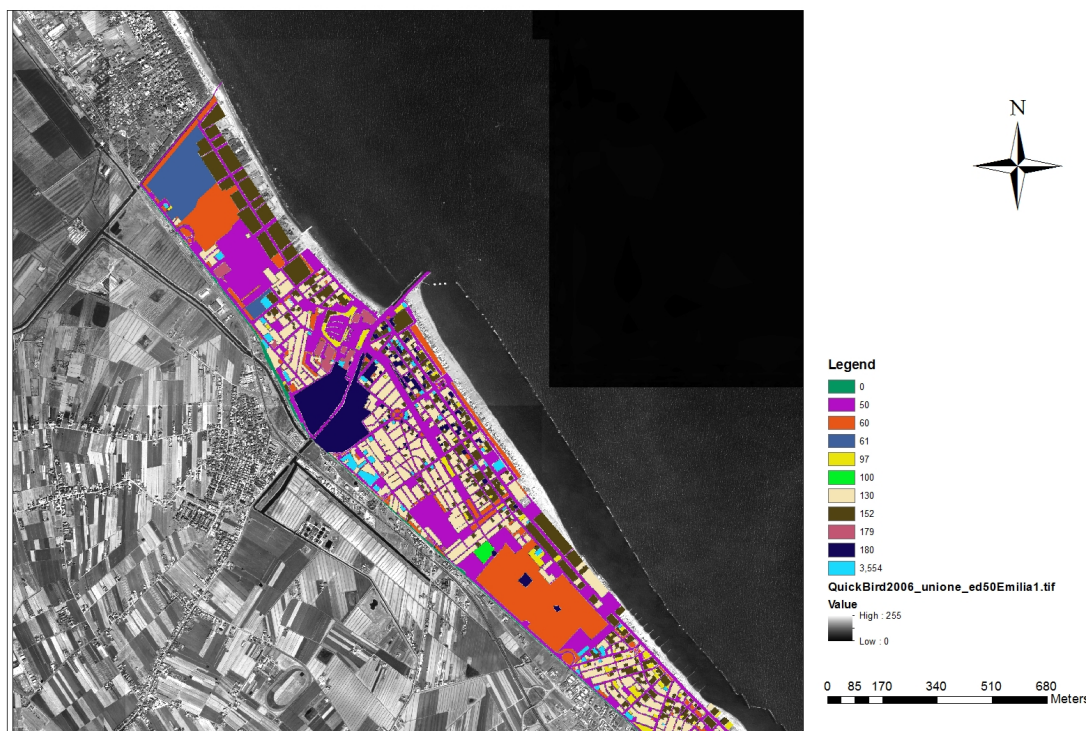


Figure 66 Cesenatico Land Use values UC_L euro/mq

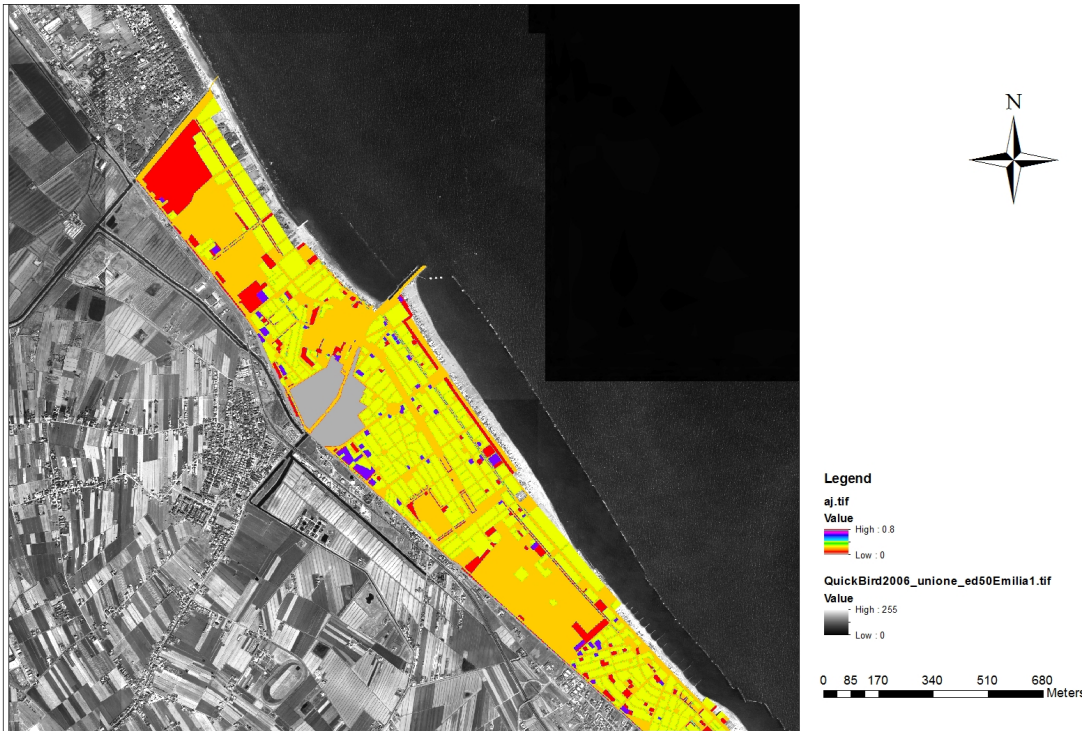


Figure 67 Cesenatico *aj* proportional constant



Figure 68 Cesenatico *bj* proportional constant

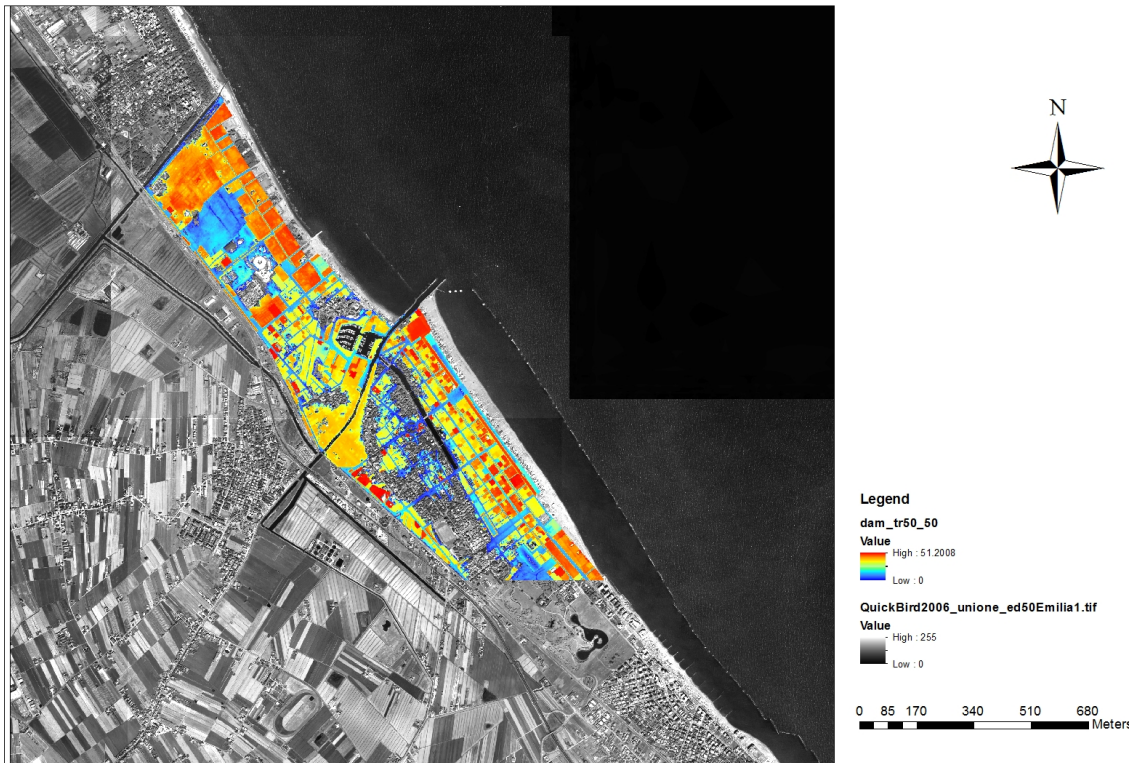


Figure 69 Cesenatico Economic Damage Map

6.3 Social Damage Model

Social vulnerability is a complex phenomenon and no single measure comprehensively covers the whole spectrum of such vulnerability (Adger et al., 2005³⁹⁵). Recently, the Social Vulnerability Index (SoVI) has been suggested as a comparative spatial assessment of human-induced vulnerability to environmental hazards (Cutter et al., 2003³⁹⁶; Wisner et al., 2004³⁹⁷). The SoVI is based on a large set of measurable variables that can be grouped into main common factors such as: population structure, gender, income, socio-economic status, and renters (www.csc.noaa.gov/slr). Analysis and mapping of social vulnerability should also consider identifying critical facilities or resources to help prioritize potential hazard mitigation.

In the developed Web-GIS DSS the social vulnerability is modelled considering two main aspects: number of people exposed and the expected number of fatalities.

Expected number of fatalities:

Alongside economic damage expectations, policy and decision-makers are also interested in the potential number of fatalities associated with a hazard. An estimate of the number of

fatalities due to a flood event is based on: 1) information regarding the flood characteristics; 2) an analysis of the exposed population and evacuation possibilities; and 3) an estimate of mortality among the exposed population.

Relevant flood characteristics include water depth, the rate at which the flood water rises, and the flow velocity. The exposed population equals the number of inhabitants of the flooded area minus the part of the population that is able to evacuate the area or find shelter elsewhere in the area. An example of a mortality function for the rapidly rising zone is shown in Figure 70. Based on this method the loss of life can be estimated for a given flood scenario. The loss of life estimates are presented as a separate output of the model and are not monetised.

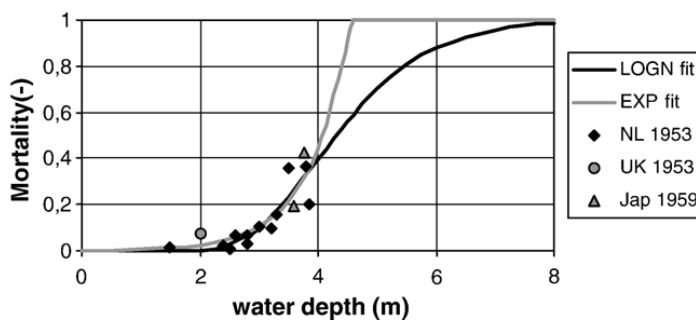


Figure 70 Observed and fitted mortality function for zone with rapidly rising flood water (Jonkman, 2007³⁹⁸)

The (flood) hazard rate to people implemented in the Web-GIS MARASMA DSS is calculated using the following equation (DEFRA, 2006):

$$Hazard_People(i, j) = (WD(i, j) * (V(i, j) + 1, 5))Eq. 19$$

where $Hazard_People(i, j)$ = hazard score for people, WD = water depth (m), V = velocity ($m\ s^{-1}$).

Above equation allows one to produce a hazard map, where the resolution depends on the outcomes and resolution of the hydraulic modelling and/or the historical data set used to calculate and/or retrieve the physical metrics.

Number of People Exposed

The following criteria were considered as tremendously important for being part of our integrated urban criteria set: the affected (total) population (excluding children and the elderly), the number of children, the number of elderly people, and the number of social hot spots (cf. also King and MacGregor, 2000³⁹⁹).

Humans are the most important value in flood protection. Next to direct physical harm, humans may suffer damage from extreme floods due to psychic trauma, stress and con-

taminated drinking water (Gruenwald, 2001⁴⁰⁰; Tapsell et al., 2002⁴⁰¹). Elderly people and children represent age classes which are particularly vulnerable to floods (Meyer et al., 2009⁴⁰²) as they depend on support in case of a flood event. Moreover, flood damage to nursing homes, kindergartens and schools poses unexpected financial discomforts for parents, relatives and the staff. Furthermore, elderly people are at risk again due to their lower constitutional mobility (Cutter et al., 2003⁴⁰³).

The criteria of the affected population, children, and elderly people are quantified by means of a micro-scale approach: census data at municipality district level were taken and downscaled.

The percentage of the Population Aged (Pa) can be derived from demographic data (ISTAT, 2009⁴⁰⁴) or referred to national middle average.

Places with social and health care and related infrastructure facilities play an important role in ensuring the quality of life of the urban population. Thus, damages caused by flood events could lead to substantial losses of such infrastructure. In order to capture such damage potential the following infrastructure facilities were considered: schools, kindergartens, pensioners' homes, fire stations, and hospitals.

In the next figures are reported the damage assessment for population in Cesentaico. In particular the Damage function for people exposure is evaluated crossing the water depth (Scenario 2020 with TR50 years) due to flooding and the density of population downscaled to residential building.

In Figure 71 and Figure 72 are displayed respectively the population in census area (ISTAT 2001) and the relative density of population. In Figure 73 is reported the presence of residential buildings (point) and in Figure 74 the relative flood hazard indicator for residential exposed population obtained multiplying the density of residential population by the water depth.

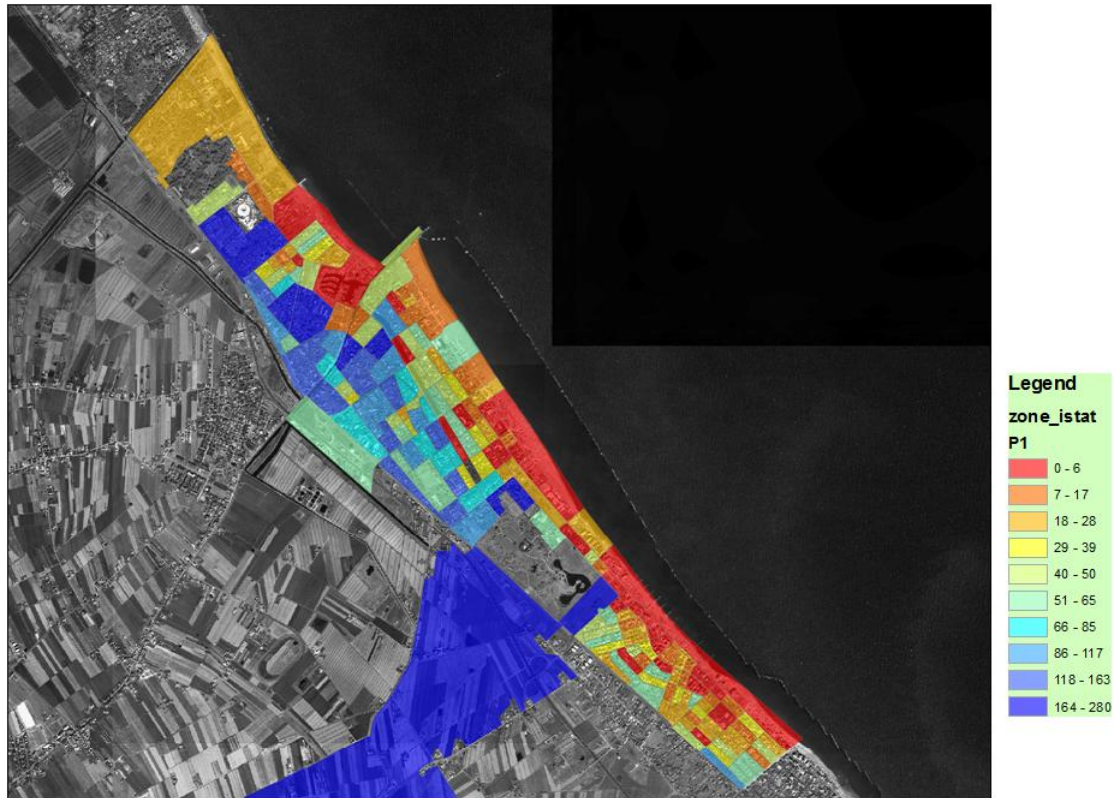


Figure 71 Population in Cesenatico

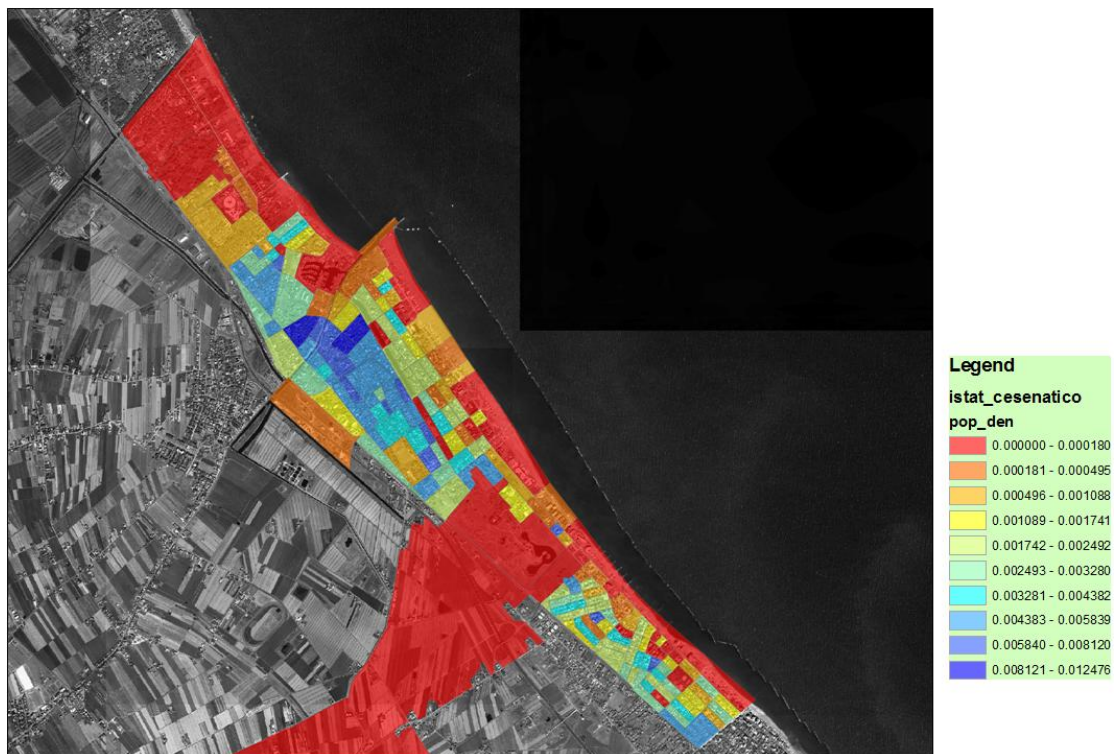


Figure 72 Population density in Cesenatico

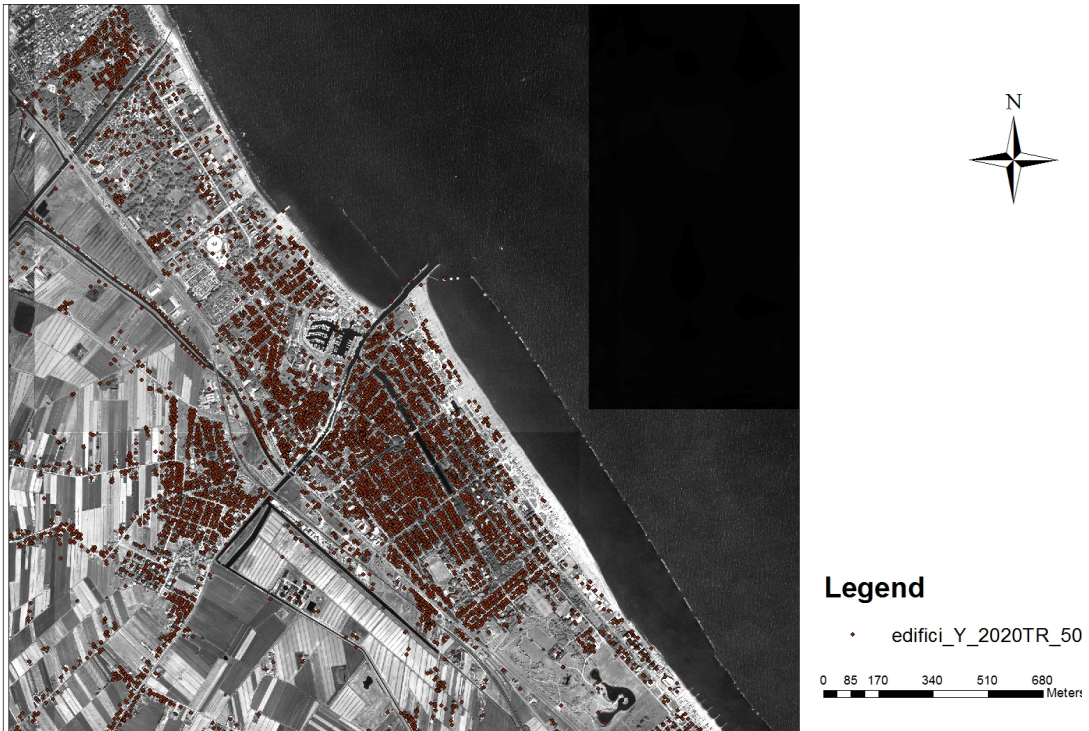


Figure 73 Cesenatico Residential Building

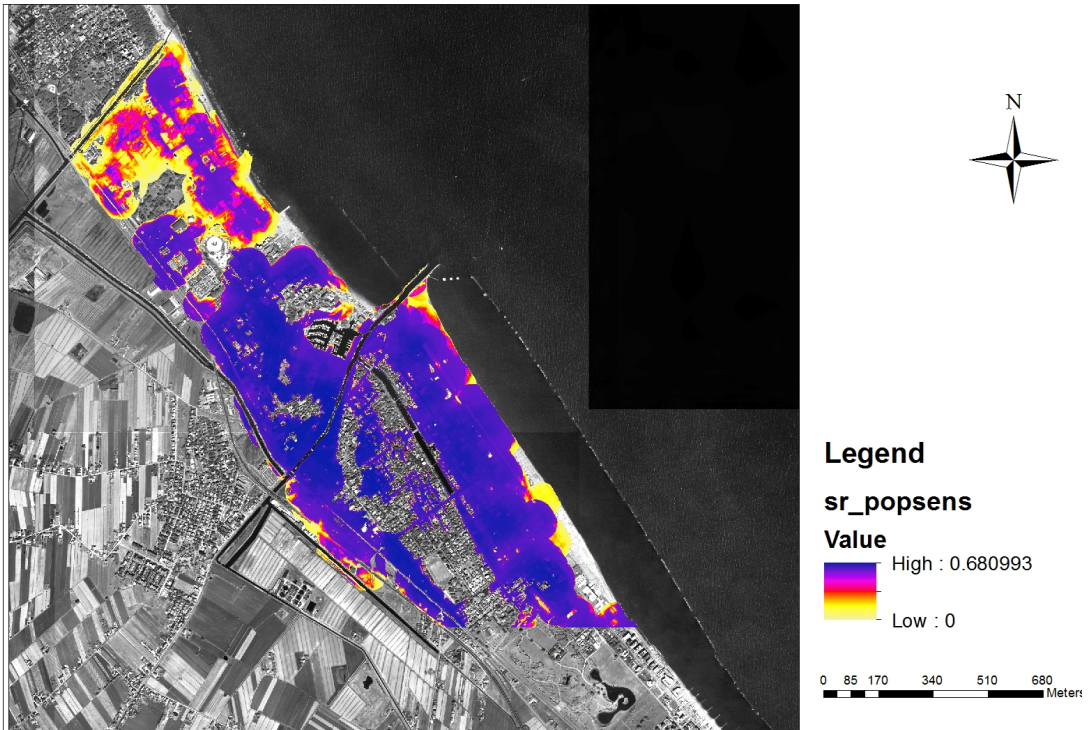


Figure 74 Cesenatico indicator of exposed Population

6.4 Environmental Damage Model

To assess the vulnerability of ecosystems to changes induced by flooding in the coastal area, an index was adopted in the DSS. This index provides a rapid and standardized method for characterizing vulnerability across coastal systems and identifies issues that may need to be addressed in order to reduce vulnerability.

Outcomes are categorical based on thresholds for the transition between the following states: 0) existing state remains with minimal / no change; 1) damage to the habitat occurs but natural recovery possible without human intervention within one year; 2) damage to the habitat is more substantial but recovery is possible with some human interventions (e.g. re-planting, stabilisation of substratum) 3) irreversible loss of existing habitat. Where outcomes result in irreversible loss of an existing habitat the most likely transition to a new habitat type is indicated for example where terrestrial habitats become flooded on a regular basis it is anticipated that a saltmarsh community will be formed.

The advantage of using an index is that allows key step changes or tipping points (Scheffer et al. 2009⁴⁰⁵ see also Rietkerk et al. 2004⁴⁰⁶) in a habitats properties to be captured as it is these dynamic changes of an ecosystem that is of interest rather than the transition from one ecosystem to another. A second advantage is that it provides a standardised method for characterising vulnerability across different coastal habitats and one that can be applied to all study sites. The EVI allows the user to identify issues that may need to be addressed in order to reduce vulnerability of a given habitat (EVI SOPAC UNEP 2011).

	Negligible	Transient effect (no long term change anticipated)	Moderate effect/Semi permanent change	Permanent effect/change
EVI Index	0	1	2	3
Habitat/ Key species	Negligible impact to habitats / species	Changes within the range of Receptor's natural seasonal variation and full recovery is likely within a season	Changes are beyond Receptor's natural seasonal variation. Partial recovery is possible within several seasons, but full recovery is likely to require human intervention, or greater than 20 years for natural recovery	Changes are so drastic that natural recovery of receptor is very unlikely without human intervention. Or natural recovery will take longer than 20 years

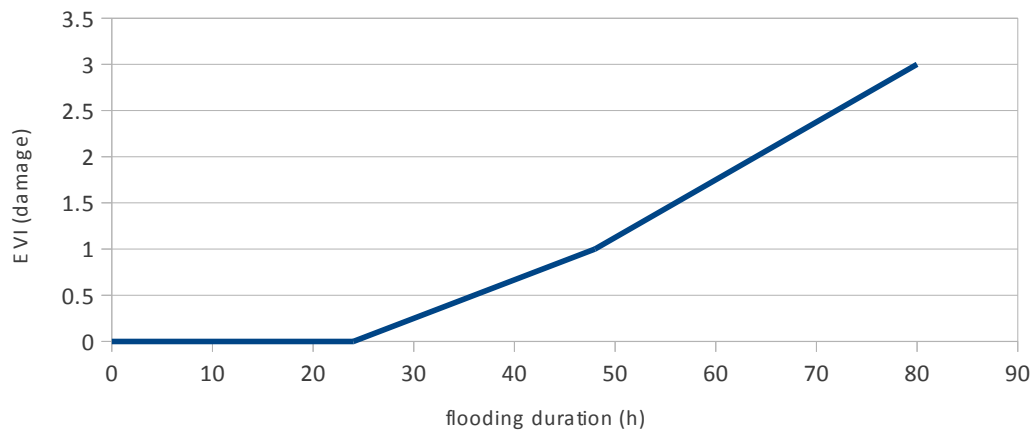
Table 17 Step change categories for EVI

The Ecological Damage function implemented in the Web-GIS MARASMA DSS are based on Environmental Vulnerability index (EVI).

For each sensible habitat the user can define a specific EVI-flood duration-water depth damage relations as illustrated in the next figures.

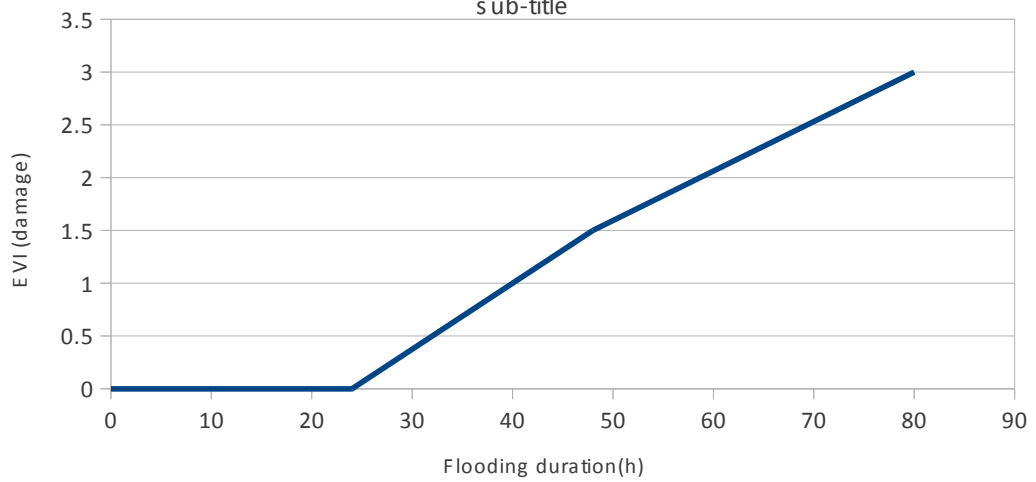
Pinewood damage curve (SLR:0 cm)

sub-title



Pinewood damage curve (SLR:13 cm)

sub-title



Pinewood damage curve (SLR:22cm)

sub-title

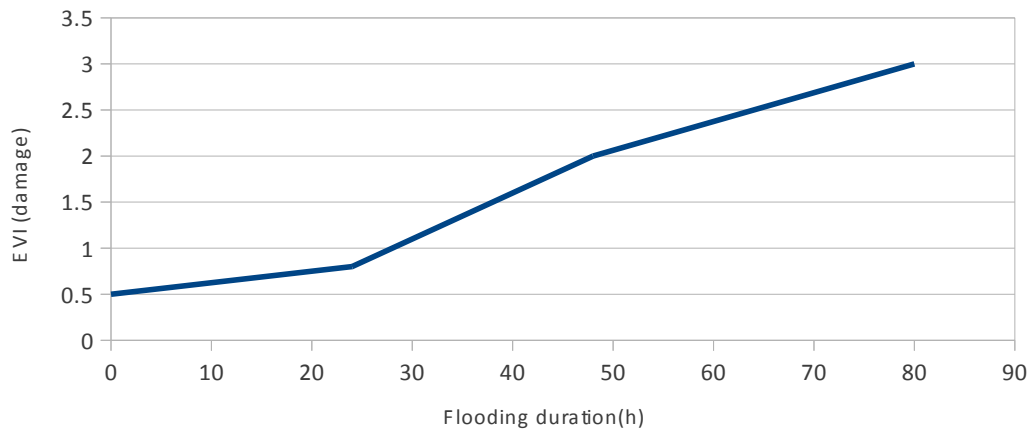


Figure 75 EVI – Flow Duration

7 Quantitative GIS-Based risk evaluation

The term risk is hereby understood as the probability of negative consequences and is measured by the formula

risk = probability * negative consequence (see e.g. Gouldby & Samuels 2005⁴⁰⁷)

In other words this is the expected annual average negative consequence of flooding, whereas “negative consequences” covers economic, social as well as environmental consequences. This formula goes back to the definition of risk introduced by Knight 1921⁴⁰⁸, see e.g. Hansjürgens 2004⁴⁰⁹ and Köck 2001⁴¹⁰) and is based on the assumption that risks are measurable.²

For the practical application of flood risk assessment this means that the negative consequences have to be evaluated for flood events of different probability in order to construct a damage-probability curve .

The risk (or the annual average damage) is shown by the area or the integral under the curve (Meyer et al. 2007⁴¹¹).

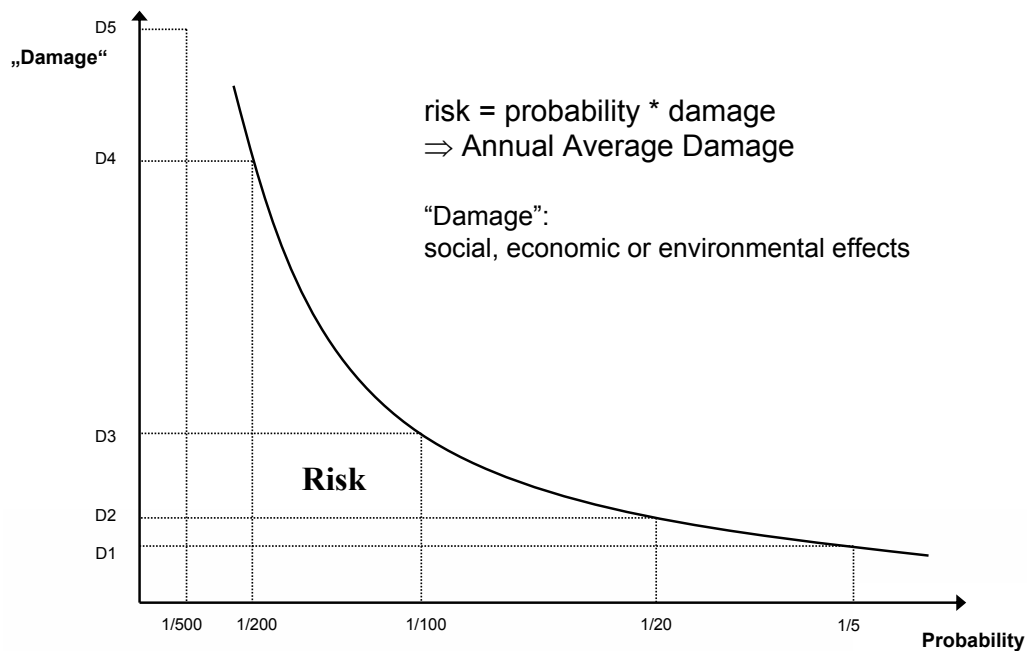


Figure 76 Risk – Damage Vs Probability Meyer et al. 2007⁴¹²

The flood damage as reported in previous section, are estimated under the assumption that, for given environmental, social and economic conditions, damage is a function of floodwater characteristics such as water depth, velocity and duration.

The information concerning the probability of flood events, storm surge and wave height, are derived from joint probability frequency function reported in chapter 5.7 and expressed in terms of Return Period.

The return period represents the chance of the occurrence of a flood with a certain water level in the floodplain.

In the final step, the different damage maps for each return period are combined into one risk map.

Two different methods for combining multiple damage maps with different return period were evaluated in this thesis.

The first is proposed in the FLOODSITE project by Meyer et al. 2007⁴¹³ and assume a linear run of the curve between each of know points computing the average damage and assessing the area of risk curve using the trapezoidal rule (DVWK 1985⁴¹⁴):

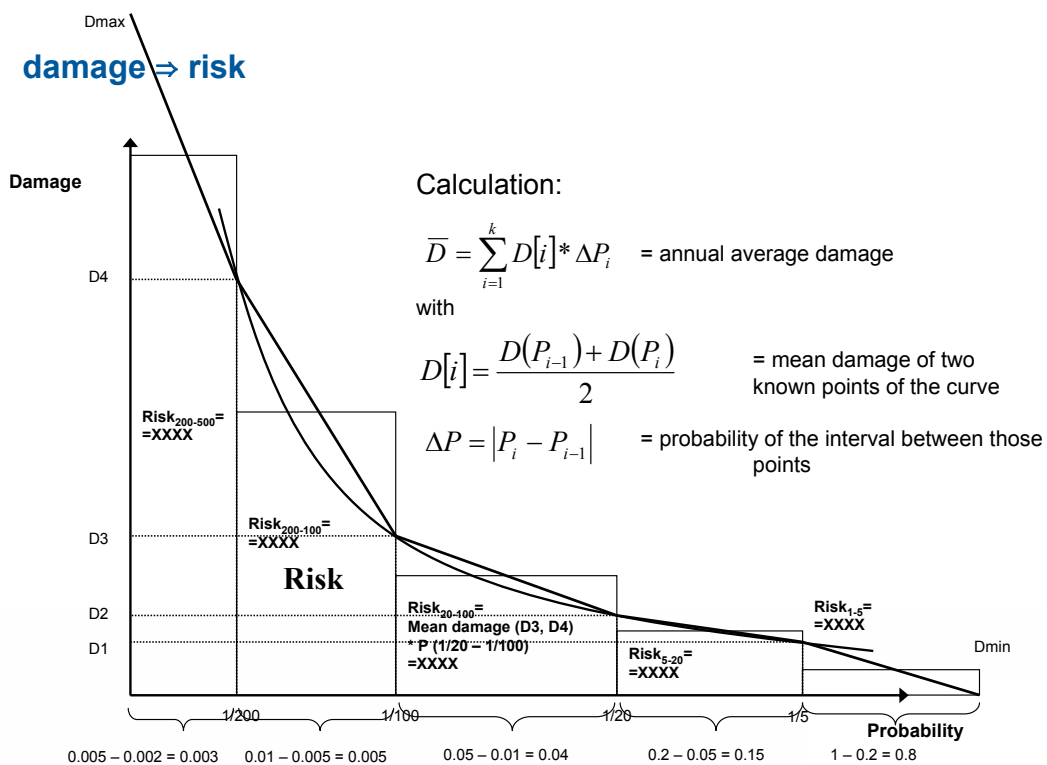


Figure 77 Risk – Trapezoidal Rule Meyer et al. 2007⁴¹⁵

The second formulation proposed by Vanneville et al. 2003⁴¹⁶ in LATIS evaluate the risk (expressed as the mean annual damage per surface unit per year) equal to the damage caused by a n event with a 1-year return period, plus half of the damage difference between a 2-year flood and a 1-year flood, plus one-third of the damage difference between a 3-year

flood and a 2-year flood, and so forth. The mathematical explanation of this procedure is explained in Equations:

$$R = \sum_{i=1}^n \frac{1}{i} (S_i - S_{i-1})$$

Or

$$R = \frac{1}{1}S_1 + \frac{1}{2}(S_2 - S_1) + \frac{1}{3}(S_3 - S_2) + \dots + \frac{1}{n}(S_n - S_{n-1})$$

Eq. 20

R risk S_i the damages related to a flood with a return period of i years n the highest return period

As explained above, the creation and validation of flood maps is time-consuming, so only a few have been created. To calculate risk in practice, it is assumed that linear interpolation of the flood damage between two return periods is valid, so the formula (in the case of return periods of 1, 2, 5, 10, 25, 50 and 100 years) can be simplified to ():

$$R = \frac{1}{1}S_1 + \frac{1}{2}(S_2 - S_1) + \frac{\frac{1}{3} + \frac{1}{4} + \frac{1}{5}}{5 - 2}(S_5 - S_2) + \frac{\frac{1}{6} + \frac{1}{7} + \frac{1}{8} + \frac{1}{9} + \frac{1}{10}}{10 - 5}(S_{10} - S_5) + \dots$$

(4.4)

Equation 4.4 can be further simplified to:

$$R = 0.5 \times S_1 + 0.2389 \times S_2 + 0.132 \times S_5 + 0.07 \times S_{10} + 0.0318 \times S_{25} + 0.0135 \times S_{50} + 0.0138 \times S_{100}$$

(4.5)

GIS modeling potentiality are crucial for natural hazard risk assessment and mitigation. In relation to flood hazard, several approaches and models are used for assessing the related risks, depending on the context, existing datasets and objectives of the evaluation. The work published by Merz et al., 2010⁴¹⁷ resume different methods and approaches used to assess potential flood damages and risk worldwide.

Concerning the implementation of risk calculation in a GIS-based framework, for each grid cell the risk needs to be evaluated. The GIS method developed and implemented in this thesis is a raster-based type and consists in a set of simple map algebra calculations.

The calculation of damage and risk consists of three steps, namely (i) defining probability and extent of flooding, (ii) determining expected damage, and (iii) defining risk. The different steps are schematically presented in Figure 78.

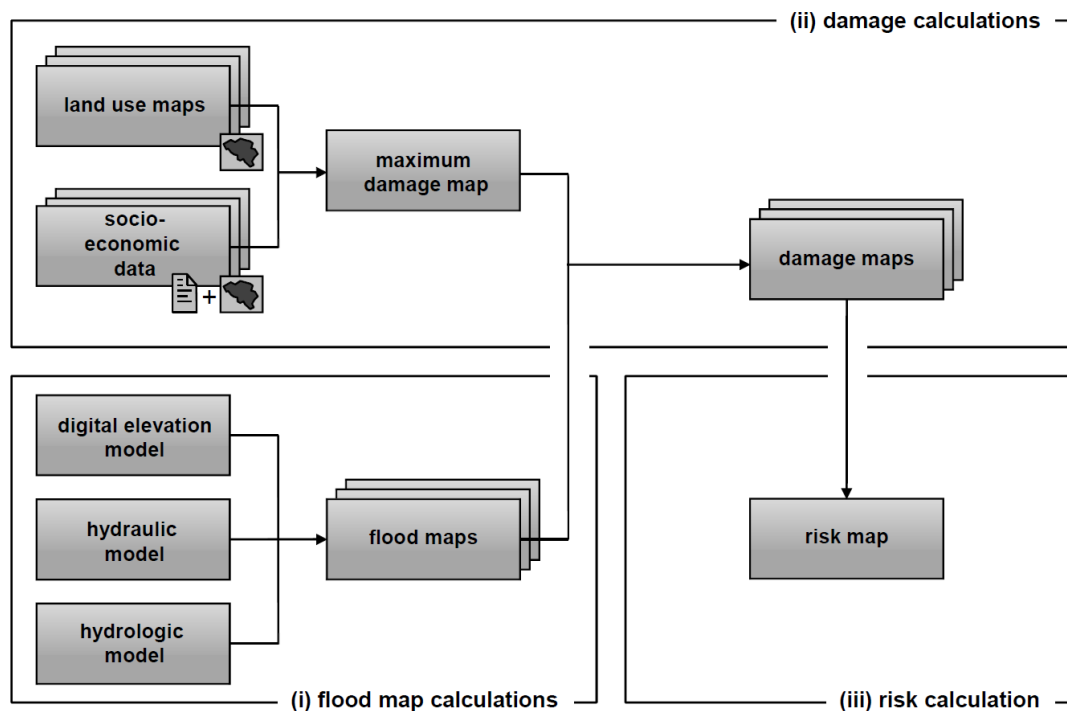


Figure 78 Raster Based Risk Framework - Vanneuille et al. 2003

The basis for all damage evaluations are the map of flooding characteristics, such as water depth, velocity and duration, of different exceedance probability or return period (TR10=1:10, TR50=1:50, ...). The maps are calculated by the raster based model discussed in chapter 6. Damage is calculated for each of these grid cells, so that a damage map for each of the events mentioned above is produced. By using the risk formula described above, the annual average damage per grid cell can be computed.

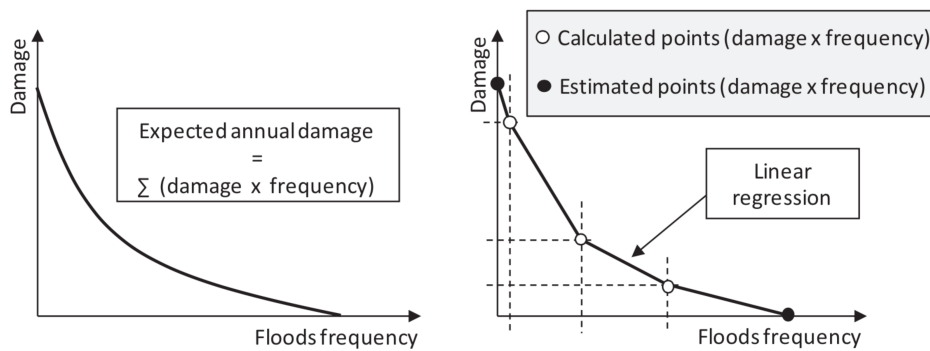
Secondly, land use information and socio-economic data is used to produce maximum damage maps. When combining the latter with the flood maps, expected damage for a given inundation can be calculated. Besides this, land use information can be derived out of a variety of land use maps, based on topographic maps, satellite imagery, orthophotographs, CORINE Land Cover, etc. In addition, socio-economic data is gathered. E.g. the number of persons and vehicles per surface area, values for a great number of goods, land use categories, buildings, etc. Thus, to determine the expected damage for a given flood, the replacement value of goods is used, not the original value of purchase. Based on this information, a maximum damage is computed by unit of surface for each land use category (buildings, industry, pastures, etc.).

These categories all have different relations between maximum damage and water depth, called damage functions or a-factors. The expected damage inside an inundation area is then calculated by multiplying the maximum damage of each land use category with the

corresponding a-factors and by subsequently summarizing these with all different land use categories of a certain area.

The last step calculates assets expected annual damage (EAD), which is an index commonly used to express the risk in terms of exceedance probabilities (Beard, 1997⁴¹⁸; CIEWR-HEC, 1989⁴¹⁹; Messner et al., 2007⁴²⁰). Its calculation enables to define the average annual damage for the elements at risk based on the probability of damage caused by floods.

A raster-based routines were developed and embedded in the MARASMA DSS in order to run the above described procedure. The routine were written in python and are based on map algebra library such as GDAL.



Eq. 21 Calculation of expected annual damage

8 Multicriteria Risk Assessment

For natural hazards, risk-based decision-making is a multidimensional and multidisciplinary activity embracing environmental, socio-economic and management-related factors at different spatial and temporal scales.

The comprehensive analysis and assessment of flood risk is an essential part of the risk management approach, which is the conceptual basis for the new EU “directive on the assessment and management of flood risk” (EU 2006/C 311 E/02).

Risk assessment is conducted in order to identify the magnitude and spatial distribution of flood risks. Most current approaches focus only on economic risks. Environmental, social and cultural risks are often neglected or mentioned as a side product.

Multicriteria Analysis enables consideration of all relevant risks, is an appropriate method of incorporating all relevant types of consequences without measuring them on one monetary scale. It provides an alternative to the complex monetary evaluation (CBA) and internalisation of intangible consequences. Cost-benefit analysis (CBA) for flood management and coastal defence is well established but there is growing concern that it fails to take full account of social and environmental factors. Multi-criteria Analysis (MCA), in contrast, allows a comparison between different alternatives by a broader set of criteria which can all be expressed in their own different dimensions, be it qualitative or merely ranked (-- to + +).

In this thesis MCA is combined with Geographical Information Systems (GIS) (Geneletti, 2005⁴²¹, 2004⁴²²; Malczewski, 1999⁴²³) in order to display the spatial distribution of flood risks and risk reducing effects, respectively. Different *areas* are compared and evaluated with regard to different risk criteria. The result of GIS-based multicriteria risk analysis is a map which allows a ranking of risk areas under multiple mitigations option scenario.

Multicriteria Analysis can be used in the two stages of the flood risk management process mentioned above:

- *Multicriteria risk assessment* First of all, the problem is to identify, *where* the coastal flood risk is too high. Often there is in the beginning only a vague awareness that flood risk might be high. I.e. the current magnitude and spatial distribution of flood risk needs to be identified in order to find out where further mitigation measures are necessary. The objective is to identify areas where flood risk needs to be reduced and where not. This multicriteria assessment of different areas is therefore an important prerequisite of step 2 as it is an important part of the

problem definition of step 2. The alternatives considered here are the different areas (Where is risk highest?). The evaluation criteria are the different risk categories (social, economic and environmental risk criteria, which can be further differentiated into sub-criteria).

- *Multicriteria project appraisal* After identifying high risk areas, the second part of the decision problem is to find the best strategies or measures to reduce flood risk to an appropriate level. These mitigation measures need to be evaluated in order to find the best alternative or combination of alternatives. In this step the decision alternatives are measures which have a certain effect on the risk criteria. The evaluation criteria are therefore the expected reduction of social, economic and environmental risks caused by the measure. Additionally, the costs of the measure are an important criterion. Hereby, the spatial distribution of these risk reducing effects is rarely considered at present. I.e. in most cases only the overall effects of alternative measures are evaluated. A GIS-based mapping of the effects of each measure may also help to highlight who and where the winners (and perhaps losers) are.

A stepwise procedure of Multicriteria Risk Mapping approach is implemented in the Web-GIS MARASMA DSS (Meyer et al. 2007⁴²⁴, 2008⁴²⁵, 2009⁴²⁶) and tested at the Cesenatico case study in Italy.

As displayed in Figure 79, the process of MCA can be divided into different steps (based on Munda 1995⁴²⁷, Rauschmayer 2000⁴²⁸; Malczewski 1999⁴²⁹):

1. Scenario and Problem Definition
2. Evaluation Criteria
3. Alternatives
4. Criteria Evaluation
5. Weighting
6. Decision Rules
7. Sensitivity and Uncertainty
8. Ranking

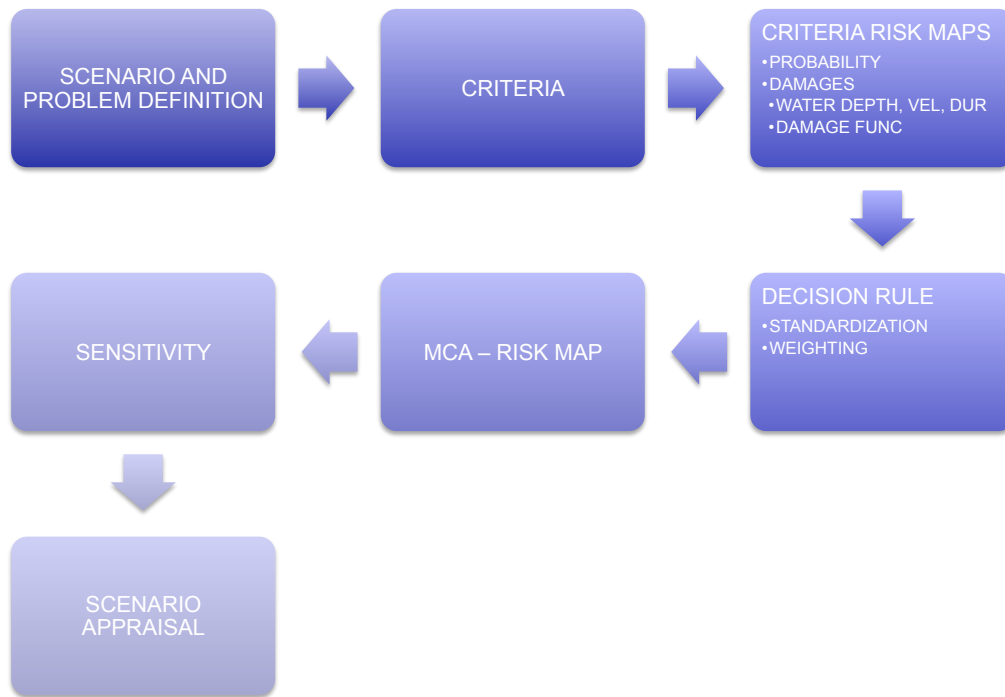


Figure 79 MCA Steps wise procedure

Problem and Scenario Definition

At the beginning of any decision making process the problem needs to be recognized and defined. Malczewski (1999) defines the decision problem broadly as “a perceived difference between the desired and existing states of a system”. In the case of flooding, the problem seems to be quite clear: Floods obviously cause huge damage and, in the worst cases, even casualties. Consequently, there is a high need to reduce the risk of flooding.

Multiple coastal flooding scenario can be evaluated, in particular the user can select among the following of scenario:

- Climate and environmental scenarios, which can be a predefined set of conditions derived by scientists (wave height, storm surge, sea- level rise, etc.) for short, medium and long term or intervals of these parameters the user can combine based on the kind of scenario he/she wishes to try, ordinary or extreme;
- Economic and social scenarios, essentially based on expected changes or trends of the population and on the gross domestic product; also in this case the user can select the trend value within the range of values suggested by the scientists;
- Environmental scenarios, limitedly for now to subsidence; in future versions scenarios of habitat change based on changes of temperature, social and economic development, etc. may be included.
- Mitigation option scenarios, represented by adoption of structural infrastructures such as dike, sea gate and wave energy converters. Other mitigation measure are represented by land use change trough specific planning policies.

Through the GUI of MARASMA-DSS the user can select and define multiple risk scenario and upload the associated raster maps, for example a new DEM where there is the dike presence or a new land use with a different asset dislocation.

In the next figure is reported an example of risk reduction benefit in terms of realization of a dike for coastal protection.

Evaluation of measures by Cost-benefit analysis: risk reduction = benefit

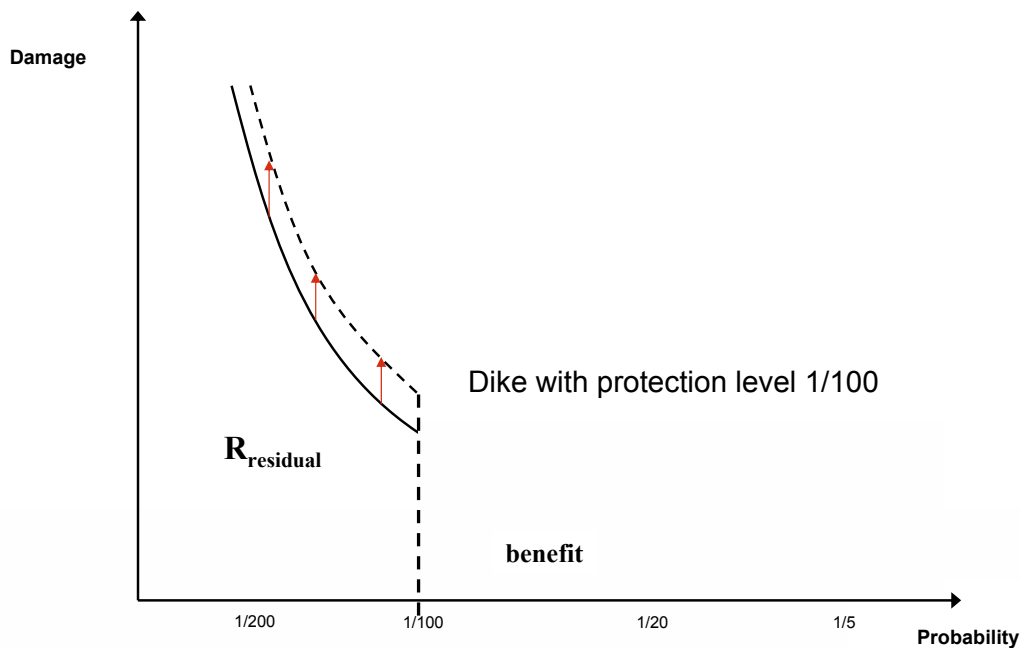


Figure 80 Risk Reduction Example Meyer et al. 2007⁴³⁰

Selecting the Evaluation Criteria

In the second step of MCA the evaluation criteria have to be selected. The inclusion or exclusion of criteria can greatly influence the results of the evaluation process, so it is important that stakeholders and decision makers participate in this selection process. The evaluation criteria should be complete on the one hand to make sure that the whole problem is encompassed, on the other hand the set of criteria should be kept minimal to reduce the complexity of the evaluation process. Regarding flood risk analysis the criteria should cover the whole range of economic, social and environmental risks.

The most common economic criterion is the expected annual flood damage. Sometimes also indirect losses, e.g. due to business or transport interruption are considered. Regarding social risk criteria, often simply the number of affected persons is used as a simple indicator for the harmful effects flooding may cause to people. But of course these effects can be

differentiated in e.g. loss of life, health effects, stress, safety, equity and community. Also the damage to cultural goods such as cultural heritage can be considered here.

Environmental criteria measure e.g. the performance of fauna & flora habitats, of water quality and quantity, soil quality or the effects on landscape scenery. Note that especially in this category flooding can also have positive effects on the criteria performance.

Publication	Criteria used
(RPA 2004)	Economic Assets Land use Transport Business development Environmental Physical habitats Water quality Water quantity Natural processes Historical environment Landscape Social Recreation Health and safety Availability of services Equity Sense of community Costs criteria
(Penning-Rowsell et al. 2003)	Risk to life Failure mode Reliability Local socio-economic impact Positive environmental Negative environmental impacts Flood losses Other benefits Costs Maintenance costs Benefit-cost-ratio
(Brouwer & van Ek 2004)	Environmental Nature conservation Economic Costs (land use change, agricultural compensation payments, infrastructure protection, operation and maintenance) Benefits (damages avoided, recreational benefits) Social (qualitative score card) Impact on functions perception of landscape change risk perception communication efforts participation possibilities
(Bana E Costa et al. 2004)	Environmental: Water (5) Soil (2) Fauna & Flora (1) Landscape (2) Social Risk perception Effects on social fabric Public health Technical Complexity of intervention Complexity of maintenance Level of protection

Publication	Criteria used
(Olfert 2006)	Hydrological & hydraulic effects Ecological criteria Water (biological, hydromorphological, chemical) Social Health Social stability Cultural & natural heritage Economic Annual average damage (AAD) Indirect Direct cost Indirect costs
(De Bruijn 2005)	People Affected persons Casualties Economic AAD Costs Economic opportunities Environmental Change in natural area Landscape Flexibility Robustness
(Simonovic & Nirupama 2005)	Water depth Flood damage
(Akter & Simonovic 2005)	Social: 1. Community involvement (participation, involvement, local leadership etc.) 2. amount of personal loss (economic, health, stress, safety, control)
(Tkach & Simonovic 1997)	Flood Depth Building damage Benefit from flooding upstream areas

Figure 81 Example of criteria used in flood risk MCA Meyer et al. 2007⁴³¹

The evaluation criteria implemented in the Web-GIS DSS in order to assess the flood risks are the following:

- Economic
 - Annual Average Damage
- Social
 - Annual average flood affected population
 - Annual average sensible population affected
 - Probability of social hot spots (hospital, schools, tourism, ect) being affected
- Environmental
 - EVI

The choice of evaluation criteria is always a trade-off between completeness and applicability. This is also true for this set of criteria. On the one hand the intention is at least to cover the three main dimensions of flood risk: economic, social and environmental risks, on the other hand this list is kept minimal and simple for reasons of applicability. For a more

sophisticated and comprehensive analysis it might be good to extend this set by more criteria and/or to improve the criteria.

Criteria Evaluation: Risk Assessment

For each alternative the performance of each criterion needs to be evaluated. The result is a decision matrix which builds the basis for the multicriteria evaluation. Regarding GIS-based flood risk analysis, the result of each criterion evaluation is a risk map for each criterion.

Each criteria, economic, social and environmental is evaluated in term of risk maps as described in the section 7.

Standardization/Normalization is the procedure of transforming criteria values of different metrics into a dimensionless number, usually between 0 and 1, with an aim to allow for valuation comparison, and aggregation of indicators with different units of measure. There exist a number of different normalization functions. Some other normalization procedures are mentioned beneath,

- Ranking
- Standardization (z-score)
- Value functions
- Min-max normalization
- Distance to a reference measures
- Categorical scales
- Methods of cyclical indicators

The type of normalization function depends on the indicators under consideration and the preferences of the decision makers. The simplest normalization method consists in *ranking* each indicator. The main advantages of ranking approach are its simplicity and the independence to outliers. Disadvantages are the loss of information on absolute levels and the impossibility to draw any conclusion about difference in performance. One of the most commonly used normalization procedure is *Standardization (z-score)* in which all indicators can be converted into a common scale with an average of zero and standard deviation of one. The *min-max* normalization is achieved through determine desirable and least acceptable (best and worst) values and to normalize the measured value between the two threshold values. *Value function* is one of the widely used normalization procedure. *Value functions* are mathematical representations of human judgments, which offer the possibility of treating people's values, and judgments explicitly, logically, and systematically (Beinat, 1997). *Distance to a reference measures* takes the ratios of the indicator for a generic value with respect to the reference value. The reference could be a target to be reached in a given

time frame. In determining *categorical scale*, first, the categories are selected. They can be numerical, such as one, two, or three stars, or qualitative, such as ‘fully achieved’, ‘partly achieved’, or ‘not achieved’. Each category is then assigned a score, which is, to a certain extent, arbitrary. Most institutes conducting business tendency surveys select a set of survey series and combine them into *cyclical composite indicators*. This is done in order to reduce the risk of false signals, and to better-forecast cycles in economic activities (Nilsson, 2000).

Weighting is the procedure to express the relative relevance of individual indicators in composite indicators/indexes. Weights are essentially value judgments, thus essentially subjective, and have the property to make the objectives underlying the construction of a composite explicit. Depending on the subjective judgment, different weights may be assigned to different indicators and there is no uniformly agreed methodology to weight individual indicators before aggregating them into a composite indicator or index. Therefore, weights usually have an important impact on the composite indicator value and this is why weighting models need to be made explicit and transparent through involving the stakeholders. To construct composite indicator value and/or index, the weighting of indicators are carried out reflecting stakeholders’ views.

Commonly used weighting procedures are as follows:

Statistical weighting methods:

- Equal weights
- Principal Component Analysis
- Factor Analysis
- Multiple Regression Models
- Participatory weighting methods
- Expert judgment
- Public opinion
- Pair-wise comparison
- Conjoint analysis

Decision Rules - Aggregation:

In the indicator-based assessment, the outcome (i.e. the index) is the result of a hierarchical combination of several indicators that need to be aggregated in each node in which they converge. Aggregation of indicators is obviously not a trivial task since the chosen (among many) methodology has meaningful impacts on the computation of the final index;

furthermore, the choice of the aggregation method typically involves trade-offs between loss of information, computational complexity, adherence to decision makers' preference structure, transparency of procedure, etc.

The user of Web-GIS DSS software tool can choose between two different multicriteria decision rules, a disjunctive approach (see e.g. Zimmermann & Gutsche 1991) and a simple additive weighting approach (see e.g. Malczewski 1999)

The general idea of the disjunctive approach is that the decision maker has to define a threshold level for each criterion. E.g. in order to select areas which have a high risk of flooding, the decision maker has to determine for each risk criterion a critical value which defines the border between low/acceptable risk and high/unacceptable risk. If this threshold value is exceeded in only one of the criteria, the area is selected as a high risk area. Such a simple approach can be used for example for a quick screening and pre-selection of high risk areas.

The additive weighting approach applies the following model:

$$U_i = \sum_j w_j u_{ij}$$

where U_i is the overall value or utility of the alternative i , u_{ij} is the value or utility of the alternative i regarding criterion j and w_j is the standardised weight for criterion j .

Uncertainty. Estimates of vulnerability and risk are pervaded by significant uncertainty due at least to the uncertainty in data, indicators, and models, which use data and indicators as inputs. Neglecting uncertainties can lead to flawed estimates, thereby hindering the desired reduction of vulnerability to acceptable levels or to overestimations of vulnerability, resulting in uneconomic mitigation countermeasures. The source of uncertainty associated with each assessment stage and techniques of treating uncertainty are shown in Figure 12 and Table 3 respectively

Ranking and Scenario Appraisal

The multicriteria analysis ends with a more or less stable ranking of the given alternatives and hence a recommendation as to which alternative(s) should be preferred. Regarding our problem 1 (risk assessment), the result will be a ranking or categorisation of areas with regard to their risk level and hence a recommendation where mitigation action is most required. For problem 2, the selection of mitigation measures, the result of this step will be a ranking of measures.

The entire step wise map-based MCA is implemented in the Web-GIS, the user can interact with dedicate tolls and masks developed in a wizard mode.

All the calculation are performed in a raster environment using map algebra operators available in GDAL Python libraries.

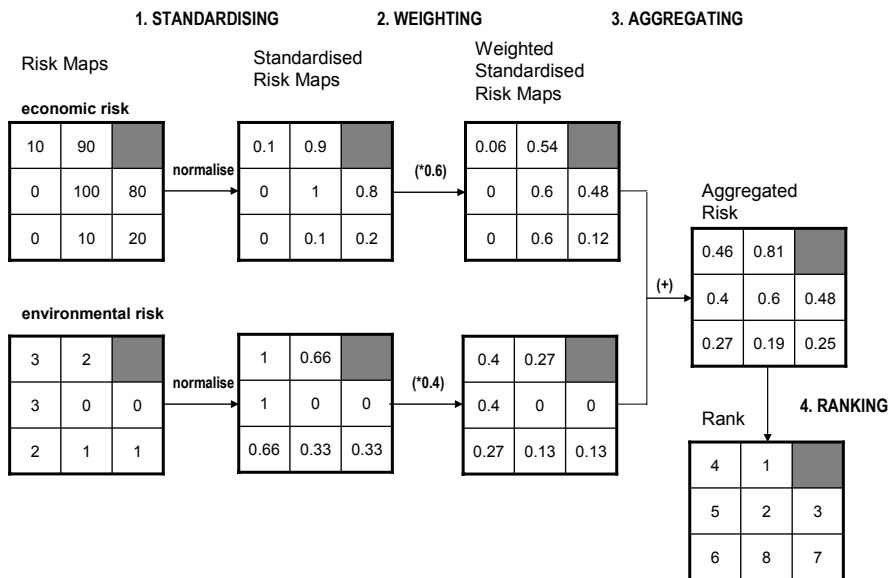


Figure 82 MCA approach for flood risk maps - Malczewski, 1999⁴³²

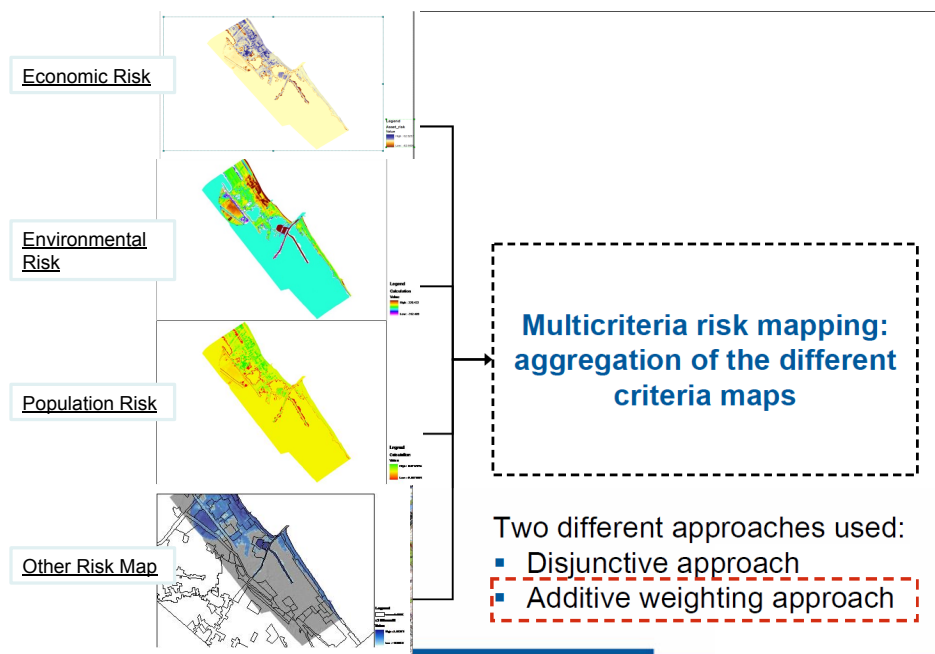


Figure 83 Multicriteria Risk Mapping Framework

9 MARASMA: A web GIS DSS for mapping coastal risk assessment and mitigation planning

9.1 What is a Decision Support System (DSS)?

Even if there is not a universally accepted definition for DSS, in this work we will accept Dan Power's definition "A *Decision Support System (DSS)* is an interactive computer-based system or subsystem intended to help decision makers use communications technologies, data, documents, knowledge and/or models to identify and solve problems, complete decision process tasks, and make decisions... five more specific DSS types include: Communications-driven DSS, Data-driven DSS, Document-driven DSS, Knowledge-driven DSS and Model-driven DSS." (<http://dssresources.com/>).

DSS are not a unique distinct set of tools, but a fuzzy set of frameworks, models and representation environments that help people (from high street to wall street) cope with a wide range of problems. In essence, every quantitative model that is able to make some kind of prediction, departing from a set of data and hypothesis, can be considered a DSS, although in practice this denomination is usually reserved to models with some special features: scenario analysis, cooperative model construction, combination of hard (physical) and soft (socioeconomic) variables, etc.

The increasing popularity of DSS has also profound sociological roots, and some social scientist would argue that the deterministic and mechanistic sprethat present advanced societies show is linked to a parallel destruction of many old structures and new individuation processes and relation patterns. In this project a positive approach will be mainly adopted, although with some restrictions and caveats.

In the context of natural hazards and climate change, DSSs are considered useful tools to cope with climate change related issues and support decision makers in a sustainable management of natural resources and in the definition of mitigation and adaptation measures. These tools can be characterized by a framework and a structure. The first one refers to the assessment and management issues to which the DSS responds and for which it

offers a specific functionalities while the structure describes the main components of the system in terms of database, model and graphical interface (Agostini et al. 2009⁴³³).

As stated by Janssen 1992⁴³⁴, a DSS is expected to support rather than replace judgement of decision makers, to assist them and to improve effectiveness of decision making rather than its efficiency.

There are different types of DSS, such as spatial DSS and environmental DSS. As stated by Densham 1991⁴³⁵, spatial DSS are “explicitly designed to provide the user with a decision-making environment that enables the analysis of geographical information to be carried out in a flexible manner”. The Spatial DSS version usually is developed recurring to mapping and GIS environments.

An environmental DSS consists of various coupled environmental models, databases and assessment tools, which are integrated under a graphical user interface, often realized by using spatial data management functionalities provided by geographical information systems (GIS) (Matthies, 2005⁴³⁶). A DSS applied in a coastal zone management perspective need to be at the same time spatial and environmental.

A Spatial Decision Support System (SDSS) is a computer-based software that integrate the relevant environmental models, database and assessment tools - coupled within a Graphic User Interface (GUI) - for functionality within a Geographical Information System (GIS).

A Geographic Information System (GIS) is a computer-based information system used to digitally represent and analyse geographic features. It is used to input, store, manipulate, analyse and output spatially referenced data (Burrough and McDonnell, 1998⁴³⁷)

In some detail, GIS is a set of computer tools that can capture, manipulate, process and display spatial or geo-referenced data in which the enhancement of spatial data integration, analysis and visualization can be conducted. These functionalities make GIS-tools useful for efficient development and effective implementation of SDSS within the management process. For this purpose they are used either as data managers (i.e. as a spatial geo-database tool) or as an end in itself (i.e. media to communicate information to decision makers). The use of GIS for coastal zone management has expanded rapidly during the past decade and references are numerous (Durand, 1994⁴³⁸; Wright and Bartlett, 2000⁴³⁹).

In this sense, the development of the Web-GIS-MARASMA DSS pursued in this thesis is focused on a Model-driven SDSS with a relevant spatial component.

9.2 DSS in the context of coastal flood risk assessment: A review

While planning coastal risk management strategies, coastal managers need to assess risk across a range of spatial and time scales. GIS-based tools may be an efficient way to support them in the decision making process through a scenarios analysis starting from social, economic and environmental information integrated in a common platform. This integration process however requires a huge effort from scientists in terms of a) identifying the appropriate scales and data resolution for analysing social, environmental, economic issues; b) setting the needed simplifications of scientific methodologies and results; c) developing multi-criteria analysis to integrate social, environmental, economic impacts; d) representing key challenging research issues, such as risk perception and social resilience; e) accounting for the expectations of the stakeholders and therefore optimizing the chances for them to interact with the tool development and with the final tool itself.

Improving the adaptive capacity of individuals, groups or organizations requires communicating coastal risk and building awareness of potential impacts.

One of the biggest criticisms of much research is that it is not accessible, including policymakers whose decisions help to shape our future world. This is especially true for multi-dimensional problems, where a systems view is most effective at capturing the key issues. However, this necessitates multi-disciplinary working and often engagement with the relevant stakeholders.

A good example issue is coastal flooding and erosion risk management where multiple factors embracing, human safety, the environment and society must be considered, requiring a coastal system perspective (Narayan et al. 2012⁴⁴⁰).

In assessing the flooding risk in coastal areas, the main objectives of the reviewed DSSs are the analysis of vulnerability, impacts and risks, and the identification and evaluation of related management options, in order to guarantee robust decisions required for sustainable management. Specifically, the objectives of the examined DSS are concerned with three major issues: (1) the assessment of vulnerability to natural hazards and climate change (DIVA, RegIS, CVAT, DESYCO, KRIM, Coastal Simulator); (2) the evaluation of present and potential climate change impacts and risks on coastal zones and linked ecosystems, in order to predict how coastal regions will respond to climate change (RegIS, CVAT, Coastal Simulator); (3) the evaluation or analysis of management options for the optimal utilisation of coastal resources and ecosystems through the identification of feasible measures and

adequate coordination of all relevant users/stakeholders (COSMO, WADBOS, SIMCLIM, RAMCO, LAVIS⁴⁴¹).

Review of existing exploratory tools that can be used for supporting decisions applied to coastal areas. These GIS-based tools perform scenario construction and analysis. To be continued.

Name	Year	Ref	Processes	Functionalities
COSMO	1992	Feenstra et al. (1998)	Sea-level rise	Problem characterization (e.g. water quality, coastal erosion.) Impact evaluation of different development and protection plans Multi-criteria decision analysis Ecosystem-based
Coastal Simulator	2000-	Mokrech et al. (2009) Dawson et al. (2009)	Storm surge Flooding Coastal erosion Sea-level rise	Environmental status evaluation Risk analysis Management strategies identification and evaluation Uncertainty analysis
CVAT	1999-	Flax et al. (2002)	Socio-economic scenarios Multi-hazard Extreme events Storm surge	Integrated risk assessment Hazard analysis Social, economic and environmental vulnerability indicators Mitigation options analysis
DESYCO	2005-2010	Torresan et al. (2010)	Sea-level rise Storm surge Flooding Coastal erosion	Risk analysis at regional scale Impacts and vulnerability analysis Adaptation options definition Multi-criteria decision analysis Regional risk assessment
DIVA	1999-	Vafeidis et al. (2008) Hinkel and Klein (2009)	Water quality Sea-level rise Coastal erosion Storm surge Flooding Wetland loss and change	Environmental status evaluation Impact analysis Adaptation options evaluation Cost-benefit analysis
KRIM	2001-2004	Schirmer et al. (2003)	Salinisation Sea-level rise Extreme events Coastal erosion	Environmental status evaluation. Adaptation measures evaluation Information for nontechnical users Risk analysis
RegIS	2003-2010	Holman et al. (2008)	Coastal and river flooding Wetland loss and change Sea-level rise Emission scenarios	Implementation of DPSIR conceptual model Management measures evaluation Impact analysis. Integrated risk assessment
RAMCO	1996-1999	De Kok et al. (2001) http://www.riks.nl/resources/papers/RamCo2.pdf	Socio-economic scenarios Socio-economic scenarios Coastal and river flooding Policy options Impact of human activities	Information for nontechnical users Environmental status evaluation Management measures evaluation.
SimCLIM	2005-	Warrick (2009)	Integrated management Sea-level rise Coastal flooding Coastal erosion	Environmental status evaluation Impact and vulnerability evaluation Adaptation strategies evaluation Cost/benefit analysis
WADBOS	1996-2002	Van Buuren et al. (2002)	Socio-economic scenarios Policy options Impact of human activities Integrated management	Socio-economic, hydrological, environmental, ecological data Socio-economic, ecological, landscape models Management measures identification and evaluation
CLIMSAVE	2010-2013	Harrison et al. (2013)	Emission scenarios Agriculture Forests Water Resources Coastal and river flooding Urban development	Implementation of DPSIR conceptual model Impact analysis Adaptation strategies
THESEUS	2010-2013	(this paper)	Sea-level rise Coastal flooding Coastal erosion Socio-economic scenarios	Hydraulic, social, economic, ecological vulnerability Combination of engineering, social, economic and ecologically based mitigation options Multi-criteria analysis High resolution risk assessment

Table 18 Review of existing DSS for coastal risk assessment

DIVA, acronym for Dynamic Interactive Vulnerability Assessment is a tool for integrated assessment of coastal zones produced by the EU-funded DINAS-Coast consortium in 2004. DIVA is specifically designed to explore the vulnerability of coastal areas to sea level rise. It comprises a global database of natural system and socioeconomic factors, relevant scenarios, a set of impact-adaptation algorithms and a customized graphical-user interface. DIVA is able to consider several factors such as erosion, flooding and wetland loss. This software tool, which is freely distributed, is designed for national, regional and global scale analysis of coastal vulnerability and covers all coastal nations. The user can chose between different scenarios and include some adaptation options.

The Regional Impact Simulator was developed as part of the RegIS2 project, which was funded by the Department for Environment, Food and Rural Affairs (Defra), with support from UK Water Industry Research (UKWIR). The initial RegIS was the first attempt in the UK to produce an integrated snapshot of possible regional futures, in East Anglia and the North West of England taking into account both climate change and demographic and socio-economic trends.

RegIS looked in detail at how the major sectors driving landscape change in each of these regions might respond under two contrasting storylines of climate and socio-economic change. However, this initial version required long model run times and lacked of interlinking between the different models and data exchange.

RegIS2 continued the stakeholder-led approach and developed a tool that was simpler and faster, could be installed on a PC and used by users as and when required. The resulting Regional Impact Simulator contains a suite of computer models and datasets within a user-friendly interface that allows the user to: Rapidly identify the sensitivity of an indicator to climate and/or socio-economic change; investigate the effects of uncertainty in the future scenarios; and investigate regional adaptive response to future change.

The linked models are run in sequence describing the impacts on coastal and river flooding, rural land use and cropping, water resources (supply and demand) and biodiversity (species and habitat). Moreover, the Regional Impacts Simulator also allows the user to explore the effectiveness of a wide range of adaptation response in terms of reducing or minimizing the impacts.

The Tyndall Coastal Simulator aims to provide a range of predictions for the future evolution of the coast under a series of climate and socio-economic futures and localized shoreline management options. The Simulator is able to produce a downscaled analysis applied to a coastal region. Starting with downscaled Global Climate Models, regional climate change including sea-level rise, storm surges and waves are included in the analysis. The dynamics are then linked to shoreline erosion and profile evolution using the process-based models and coupled with a flood model to conduct a coastal flood and erosion risk assessment under the full range of scenarios. The Tyndall Coastal Simulator is therefore design to address problems at a very high spatial resolution and using complex models, which limits the spatial area to be covered in the analysis as well as the number of scenarios to be

considered.

Ward et al 2010⁴⁴², developed a GIS-based decision support tool originally designed for mapping permanent coastal inundation, for use in inundation mapping and damage exposure estimation for extreme coastal flood events in cities, and applied the tool to the case study of Jakarta. They set up a GIS-based flood model of northern Jakarta to simulate inundated area and value of exposed assets. Under current conditions, estimated damage exposure to extreme coastal flood events with return periods of 100 and 1,000 years is high

LATIS (Kellens et al 2008⁴⁴³) is a GIS based DSS implementing a risk-based methodology for flood risk assessment developed by Flanders Hydraulics Research and Ghent University. LATIS is built on Microsoft.NET technology in combination with the raster GIS package Idrisi (Clark Labs). The user interface of the application and algorithm of the model were implemented in the programming language C#.NET. For all the geospatial operations, LATIS uses the optimal computing capacity and built-in standard modules (stand-alone executable files) of Idrisi⁴⁴⁴. The tool performs all necessary actions with the corresponding parameters so the user only has to take care of the input data.

The effect calculation of climate change scenarios in Flanders has been one of the first projects for which the LATIS tool is used. These climate change scenarios are based on regional climate models for different emissions scenarios.

In the next paragraphs the thesis describes the conceptual and technological frameworks around which MARASMA DSS was built.

9.3 The Web-GIS MARASMA DSS Frameworks

The MARASMA-DSS is a Model-driven Decision Support System with a relevant spatial component based on a Web-GIS platform. In order to build a DSS it is common to define 3 general frameworks (Figure 84):

- A Conceptual Framework, which seeks to understand and formalize the vision and goals of the DSS.
- A Methodological Framework, which is a translation of the conceptual framework into an analysis process containing data, algorithms, methods and model interactions.

- A Technological Framework, which considers the software and associated development, protocols to be used to enact the methodology framework.



Figure 84 Conceptual, methodological and technological frameworks

These frameworks provide a platform for decision makers to assess and evaluate flood risk assessment and mapping strategies in the context of long-term planning. This requires a description of:

- data to represent the source, pathway and receptor terms;
- external drivers of change in these terms – represented via scenarios;
- internal drivers of change in these systems – represented via strategic alternatives;
- representation of the output risk metrics in a format that assists decision makers in evaluating combinations of management measures;
- an approach for handling uncertainty; and
- a generic means for combining and evaluating this information.

Here, the term ‘generic’ implies no restrictions on, for example:

- - spatial or temporal scale;
- - location e.g. rivers, estuary or coast;
- - nature of input data e.g. detailed 3D point velocities versus section-average velocity;
- - number of receptors terms e.g. people, property, transport infrastructure;
- - other

9.3.1 Conceptual Framework:

The European Directive on the assessment and management of flood risk reinforces a risk based approach as being fundamental to good decision making. The concept of risk however is only one component of good flood management which demands integration across sectorial interests as well as spatial and temporal domains.

The primary objective of MARASMA-DSS is to provide an integrated Web-GIS DSS for mapping coastal flooding and planning mitigation measures which addresses social, economic and environmental aspects in a multicriteria scheme. The Web-tool support an assessment of the change in risk due to a range of scenarios (climate change and subsidence) and selection of the most appropriate intervention measures from an available portfolio of engineering, ecological and social measures.

The primary end-users are intermediate-level coastal managers who need to make sound evidence-based decisions regarding spatial planning and coastal protection.

MARASMA DSS guiding concepts are the same of THESEUS DSS. The Project builds on this experience by developing a comprehensive Web-GIS-based DSS including visualisations whose design, development and application is described in this thesis.

Some example questions this DSS allows to answer include:

- How will flood risk change if I do nothing?
- Should I use soft or hard approaches?
- Can enhancing habitats benefit human safety?
- Can the risk-sharing embodied in insurance benefit community resilience?
- Where and which mitigation option the coastal manager can implement in order to maximize the mitigation of coastal risk evaluated in a multicriteria paradigm (environmental, economical and societal)?

The We-GIS DSS is intended as a vehicle for communication, training, forecasting and experimentation. It fills a gap among the existing tools, based on the following pillars:

- seamless integration of disciplines: physics, engineering, ecology, social sciences and economy;
- intermediate spatial scales (10- 100 km) and medium-to- long time spans (10-100 years);
- representation of a portfolio of mitigation options such as engineering defences (i.e. barriers, wave farms, etc.), ecologically based solutions (i.e. biogenic reefs, sea-grasses, etc.) and socio-economic mitigations (i.e. insurance, change of land use, etc.);

- decision-making based on a balance between deterministic models and expert, discussion-based assumptions.

9.3.2 Methodological Framework: The SPRC methodology

The Methodological Framework (MF) of MARASMA-DSS is based on SPRC model described in paragraph 5.7.

The MF integrated in the Web-GIS DSS and reported in Figure 85 and **Error! Reference source not found.**Figure 86 is composed by the following main elements:

- A set of raster-based models,
- A spatial database
- Graphical User friendly Interface (GUI).

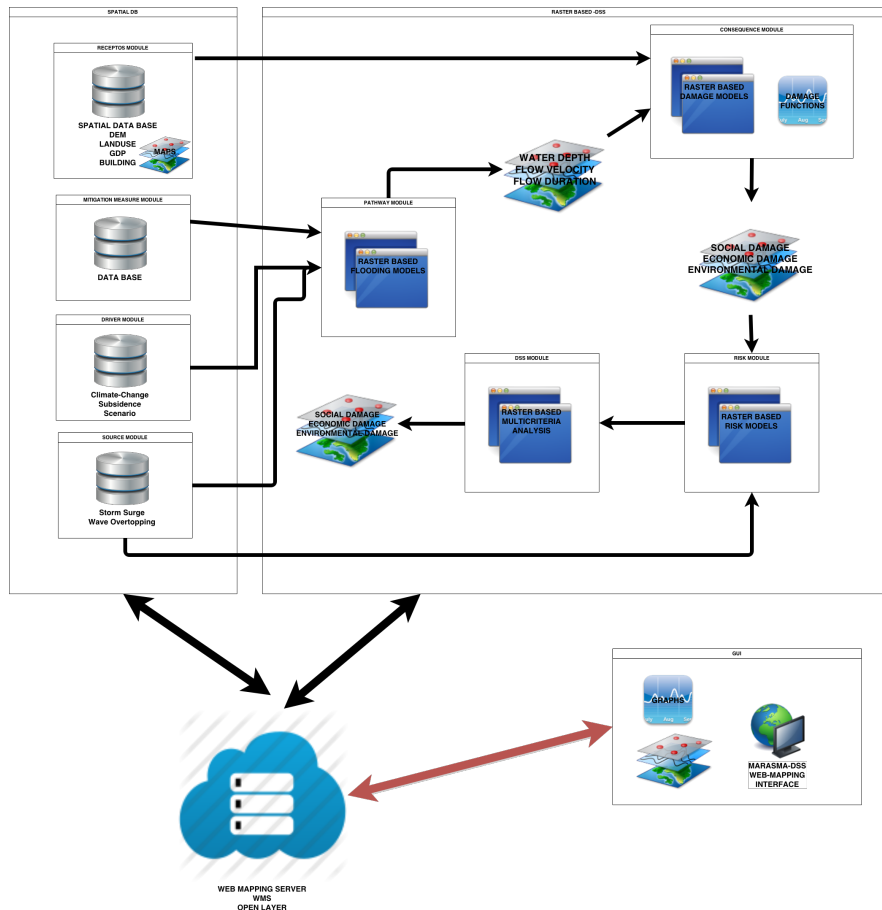


Figure 85 Methodological framework of MARASMA DSS

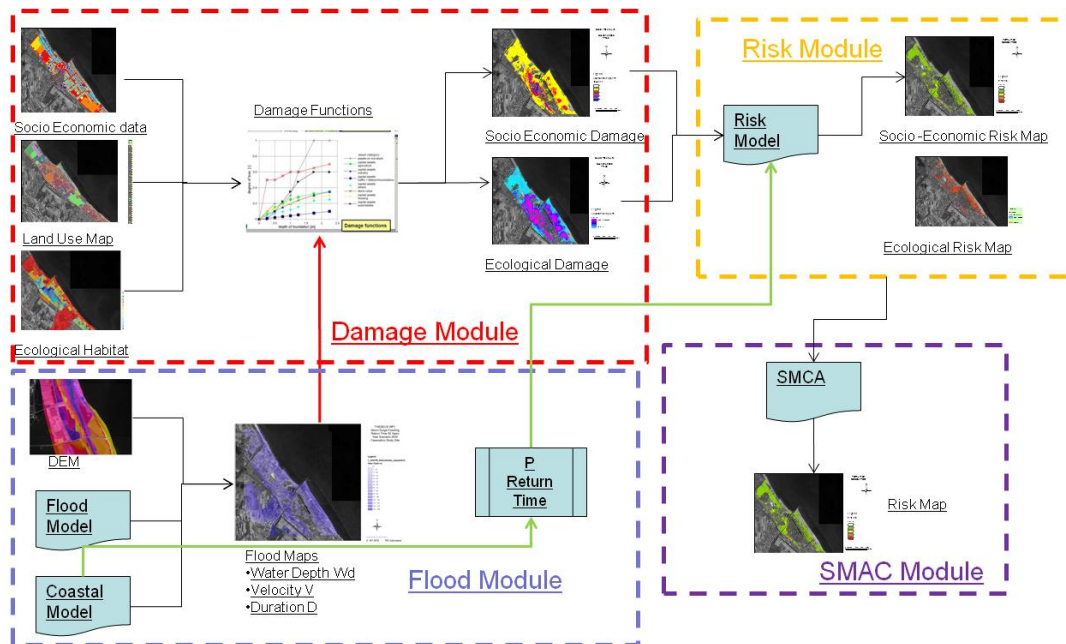


Figure 86 Methodological framework of MARASAM DSS – detail RASTER BASED MODULE

Source module. Traditionally (Sayers *et al*, 2002), the source module is used to derive the source terms which are for the developed Web-GIS DSS the storm surge levels and wave overtopping volume. Source module consists in a database where the user can retrieve specific storm surge and wave height data representative of specific actual or climate driven scenarios. The GUI of MARASMA DSS assist the user in selecting pre-loaded source scenarios or in creating new tailored source data.

Pathway module. This module contains the raster-based routine able to map and describe the important characteristics of that coastal flood, for example inundation depth, duration and velocity taking account of defences (geometry and conditions), morphology, floodplain barriers etc. This is termed 'pathway' as it relates to the path that the water follows when being conveyed from source (as defined above) through to the receptor terms in the floodplain.

Receptor module. This is where the receptor information is collated i.e. the receptor exposure based on location, number and characteristics. This includes the location of residential property, installations, schools, hospitals, infrastructure and designated habitats within the undefended floodplain. This module is distinguishable from the consequences module (below) in that it does not include damage or vulnerability.

Consequence module. This is where the receptor damage and vulnerability is determined. The framework will provide the flexibility to, as a minimum; include any receptor impact provided the spatial location and depth damage relationship is known. More complex

impacts such as social equity, environmental degradation, habitat reduction etc. are an integral component of the receptor analysis and as such these are included in the overall MF, however methods for quantifying these in terms of economic damage are still at an the embryonic stage.

Risk module. The risk module integrates the outputs from the pathway (e.g. probabilistic flood depth or velocity grid) and consequences modules (e.g. property depth-damage curves), to provide the basic risk metrics. The outputs are expressed quantitatively (e.g. monetary value, expected economic damage), by category (e.g. high, medium, low) or descriptively. The may include wider risks metrics such as ecological risks, for example, toxicological risks due to flood-induced heavy metal fluxes. The risk module does not include any post- processing of the basic risk metrics – any additional manipulation takes place in the decision support module.

External driver module. This is used to define the changes in the flood risk system due to autonomous events or ‘external drivers’ i.e. events which the flood risk manager has no influence over. These are implemented at different stages of the analysis as they affect different terms, for example:

- changes to the *source* e.g. climate change influences such as increased or decreased rainfall, spatial change in weather patterns, sea level rise, changed storminess and or storm sequencing;
- changes to the *pathways* e.g. land subsidence altering defence crest levels;
- changes to the *receptors* e.g. urbanisation, land-use etc;
- changes to the *consequences* e.g. economic growth, improved medical care etc;

Decision support module. This deals with the translation of the integrated results from the previous modules, i.e. risk metrics, into performance indicators for pre-specified criteria which can then be used for the evaluation of different strategies and scenarios. These criteria will then be utilised in the context of different analyses e.g. present value calculation (PV), risk reduction, benefit-cost analyses (BCA), multi-criteria analysis (MCA) etc. to provide useful and credible guidance to decision makers on the utility of alternative long term management strategies.

This modular framework is independent of the precise models and calculations to be used, for example, the inundation model chosen to spread the flood or the breach model for a given defence. However, the way in which each module is used and interacts with other modules within the context of the overall MF is the same.

The previous modules can be grouped in the following main components:

- 1) A Web-GIS-based graphical user-interface
- 2) A database, mainly accessible through the user-interface
- 3) A set of raster-based models and utilities
- 4) An intelligence engine that manages the connectivity among the user-interface, the database and the raster-based models (including inter-model relationships)

It can be useful to establish a musical parallelism, in order to understand the relationship between these components:

- the intelligence engine acts as the orchestra conductor
- the Web-GIS-based interface are the musical instruments
- the database is the musical language
- the raster-based models are the musical scores for each group of instruments that intertwine
- the user is the composer
- the decision-maker is the audience.

WebGIS-based user-interface.

The user-interface has the following functions:

- Represents geographic data and spatial variable
- Allows a physical tessellation of the project domain
- Allows the visualization of results
- Allows the creation of new physical configurations (alternative analysis)
- Define risk assessment scenario and running simulation
- Interacts with the database, transcribing spatial information to model-specific inputs.

Database:

- The database includes all type of information organized in several layers: geographical, climatic, environmental, socioeconomic, etc. It interacts with the user-interface, extracting information needed for each particular mode, and includes pre-processing tools, that provide linkage utilities between the user interface and the database, on how to translate the physical space to the language of each particular model. It is important that the database allows easy or even automatic import/export operations with official databases.

Raster-Based Modeling

Consists in a set of specifically designed raster based models able to quickly evaluate and mapping the flooding characteristics, the related damages and risk for receptors (social, economic and environmental) and finally to merge multiple risk criteria in a single one.

Knowledge engine:

The knowledge engine will coordinate the different process-specific modules, facilitating the communication among them. It will have the following functions:

- The creation of scenarios, including all types of variables and internal evolution rules.
- Sensitivity analysis of some results, with respect to specific drivers.
- Integration of results from the different modules.

9.3.3 Technological Framework: Architecture and Software

The Technological Framework (TF) describes out the means with which to enact the MF. This is described in terms of identifying:

- the users and their requirements;
- the methods;
- the system architecture and related software/hardware requirements; and

9.3.3.1 The user requirements

The MARASMA-DSS is focused in providing decision support to coastal managers and land user planning in order to map costal flooding related risks with the purpose of localizing high risk area and identify mitigation measures in order to reduce risk.

Coastal Managers and spatial planners with intermediate level in coastal flooding engineering are identified as the main users.

9.3.3.2 The methods

TF determines which of the methods described in the MF are to be enacted within the tool based on, for example, proposed solution technique, use of an embedded model/calculation, computational speed of calculation, dependence on proprietary software, option for pre-cooked database of results, user preferences etc

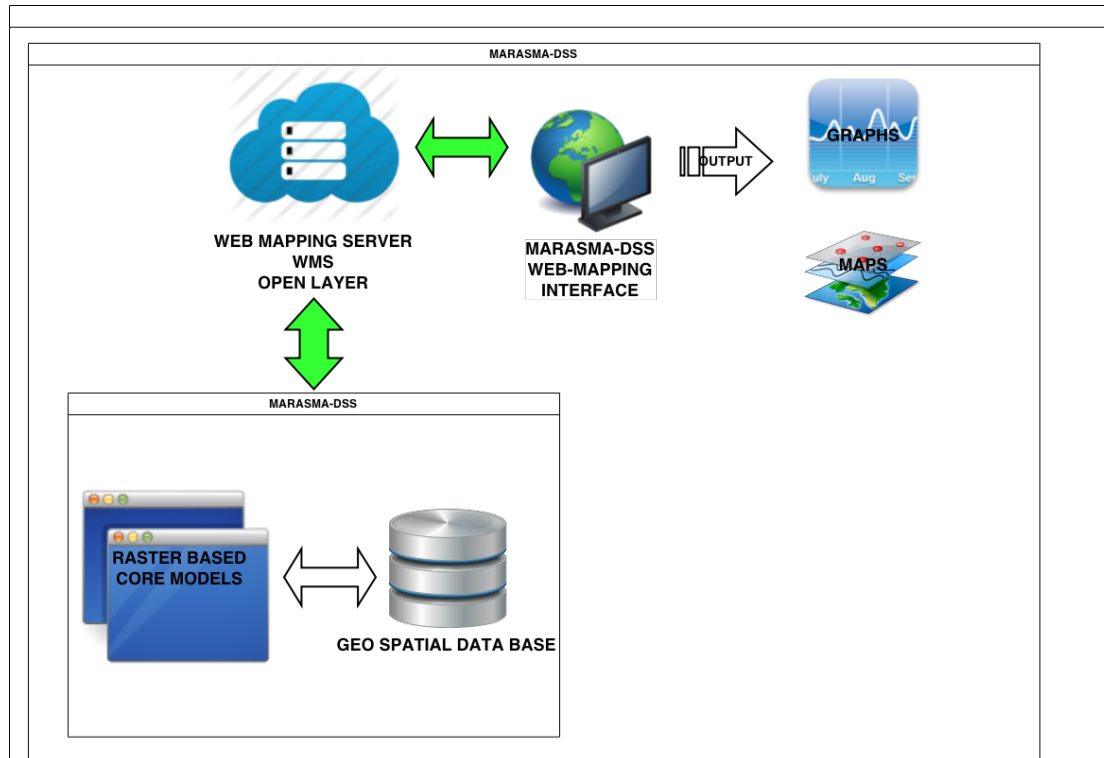
In the MARASMA-DSS each module is developed using open-source software:

- Source Module: consists in a spatial database containing pre-cooked storm surges and volume overtopping scenarios
- Pathway Modue integrates the raster based model for predicting water depth, flow velocity and flood duration. The raster-based models are completely embedded in the Web-GIS DSS.
- Receptor Module consists in a spatial data base of information related to receptor caracteristichs, location and vulnerability
- Consequence Module integrate damage curve model and raster based module for damage assessment and mapping
- Risk Module integrates a raster based model for mapping risk
- External Drivers
-

9.3.3.3 System Architecture and Software

The Web-based architecture of MARASMA DSS consists in four main components:

- A web mapping server
- A web interface- GUI
- A Spatial DataBase
- A set of raster based models



9.3.3.3.1 A web mapping server

WebGIS -DSS primary objective is to provide an integrated methodology implemented into a software tool for mapping coastal flooding risk and supporting coastal managers in sustainable defense strategies, which addresses technical, social, economic and environmental aspects. The geographic implications of these aspects are evident; therefore the implementation of a Geographic Information System (GIS) based Decision Support System (DSS) is required.

Development of web GIS (i.e., integrated product of GIS and internet technologies) based environmental applications have many advantages like ease in access, data transparency,

platform independence, no additional hardware/software requirement, better visualization and also cost effectiveness (Kulkarni et al. 2014⁴⁴⁵). Access to web GIS based environmental solutions also help the stake holders or local communities to participate in the environmental issues that directly affect them (Al-Sabhan et al., 2003⁴⁴⁶). Researchers have made the environmental applications more accessible by integrating them with web GIS. Lohani et al. (2002⁴⁴⁷) described integration of Hydrological Simulation Program Fortran (HSPF) with web, to assess the impact of land use change on catchment hydrology. Engel et al. (2003⁴⁴⁸) described a web based DSS for hydrologic impact evaluation of small watershed on land use changes based on the distributed conceptual model. Hulchy et al. (2004⁴⁴⁹) presented flood forecasting for a river basin, based on integrated meteorology, hydrology and hydraulic models using web based grid computing techniques. Choi et al. (2005⁴⁵⁰) developed a web based spatial decision support system (SDSS) which integrated the hydrologic model, web GIS and databases. SDSS' capabilities included watershed delineation and impact evaluation of land use change and non point source pollution using the Long Term Hydrologic Impact Assessment (L-THIA) model. Lim et al. (2005⁴⁵¹) described a web GIS based hydrograph analysis tool for separating the base flow component using digital filter methods. Cate et al. (2007⁴⁵²) developed a web GIS based tool that was connected to a spatial and non-spatial database server as well as an application server storing two hydrological models. The tool provided for 'what if analysis' through user interface to run the hydrological models. Jia et al. (2009⁴⁵³) developed a web GIS based rainfall runoff prediction system using a distributed conceptual model. Thus, researchers have developed many hydrological tools for decision making by harnessing the power of www and GIS. However, past studies have mostly used conceptual hydrological models because of fewer data and parameter requirements. Distributed physics based model based on partial differential equations bring out the actual hydrodynamic behavior. Such models are computationally intensive and also a challenge to researchers when running on web servers. Model computational time and reliable precipitation estimates are also challenges that are being addressed for even a real time flood forecasting system based on distributed models (Henonin et al., 2010).

The web mapping application of MARASAM DSS is developed recurring to MapServer (<http://mapserver.org/>) and OpenLayers (<http://openlayers.org>)

MapServer is an Open Source platform for publishing spatial data and interactive mapping applications to the web. Originally developed in the mid-1990's at the University of

Minnesota, MapServer is released under an *MIT-style license*, and runs on all major platforms (*Windows, Linux, Mac OS X*).

MapServer is a Common Gateway Interface (CGI) application written in the C programming language that can be installed on any operating system (Gkatzoflias et al., 2013⁴⁵⁴ and Vatsavai et al., 2006⁴⁵⁵). The C implementation also gives MapServer exceptional performance compared to the Java implementations of the other projects (OSGeo, 2014⁴⁵⁶). It is capable of serving spatial datasets as OGC web services including OGC-WMS, OGC-WFS, and OGC-WCS. MapServer supports numerous raster and vector data formats via the GDAL libraries including TIFF, GeoTIFF, ESRI shapefiles, and PostGIS.

MapServer is configured via special files called Mapfiles. It also includes an Application Programming Interface (API) called MapScript that can be used to configure the server and interact with the server's data programmatically. MapScript is available for several programming languages including Python, Java, and PHP. The datasets that MapServer serves can be stored on the file system of the server or in spatially enabled databases (such as PostGIS).

OpenLayers is a web-mapping client library for rendering interactive maps on a web page (Hazzard, 2011⁴⁵⁷). It is a pure JavaScript library for building rich web-based geospatial applications similar to Google Maps™. OpenLayers is capable of rendering vector and raster data from a variety of formats including GeoJSON, OGC-KML, OGC-GML, and OGC web services. It leverages WebGL and Canvas 2D for better performance. OpenLayers also provides methods for drawing on the map and editing data interactively. It allows developers to use a variety of services for base maps including Open Street Map, Bing, MapQuest, and Google. OpenLayers does not currently support a 3D globe-type environment. It does not require a plugin and does not have the use restrictions that are imposed by the Google license (Steiniger and Hunter, 2012⁴⁵⁸ and Steiniger and Hunter, 2012⁴⁵⁹), although using some of the proprietary base maps (e.g.: Google and Bing) used in OpenLayers may invoke licensing restrictions.

9.3.3.3.2 The web GUI

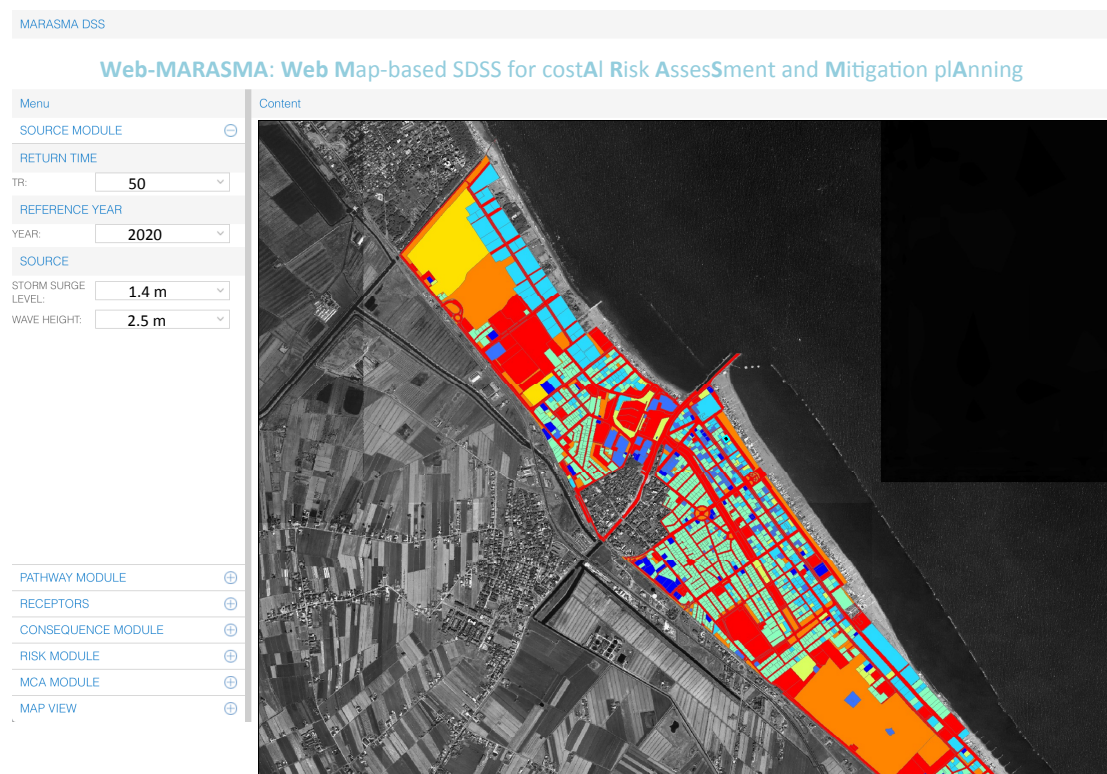
The web-GIS MARASMA DSS is implemented with an easy-to-use Graphical User Interface (GUI) with minimum data inputs so that it can be simulated even by a non-expert user through the browser. In this way, users can access GIS datasets, run simulations and

visualize results from different geographic locations, independent of the computing platform.

The GUI (Graphical User Interface) consists in a web map application developed using the Open Layer web mapping technology. The GUI is developed using PHP, the mainly used programming language with the support of the MapScript library that is embedded into MapServer. HTML, JavaScript, jQuery and Sencha (<https://www.sencha.com/>) libraries are used mainly to support the interface design and interaction.

The Web GUI has two main sections. The first is the menu section where the user can browse through the Source, Pathway, Receptors, Consequence, Risk and MCA modules. Each module has a dedicated mask for the definition of inputs and parameters of raster-based models.

The second section of the GUI is the mapping environment where the user can display and navigate (zoom in/out, pan, identify) through the input and generated maps.



Web-MARASMA: Web Map-based SDSS for costAI Risk AssesSment and Mitigation plAnning

Menu

- SOURCE MODULE (+)
- PATHWAY MODULE (-)
- DEM
Filename DEM:
- SUBSIDENCE
Yes/NO: sub
- COSTAL FLOODING MODEL
STORM SURGE LEVEL:
MAX WAVE HEIGHT:
- RECEPTORS (+)
- CONSEQUENCE MODULE (+)
- RISK MODULE (+)
- MCA MODULE (+)
- MAP VIEW (+)

Content

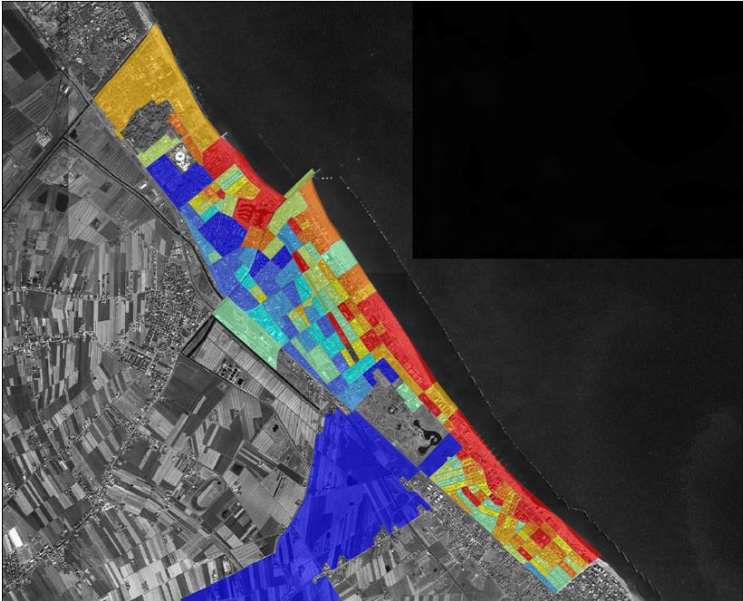


Web-MARASMA: Web Map-based SDSS for costAI Risk AssesSment and Mitigation plAnning

Menu

- SOURCE MODULE (+)
- PATHWAY MODULE (+)
- RECEPTORS (-)
- LANDUSE MAP
Landuse file:
- POPULATION MAP
Pop file:
- HABITATS
Ecological Habitat:
- CONSEQUENCE MODULE (+)
- RISK MODULE (+)
- MCA MODULE (+)
- MAP VIEW (+)

Content



zone_istat
0 - 6
7 - 17
18 - 28
29 - 39
40 - 50
51 - 65
66 - 85
86 - 117
118 - 163
164 - 280

Web-MARASMA: Web Map-based SDSS for costAI Risk AssesSment and Mitigation plAnning

Menu

SOURCE MODULE ⊕

PATHWAY MODULE ⊕

RECEPTORS ⊕

CONSEQUENCE MODULE ⊖

ECONOMIC

DAMAGE FUNC.: $EC = v_0 \cdot b_1 \cdot Fd + v_0 \cdot a_1 \cdot \sqrt{Fy}$

SOCIAL

DAMAGE FUNC.: $H_{people} = d \cdot (v + 1.5) + DF$

ENVIRONMENTAL

DAMAGE FUNC.: $EVI = f(\text{depth}, \text{duration})$

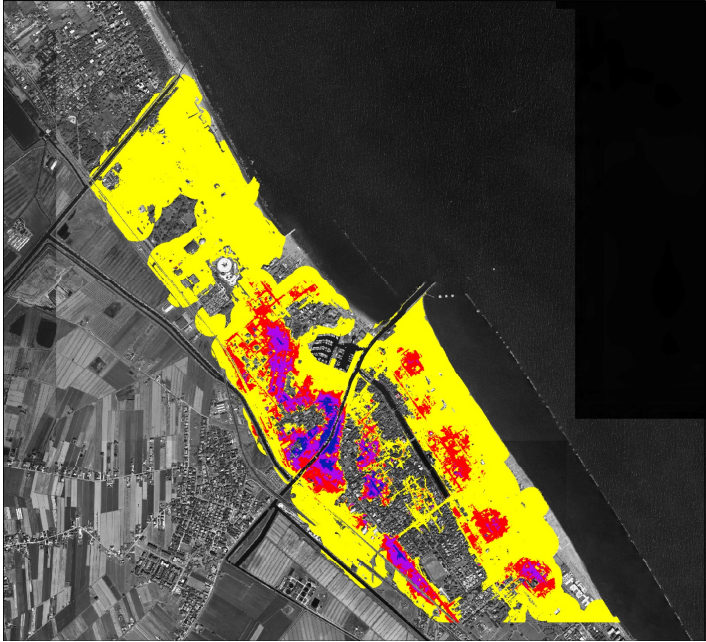
RUN DAMAGE MODELS

RISK MODULE ⊕

MCA MODULE ⊕

MAP VIEW ⊕

Content



Menu

SOURCE MODULE ⊕

PATHWAY MODULE ⊕

RECEPTORS ⊕

CONSEQUENCE MODULE ⊕

RISK MODULE ⊖

TR10:

TR20:

TR50:

TR80:

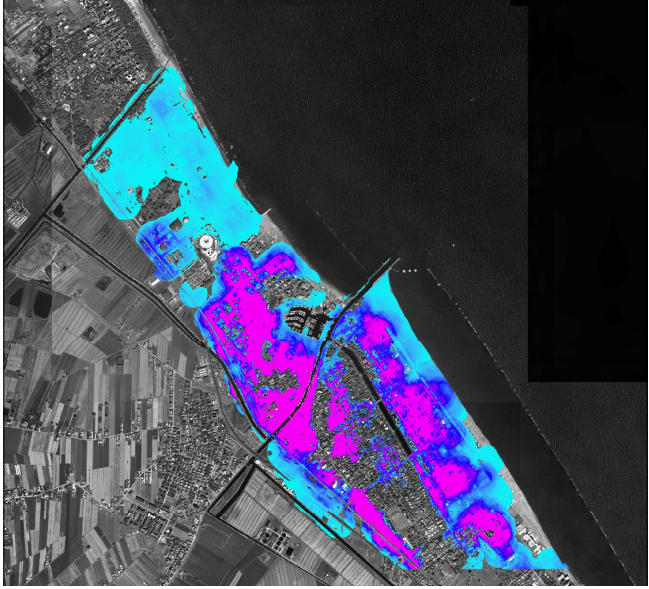
ALL TR:

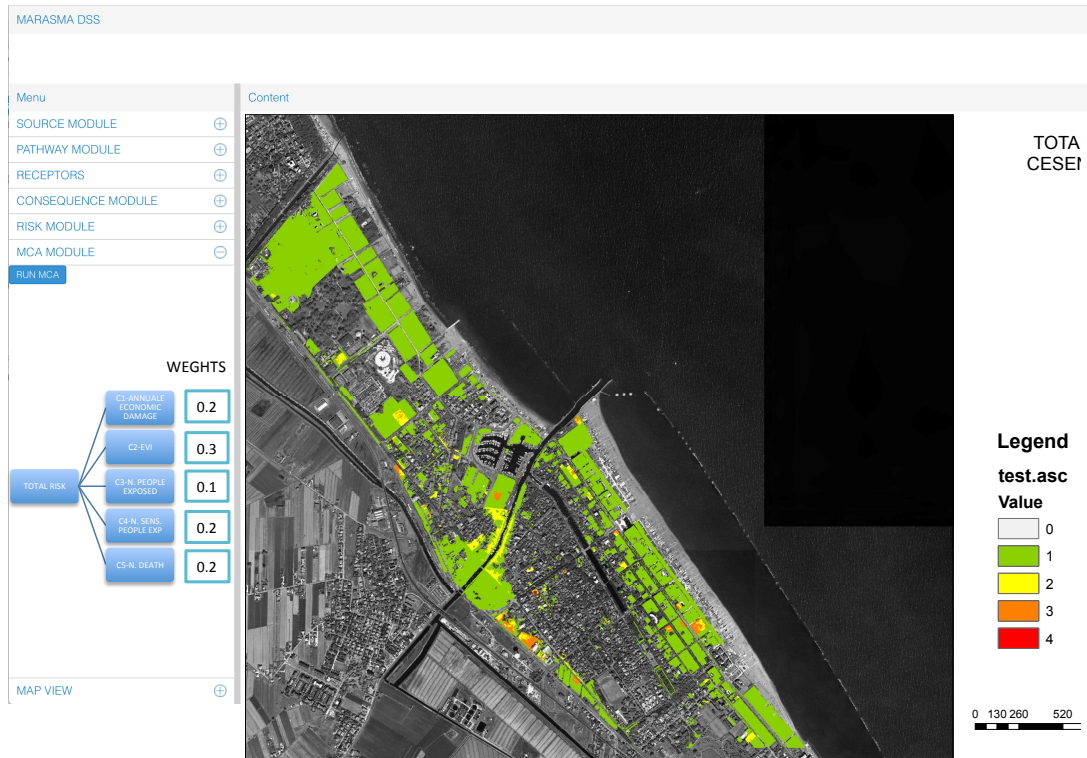
RUN RISK MODULE

MCA MODULE ⊕

MAP VIEW ⊕

Content





9.3.3.3.3 Spatial DB

Spatial databases store geographical data in a file system that is suitable for large datasets with thousands of features and provide an efficient mechanism to store, query, analyze, and update these data (Steiniger and Hunter, 2012⁴⁶⁰ and Steiniger and Hunter, 2012⁴⁶¹).

The Web-GIS DSS MARASMA DB is developed recurring to SpatiaLite. SpatiaLite is the spatial extension for the SQLite database (Steiniger and Hunter, 2012⁴⁶²). The project aims to be roughly equivalent to PostGIS, but far lighter weight in the SQLite fashion. It uses the geometry library of GEOS (Foundation, 2014) to implement OGC-SFS (Zhao et al., 2012⁴⁶³). Like PostGIS, SpatiaLite boasts a large library of database functions for performing spatial analysis (~400 in version 4.2 not counting variants). However the functions assume planar geometry and effectively ignore the spatial reference system of the data. SQLite performs well in single user environments, but it is not well equipped to handle multiple concurrent connections as occurs often in a web environment (Furieri, 2008⁴⁶⁴).

9.3.3.3.4 Raster Based Models

The web-GIS DSS integrates simple raster based equilibrium flooding models for mapping coastal flooding hazard such as flood extent, velocity and duration. Through map algebra GDAL and Numpy library hazard maps are converted in damage and risk maps, through the use of damage function. Finally the web service provide a final total risk map merging in a multi criteria scheme the risk computed for the different receptors type.

This module contains the developed and fully embedded raster based models for coastal flooding simulation, damage and risk assessment mapping.

All the models are raster-based, this mean that are developed recurring to map-algebra or GIS spatial function. In this case map-algebra routines were developed using Python programming languages and OGL/GDAL, PIL and Mamba libraries.

The cost-distance function required for the implementation of flow velocity algorithm is provided by SAGA-GIS software (<http://www.saga-gis.org>)

9.3.4 Scenario Generation

Similarly to what developed in the THESEUS DSS, the MARASAM DSS is based on scenarios analysis and specifically includes:

- Climate and environmental scenarios, which can be a pre-defined set of conditions derived by scientists (wave height, storm surge, sea- level rise, etc.) for short, medium and long term or intervals of these parameters the user can combine based on the kind of scenario he/she wishes to try, ordinary or extreme;
- Economic and social scenarios, essentially based on expected changes or trends of the population and on the gross domestic product; also in this case the user can select the trend value within the range of values suggested by the scientists;
- Environmental scenarios, limitedly for now to subsidence; in future versions scenarios of habitat change based on changes of temperature, social and economic development, etc. may be included.

9.3.5 Source of Flooding

The DSS needs the definition by the site manager of the following elements (lines, points) that are relevant for modelling the hydraulic processes.

Waves: the position of the point/s or line/s for off-shore generation has to be identified based on the indication of the water depth where climate scenarios are provided by the scientists; this is the off-shore depth from which waves are transferred to shore.

Shore line and sea bank line: these lines represent the water/beach boundary relative to which beach retreat is determined, and the water/land boundary where flooding starts, respectively.

Water sources: one or more punctual sources where flooding will be initiated for each coastal segment depending on the minimal resolution adopted for describing the area.

10 MARASMA DSS: Cesenatico Case Study

10.1 Cesenatico Study Area

The Web-GIS MARASMA DSS is tested in a real case study represented by the coastal area of Cesenatico (Italy).

Cesenatico municipality is a well-known touristic resort in the province of Forlì-Cesena. The coastline is approximately 7 km long and is divided by the harbour jetties and the different defences into a Northern and a Southern area (Fig. 4). The hydraulic network close to the urban area (scheme in Fig. 5) is composed by the following main channels: Canale Allacciamento, Rio Granarolo, Rio della Valle, Canale Mesola, Vena Madonnina, Canale Fossatone, Porto Canale di Cesenatico, Canale Tagliata. Rio Granarolo, Rio della Valle, Canale Mesola flow into the Canale Allacciamento and form Canale Fossatone that feeds – together with Vena Madonnina from the South – the Porto Canale di Cesenatico, i.e. the Canal Harbour. Canale Allacciamento is closed by a valve just after the Canale Fossatone, thereafter its part flowing to the sea is named Canale Tagliata; in Canale Tagliata, a by-pass system pumps water from the low-lying areas to the North of Cesenatico.



Figure 87 Aerial view of the site

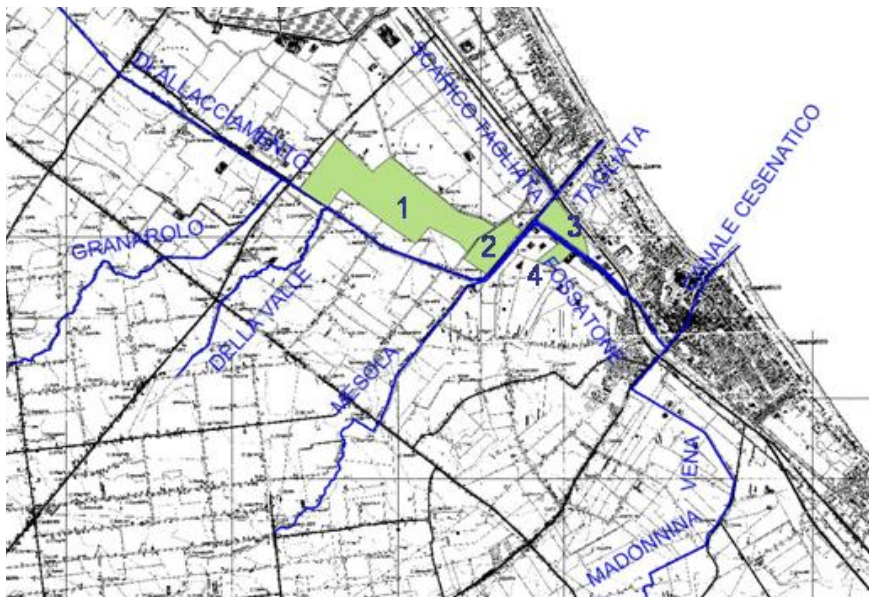


Figure 88 Hydraulic network with indication of the lamination basins in green colour

Since the 70's the area suffered also for anthropogenic subsidence due to extraction of water for industrial and agricultural use. Flooding and erosion motivated the construction of the first defences:

- Cesenatico South: emerged (crest level: 1-1.5 m s.l.m) barriers in 1974;
- Cesenatico North: in 1978 Longard tubes were placed along the shoreline but were damaged by the sea and removed after a few years; in 1983 a nourishment (150'000 m³) was performed and geo-synthetic submerged barriers were built.

In 1982, extractions were forbidden by law and the lowering trend slowly decreased to the natural subsidence. Unfortunately the land lowering was already dramatic, i.e. 116 cm in the period 1950-2005, causing evident flooding and erosive problems.

Flooding became very frequent and the main pathways were the beach overtopping and canal harbour intake, due to insufficient water drainage in the Tagliata-Porto canale system.

The national government therefore renewed the existing defences and planned new interventions:

- Center of Cesenatico: defence of the area immediately to the South of the Jetty with emerged barriers in 1997;
- Cesenatico North: Construction of a submerged (crest level: -0.5 m s.l.m) barrier 0.8 km long, 12 m wide, 250 m distant from the shoreline to replace the geosynthetic barrier. Nourishment with 160'000 m³ of sand. Removal of a 70 m long groin placed 400 m Northward of the jetty (2003-2005)
- Valverde, Southern adjacent beach: change of the layout of three emerged barriers, removal of 16 groins, construction of three new groins and nourishment with 160'000 m³ of sand (2003-2005); removal of a stone revetment with beneficial effects on the beach stabilisation. Due to the relatively little distance among the beach and the barriers, the interaction among the structures and the seabed induced erosive

tendencies and rip-currents formations.

The following specific defences to high water events were designed by the Regional Authority in 2005 (Brath, 2007):

- construction of a sea gate, “Porte Vinciane” (Fig. 6), 2.0 m high a.s.l., closing the canal harbour for water level exceeding 0.9 m a.s.l.; to face sedimentation at the entrance of the canal harbour, dredging operations have to be performed usually twice per year or exceptionally after intense storms;
- set-up of a pumping system in connection with “Porte Vinciane”, whose operating capacity of 18 m³/s is much greater than what is necessary to drain an extreme rain event; in case of combined flood and sea storm with closure of the sea gate, it is assumed that the plant can still drain into the sea up to 8 m³/s, whereas the rest has to be discharged by Canale Tagliata;
- widening of Canale Tagliata (new section 20 m wide, slopes 1:2, height of river walls 3 m a.s.l) to assure the outflow up to the reference discharge of 90 m³/s, based on the indication of the “Bacini Romagnoli” Authority;
- set-up of a sewer-drain by-pass system of the railway and streets crossing Canale Tagliata;
- increasing the potential (from 10 to 17 m³/s) of the pumping system of the Canale Tagliata; the plant collect the water drained from the low-lying areas of Cervia and Cesenatico;
- construction of a series (4) lamination basins;
- construction of a gate on the Canale Vena, upstream the Porto Canale;
- control and upgrade (in terms of section and height) of channel banks and streets crossing the channels.

To protect the low-lying urban areas, the Municipality built a soil dike (Fig. 6) in 2005, integrated into the urban use of the back beach, 20 m wide, 1 m high, 1.4 km long, starting from the southern jetty (extending Southward).

The estimated costs of all these works exceeds 30 MEuro.



Figure 89 Mitigation measures: the “Gardens of Cesenatico”: dike behind bathing facilities; sea gate in correspondence of the Canal Harbour

The main periodical beach maintenance consists of:

- a seasonal dune 1.4 m high during the winter time to defend the bathing facilities. Its width is variable from point to point but it is always sufficiently wide to ensure a resistance to the storm events.
- yearly nourishments that are typically carried out Northward and Southward of the port of about 16'000 and 20'000 m³/y respectively.

By assuming that the high water defence system detailed above is properly working, the two main **failure conditions** of the coastal system in Cesenatico are

- beach erosion;
- impossibility to close the Porte Vinciane due to sedimentation at the gates and inside the canal harbour.

10.2 Cesenatico Coastal Flooding Risk Assessment

The next map in **Error! Reference source not found.**Figure 90 reports an example of the final output provided by MARASMA-DSS in term of coastal risk assessment under a Multicriteria paradigm.

The map represents the re-classified, red high risk green low risk, total flooding risk for the social, economic and ecological asset in Cesenatico.

The maps refers to a specific flooding scenario input data, such as the Storm Surge Level, the Return Time mitigation option, climate change or subsidence scenario, MCA parameters, etc..

Trough the MARASMA-DSS the user can quickly, less than 5 min, obtain the map of total flooding risk for comparison purposes with the aim of supporting the planning of mitigation measures.

The map here reported for example underline to the costal manager where are located the area at high risk, in this way is possible to efficiently manage and allocate economical and human resources based on objective evaluations and not only on subjective interpretations.

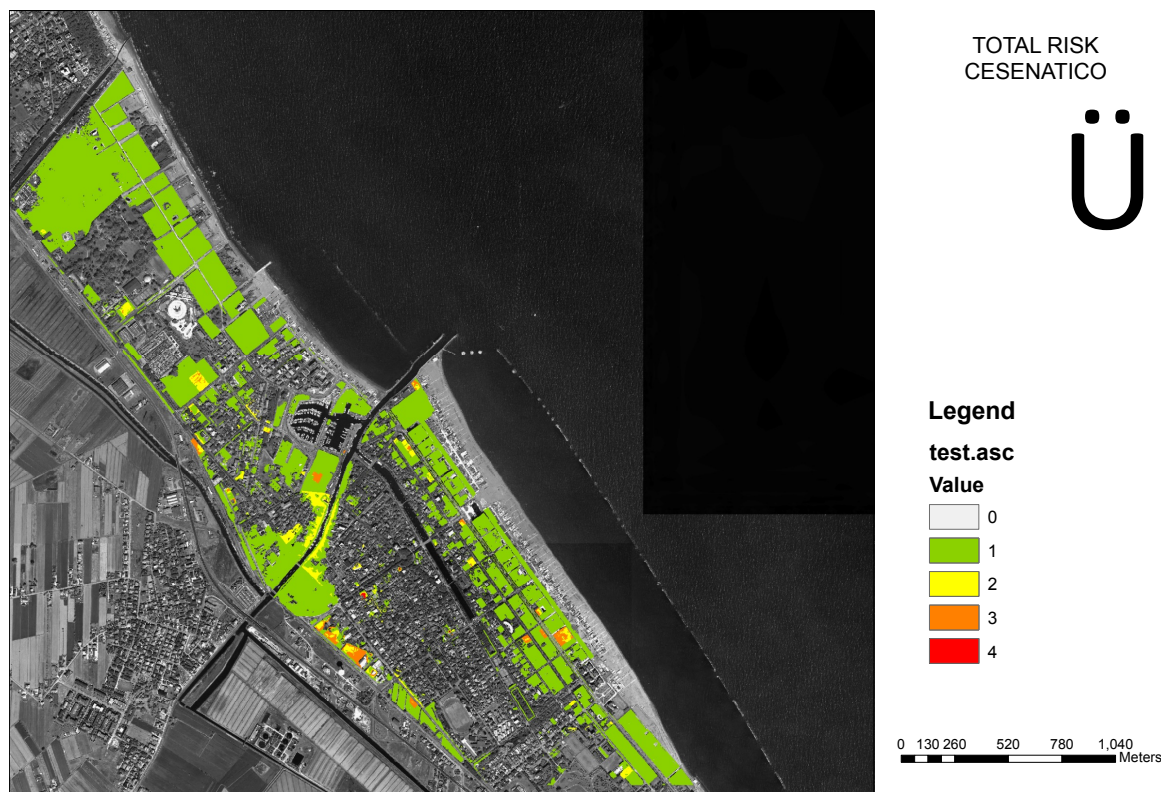


Figure 90 Total Flooding Risk - Cesenatico

11 Conclusions

The aim of this research was to develop, apply and implement a methodology to evaluate and improve the understanding of coastal flood risk via the development of a new Web-based DSS and its application to a case-study.

The new and innovative Web-GIS DSS named MARASMA was developed with the purpose to assist coastal managers and land use planners in present and future flood risk assessment and at supporting a sustainable long-term planning of mitigation strategies.

The Web-GIS DSS is fully open source and parametric so that it can be applied, in principle, to any coastal area independent of scale issues. However it requires appropriate site data, both to simulate inundation with a sufficient degree of accuracy (needing a high resolution DEM) and to represent social and economic vulnerability and the range of mitigation options.

The tool was designed to allow the user step by step interaction by setting up scenarios, selecting mitigation options, and changing weights within the multi-criteria risk analysis. The possibility to run and compare many different conditions allows the users to explore flood risk and to develop an impact-oriented approach to coastal risk mitigation across multiple criteria. This process of course depends on the technical skills of the user and their local site-specific background.

The web service ensure a rapid run-time and a quick response to the user. Hence, it is most useful in the preliminary risk assessment phase, identifying the most threatened areas, and in the preliminary planning phase, verifying the most promising portfolio of mitigation solutions. Hence its role is to structure the analysis, including selection and use of more sophisticated models for subsequent more detailed analysis.

Particular effort in this thesis is dedicated in developing new simple raster-based model able to map and predict the main flood effects in terms of water depth, flow velocity and time duration. The developed models were testes comparing results obtained with numerical hydrodynamic models such as Mike 21 and Telemac.

The main novelties of this research are primarily due to the combination of:

- Development of new raster-based flood models fully embedded in the Web-GIS DSS, to quickly mapping and simulate the flood characteristics, water depth, flow velocity and flood duration;

- Integration of MCA approach in order to appropriately evaluate the flood risk incorporating all relevant types of consequences without measuring them on one monetary scale;
- Integration of coastal risk assessment methodology in a Web-GIS MARASMA DSS developed to perform quickly a simplified, but still enough accurate, coastal risk assessment evaluation directly from the web without installing locally (desktop) complex software, numerical models etc., and without requiring high scientific knowledge in the field of hydrodynamic modeling and risk assessment;

12 Appendix

12.1 FLOODSURGEMAP

```
# FLOODING_MODEL_VOLUME_MP_1.0.py
# DATE 23 MAY 2012
# VERSION 1.0 FINITE VOLUME MULTIPOINT
# Watershed transformation using HQ and image slicing performed on 32-bit Mamba image.
# Contribution:
# Stefano Bagli, PhD DICMA UNIBO (stefano.bagli@unibo.it)
# Nicolas BEUCHER (nicolas.beucher@ensta.org)
# The model compute the flooding area and the water depth Watershed flooding
# with a specific Storm Surge Level and Overtopping volume in cubic meters
# INPUT
# DEM Float 32 with number of column and rows non exceeding 4032 and row num multiple of 4
# TEXT File with the list of storm surge level point and overtopping points . Each row contain the following info
# X-coord Y-Coord Level
# X-coord Y-Coord Volume
# X-coord Y-Coord Volume
# X-coord Y-Coord Volume
# X-coord Y-Coord Volume

#COMPILING INSTRUCTION
# Compiled and command line
# import py_compile
# py_compile.compile("mymodule.py")
#py_compile.compile("F:/THESEUS/DSS/DSS_functions_prd/flood_levelvolume_mp_time_iso_2_2_10.py")

import sys,os,time,gc
import math,numpy
import gdal,gdalconst
import mamba,mambaCore,mambaComposed

X_DEBUG = False
X_VERSION = "2.2.10"

#-----
# Version 2.2.10
#-----
# vol reduction routine
# set water pixel at 0
#-----
# Version 2.2.8
#-----
# finite volume level step as parameters
#-----
# Version 2.2.7
#-----
# water depth in m

#-----
# Version 2.2.6
#-----
# Fixed bug in Numpy2Mamba
# - swapped rows with columns
# - removed some unused e wrong lines : w,h = DEM.shape instead of h,w = DEM.shape
# but values w,h was never used...

#-----
# Version 2.2.5
#-----
# Fixed bug in reading the pointfile.txt
# - error in reading number points and timesteps

#-----
# Version 2.2.4
```

```

#-----
# In previous version ISO was saved in 64 bit x pixel and WD in 32 bit x pixel
# Now ISO image is 8 bit x pixel and WD image is 32 bit x pixel.
# - reintroduction of name_scenario as prefix output name
# - more robust parsing of volume filepoint. You can put lines with comment (#)
# empty lines and introducing point in this way (x,y,z) or (x y z) or x,y,z
# or x y z.
# - Check at time of argument control if the seapoint is placed in the sea and
# if following points are placed on the ground.

#-----
# Version 2.2.3
#-----
# Some trouble with X_DEBUG. Now it's possible to run it in DEBUG mode

#-----
# Version 2.2.2
#-----
# Many correction to the program to make results as version 2.1
# This is the first valid version in terms of calcolous after version 2.1

#-----
# Version 2.2.0
#-----
# Restyling of version 2.1 using Numpy and GDAL instead of Mamba and PIL
# The program depends now on Numpy,GDAL a Mamba just for the watershed function
# - added support to ESRI (AAIGRID) file
# - more manageable code to control memory consumption
# - If input file is in ESRI format ouput is in ESRI format

#-----
# Version 2.1.3
#-----
# Correction of troubles with createFromDEM TIFF for image that aren't multiple
# of 64 pixel width

#-----
# Version 2.1.2
#-----
# Speedup createFromDEM TIFF function

#-----
# Version 2.1
#-----
# Original version based on GDAL, Mamba and PIL

#-----
# main - The Main loop
#-----
def main(argv):

    t0=time.time()

    if not X_DEBUG:
        print Credits()

    #Verifica le Pre-condizioni
    working_dir,dem_filename,name_scenario,pointfilename,unit,levelstep,volreduc = ContolloArgomenti(argv)

    # Elaborazione
    flooding(working_dir,dem_filename,name_scenario,pointfilename,unit,levelstep,volreduc)

    #Verifica le Post-condizioni
    #Il file di output deve esistere..
    if not os.path.isfile(working_dir+dem_filename):
        print "Something goes wrong. Verify that working dir <%s> is writable. If not contact:
stefano.bagli@unibo.it"%(working_dir)
        sys.exit(1)

    #Success
    print "Done in %ds!"%(time.time()-t0)

```

```

sys.exit(0)

#-----
# die
#-----
def die():
    sys.exit(1)

#-----
# memory_used - expressed in MByte
#-----
def memory_used(message=""):
    import os
    try:
        from wmi import WMI
        result = WMI('.').query("SELECT WorkingSet FROM Win32_PerfRawData_PerfProc_Process WHERE IDProcess=%d" %
os.getpid())
        result = float(result[0].WorkingSet)/1000000

        if X_DEBUG:
            print "-----"
            print "|           Memory used %s %.2f MByte" % (message,result)
            print "-----"
        return result
    except ImportError:
        pass

#-----
# Credits
#-----
def Credits():
    return """
*****
*
*                               *
* UNIBO-THESEUS-Watershed Segmentation Flooding Model                *
* STORM SURGE LEVEL + VOLUME OVERTOPPING MULTIPOINT                  *
* contact stefano.bagli@unibo.it                                     *
* FINITE VOLUME MULTIPOINT version %s                               *
*
*                               *
* Watershed transformation using HQ and image slicing performed on 32-bit *
* Mamba image.
*
*                               *
* Contribution:
* Stefano Bagli, PhD DICMA UNIBO (stefano.bagli@unibo.it)          *
* Valerio Luzzi - GECOSISTEMA (www.gecosistema.eu)                 *
* Nicolas BEUCHER (nicolas.beucher@ensta.org)                       *
* The model compute the flooding area and the water depth Watershed flooding *
* with a specific Storm Surge Level and Overtopping volume in cubic meters *
*
*                               *
*****
"%(X_VERSION)

#-----
# usage
#-----
def usage(message):
    return "\n\n\t\t"+message +"\n\n
Usage:
python dir+flood_levelvolume_mp_time_iso_2_2_6.pyc [working_dir] [dem_filename] [name_scenario] [pointfilename]
[dem_unit] [levelstep] [volred]"
    where
    [working_dir] = is the directory for the input / output
    [dem_filename] = is the input DEM file (it must be a GeoTiff file or ESRI AAIGrid file)
    [name_scenario]= is the prefix-name of output filename

    [pointfilename] = text filename where are stored
    [volred]= volume reduction algorithm 1 yes 0 no

the first line refers to the number of point sources
the second line refers to the number of time step

```

the third line refers to the value of each time step in sec or minute
the rest of lines concerns the X,Y coord of each source point with the value of volume/level for each time step
the first point refers to a storm surge point that must be located in the sea, the value associated to the storm surge is always a level

the following lines contain the X,Y, and Volume value of multiple point where the overtopping can occur, the value refers to cumulative volume in unit^3

example pointfilename.txt file

```
2 # number of source point
3 # number of time step
0 10 100 # time steps values
437807.212 4814576.444 200 # storm surge point at time step 0 (X,Y, level value)
436482.342 4814777.395 150000 # overtopping point at time step 0 (X,Y, voume value)
437807.212 4814576.444 300 # storm surge point at time step 10 (X,Y, level value)
436482.342 4814777.395 180000 # overtopping point at time step 10 (X,Y, voume value)
437807.212 4814576.444 400 # storm surge point at time step 100 (X,Y, level value)
436482.342 4814777.395 190000 # overtopping point at time step 100 (X,Y, voume value)
```

example volpintimeuk1.tif

```
1 # 1 storm surge point - NO OVERTOPPING
4 # 4 timesteps
0 30 60 90 # time steps values
294524 71451 295 storm surge point at time step 0 (X,Y, level value) THIS POINT MUST BE IN THE SEA - STORM
SURGE POINT
294524 71451 300 storm surge point at time step 0 (X,Y, level value) THIS POINT MUST BE IN THE SEA - STORM
SURGE POINT
294524 71451 324 storm surge point at time step 0 (X,Y, level value) THIS POINT MUST BE IN THE SEA - STORM
SURGE POINT
294524 71451 359 storm surge point at time step 0 (X,Y, level value) THIS POINT MUST BE IN THE SEA - STORM
SURGE POINT
```

...

[dem_unit] = the DEM unit (1 is meter, 10 dcm, 100 cm)
[levelstep]= level step for finite volume computation (1 cm, 10 cm, 5 cm)
Example:

```
python flood_levelvolume_mp_time_iso_2_2_8.pyc dtm4ws_canta_l1.tif test volpoint.txt 100 10 1
```

or using ESRI asc file ...

```
python flood_levelvolume_mp_time_iso_2_2_8.pyc dtm4ws_canta_l1.asc test volpoint.txt 100 10 1
```

```
"""
#-----
# ControlloArgomenti
#-----
def ControlloArgomenti(argv):

    #Devono essere 7 compreso il comando
    if len(argv)< 8:
        print usage("Wrong number of arguments:")
        sys.exit(1)

    working_dir = sys.argv[1]
    dem_filename = sys.argv[2]
    name_scenario = sys.argv[3]
    pointfilename = sys.argv[4]
    unit = sys.argv[5]
    levelstep = sys.argv[6]
    volreduc = sys.argv[7]

    # WORKING DIRECTORY
    #The working_dir must ends with slash or backslash if not complete it
    #The working_dir must exist if not exit
    working_dir = working_dir.strip("\ " " ")
    working_dir = os.path.abspath(working_dir)+os.sep
    if not os.path.isdir(working_dir):
        print usage("Working dir <%s> does not not exists"%(working_dir))
        sys.exit(1)

    # DEM
    # Dem must exist, it must be a Tiff (GeoTiff?)
    # Width must be multiple of ( ) if not complete it
```

```

dem_filename = dem_filename.strip("\ " ")
if not os.path.isfile(working_dir+dem_filename):
    print usage("File <%s> does not exists in <%s>"%(dem_filename,working_dir))
    sys.exit(1)

# PIXELSIZE (GDAL detected) We assume that x-pixelsize == y-pixelsize
#Get the PixelSize with GDAL if zero it's not correctly geo-referenced
pixelsize = getPixelSize(working_dir+dem_filename)
if pixelsize==0.0:
    print usage("File <%s> must be a GeoTiff"%(dem_filename))
    sys.exit(1)

#SCENARIO
#Must be a valid filesystem name otherwise correct-it
#TODO ...

# Point filename
# It must exists
if not os.path.isfile(working_dir+pointfilename):
    print usage("File <%s> not exists in <%s>"%(pointfilename,working_dir))
    sys.exit(1)

# All points in pointfile must be in the image area
# The first point must be placed in the sea
nsp,nts,timesteps,points = ParseVolumePointFile(working_dir+pointfilename)
if len(timesteps)<>nts:# or len(points)<>nsp:
    print usage("Wrong file %s. Control the file %s."%(pointfilename,pointfilename))
    sys.exit(1)
#Open the DEM for controlling the correct point location
data,gt,proj = GDAL2Numpy(working_dir+dem_filename)
# TODO ...
[minX1,pixelWidth,rot1,maxY1,rot2,pixelHeight] = gt
(rows,cols) = data.shape
j = 0
for (x,y,lev) in points:
    colnum=int((x-minX1)/pixelWidth)
    rownum=int((maxY1-y)/pixelWidth)
    if not (colnum in range(0,cols) and rownum in range(0,rows)):
        print usage("Point (%.4f,%.4f) is not in the image area. Control the file %s."%(x,y,pointfilename))
        sys.exit(1)
    #The first point must be placed in the sea...
    colnum=int((x-minX1)/pixelWidth)
    rownum=int((maxY1-y)/pixelWidth)
    if j==0:
        if data[rownum,colnum]<>0:
            print usage("The source of storm surge (%.4f,%.4f) must be placed in the sea.Control the file
%s."%(x,y,pointfilename))
            sys.exit(1)
        #else:
        #All the other points must be placed on terrain
        # if data[rownum,colnum]==0:
        #     print usage("The point (%.4f,%.4f) must be placed on the ground.Control the file %s."%(x,y,pointfilename))
        #     sys.exit(1)
        j+=1
    del data,gt,proj

# unit
# It must be an Integer if not convert it
unit = int(unit)
volreduc=int(volreduc)

return [working_dir,dem_filename,name_scenario,pointfilename,unit,levelstep,volreduc]

#-----
# ParsePoint
#-----
def ParsePoint(line):
    #remove comments
    line = line.split("#")[0].strip()
    #parse this format (x,y,lev) or x,y,lev or x y lev
    #remove "(" " ")"

```

```

line = line.replace(",","").replace(")","")
line = line.replace(" ","")
point = line.split(" ")
point = [item for item in point if len(item.strip())>0]
if len(point)>2:
    x = float(point[0])
    y = float(point[1])
    lev = int(float(point[2]))
    return (x,y,lev)
return ()

#-----
# ParseVolumePointFile
#-----
def ParseVolumePointFile(pathname):
    # Open the volpoint.txt file with the storm surge or volume values
    volumefile= open(pathname, 'r')
    lines = volumefile.readlines()
    # Remove all comments
    lines = [item.split("#")[0].strip() for item in lines]
    # Remove all empty lines
    lines = [item for item in lines if len(item)>0]
    if len(lines)<4:
        return [-1,-1,[],[]]
    nsp = int(lines[0]) #Number of sources
    nts = int(lines[1]) #Number of timestep
    timesteps = lines[2].split(" ")
    timesteps = [item for item in timesteps if len(item.strip())>0]
    lines = lines[3:]
    points = []
    for line in lines:
        points.append(ParsePoint(line))

    return [nsp,nts,timesteps,points]

#-----
# GDAL2Numpy
#-----
def GDAL2Numpy(pathname):
    dataset = gdal.Open(pathname,gdalconst.GA_ReadOnly)
    band = dataset.GetRasterBand(1)
    cols = dataset.RasterXSize
    rows = dataset.RasterYSize
    geotransform = dataset.GetGeoTransform()
    projection = dataset.GetProjection()
    wdata = band.ReadAsArray(0, 0, cols, rows).astype("float32")
    return (wdata,geotransform,projection)

#-----
# Numpy2GTiff
#-----
def Numpy2GTiff(arr ,geotransform,projection,filename):
    if isinstance(arr,numpy.ndarray):
        rows,cols = arr.shape
        if rows>0 and cols>0:
            dtype = str(arr.dtype)
            if dtype in ["uint8"]:
                fmt = gdal.GDT_Byte
            elif dtype in ["uint16"]:
                fmt = gdal.GDT_UInt16
            elif dtype in ["uint32"]:
                fmt = gdal.GDT_UInt32
            elif dtype in ["float32"]:
                fmt = gdal.GDT_Float32
            elif dtype in ["float64"]:
                fmt = gdal.GDT_Float64
            else:
                fmt = gdal.GDT_Float64

            driver = gdal.GetDriverByName("GTiff")
            dataset = driver.Create( filename, cols, rows, 1, fmt )
            if (geotransform!=None):

```

```

        dataset.SetGeoTransform( geotransform )
    if (projection!=None):
        dataset.SetProjection(projection)
    dataset.GetRasterBand(1).WriteArray( arr )
    dataset = None
    return filename
return None
#-----
# Numpy2AAIGrid
#-----
def Numpy2AAIGrid(data,geotransform,filename):
    (x0, pixelXSize, rot, y0, rot, pixelYSize) = geotransform
    (rows,cols) = data.shape
    stream = open(filename,"wb")
    stream.write("ncols    %d\r\n"%(cols))
    stream.write("nrows    %d\r\n"%(rows))
    stream.write("xllcorner  %d\r\n"%(x0))
    stream.write("yllcorner  %d\r\n"%(y0 + pixelYSize*rows))
    stream.write("cellsize   %d\r\n"%(pixelXSize))
    stream.write("NODATA_value %d\r\n"%(-9999))
    template = ("%g " * cols) + "\r\n"
    for row in data:
        line = template % tuple(row.tolist())
        stream.write(line)
    stream.close()
    return filename

#-----
# Numpy2Gdal
#-----
def Numpy2Gdal(data,geotransform,projection,filename):
    ext = os.path.splitext(filename)[1][1:].strip().lower()
    if ext == "tif" or ext == "tiff":
        return Numpy2GTiff(data,geotransform,projection,filename)
    elif ext == "asc":
        return Numpy2AAIGrid(data,geotransform,filename)
    else:
        return ""

#-----
# Numpy2Mamba
#-----
def Numpy2Mamba(arr):
    (rows,cols) = arr.shape
    (W,H) = (int(64*math.ceil(float(cols)/64)),int((2*math.ceil(float(rows)/2))))
    if rows!=H:
        arr.resize((H,cols))
    if cols!=W:
        zeros = numpy.zeros((H,W-cols))
        arr = numpy.append(arr,zeros,1)
    if str(arr.dtype)=="uint8":
        arr = arr.astype("uint8")
        arr = arr.tostring("C") # C format
        im32 = mamba.imageMb(cols,rows, 8 )
    else:
        arr = arr.astype("uint32")
        arr = arr.tostring("C") # C format
        im32 = mamba.imageMb(cols,rows, 32 )
    err = mambaCore.MB_Load(im32.mblm, arr, len(arr))
    mamba.raiseExceptionOnError(err)
    return im32

#-----
# Mamba2Numpy
#
# Creates an 2D array containing the same data as in 'imIn'. Only
# works for greyscale and 32-bit images. Returns the array.
#
#-----
def Mamba2Numpy(imIn):

    if imIn.getDepth()==8:

```

```

dtype = numpy.uint8
elif imIn.getDepth()==32:
dtype = numpy.uint32
else:
import mambaCore
raiseExceptionOnError(mambaCore.ERR_BAD_DEPTH)

(w,h) = imIn.getSize()
# First extracting the raw data out of image imIn
data = imIn.extractRaw()
# creating an array with this data
# At this step this is a one-dimensional array
array1D = numpy.fromstring(data, dtype=dtype)
# Reshaping it to the dimension of the image
array2D = array1D.reshape((h,w))
return array2D
#-----
# DEM2Mamba
#-----
def DEM2Mamba(pathname):
dataset = gdal.Open(pathname,gdalconst.GA_ReadOnly)
band = dataset.GetRasterBand(1)
cols = dataset.RasterXSize
rows = dataset.RasterYSize
wdata = band.ReadAsArray(0, 0, cols, rows)
wdata = wdata.reshape(rows,cols)
(W,H) = (int(64*math.ceil(float(cols)/64)),int((2*math.ceil(float(rows)/2))))
if rows!=H:
wdata.resize((H,cols))
if cols!=W:
zeros = numpy.zeros((H,W-cols))
wdata = numpy.append(wdata,zeros,1)
wdata = wdata.astype("uint32")
wdata = wdata.tostring("C") # C format
im32 = mamba.imageMb(cols,rows, 32 )
err = mambaCore.MB_Load(im32.mblm, wdata, len(wdata))
mamba.raiseExceptionOnError(err)
return im32
#-----
# getPixelSize
#-----
def getPixelSize(pathname):
return int(gdal.Open(pathname,gdalconst.GA_ReadOnly).GetGeoTransform()[1])
#-----
# getBytePlane0
#-----
def getBytePlane0(arr):
return numpy.bitwise_and(arr,0b00000000000000000000000011111111).astype("uint8")
#-----
# getBytePlane3
#-----
def getBytePlane3(arr):
tmp = numpy.bitwise_and(arr,0b11111111000000000000000000000000)
return numpy.right_shift(tmp,24).astype("uint8")
#-----
# watershedSegment32
#-----
def watershedSegment32(imIn, imMarker, grid=mamba.DEFAULT_GRID, max_level=-1):
"""
This is the complete equivalent of the watershedSegment Mamba function but
this one works on 32-bit images instead of 8-bit images.

If 'max_level' is negative the function will continue until the whole
image is flooded.
"""
imWrk1 = mamba.imageMb(imIn)
imWrk2 = mamba.imageMb(imIn)
imWrk3 = mamba.imageMb(imIn, 8)
imMask = mamba.imageMb(imIn)
imBinMask = mamba.imageMb(imIn, 1)
(mi, ma) = mamba.computeRange(imIn)

```

```

current_level = mi
if max_level < 0:
    high_level = ma+1
else:
    high_level = min(max_level,ma+1)
mamba.subConst(imIn, mi, imWrk1)
imMask.fill(255)
mamba.logic(imWrk1, imMask, imWrk2, "inf")
mamba.copyBytePlane(imWrk2, 0, imWrk3)
if high_level-current_level<256:
    if high_level>=(ma+1):
        level=256
    else:
        level=high_level-current_level
else:
    level=255

memory_used("at Watershed32 1")
mamba.watershedSegment(imWrk3, imMarker, grid=grid, max_level=level)
current_level += level
while current_level<high_level:
    mambaComposed.floorSubConst(imWrk1, 254, imWrk1)
    mamba.copyBytePlane(imMarker, 3, imWrk3)
    mamba.threshold(imWrk3, imBinMask, 0, 254)
    mamba.convertByMask(imBinMask, imWrk2, 0, mamba.computeMaxRange(imWrk2)[1])
    mamba.logic(imMarker, imWrk2, imMarker, "inf")
    mamba.logic(imWrk1, imMask, imWrk2, "inf")
    mamba.copyBytePlane(imWrk2, 0, imWrk3)
    if high_level-current_level<256:
        if high_level>=(ma+1):
            level=256
        else:
            level=high_level-current_level
    else:
        level=255
    mamba.watershedSegment(imWrk3, imMarker, grid=grid, max_level=level)
    current_level += level
memory_used("at Watershed32 2")

#-----
# NumpyWatershedSegment32
#-----
def NumpyWatershedSegment32(DEM,FLOOD, grid = mamba.DEFAULT_GRID, level = -1):
    imDem = Numpy2Mamba(DEM)
    imFlood = Numpy2Mamba(FLOOD.astype("uint32"))
    watershedSegment32(imDem, imFlood, grid,level)
    imDem = None
    FLOOD = Mamba2Numpy(imFlood).astype("uint8")
    imFlood = None
    return FLOOD

#-----
# NumpyComputeFloodVolume
#
# Computes and returns the volume of *water* needed to flood completely
# the area described by 'imFloodArea' in image 'imDEM'.
#-----
def NumpyComputeFloodVolume(DEM, FloodArea):
    ma = numpy.float32((DEM*FloodArea).max())
    return ( ma *FloodArea - DEM ).sum()

#-----
# volumeControlledFlood
#
# This computes the flood area in imDEM given a certain amount of water
# as given by 'targetVolume'. The flood starting point must be given
# in 'imFlood'. This image will also contains the resulting flooded
# area. The function returns the level reached by water and the actual
# volume needed to perform the flood (greater or equal to targetVolume).
#-----

```

```

def volumeControlledFlood(DEM, FLOOD, targetVolume, thepx, theunit, maxlevel, minpixlevel,
levelstep,grid=mamba.DEFAULT_GRID):

    #theseapixel=computeSeaWaterPixels(imDEM, imFlood)
    theseapixel=0
    print "seapixel = %.2f"%(theseapixel)

    (mi, ma) = (DEM.min(),DEM.max())
    ma=min(ma,maxlevel)
    mi=max(mi,minpixlevel)

    # First we check if the targetVolume will flood the
    # maximum level. In this case the flooded area is the whole image
    ones = numpy.ones_like(DEM)
    vol = NumpyComputeFloodVolume(DEM, ones)
    del ones

    print "TOTAL VOL=%.4g"%(vol)

    if vol<targetVolume:
        # A complete flooding is not sufficient to reach
        # target volume. We stop here and return the maximum level
        # and the associated volume
        return (ma+1, vol)

    # Using a dichotomy approach, we determine the level for which
    # the flood volume becomes equal or greater to target volume.
    #inc = 10 # livello di dettaglio DEM
    inc=int(levelstep)
    level = mi #parte dal livello minimo
    vol = 0
    realvol=0

    while inc>0:
        while vol<targetVolume and level<=ma:

            FLOOD2 = NumpyWatershedSegment32(DEM, FLOOD,grid, level)
            vol = numpy.maximum( ( numpy.float32(level) *FLOOD2 - DEM) , numpy.float32(0.0)).sum()*(thepx*thepx/theunit)

            print "LEVEL,VOLUME = (%.2f,%.2f)"%(level,vol)
            memory_used("at volumeControlledFlood")
            level += inc

            # Changing the level to the previous level for which the flood volume
            # was below the target volume
            level -= 2*inc
            # Decreasing increment for better precision
            inc = inc/10

        return (level+2, vol, FLOOD2)
#-----
def Volumereduction(targetVolume,FLOOD,WATERMASK,thepixelsize,unit,levelwater):
    mosaic = numpy.maximum( WATERMASK ,FLOOD)

    #Numpy2GTiff(mosaic ,geotransform,projection,'F:/THESEUS/DSS/watershed/NED_10m_TIFF/mosaic.tif')

    WDgrid=mosaic

    Area=thepixelsize*thepixelsize
    maxlevel=numpy.max(WDgrid)

    markersea=numpy.where(WDgrid==1.0,WDgrid,0) #set max level var
    seamask=numpy.where(WDgrid==1.0,WDgrid,0)
    volsea=(numpy.sum(seamask)*Area)/(unit)
    vol=(numpy.sum(WDgrid)*Area/unit)-(volsea)
    #print "seavol"+str(volsea)
    #WDgrid=numpy.where(WDgrid==1.2,0,WDgrid)

    print "first tentative volume 0"+str(vol)

```

```

kk=0
while vol>targetVolume:
    #print "START"+str(vol)
    #print "target"+str(targetVolume)
    WDgridmask=numpy.where(WDgrid>0,1,0)
    WDMamba=Numpy2Mamba(WDgridmask)
    imout=WDMamba
    mambaComposed.gradient(WDMamba, imout)

    border=Mamba2Numpy(imout)
    border=numpy.where(border==1,0,1)
    #remove border
    WDgrid=WDgrid*border
    #remove island not connected to the sea/channel
    WDgridDEM=numpy.where(WDgrid==0,9999,WDgrid)
    WDgridDEM=numpy.float32(WDgridDEM)

    grid = mamba.DEFAULT_GRID
    islandmask=NumpyWatershedSegment32(WDgridDEM,markersea,grid, level=int(maxlevel+1))
    WDgrid=WDgrid*islandmask
    vol=(numpy.sum(WDgrid)*Area/(unit))-volsea

    #print "end"+str(vol)
    #print "target"+str(targetVolume)
    kk=kk+1
    #print str(kk)

    del WDgridDEM

    del WDMamba
    del imout
    print "final reduced volume="+str(vol)
    WDgrid=WDgrid/levelwater
    return WDgrid

#-----
#
# flooding - ...
#
# This part illustrates how to use this transformation on a DEM image.
# A flooding demo with display has been designed to see the flooding process
# step by step. Due to the display, the transformation is much slower than it is
# when display is off.
#
#-----
def flooding(working_dir,dem_filename,name_scenario,pointfilename,unit,levelstep,volreduc):

    # UNIT MEASURE LABEL

    if unit == 1:
        labelunit="m"
    elif unit==10:
        labelunit="dm"
    else:
        labelunit="cm"

    # SCENARIO
    ext = os.path.splitext(dem_filename)[1][1:].strip().lower()

    memory_used("at flooding function 1)")

    # Open the DEM file
    (DEM,geotransform,projection) = GDAL2Numpy(working_dir+dem_filename)
    (minX1, pixelsize, rot, maxY1, rot, pixelHeight) = geotransform

    memory_used("at flooding function 2)")

    #WATER_MASK =numpy.logical_and(DEM ==0, DEM==0)
    DEM_VOL = numpy.logical_and(DEM ==0, DEM==0) #Optimize memory using the same table

```

```

DEM_VOL = ( numpy.float32(99999.00) * DEM_VOL + DEM)

#del WATER_MASK
(minleveldem, maxleveldem) = (DEM_VOL.min(),DEM_VOL.max())
mosaic = numpy.float32(0)

gc.collect()
memory_used("at flooding function 3)")

nsp,nts,timesteps,points = ParseVolumePointFile(working_dir+pointfilename)

lineid=0
for ts in timesteps:
    #Per il numero di sorgenti dichiarato nel file
    for sp in range(0,nsp):

        #(Xp,Yp,lev_volume) = points[sp]
        (Xp,Yp,lev_volume) = points[lineid]
        print Xp,Yp,lev_volume
        lineid=lineid+1

    print "Elaborating Source Point %s x,y = (%.3f,%.3f)" % (sp,Xp,Yp)

    rownum=int((Xp-minX1)/pixelsize)
    colnum=int((maxY1-Yp)/pixelsize)
    # watershed segmentation
    # correction of target volume in order to take into account the pixel dimension and the cm unit of the elevation
    FLOOD = numpy.zeros_like(DEM).astype("uint32")
    FLOOD[colnum,rownum] = 1
    memory_used("at flooding function 4)")

    print "Source point # :%d" %sp
    if sp==0:
        seapixel = DEM[colnum,rownum]
        if seapixel<=0:
            sys.exit("the source of storm surge must be placed in the sea (pixel value =0)")
            print "Level" + labelunit + " = %s" % (lev_volume)
            FLOOD = NumpyWatershedSegment32(DEM, FLOOD, level=lev_volume)
            WD = lev_volume
            print volreduc

            #create a water mask for volume reduction
            WATERMASK = numpy.zeros_like(DEM).astype("uint32")
            WATERMASK[colnum,rownum] = 1
            WATERMASK = NumpyWatershedSegment32(DEM, WATERMASK, level=20) #min level to have water mask

            #Numpy2GTiff(WATERMASK ,geotransform,projection,'F:/THESEUS/DSS/watershed/NED_10m_TIFF/wm.tif')

        if sp>0:
            # Our flood starting point
            neigh = DEM[colnum-1:colnum+2,rownum-1:rownum+2]
            minvalue=numpy.min(neigh[neigh!=0])

            (level, volume,FLOOD) = volumeControlledFlood(DEM_VOL, FLOOD, lev_volume, pixelsize, unit, maxleveldem,
            int(minvalue), levelstep, grid=mamba.SQUARE)
            WD = level

    print "LEVEL,VOLUME (M3) = (%.2f,%.2f)"%(level,volume)
    if volreduc==1:
        #print FLOOD
        FLOODTEMP=(numpy.float32(WD)*FLOOD)-DEM
        #FLOODTEMPfilename=working_dir+"tempflood.tif"
        #Numpy2Gdal(FLOODTEMP,geotransform,projection,FLOODTEMPfilename)
        FLOOD=Volumereduction(lev_volume,FLOODTEMP,WATERMASK,pixelsize,unit,WD)

```

```

mosaic = numpy.maximum( numpy.float32(WD)*FLOOD ,mosaic)

del FLOOD
gc.collect()

#-----
# Preparing Output
#-----
mask = numpy.greater(mosaic-DEM, numpy.float32(0)).astype("uint8")

watershed=(((mosaic-DEM)*mask)/100.00)
#(seamask,geotransform,projection) = GDAL2Numpy(working_dir+"wm.tif")
watershed=numpy.where(WATERMASK==1,0.00,watershed)

#Writing the output ISO
isofilename = "%s%s_ISO_TS%s.%s"%(working_dir,name_scenario,ts,ext)
Numpy2Gdal(mask,geotransform,projection,isofilename)
del mask

#Writing the output WD
wdfilename = "%s%s_WD_TS%s.%s" %(working_dir,name_scenario,ts,ext)
Numpy2Gdal(watershed,geotransform,projection,wdfilename)
del watershed

del DEM,DEM_VOL,mosaic,WATERMASK
gc.collect()
memory_used("at end of flooding")

#-----
#
# Quando viene lanciato da linea di comando ...
#
#-----
if __name__ == '__main__':

    if X_DEBUG:
        os.chdir(r"F:\THESEUS\DSS\DSS_functions_prd")
        #os.chdir(r"C:\Users\Valerio\Google Drive\FLOODING")
        #sys.argv = 'flood_levelvolume_mp_time_iso_2_2_5.py F:/THESEUS/DSS/watershed/NED_10m_TIFF/ dem_25m_tel9.tif gir
volpointtimegir1.txt 100'.split(" ")
        #sys.argv = 'flood_levelvolume_mp_time_iso_2_2_4.py C:/flooding/ ukdem_3h_v4.tif ukt volpointtimeuk3.txt 100'.split("
")
        #sys.argv = 'flood_levelvolume_mp_time_iso_2_2_2.pyc F:/THESEUS/DSS/watershed/NED_10m_TIFF/
dtm4ws_canta_l1.tif trez volpoint.txt 100'.split(" ")
        #sys.argv = 'flood_levelvolume_mp_time_iso_2_2_2.pyc F:/THESEUS/DSS/watershed/NED_10m_TIFF/
dtm4ws_canta_l1.asc testasc volpoint.txt 100'.split(" ")
        #sys.argv = 'flood_levelvolume_mp_time_iso_2_2_4.py F:/THESEUS/DSS/watershed/NED_10m_TIFF/ dtm4ws_ces_cl.tif
lolla volpointtimeces.txt 100'.split(" ")
        sys.argv = 'flood_levelvolume_mp_time_iso_2_2_9.py F:/THESEUS/DSS/watershed/NED_10m_TIFF/
dtm4ws_ces_full_2m.tif post1m inputWS.txt 100 1 1'.split(" ")
        #sys.argv = 'flood_levelvolume_mp_time_iso_2_2_9.py F:/THESEUS/DSS/watershed/NED_10m_TIFF/
dtm4ws_ces_full_2m.tif post2m inputWS.txt 100 1'.split(" ")
        sys.exit(main(sys.argv))

```

12.2 VELOCITY

```
import Image
import struct

import time
import sys
import gdal
from gdalconst import *
import numpy
import ogr
import osr
import sys
import os
import ImageMath
import ImageOps
import ImageChops
##workdir=sys.argv[1]
##slopefilename=sys.argv[2]
##amapfile=sys.argv[3]
##NameScenario=sys.argv[4]
##timestep=sys.argv[5]

slopefilename='slope_ces.tif'
NameScenario='cesub'
amapfile='a_ces_v2.tif'

pointfilename='volpointtimeces.txt'

workdir="E:/THESEUS/DSS/watershed/NED_10m_TIFF/"
timestep=1

def floodvel(slopefile,amapfile):
    driver = gdal.GetDriverByName('GTiff')
    driver.Register()

    amap = gdal.Open(amapfile, GA_ReadOnly)
    aband = amap.GetRasterBand(1)
    a = aband.ReadAsArray(0, 0, cols1, rows1)

    slopemap = gdal.Open(slopefile, GA_ReadOnly)
    slopeband = slopemap.GetRasterBand(1)
    slope = slopeband.ReadAsArray(0, 0, cols1, rows1)

    velocity=(a*numpy.sqrt(slope))/3.2808
    return velocity

amap = gdal.Open(workdir+amapfile, GA_ReadOnly)
cols1 = amap.RasterXSize
rows1 = amap.RasterYSize
bands1 = amap.RasterCount
aband = amap.GetRasterBand(1)
transform1 = amap.GetGeoTransform()
minX1 = transform1[0]
maxY1 = transform1[3]

pixelWidth1 = transform1[1]
pixelHeight1 = transform1[5]
maxX1 = minX1 + (cols1 * pixelWidth1)
minY1 = maxY1 + (rows1 * pixelHeight1)

velocity=floodvel(workdir+slopefilename,workdir+amapfile)
```

```

driver = gdal.GetDriverByName('GTiff')
#create the watershed image
velDs = driver.Create(workdir+str(NameScenario)+'_'+V_TS'+str(timestep)+'.tif', cols1, rows1, 1, GDT_Float32)
print 'save image'+workdir+str(NameScenario)+'_'+V_TS'+str(timestep)+'.tif'

if velDs is None:
    print 'Could not create image'
    sys.exit(1)
VBand = velDs.GetRasterBand(1)
velocity=(velocity).astype(float)
VBand.WriteArray(velocity)
geotransform = [minX1, pixelWidth1, 0, maxY1, 0, pixelHeight1]
velDs.SetGeoTransform(geotransform)
velDs.SetProjection(amac.GetProjection())
velDs=None
#del slope
del velocity

```

12.3 FLOW DURATION

```

import Image
import struct

import time
import sys
import gdal
from gdalconst import *
import numpy
import ogr
import osr
import sys
import os
import ImageMath
import ImageOps
import ImageChops
workdir=sys.argv[1]
waterdepthfilename=(sys.argv[2])
porosity=float(sys.argv[3])
watertable=sys.argv[4]
infilfilename=sys.argv[5]
NameScenario=sys.argv[6]
timestep=sys.argv[7]

##workdir="E:/THESEUS/DSS/watershed/NED_10m_TIFF/"
##waterdepthfilename="cesub_WD_TS0.tif"
##porosity=0.2
##watertable=100
##infilfilename='ltot_v6.tif'
##NameScenario='cesub'
##timestep=1

def flood_duration(waterdepthfile, porosity, watertable, infiltrationfile):
    WDmap = gdal.Open(waterdepthfile, GA_ReadOnly)
    WDband = WDmap.GetRasterBand(1)
    watershed = WDband.ReadAsArray(0, 0, cols1, rows1)

    infiltrationmap = gdal.Open(infiltrationfile, GA_ReadOnly)
    Dband = infiltrationmap.GetRasterBand(1)
    infilt = Dband.ReadAsArray(0, 0, cols1, rows1)

    runoff=(watershed-(float(porosity)*float(watertable)))
    duration=numpy.divide(runoff,infilt)
    return duration

WDmap = gdal.Open(workdir+waterdepthfilename, GA_ReadOnly)

```

```

cols1 = Wdmap.RasterXSize
rows1 = Wdmap.RasterYSize
bands1 = Wdmap.RasterCount
aband = Wdmap.GetRasterBand(1)
transform1 = Wdmap.GetGeoTransform()
minX1 = transform1[0]
maxY1 = transform1[3]

pixelWidth1 = transform1[1]
pixelHeight1 = transform1[5]
maxX1 = minX1 + (cols1 * pixelWidth1)
minY1 = maxY1 + (rows1 * pixelHeight1)

duration=flood_duration(workdir+waterdepthfilename, porosity, watertable, workdir+infiltrfilename)

driver = gdal.GetDriverByName('GTiff')
#create the watershed image
DTDs = driver.Create(workdir+str(NameScenario)+'_'+D_TS'+str(timestep)+'.tif', cols1, rows1, 1, GDT_Float32)
print 'save image'+workdir+str(NameScenario)+'_'+D_TS'+str(timestep)+'.tif'

if DTDs is None:
    print 'Could not create image'
    sys.exit(1)
DBand = DTDs.GetRasterBand(1)
duration1=(duration).astype(float)
print duration1
DBand.WriteArray(duration1)
geotransform = [minX1, pixelWidth1, 0, maxY1, 0, pixelHeight1]
DTDs.SetGeoTransform(geotransform)
DTDs.SetProjection(Wdmap.GetProjection())
DTDs=None
#watershed=None
#duration=None
infiltr=None
del duration

del duration1

```

13 Bibliography

-
- 1 Zanuttigh B., Dario Simcic , Stefano Bagli , Fabio Bozzeda , Luca Pietrantonì , Fabio Zagonari , Simon Hoggart , Robert J. Nicholls. THESEUS decision support system for coastal risk management. *Coastal Engineering* 87 (2014) 218–239
- 2 M.E. Castillo, E. M. Baldwin, R. S. Casarin, G. P. Vanegas, M. A. Juárez Characterization of Risks in Coastal Zones: A Review *Clean – Soil, Air, Water* 2012, 40 (9), 894–905 WILEY-VCH Verlag GmbH & Co. KGaA, Weinheim 10.1002/clen.201100679
- 3 Nicholls, R.J., 1995. Coastal megacities and climate change. *Geojournal* 37 (3), 369–379.
- 4 Turner, R.K., Subak, S., Adger, W.N., 1996. Pressures, trends, and impacts in coastal zones: interactions between socio- economic and natural systems. *Environmental Management* 20 (2), 159–173
- 5 A. Jha, J. Lamond, R. Bloch, N. Bhattacharya, A. López, N. Papachristodoulou, A. Bird, et al., Five Feet High and Rising Cities and Flooding in the 21st Century, World Bank Policy Research Working Paper 5648, The World Bank Group, Washington, DC 2011
- 6 M.E. Castillo, E. M. Baldwin, R. S. Casarin, G. P. Vanegas, M. A. Juárez Characterization of Risks in Coastal Zones: A Review *Clean – Soil, Air, Water* 2012, 40 (9), 894–905 WILEY-VCH Verlag GmbH & Co. KGaA, Weinheim 10.1002/clen.201100679
- 7 Dasgupta S, Laplante B, Meisner C, Wheeler D, Yan J (2009) The impact of sea level rise on developing countries: a comparative analysis. *Climatic Change* 93:379–388. doi:10.1007/s10584-008-9499-5
- 8 Nicholls RJ (2004) Coastal flooding and wetland loss in the 21st century: changes under the SRES climate and socio-economic scenarios. *Global Environ Chang* 14:69–89. doi:10.1016/j.gloenvcha.2003.10.007
- 9 Nicholls RJ, Hanson S, Herweijer C, Patmore N, Hallegatte S, Corfee-Morlot J, Chau^teau J, Muir-Wood R (2008) Ranking port cities with high exposure and vulnerability to climate extremes: exposure estimates. *OECD environment working papers No. 1, ENV/WKP(2007)*. OECD, Paris, France, [http://www.ois.oecd.org/olis/2007doc.nsf/linkto/env-wkp\(2007\)1](http://www.ois.oecd.org/olis/2007doc.nsf/linkto/env-wkp(2007)1)
- ¹⁰ P. J. Ward • M. A. Marfai • F. Yulianto • D. R. Hizbaron • J. C. J. H. Aerts Coastal inundation and damage exposure estimation: a case study for Jakarta *Nat Hazards* (2011) 56:899–916 DOI 10.1007/s11069-010-9599-1
- ¹¹ P. Vellinga, R. J. T. Klein, *Climate Change, Sea Level Rise and Integrated Coastal Zone Management: An IPCC Approach, Ocean Coastal Manage.* 1993, 21, 245–268
- ¹² R. C. Ballinger, H. D. Smith, L. M. Warren, *The Management of the Coastal Zone of Europe, Ocean Coastal Manage.* 1994, 22, 45–85
- ¹³ A. Zenger, D. I. Smith, G. J. Hunter, S. D. Jones, *Riding the Storm: A Comparison of Uncertainty Modelling Techniques for Storm Surge Risk Management, Appl. Geogr.* 2002, 22, 307–330.
- ¹⁴ . Duxbury, S. Dickinson, *Principles for Sustainable Governance of the Coastal Zone: In the Context of Coastal Disasters, Ecol. Econ.* 2007, 63, 319–330

-
- ¹⁵ AU IPCC, Workshop Report of the Intergovernmental Panel on Climate Change Workshop on Sea Level Rise and Ice Sheet Instabilities (Eds.: T. F. Stocker, D. Qin, G. K. Plattner, M. Tignor, S. Allen, P. M. Midgley), IPCC Working Group I Technical Support Unit, Bern 2007
- ¹⁶ M. El-Raey, Vulnerability Assessment of the Coastal Zone of the Nile Delta of Egypt, to the Impacts of Sea Level Rise, *Ocean Coastal Manage.* 1997, 37 (1), 29–40.
- ¹⁷ R. J. Nicholls, F. M. J. Hoozemans, M. Marchand, Increasing Flood Risk and Wetland Losses due to Global Sea-level Rise: Regional and Global Analyses, *Global Environ. Change* 1999, 9, 69–87.
- ¹⁸ A. Magnan, B. Garnaud, R. Bille', F. Germente, I. S. Hallegatte, The Future of the Mediterranean from Impacts of Climate Change to Adaptation Issues, IDDRI, Paris, France 2009
- ¹⁹ IPCC (2007) *Climate Change 2007: impacts, adaptation and vulnerability. Contribution of working group II to the fourth assessment report of the intergovernmental panel on climate change.* Cambridge University Press, Cambridge, UK
- ²⁰ Rosenzweig C, Solecki W (2001) *Climate change and a global city; the potential consequences of climate variability and change—metro east coast.* Report for the US global change program. Columbia Earth Institute, New York, USA
- ²¹ P. J. Ward • M. A. Marfai • F. Yulianto • D. R. Hizbaron • J. C. J. H. Aerts Coastal inundation and damage exposure estimation: a case study for Jakarta *Nat Hazards* (2011) 56:899–916 DOI 10.1007/s11069-010-9599-1
- ²² Peltier WR (1998) Postglacial variations in the level of the sea: implications for climate dynamics and solid-earth geophysics. *Rev Geophys* 36:603–689
- ²³ Meckel TA, Ten Brink US, Williams SJ (2007) Sediment compaction rates and subsidence in deltaic plains: numerical constraints and stratigraphic influences. *Basin Res* 19:19–31. doi:10.1111/j.1365- 2117.2006.00310.x
- ²⁴ Ericson JP, Vo'ro'smarty CJ, Dingman SL, Ward LG, Meybeck M (2006) Effective sea-level rise and deltas: causes of change and human dimension implications. *Global Planet Change* 50:63–82. doi:10.1016/j.gloplacha.2005.07.004
- ²⁵ Nicholls RJ, Hanson S, Herweijer C, Patmore N, Hallegatte S, Corfee-Morlot J, Cha^teau J, Muir-Wood R (2008) Ranking port cities with high exposure and vulnerability to climate extremes: exposure estimates. OECD environment working papers No. 1, ENV/WKP(2007). OECD, Paris, France, [http://www.ois.oecd.org/olis/2007doc.nsf/linkto/env-wkp\(2007\)1](http://www.ois.oecd.org/olis/2007doc.nsf/linkto/env-wkp(2007)1)
- ²⁶ IPCC (2007) *Climate change 2007: the physical science basis. Contribution of working group I to the fourth assessment report of the intergovernmental panel on climate change.* Cambridge University Press, Cambridge, UK
- ²⁷ Nicholls RJ, Hanson S, Herweijer C, Patmore N, Hallegatte S, Corfee-Morlot J, Cha^teau J, Muir-Wood R (2008) Ranking port cities with high exposure and vulnerability to climate extremes: exposure estimates. OECD environment working papers No. 1, ENV/WKP(2007). OECD, Paris, France, [http://www.ois.oecd.org/olis/2007doc.nsf/linkto/env-wkp\(2007\)1](http://www.ois.oecd.org/olis/2007doc.nsf/linkto/env-wkp(2007)1)
- ²⁸ Church, J.A., Gregory, J.M., Huybrechts, P., Kuhn, M., Lambeck, K., Nhuan, M.T., Qin, D. & Woodworth, P.L., Changes in Sea Level. *Climate Change 2001: The Scientific Basis. Contribution of Working Group 1 to the Third Assessment Report of the Intergovernmental Panel on Climate Change* [Houghton, J.T., Y. Ding, D.J. Griggs, M. Noguer, P.J. van der Linden, X. Dai, K. Maskell, and C.A. Johnson (eds.)], Tech. Rep. 881pp, 2001.

-
- ²⁹ Bouwer LM, Bubeck P, Wagtendonk AJ, Aerts CJH (2009) Inundation scenarios for flood damage evaluation in polder areas. *Natural hazards and earth system sciences* 9:1995–2007. www.nat-hazards-earth-syst-sci.net/9/1995/2009/
- ³⁰ Dasgupta S, Laplante B, Meisner C, Wheeler D, Yan J (2009) The impact of sea level rise on developing countries: a comparative analysis. *Climatic Change* 93:379–388. doi:10.1007/s10584-008-9499-5
- ³¹ Leskens J.C., M. Brugnach , A.Y. Hoekstra , W. Schuurmans 2014. Why are decisions in flood disaster management so poorly supported by information from flood models?. *Environmental Modelling & Software* 53 (2014) 53-61
- ³² Smith, K and Ward R, 1998, *Floods: Physical Processes and Human Impacts*, John Wiley and Sons, Chichester, USA.
- ³³ United Nations General Assembly, 1992: United Nations framework convention on climate change. Article 1. United Nations, New York.
- ³⁴ Christensen, J., Christensen, O., 2007. A summary of the PRUDENCE model projections of changes in European climate by the end of this century. *Climatic Change* 81, 7–30, <http://dx.doi.org/10.1007/s10584-006-9210-7>.
- ³⁵ Mitchell, J., 2003. European river floods in a changing world. *Risk Analysis* 23, 567– 574, <http://dx.doi.org/10.1111/1539-6924.00337>.
- ³⁶ Fowler, H., Ekström, M., 2009. Multi-model ensemble estimates of climate change impacts on UK seasonal precipitation extremes. *International Journal of Climatology* 29, 385–416, <http://dx.doi.org/10.1002/joc.1827>
- ³⁷ van der Linden, P., Mitchell, J., 2009. ENSEMBLES: Climate change and its impacts: Summary of research and results from the ENSEMBLES project. Technical Report. Met Office Hadley Centre. URL: http://ensembles-eu.metoffice.com/docs/Ensembles_final_report_Nov09.pdf.
- ³⁸ Nikulin, G., Kjellström, E., Hansson, U., Strandberg, G., Ullerstig, A., 2011. Evaluation and future projections of temperature, precipitation and wind extremes over Europe in an ensemble of regional climate simulations. *Tellus A* 63, 41–55, <http://dx.doi.org/10.1111/j.1600-0870.2010.00466.x>.
- ³⁹ Dankers, R., Feyen, L., 2009. Flood hazard in Europe in an ensemble of regional climate scenarios. *Journal of Geophysical Research* 114, 1–16, <http://dx.doi.org/10.1029/2008JD011523>.
- ⁴⁰ Whitfield, P., 2012. Floods in future climates: a review. *Journal of Flood Risk Management* 5, 336–365, <http://dx.doi.org/10.1111/j.1753-318X.2012.01150.x>.
- ⁴¹ IPCC, 2007: *Climate Change 2007: The Physical Science Basis*. Contribution of Working Group I to the Fourth Assessment Report of the Intergovernmental Panel on Climate Change, S. Solomon, D. Qin, M. Manning, Z. Chen, M. Marquis, K. B. Averyt, M. Tignor, and H. L. Miller, Eds., Cambridge University Press, Cambridge, United Kingdom and New York, 996 pp
- ⁴² T.W. Gallien et al. Predicting tidal flooding of urbanized embayments: A modeling framework and data requirements / *Coastal Engineering* 58 (2011) 567–577
- ⁴³ Heberger, M., Cooley, H., Herrera, P., Gleick, P.H., Moore, E., 2009. The impacts of sea-level rise on the California coast. California Climate Change Center, Sacramento.
- ⁴⁴ Kingma, Nanette C., 2002 *Flood Hazard Assessment and Zonation, Lecture Note*, ITC, Enschede, The Netherlands.
- ⁴⁵ Few, 2003 R. FewFlooding, vulnerability and coping strategies: local responses to a global threat *Prog. Dev. Stud.*, 3 (1) (2003), pp. 43–58

-
- ⁴⁶ Alexander, J., and S. Marriott, 1999: Introduction. *Floodplains: Interdisciplinary Approaches*. S. B. Marriott, and J. Alexander, Eds., The Geological Society of London, Special Publication No. 163, The Geological Society Publishing House, Bath, UK, 1–13
- ⁴⁷ Bridge, J. S., 2003: *Rivers and Floodplains: Forms, Processes, and Sedimentary Record*. Blackwell Science
- ⁴⁸ Blaikie, P., T. Cannon, I. Davis, and B. Wisner, 2003: *At Risk Natural Hazards, People's Vulnerability and Disasters*. 2nd ed., Routledge, 496 pp
- ⁴⁹ Handmer, J., E. Penning-Roswell, and S. Tapsell, 1999: *Flooding in a warmer world: the view from Europe*. *Climate, Change and Risk*. T. E. Downing, A. A. Olsthoorn, and R. S. J. Tol, Eds., Routledge, London
- ⁵⁰ He Y., F. Pappenberger, D. Manful, H. Cloke, P. Bates, F. Wetterhall, B. Parkes. Flood inundation dynamics and socioeconomic vulnerability under environmental change. *Climate Vulnerability*, Volume 5 <http://dx.doi.org/10.1016/B978-0-12-384703-4.00508-6>
- ⁵¹ EC, 2010. Council of European Union, Risk assessment and mapping guidelines for disaster management; Brussels, 2010, http://www.consilium.europa.eu/uedocs/cms_data/docs/pressdata/en/jha/121462.pdf
- ⁵² EC, 2009. Council of European Union, Council Conclusions on a Community framework on disaster prevention within the EU. Brussels 2009, http://www.consilium.europa.eu/uedocs/cms_data/docs/pressdata/en/jha/111537.pdf
- ⁵³ EC, 2010. Council of European Union, Risk assessment and mapping guidelines for disaster management; Brussels, 2010, http://www.consilium.europa.eu/uedocs/cms_data/docs/pressdata/en/jha/121462.pdf
- ⁵⁴ EC, 2009. Council of European Union, Council Conclusions on a Community framework on disaster prevention within the EU. Brussels 2009, http://www.consilium.europa.eu/uedocs/cms_data/docs/pressdata/en/jha/111537.pdf
- ⁵⁵ M. G. Morgan, M. Henrion, in *Vulnerability, Risk and Adaptation: A Conceptual Framework* (Ed.: N. Brooks), Working Paper 38, Tyndall Centre for Climate Change Research, Norwich 2003
- ⁵⁶ Department N of Humanitarian Affairs, *Internationally Agreed Glossary of Basic Terms Related to Disaster Management*, Relief Web Report, UN Department of Humanitarian Affairs, Geneva 1992
- ⁵⁷ J. Adams, in *Vulnerability, risk and adaptation: A conceptual framework* (Ed.: N. Brooks), Working Paper 38, Tyndall Centre for Climate Change Research, Norwich 2003
- ⁵⁸ I. Kelman, *Defining Risk*, FloodRiskNet Newsletter 2003, 2, 6–8.
- ⁵⁹ S. de La Cruz-Reyna, in *Defining Risk* (Ed.: I. Kelman), FloodRiskNet Newsletter 2003, 2, 6–8.
- ⁶⁰ K. Smith, in *Defining Risk* (Ed.: I. Kelman), FloodRiskNet Newsletter 2003, 2, 6–8
- ⁶¹ B. Gouldby, P. Samuels, in *Language of Risk – Project Definitions*, FLOODsite EU Integrated Project, Research Report T32-04-01, European Community, Brussels 2005.
- ⁶² Helm, in *Defining Risk* (Ed.: I. Kelman), FloodRiskNet Newsletter 2003, 2, 6–8
- ⁶³ Safecoast, *Coastal Flood Risk and Trends for the Future in the North Sea Region*, Synthesis Report, Safecoast, The Hague 2008
- ⁶⁴ D. Bellomo, *Flood Map Modernization and FEMA Levee Policy*, FEMA – U.S. Department of Homeland Security, Hyattsville, MD 2008
- ⁶⁵ R. Wallingford, in *Language of Risk – Project Definitions*, FLOODsite EU Integrated Project, Research Report T32-04-01, European Community, Brussels 2005

-
- ⁶⁶ Balica, S.F., I. Popescu, L. Beevers, N.G. Wright. Parametric and physically based modelling techniques for flood risk and vulnerability assessment: A comparison. *Environmental Modelling & Software* 41 (2013) 84-92
- ⁶⁷ Knight, F.H., 1921. *Risk, Uncertainty, and Profit*. Hart, Schaffner & Marx; Houghton Mifflin Company, Boston, MA. Available online: <http://www.econlib.org/library/Knight/knRUP1.html>. As seen on 14th of December 2011.
- ⁶⁸ Sayers, P., Hall, J., Dawson, R., Rosu, C., Chatterton, J., Deakin, R., 29 September 2011. Risk Assessment of Flood and Coastal Defenses for Strategic Planning (rasp) e a High Level Methodology. Wallingford, as seen on. http://www.raspproject.net/RASP_defra2002_Paper_Final.pdf.
- ⁶⁹ Slovic, P., 1987. Perception of risk. *Science* 236, 280e285.
- ⁷⁰ Alexander, D., 1993. *Natural Disasters*. Chapman & Hall, New York.
- ⁷¹ IPCC, 2001. *Climate Change 2001: the Scientific Basis*. Cambridge University Press, Cambridge.
- ⁷² Plate Erich, J., 2002. Flood risk and flood management. *Journal of Hydrology* 267, 2e11.
- ⁷³ Barredo, J.I., de Roo, A., Lavalle, C., 2007. Flood risk mapping at European scale. *Water Science and Technology* 56 (4), 11e17
- ⁷⁴ Sayers, P., Hall, J., Dawson, R., Rosu, C., Chatterton, J., Deakin, R., 29 September 2011. Risk Assessment of Flood and Coastal Defenses for Strategic Planning (rasp) e a High Level Methodology. Wallingford, as seen on. http://www.raspproject.net/RASP_defra2002_Paper_Final.pdf.
- ⁷⁵ Merz, B., Thieken, A.H., Gocht, M., 2007. Flood risk mapping at the local scale: concepts and challenges. In: Begum, S., Stive, M.J.F., Hall, J.W. (Eds.), *Flood Risk Management in Europe*, 25. *Advances in Natural and Technological Hazards Research*. Springer, Netherlands, pp. 231e251.
- ⁷⁶ FLOODsite, Integrated Flood Risk Analysis and Management Methodologies, FLOODsite EU Integrated Project, Sixth Framework Programme, European Community, Brussels 2004–2009.
- ⁷⁷ ADAPT, Towards an Integrated Decision Tool for Adaptation Measures – Case Study: Floods, Final Report (Phase I), Belgian Science Policy, ADAPT, Brussels Belgium 2008
- ⁷⁸ Schanze, J., 2006. Flood risk management e a basic framework, flood risk management: hazards, vulnerability and mitigation measures NATO science Series: IV. *Earth and Environmental Sciences* 67 (Part 1), 1e20.
- ⁷⁹ CRICHTON, D. (2007) The Hull floods of June 2007: Some insurance industry Implications. Paper published by Benfield Grieg Hazard Research Centre. Available: http://www.benfieldhrc.org/floods/Crichton_Hull_2007.pdf
- ⁸⁰ Parry, M. L., Canziani, O. F., Palutikof, J. P., van der Linden, P. J., & Hanson, C. E. (2007). *Climate change 2007: Working Group II: Impacts, adaptation and vulnerability contribution of Working Group II to the Fourth Assessment Report of the Intergovernmental Panel on Climate Change, 2007*. Cambridge, UK/New York, USA: Cambridge University Press.
- ⁸¹ DEFRA, & EA. (2006). R&D outputs: Flood risks to people. Phase 2. FD2321/TR1 The flood risks to people methodology. London: Department for Environment Food and Rural Affairs and the Environment Agency.
- ⁸² Lindley, S. J., Handley, J. F., Theuray, N., Peet, E., & Mcevoy, D. (2006). Adaptation strategies for climate change in the urban environment: Assessing climate change related risk in UK urban areas. *Journal of Risk Research*, 9, 543–568
- ⁸³ IPCC, 2007a, Summary for Policymakers. In: *Climate Change 2007: The Physical Science Basis*. Contribution of Working Group I to the Fourth Assessment Report of the Intergovernmental Panel on Climate Change [Solomon, S., D. Qin, M. Manning, Z. Chen, M. Marquis, K.B. Averyt, M.Tignor and H.L. Miller]. Cambridge University Press, Cambridge, Cambridge, United Kingdom and New York, NY, USA

-
- ⁸⁴ Gabor, T., Griffith, T.K., 1980. The assessment of community vulnerability to acute hazardous materials incidents. *Journal of Hazardous Materials* 8, 323e333.
- ⁸⁵ IPCC, 2001. *Climate Change 2001: the Scientific Basis*. Cambridge University Press, Cambridge.
- ⁸⁶ Klein, R.J.T., Nicholls, R.J., Mimura, N., 1999. Coastal adaptation to climate change: can the IPCC Technical Guidelines be applied? *Mitigation and Adaptation Strategies for Global Change* 4, 51e64.
- ⁸⁷ ISDR, 2004. *International Strategy for Disaster Reduction. Living with Floods: UN Guidelines Offer Decision Makers Hope to Reduce Flood Losses*. Available from: www.unisdr.org/archive/5353 (5.04.11.).
- ⁸⁸ A. Jha, J. Lamond, R. Bloch, N. Bhattacharya, A. López, N. Papachristodoulou, A. Bird, et al., *Five Feet High and Rising Cities and Flooding in the 21st Century*, World Bank Policy Research Working Paper 5648, The World Bank Group, Washington, DC 2011.
- ⁸⁹ M. Papathoma, D. Dominey-Howes, *Tsunami Vulnerability Assessment and Its Implications for Coastal Hazard Analysis and Disaster Management Planning, Gulf of Corinth, Greece*, *Nat. Hazards Earth Syst. Sci.* 2003, 3, 733–747.
- ⁹⁰ Defra/Environment Agency, *Best Practice in Coastal Flood Forecasting, R&D Technical Report FD2206/TR1; HR Wallingford Report TR 132*, DEFRA, London, UK 2004.
- ⁹¹ A. Werritty, D. Houston, T. Ball, A. Tavendale, A. Black, *Exploring the Social Impacts of Flood Risk and Flooding in Scotland*, Scottish Executive, Edinburgh 2007
- ⁹² A. Kazmierczak, J. Handley, *The Vulnerability Concept: Use Within GRaBs*, School of Environment and Development, University of Manchester, Manchester, UK 2011
- ⁹³ S. Narayan, S. Hanson, R. Nicholls, D. Clarke, *Use of the Source–Pathway– Receptor–Consequence Model in Coastal Flood Risk Assessment*, in *European Geosciences Union General Assembly*, Copernicus Publisher, Vienna 2011
- ⁹⁴ FLOODsite, *Integrated Flood Risk Analysis and Management Methodologies*, FLOODsite EU Integrated Project, Sixth Framework Programme, European Community, Brussels 2004–2009
- ⁹⁵ THESEUS, *Flood and erosion maps at present conditions*, THESEUS Deliverable ID1.3, European Commission, Bologna, Italy 2011.
- ⁹⁶ FLOODsite, *Integrated Flood Risk Analysis and Management Methodologies*, FLOODsite EU Integrated Project, Sixth Framework Programme, European Community, Brussels 2004–2009
- ⁹⁷ Xia, Junqiang, Falconer, Roger A., Binliang, Lin, Tan, Guangming, 2011. Numerical assessment of flood hazard risk to people and vehicles in flash floods. *Environmental Modelling & Software* 26 (8), 987e998.
- ⁹⁸ Hartanto, I.M., Beavers, L., Popescu, I., Wright, N.G., 2011. Application of a coastal modelling code in fluvial environments. *Environmental Modelling and Software* 26 (12), 1685e1695.
- ⁹⁹ Gichamo, Z.,G., Popescu, I., Jonoski, A., Solomatine, D.P., 2012. River cross section extraction from ASTER global DEM for flood modeling. *Journal of Environmental Modelling & Software* 31 (5), 37e46.
- ¹⁰⁰ Pratt, C., Kaly, U., Mitchell, J., 2004. *How to Use the Environmental Vulnerability Index*, UNEP/SOPAC South Pacific Applied Geo-science Commission. Technical Report 383. www.vulnerabilityindex.net/Files/EVI%20Manual.pdf (accessed 17.09.11.).
- ¹⁰¹ Briguglio, L., 2003. *Methodological and Practical Considerations for Constructing Socio Economic Indicators to Evaluate Disaster Risk*. Institute of Environmental Studies, University of Colombia, Manizales, Colombia. Programme on Information and Indicators for Risk Management, IADB-ECLAC-IDEA.

-
- ¹⁰² Peduzzi, P., Dao, H., Herold, C., Rochette, D., Sanahuja, H., 2001. Feasibility Study Report e on Global Risk and Vulnerability Index eTrends per Year (GRAVITY). United Nations Development Programme Emergency Response Division UNDP/ ERD, Geneva.
- ¹⁰³ Sullivan, C.A., Meigh, J., 2003. Using the Climate Vulnerability Index to assess vulnerability to climate variations. Water Policy and Management. CEH Wallingford, as seen on: <http://www.ceh.ac.uk/sections/ph/ClimateVulnerabilityIndex.html>
- ¹⁰⁴ FLOODsite, in Language of Risk – Project Definitions, FLOODsite EU Integrated Project, Research Report T32-04-01, European Community, Brussels 2005.
- ¹⁰⁵ R. J. Tkach, S. P. Simonovic, A New Approach to Multi-criteria Decision Making in Water Resources, *J. Geogr. Inf. Decis. Anal.* 1997, 1 (1), 25–43.
- ¹⁰⁶ C. A. Bana, P. A. da Silva, F. N. Correia, Multicriteria Evaluation of Flood Control Measures: The Case of Ribeira do Livramento, *Water Resources Management*, Kluwer Academic Publishers, Netherlands 2004, 18, 263–283
- ¹⁰⁷ R. Brouwer, R. van Ek, Integrated Ecological, Economic and Social Impact Assessment of Alternative Flood Control Policies in The Netherlands, *Ecol. Econ.* 2004, 50, 1–21.
- ¹⁰⁸ RPA – Risk and Policy Analysts Ltd., Evaluating a Multi-criteria Analysis (MCA) Methodology for Application to Flood Management and Coastal Defense Appraisals, R&D Technical Report, DEFRA, London 2004.
- ¹⁰⁹ FLOODsite, GIS-based Multicriteria Analysis as Decision Support in Flood Risk Management, FLOODsite EU Integrated Project, Research Report T10-07-07, European Community, Brussels 2007.
- ¹¹⁰ C. A. Bana, P. A. da Silva, F. N. Correia, Multicriteria Evaluation of Flood Control Measures: The Case of Ribeira do Livramento, *Water Resources Management*, Kluwer Academic Publishers, Netherlands 2004, 18, 263–283
- ¹¹¹ Gornitz, V., White, T.W., 1992. A Coastal Hazards Database for the U.S. West Coast: ORNL/CDIAC-81, NDP-043C. Oak Ridge National Laboratory, Oak Ridge, Tenn. <http://cdiac.ornl.gov/epubs/ndp/ndp043c/43c.htm>.
- ¹¹² Gornitz et al., 1994 V.M. Gornitz, R.C. Daniels, T.W. White, K.R. Birdwell The development of a coastal vulnerability assessment database, vulnerability to sea-level rise in the U.S. southeast *J. Coast. Res. SI*, 12 (1994), pp. 327–338
- ¹¹³ Pendleton, E.A., Hammar-Klose, E.S., Thieler, E.R., Williams, S.J., 2004. Coastal Vulnerability Assessment of Cumberland Island National Park to Sea-level Rise. U.S. Geological Survey Open-File Report 2004-1021, Web Only. <http://pubs.usgs.gov/of/2004/1196/index.html>.
- ¹¹⁴ A. V. Hedge, V. R. Reju, Development of Coastal Vulnerability Index for Mangalore Coast, India, *J. Coastal Res.* 2007, 23 (5), 1106–1111.
- ¹¹⁵ V. M. Gornitz, R. C. Daniels, T. W. White, K. R. Birdwell, Multi Hazard – Identification and Risk Assessment, The Cornerstone of the National Mitigation Strategy, Federal Emergency Management Agency, New York 1997
- ¹¹⁶ R. Dal-Cin, U. Simeoni, A Model for Determining the Classification, Vulnerability and Risk in the Southern Coastal Zone of the Marche (Italy), *J. Coastal Res.* 1994, 10, 18–29
- ¹¹⁷ <http://dx.doi.org/10.1016/j.ocecoaman.2014.12.011>
- ¹¹⁸ <http://dx.doi.org/10.1016/j.ocecoaman.2014.12.011>
- ¹¹⁹ <http://dx.doi.org/10.1016/j.ocecoaman.2014.12.011>
- ¹²⁰ Schultz, C., 2013. Tropical storm Sandy was a 1-in-700-year event. *EOS Trans. Am. Geophys. Union* 94 (30), 268.
- ¹²¹ Kolen, B., Slomp, R., Balen, W.v., 2010. Learning from French Experiences with Storm Xynthia. (rijksoverheid.nl).

-
- ¹²² McGranahan, G., Balk, D., Anderson, B., 2007. The rising tide: assessing the risks of climate change and human settlements in low elevation coastal zones. *Environ. Urban.* 19 (1), 17–37
- ¹²³ Small, C., Nicholls, R.J., 2003. A Global Analysis of Human Settlement in Coastal Zones
- ¹²⁴ de Moel, H., Van Alphen, J., Aerts, J., 2009. Flood maps in Europe — methods, availability and use. *Nat. Hazards Earth Syst. Sci.* 9, 289–301
- ¹²⁵ Hanson, S., Nicholls, R.J. (Eds.), 2012. Integrated Report on Risk Assessment in Study Sites, with Appendices, Official Deliverable OD1.15. THESEUS Project (eu fp7: Grant 244104) (Available at http://www.Theseusproject.Eu/index.php?Option=com_remository& itemid=2&func=select&id=88project last accessed June 2012).
- ¹²⁶ Mokrech, M., Hanson, S., Nicholls, R.J., Wolf, J., Walkden, M., Fontaine, C.M., Sophie, N.C., Jude, S.R., Leake, J., Stansby, P., Watkinson, A., Rounsevell, M.D.A., Lowe, J., Hall, J.W., 2011. The Tyndall coastal simulator. *J. Coast. Conserv.* 15 (3), 325–335.
- ¹²⁷ Safecoast, 2008. Coastal flood risk and trends for the future in the North Sea region. Synthesis Report. Safecoast Project Team, The Hague
- ¹²⁸ Dawson, R., Dickson, M., Nicholls, R.J., Hall, J.W., Walkden, M., Stansby, P., Mokrech, M., Richards, J., Zhou, J., Milligan, J., Jordan, A., Pearson, S., Rees, J., Bates, P., Koukoulas, S., Watkinson, A., 2009. Integrated analysis of risks of coastal flooding and cliff erosion under scenarios of long term change. *Clim. Chang.* 95 (1), 249–288.
- ¹²⁹ FLOODsite, in Language of Risk – Project Definitions, FLOODsite EU Integrated Project, Research Report T32-04-01, European Community, Brussels 2005.
- ¹³⁰ Holdgate, M.W., 1979. A Perspective of Environmental Pollution. Cambridge University Press Cambridge, UK.
- ¹³¹ Evans, E., Hall, J.W., Penning-Rowell, E., Sayers, P., Thorne, C., Watkinson, A., 2006. Future flood risk management in the UK. Proceedings — Institution of Civil Engineers Water Management, p. 53
- ¹³² Sayers, P., Hall, J.W., Meadowcroft, I., 2002. Towards risk-based flood hazard management in the UK. *Civ. Eng.* 150, 36–42
- ¹³³ Bakewell, I., Luff, S., 2008. North London Strategic Flood Risk Assessment — Final Report. DEFRA, UK.
- ¹³⁴ FLOODSite Consortium, 2008. Evaluation of Inundation Models: Limits and Capabilities of Models. H R Wallingford, UK (www.floodsite.net).
- ¹³⁵ Naulin, M., Kortenhaus, A., Oumeraci, H., 2012. Reliability analysis and breach modelling of flood defences in an integrated risk analysis 4. Results of the XTREMRisk project. *Flood Risk Management: Science, Policy and Practice: Closing the Gap*, 74.
- ¹³⁶ Defra/Environment Agency, Best Practice in Coastal Flood Forecasting, R&D Technical Report FD2206/TR1; HR Wallingford Report TR 132, DEFRA, London, UK 2004
- ¹³⁷ Evans, E., Ashley, R., Hall, J.W., Penning-Rowell, E., Sayers, P., Thorne, C., Watkinson, A., 2004. Foresight Future Flooding: Scientific Summary: Volume I — Future Risks and their Drivers. Office of Science and Technology, London.
- ¹³⁸ P. Sayers, I. Meadowcroft, RASP – A hierarchy of risk-based methods and their application, Defra Flood and Coastal Management Conference, York, UK 2005
- ¹³⁹ FLOODSite Consortium, 2009. Methodology for a DSS to Support Long-term Flood Risk Management Planning. H R Wallingford.
- ¹⁴⁰ Safecoast, 2008. Coastal flood risk and trends for the future in the North Sea region. Synthesis Report. Safecoast Project Team, The Hague

¹⁴¹ North Carolina Division of Emergency Management, 2009. North Carolina Sea Level Rise Risk Management Study — Potential Impacts, Risk Assessments and Management Strategies.

142 S. Narayan, S. Hanson, R. Nicholls, D. Clarke, Use of the Source–Pathway– Receptor-Consequence Model in Coastal Flood Risk Assessment, in European Geosciences Union General Assembly, Copernicus Publisher, Vienna 2011

¹⁴³ Gouldby, B., Samuels, P., 2005. Language of Risk — Project Definitions. FLOODSite Consortium, UK.

¹⁴⁴ FLOODsite, in Language of Risk – Project Definitions, FLOODsite EU Integrated Project, Research Report T32-04-01, European Community, Brussels 2005.

¹⁴⁵ J. W. Hall, E. P. Evans, E. C. Penning-Rowsell, P. B. Sayers, C. R. Thorne, A. J. Saul, Quantified Scenarios Analysis of Drivers and Impacts of Changing Flood Risk in England and Wales: 2030-2100, Global Environmental Change Part B, Environ. Hazards 2003, 4, 51–64

¹⁴⁶ SOBEY, R.J. (2005) Extreme low and high water levels. *Coastal Engineering*, 52, 63-77.

¹⁴⁷ PIRAZZOLI, P.A. and TOMASIN, A. (2007). Estimation of return periods for extreme sea levels: a simplified empirical correction of the joint probabilities method with examples from the French Atlantic coast and three ports in the southwest of the UK. *Ocean Dynamics*, 57, 91-107.

¹⁴⁸ SANCHEZ-ARCILLA, A. (Ed.) (2007) *Report on best suitable models for a statistical analysis of joint probabilities of extreme event data*. FLOODsite report T02-07-03.

¹⁴⁹ FEMA 2005. Wave runup and overtopping. FEMA Coastal Flood Hazard Analysis and Mapping Guidelines Focused Study Report, 51 pp.

150 KEULER, K., LAUTENSCHLAGER, M., WUNRAM, C., KEUP-THIEL, E., SCHUBERT, M., WILL, A., ROCKEL, B. and BOEHM, U. (2009) Climate simulation with CLM, Scenario A1B run no.1, Data Stream 2: European region MPI-M/MaD. . World Data Center for Climate. Available at. Last accessed

151 UMGIESSER, G., CANU, D. M., CUCCO, A. and SOLIDORO, C. (2004) A finite element model for the Venice Lagoon. Development, set up, calibration and validation. *Journal of Marine Systems*, 51, (1-4) 123-145. doi 10.1016/j.jmarsys.2004.05.009

152 BELLAFIORE, D., UMGIESSER, G. and CUCCO, A. (2008) Modeling the water exchanges between the Venice Lagoon and the Adriatic Sea. *Ocean Dynamics*, 58, (5-6) 397-413. doi 10.1007/s10236-008- 0152-7

¹⁵³ Stockdon, H.F., Holman, R.A., Howd, P.A., Sallenger, A.H., 2006. Empirical parameterization of setup, swash, and runup. *Coast. Eng.* 53 (7), 573–588.

¹⁵⁴ Owen, M.W., 1980. Design of seawalls allowing for wave overtopping, Report No. EX 924, HR Wallingford, United Kingdom.

¹⁵⁵ Goda, Y. 1985. *Random Seas and Design of Maritime Structures*, University of Tokyo Press, Japan.

¹⁵⁶ Reeve, D. E., Li, Y., Larson, M., Hanson, H., Donnelly, C., Jimenez, J., Mendoza, E. T., Zech, Y., Soares Frazao, S., Bettess, R., Stripling, S. & Brampton, A. 2009. Predicting morphological changes in rivers, estuaries and coasts: executive summary. Floodsite report no. T05-07-03. Task Leader: University of Plymouth, Co-ordinator: HR Wallingford.

¹⁵⁷ Dawson, R., Speight, L., Hall, J. W., Djordavic, S., Savic, D. & Leandro, J. 2008. Attribution of flood risk in urban areas. *Journal of Hydroinformatics*, 10, 275-288.

¹⁵⁸ Marks, K. & Bates, P. 2000. Integration of high-resolution topographic data with floodplain flow models. *Hydrological Processes*, 14, 2109-2122.

-
- ¹⁵⁹ Xharde, R., Long, B. & Forbes, D. 2006. Accuracy and Limitations of Airborne LiDAR Surveys in Coastal Environment, Print ISBN: 0-7803-9510-7. Geoscience and Remote Sensing Symposium, 2006. IGARSS 2006. IEEE International Conference. Denver, CO, USA.
- ¹⁶⁰ Webster, T. L., Forbes, D. L., MacKinnon, E. & Roberts, D. 2006. Flood-risk mapping for storm-surge events and sea-level rise using lidar for southeast New Brunswick. *Can. J. Remote Sensing*, 32, 194-211.
- ¹⁶¹ Bates, P. D., Dawson, R. J., Hall, J. W., Horritt, M. S., Nicholls, R. J., Wicks, J. & Mohamed Ahmed Ali Mohamed, H. 2005. Simplified two-dimensional numerical modelling of coastal flooding and example applications. *Coastal Engineering*, 52, 793-810.
- ¹⁶² Gallien, T. W., Schubert, J. E. & Sanders, B. F. 2011. Predicting tidal flooding of urbanized embayments: A modeling framework and data requirements. *Coastal Engineering*, 58, 567-577.
- ¹⁶³ Nicholls, R. J., Mockrech, M., Richards, J., Bates, P. D., Dawson, R., Hall, J., Walkden, M., Dickson, M., Jordan, A. & Milligan, J. 2005. Assessing coastal flood risk at specific sites and regional scales: Regional assessment of coastal flood risk. Technical report No 45. October 2005, from project T2.46.
- ¹⁶⁴ Dawson, R., Hall, J., Sayers, P., Bates, P. & Rosu, C. 2005a. Sampling-based flood risk analysis for fluvial dike systems. *Stochastic Environmental Research and Risk Assessment*, 19, 388-402
- ¹⁶⁵ Brown, J. D., Spencer, T. & Moeller, I. 2007. Modeling storm surge flooding of an urban area with particular reference to modeling uncertainties: A case study of Canvey Island, United Kingdom. *Water Resour. Res.*, 43, W06402.
- ¹⁶⁶ Cugier, P. & Le Hir, P. 2002. Development of a 3D Hydrodynamic Model for Coastal Ecosystem Modelling. Application to the Plume of the Seine River (France). *Estuarine, Coastal and Shelf Science*, 55, 673-695
- ¹⁶⁷ Jonkman, S.N., Vrijling, J.K., 2008. Loss of life due to floods. *Journal of Flood Risk Management* 1, 43e56.
- ¹⁶⁸ FEMA 2003. Guidelines and Specifications for Flood Hazard Mapping Partners. Appendix A: Guidance for Aerial Mapping and Surveying, 57 pp.
- ¹⁶⁹ HAILE, A.T. and RIENTJES, T.H.M. (2005). Effects of Lidar dem resolution in flood modelling: A model sensitivity study for the city of Tegucigalpa, Honduras. ISPRS WG III/3, III/4, Workshop "Laser scanning 2005". Enschede.
- ¹⁷⁰ Middelkoop, H., Van Asselt, M.B.A., Van't Klooster, S.A., Van Deursen, W.P.A., Kwadijk, J.C.J., Buiteveld, H., 2004. Perspectives on flood management in the Rhine and Meuse rivers. *River Research and Applications* 20 (3), 327-342
- ¹⁷¹ Ashley, R.M., Balmforth, D.J., Saul, A.J., Blanksby, J.D., 2005. Flooding in the future — predicting climate change, risks and responses in urban areas. *Water Science and Technology* 52 (5), 265-273.
- ¹⁷² Hall, J.W., Sayers, P.B., Dawson, R.J., 2005. National-scale assessment of current and future flood risk in England and Wales. *Natural Hazards* 36 (1-2), 147-164.
- ¹⁷³ Dawson, R.J., Hall, J.W., Bates, P.D., Nichols, R.J., 2005a. Quantified analysis of the probability of flooding in the Thames Estuary under imaginable worst-case sea level rise scenarios. *International Journal of Water Resources Development* 21 (4), 577-591.
- ¹⁷⁴ N.M. Hunter et al. 2007, "Simple spatially-distributed models for predicting flood inundation: A review", *Geomorphology* 90 (2007) 208-225
- ¹⁷⁵ Al-Sabhan, W., Mulligan, M., Blackburn, G.A., 2003. A real-time hydrological model for flood prediction using GIS and the WWW. *Comput. Environ. Urban Syst.* 27 (1), 9e32
- ¹⁷⁶ Bates, P.D., De Roo, A.P.J., 2000. A simple raster-based model for flood inundation simulation. *J. Hydrol.* 236 (1e2), 54e77.

-
- ¹⁷⁷ De Moel, H., Aerts, J., 2011. Effect of uncertainty in land use, damage models and inundation depth on flood damage estimates. *Nat. Hazards* 58 (1), 407e425
- ¹⁷⁸ Stelling, G.S., 2012. Quadtree flood simulations with sub-grid DEMs. *Water Manag.* 165, 1e14.
- ¹⁷⁹ McCarthy, S., Tunstall, S., Parker, D., Faulkner, H., Howe, J., 2007. Risk communication in emergency response to a simulated extreme flood. *Environ. Hazards* 7 (3), 179e192.
- ¹⁸⁰ DRDE-US (Department of Regional Development and Environment-US), 1991 Primer on Natural Hazard Management in Integrated Regional Development Planning, <http://www.oas.org/usde/publications/Unit/oea66e/Contents>
- ¹⁸¹ Marfai M.A.. GIS Modelling of River and Tidal Flood Hazards in a Waterfront City Case study: Semarang City, Central Java, Indonesia. INTERNATIONAL INSTITUTE FOR GEO-INFORMATION SCIENCE AND EARTH OBSERVATION ENSCHEDE, THE NETHERLANDS 2003
- ¹⁸² Cunge, J.A., Holly, F.M., Verwey, A., 1980. *Practical Aspects of Computational River Hydraulics*. Pitman Publishing, London p. 420.
- ¹⁸³ Miller, R.C., Guertin, P.D., Heilman, P., 2004. Information technology in watershed decision making. *J. Am. Water Resour. Assoc.* 02029, 347–358.
- ¹⁸⁴ Vaze, J., Teng, J., Spencer, G. 2010. Impact of DEM accuracy and resolution on topographic indices. *Environmental Modelling and Software*. Volume: 25 Issue: 10 Pages: 1086-1098.
- ¹⁸⁵ Horritt, M.S., Bates P.D. 2001. Effects of spatial resolution on a raster based model of flood flow. *Journal of Hydrology*, 253 (1-4), 239 - 249.
- ¹⁸⁶ Bates, P. D., F. Pappenberger, and R. Romanowicz, 2012: *Uncertainty and risk in flood inundation modelling. Flood Forecasting*. K. J. Beven, and J. Hall, Eds., John Wiley & Sons, New York.
- ¹⁸⁷ Knight, D. W., and K. Shiono, 1996: *River channel and floodplain hydraulics. Floodplain Processes*. M. G. Anderson, D. E. Walling, and P. D Bates, Eds., John Wiley & Sons, Chichester, UK, 139–182.
- ¹⁸⁸ Babaeyan-Koopaei, K., D. A. Ervine, P. A. Carling, and Z. Cao, 2002: Field measurements for two overbank flow events in the River Severn. *ASCE J. Hydraul. Eng.*, 128, 891–900
- ¹⁸⁹ Nicholas, A. P., and C. A. Mitchell, 2003: Numerical simulation of overbank processes in topographically complex floodplain environments. *Hydrol. Process.*, 17 (4), 727– 746
- ¹⁹⁰ Bates, P. D., M. D. Wilson, M. S. Horritt, D. Mason, N. Holden, and A. Currie, 2006: Reach scale floodplain inundation dynamics observed using airborne synthetic aperture radar imagery: data analysis and modelling. *J. Hydrol.*, 328, 306–318.
- ¹⁹¹ Pavelsky, T. M., and L. C. Smith, 2008: Remote sensing of hydrologic recharge in the Peace-Athabasca Delta, Canada. *Geophys. Res. Lett.*, 35 (8), paper no. L08403, <http://dx.doi.org/10.1029/2008GL033268>
- ¹⁹² Schumann, G., P. Matgen, F. Pappenberger, R. Hostache, and L. Pfister, 2007: Deriving distributed roughness values from satellite radar data for flood inundation modelling. *J. Hydrol.*, 344, 96–111
- ¹⁹³ Schumann, G., P. Matgen, and F. Pappenberger, 2008: Estimating uncertainty associated with water stages from a single SAR image. *Adv. Water Resour.*, 31 (8), 1038–1047.
- ¹⁹⁴ Hromadka, T.V., Yen, C.C., 1986. A diffusion hydrodynamic model (DHM). *Advances in Water Resources* 9 (3), 118–170.
- ¹⁹⁵ Syme, W.J., 1991. Dynamically linked two-dimensional/one-dimensional hydrodynamic modelling program for rivers, estuaries and coastal waters. Unpublished MRes thesis, University of Queensland, Australia

-
- ¹⁹⁶ Katapodes, N.D., Strelkoff, T., 1979. Two-dimensional shallow water- wave model. *Journal of the Engineering Mechanics Division ASCE* 105 (EM2), 317–334.
- ¹⁹⁷ Kawahara, M., Yokoyama, T., 1980. Finite element method for direct runoff flow. *Journal of the Hydraulics Division ASCE* 106 (HY4), 519–534
- ¹⁹⁸ Iwasa, Y., Inoue, K., 1982. Mathematical simulations of channel and overland flood flows in view of flood disaster engineering. *Journal of Natural Disaster Science* 4 (1), 1–30
- ¹⁹⁹ Zhang, W.H., Cundy, T.W., 1989. Modeling of two-dimensional overland-flow. *Water Resources Research* 25 (9), 2019–2035.
- ²⁰⁰ Xanthopoulos, T., Koutitas, C., 1976. Numerical-simulation of a 2 dimensional flood wave-propagation due to dam failure. *Journal of Hydraulic Research* 14 (4), 321–331.
- ²⁰¹ Cunge, J.A., Holly, F.M., Verwey, A., 1980. *Practical Aspects of Computational River Hydraulics*. Pitman Publishing, London. 420 pp.
- ²⁰² Hromadka, T.V., Yen, C.C., 1986. A diffusion hydrodynamic model (DHM). *Advances in Water Resources* 9 (3), 118–170.
- ²⁰³ Julien, P.Y., Saghafian, B., Ogden, F.L., 1995. Raster-based hydrologic modeling of spatially-varied surface runoff. *Water Resources Bulletin* 31 (3), 523–536.
- ²⁰⁴ LHOMME J., BOUVIER C. and PERRIN J.-L. Applying a GISbased geomorphological routing model in urban catchments. *Journal of Hydrology*, 2004, 299, No. 3–4, 203–216.
- ²⁰⁵ BATES P. D. and DE ROO A. P. J. A simple raster-based model for floodplain inundation. *Journal of Hydrology*, 2000, 236, No. 1–2, 54–77.
- ²⁰⁶ Smith, G.D., 1978. *Numerical Solution of Partial Differential Equations: Finite Difference Methods*, 2nd Edition. Oxford University Press, Oxford. 304 pp.
- ²⁰⁷ Zienkiewicz, O.C., Cheung, Y.K., 1965. Finite elements in the solution of field problems. *The Engineer* 202, 507–510
- ²⁰⁸ Hirsch, C., 1988. *Numerical computation of internal and external flows. Fundamentals of Numerical Discretization*, vol. 1. Wiley, Chichester. 515 pp.
- ²⁰⁹ Liggett, J.A., Woolhiser, D.A., 1967. Difference solutions of the shallow-water equations. *Journal of the Engineering Mechanics Division — ASCE* 93 (EM2), 39–71.
- ²¹⁰ Leskens J.C., M. Brugnach , A.Y. Hoekstra , W. Schuurmans 2014. Why are decisions in flood disaster management so poorly supported by information from flood models?. *Environmental Modelling & Software* 53 (2014) 53-61
- ²¹¹ Morss, R.E., Wilhelmi, O.V., Downton, M.W., Grunfest, E., 2005. Flood risk, uncertainty, and scientific information for decision making: lessons from an inter-disciplinary project. *Bull. Am. Meteorol. Soc.* 86 (11), 1593e1601.
- ²¹² Gray, B., 1989. *Collaborating: Finding Common Ground for Multiparty Problems*. Jossey-Bass, San Francisco
- ²¹³ Janis, I.L., Mann, L., 1977. *Decision Making: a Psychological Analysis of Conflict, Choice, and Commitment*. Free Press
- ²¹⁴ Kahneman, D., Tversky, A., 1979. Prospect theory: an analysis of decision under risk. *Econom. J. Econom. Soc.*, 263e291
- ²¹⁵ MacCrimmon, K.R., Taylor, J.N., 1976. Decision making and problem solving. In: Dunnette, M.D. (Ed.), *Handbook of Industrial and Organizational Psychology*. Rand McNally, Chicago

-
- ²¹⁶ Gouldby B, Sayers P, Mulet-Marti J, Hassan M, Benwell D. 2008. A methodology for regional-scale flood risk assessment. *Proceedings of the Institution of Civil Engineers - Water Management* 161: 169–182
- ²¹⁷ Webster, T., D. Stiff, The prediction and mapping of coastal flood risk associated with storm surge events and long-term sea level changes, *WIT Transactions on Information and Communication*, Vol 39, © 2008 WIT Press www.witpress.com, ISSN 1743-3517 (on-line) doi:10.2495/RISK080141
- ²¹⁸ Cunge JA. 1975. Two-dimensional modeling of flood plains. *Water Resources Publications*, Ch. 17: 705–762
- ²¹⁹ Moussa R, Bocquillon C. 2009. On the use of the diffusive wave for modelling extreme flood events with overbank flow in the floodplain. *Journal of Hydrology* 374: 116–135.
- ²²⁰ Castellarin A, Domeneghetti A, Brath A. 2011. Identifying robust large-scale flood risk mitigation strategies: A quasi-2D hydraulic model as a tool for the Po river. *Physics and Chemistry of the Earth* 36: 299–308.
- ²²¹ Aronica, G., Hankin, B.G., Beven, K.J., 1998. Uncertainty and equifinality in calibrating distributed roughness coefficients in a flood propagation model with limited data. *Advances in Water Resources* 22 (4), 349–365.
- ²²² Bradbrook K, Waller S, Morris D. 2005. National Floodplain Mapping: Datasets and Methods - 160,000 km in 12 month. *Natural Hazards* 36: 103–123.
- ²²³ Hunter NM, Horritt MS, Bates PD, Wilson MD, Werner MGF. 2005. An adaptive time step solution for raster-based storage cell modelling of floodplain inundation. *Advances in Water Resources* 28: 975–991.
- ²²⁴ Vorogushyn S, Merz B, Lindenschmidt K-E, Apel H. 2010. A new methodology for flood hazard assessment considering dike breaches. *Water Resources Research* 46: W08541.
- ²²⁵ Wilson M, Bates P, Alsdorf D, Forsberg B, Horritt M, Melack J, Frappart F, Famiglietti J. 2007. Modeling large-scale inundation of Amazonian seasonally flooded wetlands. *Geophysical Research Letters* 34: L15404
- ²²⁶ Trigg MA, Wilson MD, Bates PD, Horritt MS, Alsdorf DE, Forsberg BR, Vega MC. 2009. Amazon flood wave hydraulics. *Journal of Hydrology* 374: 92–105
- ²²⁷ Biancamaria S, Bates PD, Boone A, Mognard NM. 2009. Large-scale coupled hydrologic and hydraulic modelling of the Ob river in Siberia. *Journal of Hydrology* 379: 136–150.
- ²²⁸ P. Sayers, I. Meadowcroft, RASP – A hierarchy of risk-based methods and their application, Defra Flood and Coastal Management Conference, York, UK 2005
- ²²⁹ PENDER, G., 2006. Briefing: Introducing Flood Risk Management Research Consortium. *Proceedings of the Institution of Civil Engineers, Water Management*, 159 (WM1), 3-8.
- ²³⁰ Gouldby B, Sayers P, Mulet-Marti J, Hassan M, Benwell D. 2008. A methodology for regional-scale flood risk assessment. *Proceedings of the Institution of Civil Engineers - Water Management* 161: 169–182.
- ²³¹ BEVEN, K.J., YOUNG, P, LEEDAL, D. AND ROMANOWICZ, R., 2008. Computationally efficient flood water level prediction (with uncertainty). In *Flood Risk Management: Research and Practice* – Samuels et al. (editors). Taylor and Francis Group, London.
- ²³² Poulter, B. and Halpin, P. N.(2008) 'Raster modelling of coastal flooding from sea-level rise', *International Journal of Geographical Information Science*, 22: 2, 167 — 182, First published on: 12 July 2007 (iFirst) To link to this Article: DOI: 10.1080/13658810701371858 URL: <http://dx.doi.org/10.1080/13658810701371858>
- ²³³ I. Brown, Modelling future landscape change on coastal floodplains using a rule-based GIS *Environmental Modelling & Software* 21 (2006) 1479 -1490
- ²³⁴ Wicks J. M., Syme B., Hassan M. A. A. M., Lin B. And Tarrant O, 2004. 2d modelling of floodplains—is it worth the effort? *Proceedings of the 39th Defra Flood and Coastal Management Conference, York*, pp. 10.1.1–10.1.11.

-
- ²³⁵ PENDER, G. (2006) - Briefing: Introducing Flood Risk Management Research Consortium, *Proceedings of the Institution of Civil Engineers, Water Management*, 159 (WMI) : 3-8.
- ²³⁶ PENDER, G. (2006) - Briefing: Introducing Flood Risk Management Research Consortium, *Proceedings of the Institution of Civil Engineers, Water Management*, 159 (WMI) : 3-8.
- 237C.B.Laney.ComputationalGasDynamics.CambridgeUniversityPress,Cambridge,1998
- 238A.J.Chorinand, J.E.Marsden. A Mathematical Introduction to Fluid Mechanics. Springer- Verlag, 1979
- 239 J.A. Liggett. Fluid Mechanics. McGraw Hill, Inc., 1994
- ²⁴⁰ ALCRUDO, F., 2004 A state of the art review on mathematical modelling of flood propagation. IMPACT project.
- ²⁴¹ WRIGHT, N.G., 2005. Introduction to numerical methods for fluid flow. In Bates, P.D., Lane, S.N., Ferguson, R.I. (editors), *Computational Fluid Dynamics: Applications in Environmental Hydraulics*. Wiley, Chichester.
- ²⁴² OTTOSEN, N.S. AND PETERSSON, H., 1992. Introduction to the Finite Element Method. Prentice Hall.
- ²⁴³ ALCRUDO, F., 2004 A state of the art review on mathematical modelling of flood propagation. IMPACT project.
- ²⁴⁴ HERVOUET, J.M., 2007. Hydrodynamics of Free Surface Flows. First Edition, John Wiley and Sons, Press 2007, ISBN-13: 978-0-470-03558-0.
- ²⁴⁵ SAUVAGET, P., DAVID, E., DEMMERLE, D. AND LEFORT, P., 2000. Optimum design of a large flood relief culvert under the A89 motorway in the Dordogne-Isle confluence floodplain. *Hydrological Processes*, 14 (13), 2311-2329.
- ²⁴⁶ CALEFFI, V., VALIANI, A., AND ZANNI, A., 2003. Finite volume method for simulating extreme flood events in natural channels. *Journal Hydraulic Research*, 41(2), 167-177.
- ²⁴⁷ Danish Hydraulic Institute (DHI), 2007b. *MIKE 21 & MIKE 3 Flow model FM*. Copenhagen, Denmark.
- ²⁴⁸ VILLANUEVA, I. AND WRIGHT, N.G., 2005. *Report on validation of TRENT solver, part I: laboratory tests*. Nottingham University.
- ²⁴⁹ ALCRUDO, F. AND MULET, J., *Conclusions and Recommendations from the IMPACT Project WP3: Flood Propagation*. IMPACT project. http://www.impact-project.net/wp3_technical.htm
- ²⁵⁰ KRAMER, S.C. AND STELLING, G.S., 2008. A conservative unstructured scheme for rapidly varied flows. *International Journal for Numerical Methods in Fluids*, 58 (2), 183- 212
- ²⁵¹ Begnudelli, L., Sanders, B.F., 2006. Unstructured grid finite volume algorithm for shallow after transport with wetting and drying. *Journal of Hydraulic Engineering* 132 (4), 371–384.
- ²⁵² Néelz S. and G Pender Environmental Agency, DEFRA. Science Report – Desktop review of 2D hydraulic modelling packages 2009
- ²⁵³ Hervouet J-M. Hydrodynamics of free surface flows: modelling with the finite element method. Wiley; 2007
- ²⁵⁴ The TELEMAC system. <<http://www.telemacsystem.com>>
- ²⁵⁵ Begnudelli, L., Sanders, B.F., Bradford, S.F., 2008. Adaptive Godunov-based model for flood simulation. *J. Hydraul. Eng.* 134 (6), 714–725.
- ²⁵⁶ Gallegos, H.A., Schubert, J.E., Sanders, B.F., 2009. Two-dimensional, high-resolution modeling of urban dam-break flooding: A case study of Baldwin Hills, California. *Advances in Water Resources* 32, 1323–1335.
- ²⁵⁷ Begnudelli, L., Sanders, B.F., 2006. Unstructured grid finite volume algorithm for shallow after transport with wetting and drying. *Journal of Hydraulic Engineering* 132 (4), 371–384.
- ²⁵⁸ Zoppou C and Roberts S., (1999), Catastrophic Collapse of Water Supply Reservoirs in Urban Areas, *ASCE J. Hydraulic Engineering* 125(7), 686-695
- ²⁵⁹ Kurganov, A.S. Noelle and G. Petrova (2001) Semidiscrete central-upwind schemes for hyperbolic conservation laws and Hamilton-Jacob equations, *SIAM Journal of Scientific Computing*, 23(3), 707- 740

-
- ²⁶⁰ Toro E., (1992), Riemann Problems and the WAF Method for Solving the Two-dimensional Shallow Water Equations, *Philosophical Transactions of the Royal Society, Series A*, 338: 43-68
- ²⁶¹ Ponce, V.M., Simons, D.B., 1977. Shallow wave propagation in open channel flow. *Journal of the Hydraulics Division, Proceedings of American Society of Civil Engineers* 103 (HY12), 1461–1476.
- ²⁶² Vieira, J.H.D., 1983. Conditions governing the use of approximations for the Saint-Venant equations for shallow surface-water flow. *Journal of Hydrology* 60 (1–4), 43–58.
- ²⁶³ Hunter N.M., P.D. Bates, M.S. Horrit, M.D. Wilson. Simple spatially-distributed models for predicting flood inundation: A review. *Geomorphology* 90 (2007) 208–225
- ²⁶⁴ Estrela, T., Quintas, L., 1994. Use of a GIS in the modelling of flows on floodplains. In: White, W.R., Watts, J. (Eds.), 2nd International Conference on River Flood Hydraulics. Wiley, Chichester, pp. 177–190.
- ²⁶⁵ Bechteler, W., Hartmann, S., Otto, A.J., 1994. Coupling of 2D and 1D models and integration into Geographic Information Systems (GIS). In: White, W.R., Watts, J. (Eds.), 2nd International Conference on River Flood Hydraulics. Wiley, Chichester, pp. 155–166.
- 266 Bates, P.D., De Roo, A.P.J., 2000. A simple raster-based model for flood inundation simulation. *Journal of Hydrology* 236 (1–2), 54–77.
- 267 Horritt, M.S., Bates, P.D., 2001a. Predicting floodplain inundation: raster-based modelling versus the finite-element approach. *Hydrological Processes* 15 (5), 825–842.
- 268 Horritt, M.S., Bates, P.D., 2001b. Effects of spatial resolution on a raster based model of flood flow. *Journal of Hydrology* 253 (1–4), 239–249
- 269 Bradbrook, K.F., Lane, S.N., Waller, S.G., Bates, P.D., 2004. Two dimensional diffusion wave modelling of flood inundation using a simplified channel representation. *International Journal of River Basin Management* 2 (3), 211–223.
- ²⁷⁰ Van Deursen, W.P.A., Wesseling, C.G., 1996. PCRaster version 2 manual. Department of Physical Geography, Utrecht University, The Netherlands
- ²⁷¹ Burrough, P.A., McDonnell, R.A., 1998. *Principles of Geographical Information Systems*. Clarendon Press, Oxford
- ²⁷² Bates PD, Horritt MS, Fewtrell TJ. 2010. A simple inertial formulation of the shallow water equations for efficient two-dimensional flood inundation modelling. *Journal of Hydrology* 387: 33–45
- ²⁷³ Dottori F, Todini E. 2011. Developments of a flood inundation model based on the cellular automata approach: Testing different methods to improve model performance. *Physics and Chemistry of the Earth* 36: 266–280.
- ²⁷⁴ Neal J, Schumann G, Fewtrell T, Budimir M, Bates PD, Mason D. 2011b. Evaluating a new LISFLOOD-FP formulation with data from the summer 2007 floods in Tewkesbury, UK. *Journal of Flood Risk Management* 4: 88–95
- ²⁷⁵ Horritt, M.S., Bates, P.D., 2001a. Predicting floodplain inundation: raster-based modelling versus the finite-element approach. *Hydrological Processes* 15 (5), 825–842.
- ²⁷⁶ Horritt MS, Bates PD. 2001b. Predicting floodplain inundation: raster-based modelling versus the finite-element approach. *Hydrological Processes* 15: 825–842.
- ²⁷⁷ Horritt MS, Bates PD. 2002. Evaluation of 1D and 2D numerical models for predicting river flood inundation. *Journal of Hydrology* 268: 87–99.

-
- ²⁷⁸ Bates, P.D., Dawson, R.J., Hall, J.W., Horritt, M.S., Nicholls, R.J., Wicks, J., Hassan, M.A.A.M. Simplified two-dimensional numerical modelling of coastal flooding and example applications. *Coastal Engineering* 52 (2005) 793–810
- ²⁷⁹ YU, D. AND LANE, S.N., 2005. Urban fluvial flood modelling using a two dimensional diffusion-wave treatment, part 2: development of a sub-grid-scale treatment. *Journal of Hydrological Processes*, 20 (7), 1567-1583.
- ²⁸⁰ Dottori F, Todini E. 2011. Developments of a flood inundation model based on the cellular automata approach: Testing different methods to improve model performance. *Physics and Chemistry of the Earth* 36: 266–280.
- ²⁸¹ Bates PD, De Roo APJ. 2000. A simple raster-based model for flood inundation simulation. *Journal of Hydrology* 236: 54–77.
- ²⁸² Argent, R.M., 2004. An overview of model integration for environmental applications e components, frameworks and semantics. *Environmental Modelling and Software* 19, 219e234.
- 283 Demirkesen, A. C., Evrendilek, F., Berberoglu, S., and Kilic, S.: Coastal flood risk analysis using Landsat-7 ETM+ imagery and SRTM DEM: a case study of Izmir, Turkey, *Environ. Monit. Assess.*, 131, 293–300, 2008
- 284 Wang, Y., Colby, J. D., and Mulcahy, K. A.: An efficient method for mapping flood extent in a costal floodplain using Landsat TM and DEM data, *Int. J. Remote Sens.*, 23, 3681–3696, 2002
- 285 Poulter, B. and Halpin, P. N.(2008) 'Raster modelling of coastal flooding from sea-level rise', *International Journal of Geographical Information Science*, 22: 2, 167 — 182, First published on: 12 July 2007 (iFirst) To link to this Article: DOI: 10.1080/13658810701371858 URL: <http://dx.doi.org/10.1080/13658810701371858>
- 286 <http://www.hydrol-earth-syst-sci-discuss.net/12/2011/2015/hessd-12-2011-2015.pdf>
- 287 Moorhead, K. K. and Brinson, M. M.: Response of wetlands to rising sea level in the lower coastal plain of North Carolina, *Ecol. Appl.*, 5, 261–271, 1995.
- 288 Titus, J. G. and Richman, C.: Maps of lands vulnerable to sea level rise: modeled elevations along the US Atlantic and Gulf coasts, *Clim. Res.*, 18, 205–228, 2001.
- 289 I. Brown, Modelling future landscape change on coastal floodplains using a rule-based GIS *Environmental Modelling & Software* 21 (2006) 1479 -1490
- 290 MOORHEAD, K.K. and BRINSON, M.M., 1995, Response of wetlands to rising sea level in the lower coastal plain of North Carolina. *Ecological Applications*, 5, pp. 261–271.
- 291 TITUS, J.G. and RICHMAN, C., 2001, Maps of lands vulnerable to sea level rise: modeled elevations along the US Atlantic and Gulf coasts. *Climate Research*, 18, pp. 205–228.
- ²⁹² Priestnall, G., Jaafar, J., Duncan, A., 2000. Extracting urban features from LiDAR-derived digital surface models computers. *Environment and Urban Systems* 24, 65e78.
- ²⁹³ Tomlin, C.D., 1990. *Geographic Information Systems and Cartographic Modeling*. Prentice Hall, Englewood Cliffs, NJ.
- ²⁹⁴ Poulter, B. and Halpin, P. N.(2008) 'Raster modelling of coastal flooding from sea-level rise', *International Journal of Geographical Information Science*, 22: 2, 167 — 182, First published on: 12 July 2007 (iFirst) To link to this Article: DOI: 10.1080/13658810701371858 URL: <http://dx.doi.org/10.1080/13658810701371858>
- ²⁹⁵ Poulter, B. and Halpin, P. N.(2008) 'Raster modelling of coastal flooding from sea-level rise', *International Journal of Geographical Information Science*, 22: 2, 167 — 182, First published on: 12 July 2007 (iFirst) To link to this Article: DOI: 10.1080/13658810701371858 URL: <http://dx.doi.org/10.1080/13658810701371858>

-
- ²⁹⁶ Gouldby, B., Sayers, P., Mulet-Marti, J., Hassan, M. and Benwell, D. (2008). "A methodology for regional-scale flood risk assessment." *Water Management* 161(3): 169-182.
- ²⁹⁷ Lhomme, J., Sayers, P., Gouldby, B., Samuels, P., Wills, M. and Mulet-Marti, J. (2008). *Recent development and application of a rapid flood spreading method*. Flood Risk 2008, Oxford.
- 298 Liu Y, Neélz S. and Pender G. (2009). "Improving the Performance of Fast Inundation Models Using v-Support Vector Regression and Particle Swarm Optimisation", The 33rd IAHR 2009 Congress, 2009, pp. 1436-1443
- 299 Wicks JM, Lardet P, Shaad K (2011) 'Developing a National Surface Water Flood Map for Scotland', CIWEM WaPUG Spring Conference, Birmingham, 18 May 2011.
- ³⁰⁰ Gouldby, B., Sayers, P., Mulet-Marti, J., Hassan, M. and Benwell, D. (2008). "A methodology for regional-scale flood risk assessment." *Water Management* 161(3): 169-182.
- ³⁰¹ Lhomme, J., Sayers, P., Gouldby, B., Samuels, P., Wills, M. and Mulet-Marti, J. (2008). *Recent development and application of a rapid flood spreading method*. Flood Risk 2008, Oxford.
- ³⁰² Gouldby, B., Sayers, P., Mulet-Marti, J., Hassan, M. and Benwell, D. (2008). "A methodology for regional-scale flood risk assessment." *Water Management* 161(3): 169-182.
- ³⁰³ HR WALLINGFORD. Rapid Flood Spreading Methodology (RFSM). Environment Agency, 2006, Thames Estuary 2100 Report, DT4.
- ³⁰⁴ Lhomme J., Recent development and application of a rapid flood spreading method, *Flood Risk Management: Research and Practice – Samuels et al. (eds), 2009 Taylor & Francis Group, London, ISBN 978-0-415-48507-4*
- ³⁰⁵ Gouldby, B., Sayers, P., Mulet-Marti, J., Hassan, M. and Benwell, D. (2008). "A methodology for regional-scale flood risk assessment." *Water Management* 161(3): 169-182.
- ³⁰⁶ HR WALLINGFORD. Rapid Flood Spreading Methodology (RFSM). Environment Agency, 2006, Thames Estuary 2100 Report, DT4.
- 307 Christopher C. Sampson, Timothy J. Fewtrell, Alastair Duncan, Kashif Shaad, Matthew S. Horritt, Paul D. Bates . Use of terrestrial laser scanning data to drive decimetric resolution urban inundation models *Advances in Water Resources* 41 (2012) 1–17, doi:10.1016/j.advwatres.2012.02.010
- 308 Bates PD, Horritt MS, Fewtrell TJ. A simple inertial formulation of the shallow water equations for efficient two dimensional flood inundation modelling. *Journal of Hydrology*. 2010;387:33–45.
- 309 Bates PD, De Roo APJ. A simple raster-based model for flood inundation simulation. *Journal of Hydrology*. 2000;236:54–77.
- 310 Hunter NM, Horritt MS, Bates PD, Wilson MD, Werner MGF. An adaptive time step solution for raster-based storage cell modelling of floodplain inundation. *Advances in Water Resources*. 2005;28:975–91.
- 311 Gouldby B, Sayers P, Mulet-Marti J, MAAM Hassan, Benwell D. A methodology for regional-scale flood risk assessment. *Proceedings of the Institution of Civil Engineers - Water Management*. 2008;161:169–82.
- 312 Shaad K. Surface water flooding: analysis and model development. Cottbus, Germany: Brandenburg University of Technology; 2009.
- 313 Zerger, A. (2002). Examining GIS decision utility for natural hazard risk modelling. *Environmental Modelling & Software*, 17(3), 287-294.
- 314 Zerger, A., Smith, D. I., Hunter, G. J., & Jones, S. D. (2002). Riding the storm: a comparison of uncertainty modelling techniques for storm surge risk management. *Applied Geography*, 22(3), 307-330
- 315 Chen, J., Hill, A. A., & Urbano, L. D. (2009). A GIS-based model for urban flood inundation. *Journal of Hydrology*, 373(1-2), 184-192

-
- 316 Wang, C., Wan, T., & Palmer, I. (2010). Urban flood risk analysis for determining optimal flood protection levels based on digital terrain model and flood spreading model. *The Visual Computer*, 1-13.
- ³¹⁷ Kass, M., Witkin, A., and Terzopoulos, D., —Snakes: active contour models , *Int'l J. Comp. Vis.*, vol. 1, pp. 321-331, 1987
- ³¹⁸ T.J. Fewtrell et al. Benchmarking urban flood models of varying complexity and scale using high resolution terrestrial LiDAR data / *Physics and Chemistry of the Earth* 36 (2011) 281–291
- ³¹⁹ Webster T. and D. Stiff The prediction and mapping of coastal flood risk associated with storm surge events and long-term sea level changes. *WIT Transactions on Information and Communication*, Vol 39, © 2008 WIT Press. doi:10.2495/RISK080141
- 320 M. G. F. Werner 2001, Impact of Grid Siz in GIS based Flood Extent Mapping Using a 1D Flow Model, *Phys. Chem. Earth*, Vol 26, N-7-8, pp. 517-522, 2001
- ³²¹ M. A. Marfai 2004 - Tidal flood hazard assessment : modeling in raster gis, case in western part of Semarang coastal area, *Indonesian Journal of Geography* Vol. 36 N 1 June 2004 pp. 25-38
- ³²² Marfai MA, King L (2008b) Tidal inundation mapping under enhanced land subsidence in Semarang, Central Java Indonesia. *Nat Hazards* 44:93–109. doi:10.1007/s11069-007-9144-z,2008
- ³²³ Hall J W, Meadowcroft I C, Sayers P B and Bramley M E (2003) Integrated flood risk management in England and Wales. *Proceedings of the American Society of Civil Engineers, Natural Hazards Review*.
- ³²⁴ Tomlin, C.D., 1990. *Geographic Information Systems and Cartographic Modeling*. Prentice Hall, Englewood Cliffs, NJ.
- ³²⁵ Meyer, F., Beucher, S., 1990. Morphological segmentation. *J. Visual Commun. Image Represent.* 1 (1), 21–46, September.
- ³²⁶ Soille, P., Ansoult, M., 1990. Automated basin delineation from digital elevation models using mathematical morphology. *Signal Process.* 20, 171–182.
- 327 Poulter, B. and Halpin, P. N.(2008) 'Raster modelling of coastal flooding from sea-level rise', *International Journal of Geographical Information Science*, 22: 2, 167 — 182, First published on: 12 July 2007 (iFirst) 10.1080/13658810701371858
- ³²⁸ Ali, A., Zhang, H., Lemckert, C.J., 2009. Numerical of hydrodynamics of a very shallow estuarine systems – Coombabah Lake, Gold Coast, Australia. *Journal of Coastal Research, Special Issue* 56, 922–926.
- ³²⁹ Weaver, R.J., Slinn, D.N., 2010. Influence of bathymetric fluctuations on coastal storm surge. *Coastal Engineering* 57, 62–70
- ³³⁰ Cea, L., French, J.R., 2012. Bathymetric error estimation for the calibration and validation of estuarine hydrodynamic models. *Estuarine, Coastal and Shelf Science* 100, 124–132
- ³³¹ Yamano, S., 2007. The use of multi-temporal satellite images to estimate intertidal reef-flat topography. *Journal of Spatial Science* 52, 73–79.
- ³³² DiGruttolo, N., Mohamed, A., 2011. Emerging unmanned aerial remote sensing system for intertidal zone modelling: a low-cost method of collecting remote sensing data for modelling short-term effects of sea level rise, Part II: Closerange airborne remote sensing. *Surveying and Land Information Science* 70 (3), 119–129
- ³³³ Coveney, S., Stewart Fotheringham, A., 2011. The impact of DEM data source on prediction of flooding and erosion risk due to sea-level rise. *International Journal of Geographical Information Science* 25 (7), 1191–1211.
- ³³⁴ Pe'eri, S., Long, B., 2011. LIDAR technology applied in coastal studies and management. *Journal of Coastal Research, Special Issue* 62, 1–5.

-
- ³³⁵ Long, B., 2005. Étude hydrodynamique, sédimentologique et biologique des sites de Maria, Saint-Siméon, Bonaventure, Newport et Cap-d'Espoir dans la baie des Chaleurs, Québec, Canada. Rapport INRS-ETE pour le Ministère des Transports du Québec, 179p.
- ³³⁶ Merwade, V., Cook, A., Coonrod, J., 2008. GIS techniques for creating river terrain models for hydrodynamic modeling and flood inundation mapping. *Environmental Modelling and Software* 23, 1300–1311
- ³³⁷ Merwade, V., Cook, A., & Coonrod, J. (2008). GIS techniques for creating river terrain models for hydrodynamic modeling and flood inundation mapping. *Environmental Modelling & Software*, 23(10-11), 1300-1311.
- ³³⁸ Hardy, R.J., Bates, P.D., Anderson, M.G., 1999. The importance of spatial resolution in hydraulic models for floodplain environments. *Journal of Hydrology* 216 (1–2), 124–136.
- ³³⁹ Horritt, M.S., Bates, P.D., Mattinson, M.J., 2006. Effects of mesh resolution and topographic representation in 2D finite volume models of shallow water fluvial flow. *Journal of Hydrology* 329 (1–2), 306–314
- ³⁴⁰ Buttner, O., 2007. The influence of topographic and mesh resolution in 2D hydro- dynamic modelling for floodplains and urban areas. *European Geosciences Union. 2007 Geophysical Research Abstracts*, 9(08232).
- ³⁴¹ Raber, G.T., Jensen, J.R., Hodgson, M.E., Tullis, J.A., Davis, B.A., Berglund, J., 2007. Impact of LIDAR nominal post-spacing on DEM accuracy and flood zone delineation. *Photogrammetric Engineering and Remote Sensing* 73 (7), 793–804.
- ³⁴² Merwade, V., Cook, A., & Coonrod, J. (2008). GIS techniques for creating river terrain models for hydrodynamic modeling and flood inundation mapping. *Environmental Modelling & Software*, 23(10-11), 1300-1311.
- ³⁴³ Soille, P., Ansoult, M., 1990. Automated basin delineation from digital elevation models using mathematical morphology. *Signal Process.* 20, 171–182.
- ³⁴⁴ Soille, P., 2003. *Morphological image analysis*. 2nd edition, Springer-Verlag, Berlin Heidelberg, New York. ISBN 3- 540-42988-3. URL <http://ams.jrc.it/soille/book2nd>.
- 345 Digabel, H., and Lantúejoul, C. Iterative algorithms. In *Actes du Second Symposium Européen d'Analyse Quantitative des Microstructures en Sciences des Matériaux, Biologie et Médecine*, Caen, 4-7 October 1977 (1978), J.-L. Chermant, Ed., Riederer Verlag, Stuttgart, pp. 85–99.
- 346 Lantúejoul, C. La squelettisation et son application aux mesures topologiques des mosaïques polycristallines. PhD thesis, Ecole des Mines, Paris, 1978.
- 347 Beucher, S., and Lantúejoul, C. Use of watersheds in contour detection. In *Proc. International Workshop on Image Processing, Real-Time Edge and Motion Detection/Estimation*, Rennes, september (1979)
- 348 Beucher, S., and Meyer, F. The morphological approach to segmentation: the watershed transformation. In *Mathematical Morphology in Image Processing*, E. R. Dougherty, Ed. Marcel Dekker, New York, 1993, ch. 12, pp. 433–481
- 349 Vincent, L., and Soille, P. Watersheds in digital spaces: an efficient algorithm based on immersion simulations. *IEEE Trans. Patt. Anal. Mach. Intell.* 13, 6 (1991), 583–598.
- 350 Serra, J. *Image Analysis and Mathematical Morphology*. Academic Press, New York, 1982.
- ³⁵¹ Haralick, R. M., and Shapiro, L. G. Survey : image segmentation techniques. *Comp. Vis. Graph. Im. Proc.* 29 (1985), 100–132.

-
- ³⁵² S. Beucher, F. Meyer, The morphological approach to segmentation: The watershed transformation, in: E.R. Dougherty (Ed.), *Mathematical Morphology in Image Processing*, Marcel Dekker Inc, New York, 1993, pp. 433}481.
- ³⁵³ S. Beucher, F. Meyer, The morphological approach to segmentation: The watershed transformation, in: E.R. Dougherty (Ed.), *Mathematical Morphology in Image Processing*, Marcel Dekker Inc, New York, 1993, pp. 433}481.
- ³⁵⁴ F. Meyer, Topographic distance and watershed lines, *Signal Processing* 38 (1) (1994) 113}125.
- ³⁵⁵ Beucher, N., Beucher, S., April 2011. Hierarchical queues: general description and implementation in mamba image library. ([http://cmm.ensmp.fr/\\$beucher/publi/HQ_algo_desc.pdf](http://cmm.ensmp.fr/$beucher/publi/HQ_algo_desc.pdf))
- ³⁵⁶ S. Beucher, F. Meyer, The morphological approach to segmentation: The watershed transformation, in: E.R. Dougherty (Ed.), *Mathematical Morphology in Image Processing*, Marcel Dekker Inc, New York, 1993, pp. 433}481.
- ³⁵⁷ KWAN, S. H. (2011) GIS modelling of flood on the South Devon Coast, MSc. Thesis Plymouth, UK; Plymouth University
- ³⁵⁸ ESRI (1996), ArcView, Spatial Analyst, Environmental Systems Research Institute, Inc. Redlands, California, USA.
- ³⁵⁹ Kreibich, H., Piroth, K., Seifert, I., Maiwald, H., Kunert, U., Schwarz, J., Merz, B., and Thielen, A. H.: Is flow velocity a significant parameter in flood damage modelling?, *Nat. Hazards Earth Syst. Sci.*, 9, 1679–1692, doi:10.5194/nhess-9-1679-2009, 2009
- ³⁶⁰ Kreibich, H., Piroth, K., Seifert, I., Maiwald, H., Kunert, U., Schwarz, J., Merz, B., and Thielen, A. H.: Is flow velocity a significant parameter in flood damage modelling?, *Nat. Hazards Earth Syst. Sci.*, 9, 1679–1692, doi:10.5194/nhess-9-1679-2009, 2009
- ³⁶¹ Mondloch R.. Characterization of agricultural floodplain scour using one-dimensional hydraulic simulation. Thesis, University of Iowa 2014. <http://ir.uiowa.edu/etd/1487>
- ³⁶² Förster, B. Kuhlmann, K.-E. Lindenschmidt, and A. Bronstert. Assessing flood risk for a rural detention area. *Nat. Hazards Earth Syst. Sci.*, 8, 311–322, 2008. www.nat-hazards-earth-syst-sci.net/8/311/2008
- ³⁶³ Förster, B. Kuhlmann, K.-E. Lindenschmidt, and A. Bronstert. Assessing flood risk for a rural detention area. *Nat. Hazards Earth Syst. Sci.*, 8, 311–322, 2008. www.nat-hazards-earth-syst-sci.net/8/311/2008
- ³⁶⁴ Holtan, H.N. and M.H. Kirkpatrick. 1950. Rainfall, infiltration, and hydraulics of flow in run-off computation. *Trans. Am. Geophys. Union* 31:771-779
- ³⁶⁵ Parker, D.J., Green, C.H., Thompson, P.M., 1987. *Urban Flood Protection Benefits—A Project Appraisal Guide*, Gower Technical Press, UK.
- ³⁶⁶ Smith, K., and R. C. Ward, 1998: *Floods: Physical Processes and Human Impacts*. Wiley.
- ³⁶⁷ Jonkman S.N. Loss of life estimation in flood risk assessment – theory and applications. PhD Thesis, Delft University, 2007
- ³⁶⁸ S. N. Jonkman, M. Bockarjova, M. Kok, P. Bernardini, *Integrated Hydrodynamic and Economic Modelling of Flood Damage in The Netherlands*, *Ecol. Econ.* 2008, 66, 77–90
- ³⁶⁹ B. Jongman et al.: Comparative flood damage model assessment *Nat. Hazards Earth Syst. Sci.*, 12, 3733–3752, 2012, www.nat-hazards-earth-syst-sci.net/12/3733/2012/. doi:10.5194/nhess-12-3733-2012
- ³⁷⁰ Merz, B., Kreibich, H., Thielen, A., and Schmidtke, R.: Estimation uncertainty of direct monetary flood damage to buildings, *Nat. Hazards Earth Syst. Sci.*, 4, 153–163, doi:10.5194/nhess-4-153- 2004, 2004

-
- ³⁷¹ MURL (Ministerium für Umwelt, Raumordnung und Landwirtschaft des Landes Nordrhein-Westfalen): Potentielle Hochwasserschäden am Rhein in Nordrhein-Westfalen Düsseldorf, 2000 (in German)
- ³⁷² Emschergenossenschaft & Hydrotec: Hochwasser-Aktionsplan Emscher, Kapitel 1: Methodik der Schadensermittlung, Emschergenossenschaft, Report, 2004 (in German)
- ³⁷³ Penning-Rowsell, E., Johnson, C., Tunstall, S., Tapsell, S., Morris, J., Chatterton, J., and Green, C.: The Benefits of Flood and Coastal Risk Management: A Manual of Assessment Techniques, Middlesex Univ. Press, UK, 2005
- ³⁷⁴ Middelman-Fernandes M.H., Flood damage estimation beyond stage^damage functions: an Australian example *JFloodRiskManagement*3(2010)88–96
- ³⁷⁵ Greenaway M.A. & Smith D.I. ANUFLOOD field guide. Canberra: Centre of Resource and Environmental Studies, Australian National University, 1983
- ³⁷⁶ Greenaway M.A. & Smith D.I. ANUFLOOD programmer's guide and user's manual. Canberra: Centre for Resource and Environmental Studies, Australian National University, 1993.
- ³⁷⁷ Penning-Rowsell E., Johnson C., Tunstall S., Tapsell S., Morris J., Chatterton J., Coker A. & Green C. The benefits of flood and coastal defence: techniques and data for 2003. London: Enfield: Flood Hazard Research Centre, Middlesex University, 2003.
- ³⁷⁸ Neubert M., Naumann T. & Deilmann C. Synthetic water level building damage relationships for GIS-supported flood vulnerability modelling of residential properties. In: P. Samuels, S. Huntington, W. Allsop & J. Harrop, eds. Flood risk management: research and practice. London: Taylor and Francis Group, 2009, 1717–1724.
- ³⁷⁹ Mertz B., H. Kreibich, R. Schwarze, and A. Thieken` Review article "Assessment of economic flood damage". *Nat. Hazards Earth Syst. Sci.*, 10, 1697–1724, 2010 www.nat-hazards-earth-syst-sci.net/10/1697/2010/ doi:10.5194/nhess-10-1697-2010
- ³⁸⁰ Messner, F., PenningRowsell, E. C., Green, C., Meyer, V., Tunstall, S. M., and van der Veen, A.: Evaluating flood damages: guidance and recommendations on principles and methods, FLOODsite, Wallingford, UK, T09-06-01, 2007.
- ³⁸¹ Merz, B., Kreibich, H., Schwarze, R., and Thieken, A.: Review article "Assessment of economic flood damage", *Nat. Hazards Earth Syst. Sci.*, 10, 1697–1724, doi:10.5194/nhess-10-1697-2010, 2010.
- ³⁸² Green, C. H., Viavattene, C., and Thompson, P.: Guidance for assessing flood losses: CONHAZ report, Flood Hazard Research Centre – Middlesex University, Middlesex, WP6 Report, 2011.
- ³⁸³ Nicholas, J., Holt, G. D., and Proverbs, D.: Towards standardizing the assessment of flood damaged properties in the UK, *Struct. Survey*, 19, 163–172, 2001
- ³⁸⁴ Zhai, G., Fukuzono, T., and Ikeda, S.: Modeling flood damage: case of Tokai Flood 2000, *J. Am. Water Resour. Assoc.*, 41, 77–92, 2005.
- ³⁸⁵ Kreibich, H., Seifert, I., Merz, B., and Thieken, A. H.: Development of FLEMOcs – A new model for the estimation of flood losses in the commercial sector, *Hydrolog. Sci. J.*, submitted, 2010
- ³⁸⁶ Smith, D. I.: Flood Damage Estimation – A Review of Urban Stage- Damage Curves and Loss Functions, *Water SA*, 20, 231–238, 1994
- ³⁸⁷ Kelman, I. and Spence, R.: An overview of flood actions on buildings, *Eng. Geol.*, 73, 297–309, 2004
- ³⁸⁸ Meyer, V. and Messner, F.: National Flood Damage Evaluation Methods – a review of applied methods in England, the Netherlands, the Czech Republic and Germany, Department of Economics, Umweltforschungszentrum Leipzig-Halle, Leipzig, Germany, 21/2005, 2005.

-
- ³⁸⁹ Green, C. H., Viavattene, C., and Thompson, P.: Guidance for assessing flood losses: CONHAZ report, Flood Hazard Research Centre – Middlesex University, Middlesex, WP6 Report, 2011
- ³⁹⁰ B. Jongman et al.: Comparative flood damage model assessment *Nat. Hazards Earth Syst. Sci.*, 12, 3733–3752, 2012, www.nat-hazards-earth-syst-sci.net/12/3733/2012/. doi:10.5194/nhess-12-3733-2012
- ³⁹¹ Merz, B., Kreibich, H., Thieken, A., and Schmidtke, R.: Estimation uncertainty of direct monetary flood damage to buildings, *Nat. Hazards Earth Syst. Sci.*, 4, 153–163, doi:10.5194/nhess-4-153-2004, 2004
- ³⁹² Hall, J. W., Tarantola, S., Bates, P. D., and Horritt, M. S.: Distributed sensitivity analysis of flood inundation model calibration, *J. Hydraul. Eng.*, 131, 117–126, 2005
- ³⁹³ De Moel, H. and Aerts, J. C. J. H.: Effect of uncertainty in land use, damage models and inundation depth on flood risk estimates, *Nat. Hazards*, 58, 407–425, 2011
- ³⁹⁴ Coastal Engineering 87 (2014) 218–239
- ³⁹⁵ Adger, W., Hughes, T., Folke, C., Carpenter, S., Rockström, J., 2005. Social–ecological resilience to coastal disasters. *Science* 309, 1036–1039.
- ³⁹⁶ Cutter, S.L., Boruff, B.J., Shirley, W.L., 2003. Social vulnerability to environmental hazards. *Soc. Sci. Q.* 84 (2), 242–261.
- ³⁹⁷ Wisner, B., Blaikie, P., Cannon, T., Davis, I., 2004. *At Risk: Natural Hazards, People's Vulnerability and Disasters*. Routledge, London.
- ³⁹⁸ Jonkman S.N. Loss of life estimation in flood risk assessment – theory and applications. PhD Thesis, Delft University, 2007.
- ³⁹⁹ King, D. and MacGregor, C.: Using social indicators to measure community vulnerability to natural hazards, *Australian Journal of Emergency Management*, 15, 52–57, 2000.
- ⁴⁰⁰ Gruenewald, U.: *Überschwemmungen, in: Naturkatastrophen. Ursachen – Auswirkungen – Vorsorge*, edited by: Plate, E. J. and Merz, B., Schweizerbart'sche Verlagsbuchhandlung, Stuttgart, 159-189, 2001
- ⁴⁰¹ Tapsell, S. M., Penning-Rowsell, E., Tunstall, S. M., and Wilson, T. L.: Vulnerability to flooding: health and social dimensions, *Philos. T. R. Soc. Lond.*, 360, 1511–1525, 2002.
- ⁴⁰² Meyer, V., Scheuer, S., and Haase, D.: A multi-criteria approach for flood risk mapping exemplified at the Mulde river, Germany, *Nat. Hazards*, 48, 17–39, 2009
- ⁴⁰³ Cutter, S. L., Boruff, B. J., and Shirley, W. L.: Social Vulnerability to Environmental Hazards, *Soc. Sci. Quart.*, 84(2), 242–261, 2003
- ⁴⁰⁴ ISTAT, 2009. http://www3.istat.it/dati/catalogo/20100526_00/Avvio2009.pdf (in Italian).
- ⁴⁰⁵ Scheffer M, Bascompte J, Brock WA, Brovkin V, Carpenter S, Dakos V, Held H, van Nes EH, Rietkerk M and Sugihara G (2009) Early-warning signals for critical transitions. *Nature* 461: 53-59.
- ⁴⁰⁶ Rietkerk M, Dekker SC, de Ruiter PC, and van de Koppel J (2004). Self-organized patchiness and catastrophic shifts in ecosystems. *Science* 305: 1926-1929.
- ⁴⁰⁷ B. Gouldby, P. Samuels, in *Language of Risk – Project Definitions*, FLOODsite EU Integrated Project, Research Report T32-04-01, European Community, Brussels 2005.
- ⁴⁰⁸ Knight F H. 1921. *Risk, Uncertainty, and Profit*. Boston
- ⁴⁰⁹ Hansjurgens, B. 2004. Economic valuation through cost-benefit analysis - possibilities and limitations. *Toxicology* 205(3): 241-252

-
- ⁴¹⁰ Köck W. 2001. Rationale Risikosteuerung als Aufgabe des Rechts - Möglichkeiten und Grenzen des Einsatzes komparativer Risikoanalysen und Kosten-Nutzen-Analysen im Rahmen administrativer Risikobewertungen, in: E. Gawel. (Eds.), *Effizienz im Umweltrecht*, Baden- Baden 2001: Nomos, S. 273-304.
- ⁴¹¹ Meyer V, Scheuer S, Haase D. 2007. GIS-based Multicriteria Analysis as Decision Support in Flood Risk Management. FLOODsite-Report
- ⁴¹² Meyer V, Scheuer S, Haase D. 2007. GIS-based Multicriteria Analysis as Decision Support in Flood Risk Management. FLOODsite-Report
- ⁴¹³ Meyer V, Scheuer S, Haase D. 2007. GIS-based Multicriteria Analysis as Decision Support in Flood Risk Management. FLOODsite-Report
- ⁴¹⁴ DVWK (Deutscher Verband für Wasserwirtschaft und Kulturbau) (1985) *Ökonomische Methoden von Hochwasserschutzwirkungen. Arbeitsmaterialien zum methodischen Vorgehen. DVWK-Mitteilungen*
- ⁴¹⁵ Meyer V, Scheuer S, Haase D. 2007. GIS-based Multicriteria Analysis as Decision Support in Flood Risk Management. FLOODsite-Report
- ⁴¹⁶ Vanneville W., De Maeyer Ph., Maeghe K., Mostaert F. (2003) Model the Effects of a Flood in the Dender Catchment, Based on a Risk Methodology. *Society of Cartography Bulletin*, 37(2), 59–64
- ⁴¹⁷ Merz, B., Kreibich, H., Schwarze, R., and Thielen, A.: Review article "Assessment of economic flood damage", *Nat. Hazards Earth Syst. Sci.*, 10, 1697–1724, doi:10.5194/nhess-10-1697-2010, 2010.
- ⁴¹⁸ Beard, L. R.: Estimating flood frequency and average annual damage, *Journal of Water Resources Planning and Management*, 123, 84-88, 10.1061/(ASCE)0733-9496(1997)123:2(84), 1997.
- ⁴¹⁹ CIEWR-HEC: Ead - expected annual flood damage computation: User's manual, Computer Program Document CPD-30, 1989.
- ⁴²⁰ Messner, F., Penning-Rowsell, E., Green, C., Meyer, V., Tunstall, S., and van der Veen, A.: Evaluating flood damages: Guidance and recommendations on principles and methods, FLOODsite Consortium, Wallingford, 179, 2007.
- ⁴²¹ Geneletti, D., 2005. Multicriteria analysis to compare the impact of alternative road corridors. A case study in northern Italy. *Impact Assessment and Project Appraisal* 22 (4), 135–146.
- ⁴²² Geneletti, D., 2004. A GIS-based decision support system to identify nature conservation priorities in an alpine valley. *Land Use Policy* 21, 149–160
- ⁴²³ Malczewski, J., 1999. *GIS and multicriteria decision analysis*. Wiley, New York.
- ⁴²⁴ Meyer V, Scheuer S, Haase D. 2007. GIS-based Multicriteria Analysis as Decision Support in Flood Risk Management. FLOODsite-Report
- ⁴²⁵ Meyer V, Scheuer S, Haase D. 2008. A multicriteria approach for flood risk mapping exemplified at the Mulde river. Germany. *Natural Hazards*
- ⁴²⁶ Meyer V, and Haase D. 2008. A multicriteria flood risk assessment and mapping approach. *Flood Risk Management: Research and Practice – Samuels et al. (eds). aaylor & Francis Group, London, ISBN 978-0-415-48507-4*
- ⁴²⁷ Munda, G. (1995). *Multicriteria Evaluation in a Fuzzy Environment - Theory and Applications in Ecological Economics*. Heidelberg, Physica Verlag.
- ⁴²⁸ Rauschmayer, F. and Wittmer, H. (2006). "Evaluating deliberative and analytical methods for the resolution of environmental conflicts." *Land Use Policy* 23(1): 108-122.
- ⁴²⁹ Malczewski, J. (1999). *GIS and multicriteria decision analysis*. New York.

-
- ⁴³⁰ Meyer V, Scheuer S, Haase D. 2007. GIS-based Multicriteria Analysis as Decision Support in Flood Risk Management. FLOODsite-Report
- ⁴³¹ Meyer V, Scheuer S, Haase D. 2007. GIS-based Multicriteria Analysis as Decision Support in Flood Risk Management. FLOODsite-Report
- ⁴³² Malczewski, J., 1999. GIS and multicriteria decision analysis. Wiley, New York.
- ⁴³³ Agostini, P., Suter, G.W.II, Gottardo, S., Giubilato, E., Indicators and endpoints for risk-based decision process with decision support systems. In Marcomini, A., Suter, G.W.II, Critto, A. (Eds). *Decision Support Systems for Risk Based Management of Contaminated Sites*. Springer Verlag, New York, 2009
- ⁴³⁴ Janssen, R., Multiobjective decision support for environmental management, *Kluwer Academic*, (Dordrecht) Boston, 1992.
- ⁴³⁵ Densham, P.J., 1991. Spatial decision support system. In: Maguire, D.J., Goodchild, M.F., Rhind, D.W. (Eds.), *Geographical Information Systems: Principle and Applications*. John Wiley and Sons, New York, pp. 403–412
- ⁴³⁶ Matthies, M., Environmental decision support systems: Current issues, methods and tools, *Environmental Modelling & Software*, 22, 123-127, 2007.
- ⁴³⁷ Burrough, P.A. and McDonnell, R.A., 1998, *Principles of Geographical Information Systems*, Oxford University Press
- ⁴³⁸ Durand H., *et al.*, 1994, An example of GIS potentiality for coastal zone management: Pre-selection of submerged oyster culture areas near Marennes Oléron (France). *EARSEL Workshop on Remote Sensing and GIS for Coastal Zone Management*. Delft, The Netherlands, 24 - 26 Oct.
- ⁴³⁹ Wright D. and Bartlett D., 2000, *Marine and Coastal Geographical Information Systems*. (London: Taylor and Francis).
- ⁴⁴⁰ Narayan, S., Hanson, S., Nicholls, R.J., Clarke, D., Willems, P., Ntegeka, V., Monbaliu, J., 2012. A holistic model for coastal flooding using system diagrams and the Source–Pathway– Receptor (SPR) concept. [in special issue Sea Hazards]. *Nat. Hazards Earth Syst. Sci.* 12 (5), 1431–1439. <http://dx.doi.org/10.5194/nhess-12-1431-2012>
- ⁴⁴¹ DOI 10.1007/978-90-481-2238-7_4,
- ⁴⁴² Ward P. J. • M. A. Marfai • F. Yulianto • D. R. Hizbaron • J. C. J. H. Aerts Coastal inundation and damage exposure estimation: a case study for Jakarta *Nat Hazards* (2011) 56:899–916 DOI 10.1007/s11069-010-9599-1
- ⁴⁴³ Kellens W., P. Deckers, H. Saleh, W. Vanneuville, Ph. De Maeyer, G. Allaert & R. De Sutter
A GIS tool for flood risk analysis in Flanders (Belgium) *WIT Transactions on Information and Communication*, Vol 39, © 2008 WIT Press www.witpress.com, ISSN 1743-3517 (on-line) doi:10.2495/RISK080031
- ⁴⁴⁴ Eastman J.R. (2006). *Idrisi Andes, Guide to GIS and Image Processing*, Clark Labs – Clark University, Worcester, USA
- ⁴⁴⁵ A.T. Kulkarni, J. Mohanty, T.I. Eldho, E.P. Rao, B.K. Mohan A web GIS based integrated flood assessment modeling tool for coastal urban watersheds *Computers & Geosciences* 64 (2014) 7–14
- ⁴⁴⁶ Al-Sabhan, W., Mulligan, M., Blackburn, G.A., 2003. A real-time hydrological model for flood prediction using GIS and WWW. *Comput. Environ. Urban Syst.* 27, 9–32.
- ⁴⁴⁷ Lohani, V., Kibler, D.F., Chanut, J., 2002. Constructing a problem solving environment tool for hydrologic assessment of land use change. *J. Am. Water Resour. Assoc.* 38 (2), 439–452.
- ⁴⁴⁸ Engel, B.A., Choi, J.Y., Harbor, J., Pandey, S., 2003. Web-based DSS for hydrological impact evaluation of small watershed land use changes. *Comput. Electron. Agric.* 39, 241–249.

-
- ⁴⁴⁹ Hulchy, L., Tran, V.D., Habala, O., Simo, B., Gatial, E., Astalos, J., Dobrucky, M., 2004. Flood forecasting in cross grid project. Second European AcrossGrids conference, 2004 Published in: Lecture notes in computer science, vol. 3165, Springer: Berlin, pp. 51–60.
- ⁴⁵⁰ Choi, J.Y., Engel, B.A., Theller, L., Harbor, J., 2005. Utilizing web-based GIS and SDSS for hydrological land use change impact assessment. *Trans. Am. Soc. Agric. Eng. (ASAE)* 48 (2), 815–822.
- ⁴⁵¹ Lim, K.J., Engel, B.A., Tang, Z., Choi, J., Kim, K., Muthukrishnan, S., Tripathy, D., 2005. Automated web GIS based hydrograph analysis tool, WHAT. *J. Am. Water Resour. Association* 04133, 1407–1416.
- ⁴⁵² Cate Jr., A., Semmens, D., Guertin, P.D., Goodrich, D.C., 2007. DOTAWGA: A case study in web-based architectures for connecting surface water models to spatially enabled web applications. In: *Proceedings of Summer Computer Simulation Conference (SCSC)*, pp. 885–892.
- ⁴⁵³ Jia, Y., Zhao, H., Niu, C., Jiang, Y., Gan, H., Xing, Z., Zhao, X., Zhao, Z., 2009. A web GIS based system for rainfall-runoff prediction and real time water resource assessment for Beijing. *Comput. Geosci.* 35, 1517–1528.
- ⁴⁵⁴ Gkatzoflias, D., Mellios, G., Samaras, Z., 2013. Development of a web GIS application for emissions inventory spatial allocation based on open source software tools. *Comput. Geosci.* 52 (0), 21e33. <http://dx.doi.org/10.1016/j.cageo.2012.10.011>.
- ⁴⁵⁵ Vatsavai, R., Shekhar, S., Burk, T., Lime, S., 2006. UMN-MapServer: a Highperformance, Interoperable, and Open Source Web Mapping and Geo-spatial Analysis System
- ⁴⁵⁶ OSGeo, 2014. Benchmarking 2011. Retrieved January 9, 2015, from http://wiki.osgeo.org/wiki/Benchmarking_2011.
- ⁴⁵⁷ Hazzard, E., 2011. *OpenLayers 2.10: Beginner's Guide*. Packt Publishing, Birmingham.
- Hill, D.J., Liu, Y., Marini, L., Kooper, R., Rodriguez, A., Futrelle, J., ... McLaren, T., 2011. A virtual sensor system for user-generated, real-time environmental data products. *Environ. Model. Softw.* 26 (12), 1710e1724.
- ⁴⁵⁸ Steiniger, S., Hunter, A.J.S., 2012. Free and open source GIS software for building a spatial data infrastructure. In: Bocher, E., Neteler, M. (Eds.), *Geospatial Free and Open Source Software in the 21st Century*. Springer Berlin, Heidelberg, pp. 247e261.
- ⁴⁵⁹ Steiniger, S., Hunter, A.J.S., 2012b. Review: the 2012 free and open source GIS software map e a guide to facilitate research, development, and adoption. *Comput. Environ. Urban Syst.* <http://dx.doi.org/10.1016/j.compenurbsys.2012.10.003>.
- ⁴⁶⁰ Steiniger, S., Hunter, A.J.S., 2012. Free and open source GIS software for building a spatial data infrastructure. In: Bocher, E., Neteler, M. (Eds.), *Geospatial Free and Open Source Software in the 21st Century*. Springer Berlin, Heidelberg, pp. 247e261.
- ⁴⁶¹ Steiniger, S., Hunter, A.J.S., 2012b. Review: the 2012 free and open source GIS software map e a guide to facilitate research, development, and adoption. *Comput. Environ. Urban Syst.* <http://dx.doi.org/10.1016/j.compenurbsys.2012.10.003>.
- ⁴⁶² Steiniger, S., Hunter, A.J.S., 2012b. Review: the 2012 free and open source GIS software map e a guide to facilitate research, development, and adoption. *Comput. Environ. Urban Syst.* <http://dx.doi.org/10.1016/j.compenurbsys.2012.10.003>.
- ⁴⁶³ Zhao, P., Foerster, T., Yue, P., 2012. The geoprocessing web. *Comput. Geosci.* 47 (0), 3e12. <http://dx.doi.org/10.1016/j.cageo.2012.04.021>.
- ⁴⁶⁴ Furieri, A., 2008. SpatialLite e a Complete Spatial DBMS in a Nutshell